Quantifying Air Quality, Human Health, and Climate Impacts from Energy Systems: Electricity and Transportation

Maninder Pal Singh Thind

A dissertation
submitted in partial fulfillment of the
requirements for the degree of

Doctor of Philosophy

University of Washington
2020

Reading Committee:
Julian Marshall, Chair
Timothy Larson
Becky Suess

Program Authorized to Offer Degree:
Civil and Environment Engineering

University of Washington

Abstract

Quantifying Air Quality, Human Health, and Climate Impacts from Energy Systems: Electricity and Transportation

Maninder Pal Singh Thind

Chair of the Supervisory Committee:

Julian Marshall

Department of Civil and Environment Engineering

Atmospheric emissions from the energy sector contribute to air pollution and climate change. Harmful gases in ambient air degrade air quality; exposure to those gases can lead to health impacts locally and regionally. Greenhouse gases perturb the energy balance of the atmosphere, leading to higher temperatures (global warming) and thus impacting climate at a global scale. Air pollution is linked to exposure disparities among demographic groups (race, income).

This dissertation explores air quality, health and climate impacts, and environmental injustice from emissions originating from energy systems. The overarching goals of this research work are to (i) quantify and compare metrics for greenhouse and noxious pollutants to evaluate environmental consequences from interventions, (ii) develop metrics and tools to quantify air

quality and human health impacts from point and line sources, (iii) explore distributions of health impacts from air pollution by race, income, and geography, and (iv) demonstrate the use a reduced-complexity air quality model to quantify impacts from multiple energy systems.

In this research, I focus on the fine particulate matter ($PM_{2.5}$) and carbon dioxide (CO_2) emissions. $PM_{2.5}$ is the air pollutant that produces the largest monetized human health impacts in the United States (U.S.) and worldwide. $PM_{2.5}$ can be directly emitted from combustion or other activities (primary $PM_{2.5}$) or formed from precursors such as volatile organic compounds (VOCs), sulfur dioxide (SO_2), oxides of nitrogen (NO_x), and ammonia (NH_3) (secondary $PM_{2.5}$). Concentrations of $PM_{2.5}$ species in the atmosphere are controlled by emissions, transport, chemistry, and deposition processes. The health impacts are a function of concentrations and the exposed population. Previous research has demonstrated the importance of fine spatial resolution for identifying and quantifying exposure disparities (environmental justice). I used a novel spatial air quality model called "Intervention Model for Air Pollution (InMAP)," combined with epidemiological research concerning air pollution and human health, to estimate health impacts of $PM_{2.5}$ at a fine resolution. To understand climate impacts, I focus on carbon dioxide (CO_2) which is a major greenhouse gas (81% of the total greenhouse gas emissions) emitted from complete combustion of carbon-containing fuels.

This dissertation consists of three original studies focused on two energy sectors in the United States (U.S.): electricity generation and freight transportation. The methods employed in this work are based on two approaches: data-driven regression analysis and mechanistic air quality modeling using InMAP.

Chapter 2 presents the data-driven empirical approach. Using linear regression between hourly changes in generation and emissions data, I investigate differences between average emission factors (AEFs) and average marginal emission factors (AMEFs) for CO_2, SO_2, and NO_x at different spatial and temporal scales for a Midwest U.S. power market called the Midcontinent Independent System Operator (MISO). AEFs and AMEFs are two commonly used metrics for estimating emission benefits from energy-efficiency strategies. This is the first study that estimates AEFs and AMEFs for a U.S. Regional Transmission Organization (RTO). I find, for example, that marginal emission factors are generally higher during late night and early morning compared to afternoons. In general, AEFs tend to be larger than AMEFs (typical difference: ~20%), and thus may overestimate emission impacts from interventions in the power sector, relative to using AMEFs.

Chapters 3 and 4 present a mechanistic modeling approach for investigating air quality and human health impacts from $PM_{2.5}$ emissions. Chapter 3 presents a study that estimates exposure to and health impacts of $PM_{2.5}$ from electricity generation in the U.S., for each of the seven Regional Transmission Organizations (RTOs), for each US state, by income, and by race. This research is the first national-scale investigation of environmental justice aspects of total $PM_{2.5}$ from electricity generation. I find that average exposures are the highest for blacks, followed by non-Latino whites. Exposures for remaining groups (e.g., Asians, Native Americans, Latinos) are somewhat lower. Levels of disparity differ by state and RTO. Exposures are higher for lower-income than for higher-income, but disparities are larger by race than by income. Geographically, I observe large differences between where electricity is generated and where people experience the resulting $PM_{2.5}$ health consequences; some states are net exporters of health impacts, other are net importers.

Chapter 4 presents a study that investigates environmental health and climate impacts from inter-state road, rail, water, and air freight transportation in the U.S. This is the first detailed study to compare health, environmental justice, and climate impacts of four freight modes, studying each route separately. Average impacts per unit mass shipped are as follows. For all three impacts studied ($PM_{2.5}$ health effects, racial-ethnic disparities in $PM_{2.5}$ exposure, CO_2 emissions), impacts are greatest for aircraft. Among non-aircraft modes: $PM_{2.5}$ health effects are largest for rail, intermediate for barge, and lowest for truck; $PM_{2.5}$ exposure disparities are largest for rail and are lower for truck and barge; climate impacts are largest for truck, intermediate for barge, and lowest for rail. Overall, inter-state freight movement in the U.S. disproportionately impacts white non-Latinos relative to other racial-ethnic groups but exposures differ by mode. Average exposures from truck and rail are the highest for white non-Latinos, barge exposure is highest for blacks, and aircraft exposure is highest for mixed/other race groups.

This dissertation presents work to investigate air quality, health and climate impacts, and environmental justice-related issues from electricity generation and freight transportation. This work can be extended to other specific sectors of the economy and can be useful to scientists, planners, and policymakers to estimate environmental benefits of energy conservation programs and create policies that address environmental injustice. The metrics developed in this work can be applied by researchers to new electricity and transportation scenarios to understand their impacts and benefits.

Preface

ੴ

"ਪਵਣੁ ਗੁਰੂ ਪਾਣੀ ਪਿਤਾ ਮਾਤਾ ਧਰਤਿ ਮਹਤੁ ॥"

- ਗੁਰੂ ਨਾਨਕ ਦੇਵ ਜੀ, ਜਪੁਜੀ ਸਾਹਿਬ, ਸ਼੍ਰੀ ਗੁਰੂ ਗ੍ਰੰਥ ਸਾਹਿਬ ਜੀ

Above verse (in quotes) from the first composition of Guru Nanak Dev Ji, "Japji Sahib" in the Sikh scripture, Sri Guru Granth Sahib Ji is pronounced as "Pawan guru paani pita, mata dhart mahat". It means Air is our teacher, Water our father, and the Great Earth is our mother. This verse is central to my efforts to study the science of air (atmosphere) – one of the important components of the Earth system necessary for the survival of human race. Humans created machines to make their lives easier; yet, this convenience often comes at the expense of creating an environmental burden by emitting harmful substances into the air. Growing up in an agrarian household on a farm in Punjab, India, I was surrounded with air pollution issues, including stubble burning in the winter months and air pollution from vehicle traffic while going to school in the city. During my bachelor's degree, I was blessed to have met and work with motivational people contributing their efforts to solve environmental and social issues. They inspired me to think differently about these issues and how to address them. I saw air pollution as a big environmental and social challenge and decided to address important questions arising from air pollution.

This dissertation aims at understanding and creating new knowledge on the air quality, human health, and climate impacts of air pollution originating from energy systems. I investigate exposure disparities among demographic groups, arising from air pollution sources. I use data-driven empirical and air quality modeling approaches to understand the impacts. I learned and used a novel atmospheric model to quantify health impacts of air pollution on human population and answer environmental justice-related questions.

This dissertation includes material previously published in the Environmental Science & Technology journal as two research papers (Chapters 2 and 3). Julian D. Marshall, Christopher W. Tessum, Inês L. Azevedo, and Elizabeth J. Wilson are co-authors of the published papers.

Chapter 2: Thind, M.P.S.; Tessum, C.W; Azevedo, I.L.; Marshall, J.D. Fine Particulate Air Pollution from Electricity Generation in the US: Health Impacts by Race, Income, and Geography. *Environ. Sci. Technol.* **2019**, 53, 14010−14019. DOI: https://doi.org/10.1021/acs.est.9b02527.

Chapter 3: Thind, M.P.S.; Wilson, E.J.; Azevedo, I.L.; Marshall, J.D. Marginal Emissions Factors for Electricity Generation in the Midcontinent ISO. *Environ. Sci. Technol.* **2017**, 51, 14445–14452. DOI: https://doi.org/10.1021/acs.est.7b03047.

Dedication

I dedicate my thesis to

Professor Julian David Marshall, my teacher and mentor

and

My family

Sukhwinder Singh Thind, my father and Manjit Kaur Thind, my mother

Late Dalip Singh Thind, my grandfather and Mahinder Kaur Thind, my grandmother

Harman Preet Singh Thind, my brother

Pawanpreet Kaur, my wife and my strength

and

People fighting with mental health challenges

Acknowledgements

I would not have been able to reach this milestone without the support of many people. First and foremost, I would like to thank my advisor and a person whose personality inspires me, Prof. Julian D. Marshall for providing me the opportunity to perform research under his guidance at the University of Washington, Seattle and the University of Minnesota, Twin Cities. I am grateful to him for his patience, effort, career advice, and many discussion sessions to help me accomplish my research goals as well as helping me navigate my personal and work lives. His dedication and firm stand towards environmental, social, and mental health issues and making efforts to solve them inspires me. I would like to thank Chris Tessum for answering my endless questions regarding Intervention Model for Air Pollution (InMAP). I sincerely thank my dissertation committee members, Prof. Timothy V. Larson, Prof. Becky Alexander, and Prof. Lyatt Jaeglé for their support and comments to improve my dissertation.

I am grateful to my family for their years of support and encouragement. Thank you, mom and dad, for your hard work in the fields to support me and my brother and investing in our education. I am here because of many valuable lessons you both taught me.

I would like to thank my colleagues, former colleagues, and friends in the Marshall Research Group: Lara Clark, Matt Bechle, Chris Tessum, Steve Hankey, Nam Nguyen, Srinidhi Murali, David Paolella, and Makoto Kelp for creating a healthy and supportive environment in the lab and making my graduate student life fun and easy. Thank you to all members of the group for answering my endless questions and curiosities on many topics ranging from life to intensive research.

I would like to thank Fred Rose for being my great mentor since my bachelor's degree, for giving me an opportunity to get involved in the Acara Institute that shaped the way I think about environmental and societal challenges, and connecting me to many inspiring people including Prof. Julian Marshall.

I thank my colleagues at the National Renewable Energy Laboratory (NREL): Garvin Heath, Yimin Zhang, Annika Eberle, and Arpit Bhatt for an incredible internship experience at NREL and for a chance to apply my doctoral skills in a project with the ExxonMobil Research and

Engineering. I thank Garvin Heath and Emily Newes for continuously supporting me in Colorado while I was completing my PhD work from Colorado.

I would also like to acknowledge the funding agencies that funded my research work: Center for Air, Climate, and Energy Solution (CACES), which was supported under Assistance Agreement Number R835873 awarded by the United States Environmental Protection Agency, Initiative for Renewable Energy & the Environment (IREE) Grant (RL-0011-13) at the University of Minnesota, Twin Cities and the Center for Climate and Energy Decision Making (CEDM) through a cooperative agreement between the National Science Foundation and Carnegie Mellon University (SES-0949710 and SES-1463492).

Contents

List of Tables

List of Figures

Chapter 1

Introduction

1.1 Background

The Earth system is comprised of four major subsystems, which are called “spheres”: "lithosphere" (land), "hydrosphere" (water), "biosphere" (living beings), and "atmosphere" (air).[1] All these spheres are interconnected and dependent on each other. Human activities on the Earth’s surface impact land, air, water, and living beings. This dissertation is focused on impacts of human activities on air and humans. Combustion and non-combustion activities in sectors such as electricity generation, transportation, and agriculture emit particles and gases into the air and cause air pollution to impact the quality of air (“air quality”).[2]

Sources of air pollution can be broadly categorized into three types: “point” or “stationary” sources such as smokestacks of power plants, “line” or “mobile” sources such as tailpipe of fossil-fueled vehicles, and “area” sources such as agriculture sites. Combustion is a common source of air pollution: a fuel containing carbon, hydrogen, and other elements, and potentially non-fuel impurities, is combusted in the presence of oxygen (air) and emits gases and particles as waste products (pollutants). U.S Environmental Protection Agency (U.S. EPA) categorizes air pollutants into various categories, such as (1) six “criteria” (common) air pollutants (CAPs): particulate matter (PM), ground-level ozone (O_3), carbon monoxide (CO), sulfur dioxide (SO_2), nitrogen oxides (NO_x), and lead;[3] (2) one hundred eighty seven hazardous air pollutants (HAPs): examples include benzene, formaldehyde, asbestos, metals such as cadmium, mercury, and chromium;[4] (3) four “greenhouse” gases (GHGs): carbon dioxide, methane, nitrous oxide, and fluorinated gases. Other harmful pollutants include ammonia and Volatile Organic Compounds (VOCs).[5] CAPs and HAPs are considered harmful to public health and the environment, and GHGs cause global warming which contributes to climate change. Under the Clean Air Act of 1990, the U.S. EPA regulates CAPs by setting concentration limits, called the National Ambient Air Quality Standards

(NAAQS).[6] Air quality is a local and regional issue where spatial location of emission sources becomes important to understand their impacts.

Particle pollution is of particular interest because chronic (long-term) exposure to it can cause serious health effects.[7] Particle pollution includes particles with aerodynamic diameter less than 10 micrometers (μm) (course particles, PM_{10}), less than 2.5 μm (fine particles, $PM_{2.5}$), and less than 0.1 μm (ultrafine particles).[8] Particles get inhaled while breathing and can pass through the respiratory tract to internal organs. $PM_{2.5}$ is small enough to penetrate the deepest part of the lungs such as the bronchioles or alveoli to cause serious health effects.[9]

$PM_{2.5}$ can be either directly emitted in the air ("primary $PM_{2.5}$") or formed in the atmosphere from precursors such as SO_2, NO_x, NH_3, and VOCs ("secondary $PM_{2.5}$").[10] Primary and secondary $PM_{2.5}$ forms the total $PM_{2.5}$. Secondary $PM_{2.5}$ is formed in the atmosphere by conversion of inorganic (SO_2, NO_x, NH_3) and organic gases (VOCs) into condensed phase material. SO_2 and NO_x are oxidized to sulfate and nitrate and react with ammonia to produce ammonium nitrate and ammonium sulfate particles. Physical processes such as coagulation, nucleation, and condensation convert gases to particles. $PM_{2.5}$ precursors can travel long distances, react in the atmosphere, and impact population spatially at far distances (~10s to ~100s of km).[11,12]

$$NH_3\ (g) + HNO_3\ (g) \rightleftharpoons NH_4NO_3\ (s)$$

$$NH_3\ (g) + H_2SO_4\ (g) \rightleftharpoons (NH_4)_2SO_4\ (s)$$

CO_2 is the major greenhouse gas that causes global warming and contributes to climate change. CO_2 accounts for 81% of the total greenhouse gas emissions in the year 2018 and is a major driver of climate change.[5] Unlike air quality, climate change is a problem at global scale. Locations of emissions are largely unimportant in climate change.

Electricity generation and transportation are two major sectors that impact air quality and human health in the U.S. by emitting primary $PM_{2.5}$, SO_2, NO_x, VOCs, and NH_3 into the air Pollutants are emitted from smokestacks of power plants after fuel (e.g., coal, natural gas, diesel) is combusted to heat the boiler to form steam which rotates turbines to generate electricity. Gasoline or diesel fuel is combusted in the combustion chamber of vehicle engine to generate pollutants emitted via the tailpipe. SO_2 is formed from the oxidation of sulfur present in fuels. NO_x emissions have several pathways: thermal NO_x from oxidation of N_2 in the air, fuel NO_x from nitrogen in fuel, and prompt NO_x from radical formation. NH_3 is mostly emitted as leakage from emission control technologies. Electricity and transportation contribute ~66% of the total CO_2 emissions in the year 2018 in the U.S.[13] CO_2 is formed from complete combustion of carbon-containing fuels in the presence of oxygen.

Many opportunities exist for reducing emissions, including energy conservation, emission control technologies (e.g., catalytic converters; power plant scrubbers), non-combustion electricity (wind, hydroelectric, waves, solar, geothermal), electric vehicles combined with lower-emission electricity systems, fuel switching (e.g., natural gas rather than coal), cleaner fuels (e.g., low- rather than high-sulfur diesel), and demand-side energy efficiency. Various economic, social, and policy strategies exist for implementing, encouraging, and accelerating those and other emission reductions.

1.1.1 Health impacts from fine particulate matter ($PM_{2.5}$)

Several epidemiological studies have established that human exposure to fine particulate matter ($PM_{2.5}$) results in premature death from diseases like stroke, heart disease, lung cancer, chronic obstructive pulmonary diseases, and respiratory infections, including pneumonia.[14-24] Here, premature death is defined as a death that would have occurred later in a population in the absence of $PM_{2.5}$ pollution.[25] A majority of the monetized damages from $PM_{2.5}$ are attributable to premature mortality; and, a majority of the total monetized damages from air pollution are attributable to mortality from $PM_{2.5}$.[26]

Global and United States context

According to World Health Organization (WHO), ambient air pollution was responsible for 4.2 million deaths in the year 2016.[27] Globally, ambient air pollution is estimated to cause ~16% of the lung cancer deaths, ~25% of chronic obstructive pulmonary disease (COPD) deaths, ~17% of ischemic heart disease and stroke, and ~26% of respiratory infection deaths.[27] Of all the pollutants, fine particulate matter ($PM_{2.5}$) poses the greatest heath risk on human health. Cohen et al. (2017) estimated $PM_{2.5}$ was the 5th-ranking mortality risk factor in 2015 globally (using 2015 Global Burden of Disease data).[28] In the U.S., $PM_{2.5}$ was the 6th largest cause of all mortalities in

2015, responsible for ~88,000 deaths (95% CI: 67,000–115,000). According to the Cohen et al. (2017) study, ~94% of ambient air pollution-related mortalities are caused by $PM_{2.5}$ and the remaining 6% are caused by ground-level O_3. Apte et al. (2018) estimates that in 2016, $PM_{2.5}$ exposure reduced average global life expectancy at birth by ∼1 year; estimated reductions were ∼1.2–1.9 years in polluted countries of Asia and Africa,[29] and ~ 0.38 year in the U.S. Several studies have estimated $PM_{2.5}$-related deaths from different energy sectors globally and in the U.S.[30-32]

$PM_{2.5}$ health impact framework

Figure 1.1 shows the impact pathway for $PM_{2.5}$ and a framework for assessing human health effects from $PM_{2.5}$ exposure. Primary $PM_{2.5}$ and precursor emissions at the source disperse, transform in the atmosphere, and are carried by wind and other physical processes to different locations, generating varying concentrations of the pollutant in the space. Exposure is the level of pollution in a person's breathing zone. Intake is the mass of a pollutant inhaled. Dose is the amount of pollutant that stays inside the body or interacts with a target biological system. Health effects can be measured using mortality or morbidity. Morbidity-related health effects from $PM_{2.5}$ show only negligible contribution to monetized health effects (Frischknecht et al. 2016, Apte et al. 2015).[33,34]

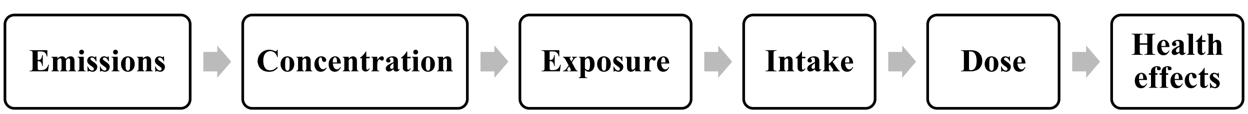

Figure 1.1 Emissions to health effects framework for fine particulate matter ($PM_{2.5}$)

Epidemiology studies relating $PM_{2.5}$ exposure to health effects

Several cohort studies have linked $PM_{2.5}$ concentrations to increased risk of mortality.[35] Concentration-response (C-R) functions or relationships are used to estimate the association between ambient concentrations of outdoor air pollution and mortality. C-R functions can be linear or non-linear, and can have a threshold or no threshold. Present scientific consensus generally suggests a linear or nearly linear C-R function with no threshold, for the range of ambient $PM_{2.5}$

concentrations experienced in the US.[35,36] For global exposures, which exhibit a wider range of concentrations than in the U.S., the integrated exposure response function employed by the Global Burden of Disease (GBD) is nonlinear.[33,35]

The most recent meta-analysis study, Pope et al. (2020) summarizes the association of increased mortality from $PM_{2.5}$ exposure from the last 25+ years of cohort studies.[35] Increased risk of mortality from $PM_{2.5}$ exposure has been studied in survival studies of several different cohorts of individuals in the U.S. and across the world (examples: Canada, Germany, Netherlands, England, China, Taiwan, Iran). The increased mortality is observed even after controlling for confounding risk factors such as age, sex, race, marital status, education, smoking, alcohol consumption, diet, and obesity in majority of the cohort studies. Hazard ratio (HR) and relative risk (RR) are two different, commonly used measures of risk in these cohort studies to express the probability of developing risk (such as premature mortality) from exposure to $PM_{2.5}$. Both measures represent ratios of risk in exposed to the unexposed populations but are estimated differently: RR is estimated by averaging events over a specific time period and HR is estimated using survival curves to give instantaneous estimates. In the air pollution literature, HR is commonly estimated using cox proportional-hazards regression modeling.[35] Table 1.1 provides examples of all-cause (i.e., all causes of death for a population) HRs per 10 $\mu g/m^3$ increase in $PM_{2.5}$ from selected large cohort studies in the U.S. and from meta-analysis of several cohort studies across the world. For example, estimated HR of 1.13 for all-cause mortality per 10 $\mu g/m^3$ of $PM_{2.5}$ means that each 10 $\mu g/m^3$ elevation in $PM_{2.5}$ exposure is associated with 13% increased risk of all-cause mortality in the population. Pope et al. (2020) estimates meta-analytic mean of the distribution of effects from cohort studies that are currently available, which provides substantial evidence of adverse air pollution associations with all-cause (HR=1.08 per 10 $\mu g/m^3$ of $PM_{2.5}$), cardiopulmonary (HR=1.11 per 10 $\mu g/m^3$ of $PM_{2.5}$), and lung cancer mortality (HR=1.14 per 10 $\mu g/m^3$ of $PM_{2.5}$).[35]

The Harvard Six-Cities study (H6C, Dockery et al., 1993) was the first study to present the HRs per 10 $\mu g/m^3$ linked to long-term exposure to $PM_{2.5}$.[14] The second study was the American Cancer Society (ACS) Cancer Prevention Study II (CPS-II), which used a larger cohort to estimate the association (Pope et al., 1995).[16] The results of these studies have been confirmed over several re-analyses, most recently in Krewski et al. (2009)[37] for the ACS study and Lepeule et al. (2012)[38]

for the H6C study. For both the H6C study and the ACS study, estimated adjusted HRs across the originally reported results, the independent reanalysis, and the various extended analyses are consistent among each other. While these publications are up to 10 years old, they are the major studies used by the U.S. EPA (e.g., to evaluate the benefits of EPA regulations for reducing particulate matter concentrations).[39] These two studies (H6C; ACS) are considered the standard among regulatory[36,39] and academic researchers.[40,41] In this dissertation, I employ all-cause HR of 1.078 per 10 μg/m^3 of $PM_{2.5}$ from the Krewski et al. (2009)[37] in the C-R function for estimating health impacts (explained in detail in section 1.3.2). HR from Krewski at al. (2019) is consistent with the Pope et al. (2020)'s meta estimate of HR for all-cause mortality (1.08 per 10 μg/m^3 of $PM_{2.5}$).

Table 1.1 Examples of hazard ratios from cohort studies in the U.S. and meta-analytic studies of several cohorts across the world

Study	Cohort details	All-cause hazard ratio (HR) per 10 μg/m^3 of $PM_{2.5}$
Dockery et al., (1993)[14]	H6C cohort; 6 US cities (n=8,111)	HR=1.13
Pope et al. (1995)[16]	ACS cohort; 151 cities (n= 552,138)	HR=1.07
Krewski et al. (2009)[37]	ACS cohort; nationwide (n= 860,000)	HR=1.078
Lepeule et al. (2012)[38]	H6C cohort; 6 US cities (n=8,096)	HR=1.14
Vodonos et al. (2018)[42] (a meta-analysis of multiple studies across world)	H6C, ACS, Medicare, and other cohorts from different studies	HR=1.129
Pope et al. (2019)[43]	National Health Interview Surveys (1986–2014), n= 1,599,329	HR=1.12
Pope et al. (2020)[35] (a meta-analysis of multiple studies across world)	H6C, ACS, Medicare and other cohorts from different studies	HR=1.08

1.1.2 Environmental justice

U.S. EPA defines "environmental justice" as "the fair treatment and meaningful involvement of all people regardless of race, color, national origin, or income, with respect to the development, implementation, and enforcement of environmental laws, regulations, and policies."[44] It further elaborates: "Fair treatment means no group of people should bear a disproportionate share of the negative environmental consequences resulting from industrial, governmental and commercial operations or policies." According to Clark et al. 2017, "environmental injustice describes conditions in which more vulnerable communities experience disproportionate burdens of environmental health risks, such as exposure to air pollution."[45] Environmental "injustice" is not same as environmental "inequality": inequality means disparity among groups (i.e., "un-equal") whereas injustice means disparity among groups with distributional impacts on fairness.[46] For example, environmental injustice from air pollution exposure may arise when exposures are larger for a disadvantaged group than for an advantaged group. Several studies have looked into environmental injustice of air pollution. Few examples: Clark et al. (2014)[47] describe spatial patterns in environmental injustice and inequality for outdoor NO_2 concentrations in the contiguous U.S. and Clark et al. (2017)[45] explore disparities in exposure to outdoor NO_2 concentrations the U.S. and found that non-whites are exposed to higher NO_2 concentrations than whites. Tessum et al. (2019) explored racial–ethnic disparities in the causation and effect of exposure to $PM_{2.5}$ in the United States.[48]

1.1.3 Factors impacting concentrations, health impacts, and exposure disparity

Figure 1.2 provides an overview of factors that impact each stage of emissions to damage framework for $PM_{2.5}$. Pollutant mass emitted at the source depends on the characteristics of the emitting source (e.g., for combustion sources: fuel type, combustion technology, emission control technology). Ambient $PM_{2.5}$ concentrations depend on the geographic location of an emission source, the emission height, the type of $PM_{2.5}$ precursor, meteorology, atmospheric aerosol chemistry of secondary $PM_{2.5}$ formation, and physical processes such as wet and dry deposition, advection, and turbulent mixing. People are exposed to varying concentrations in space. Intake fraction is the ratio of mass of pollutant inhaled to the mass of pollutant emitted at the source.

Pollutant mass intake is a function of three core variables: concentration, breathing rate, and time. Choice of concentration-response function is important for quantification of health endpoints.

Health disparities from $PM_{2.5}$ can arise when exposure to one demographic group (race, income) is greater than the other group. Spatial pattern of population of demographic groups and concentrations determine disparity.

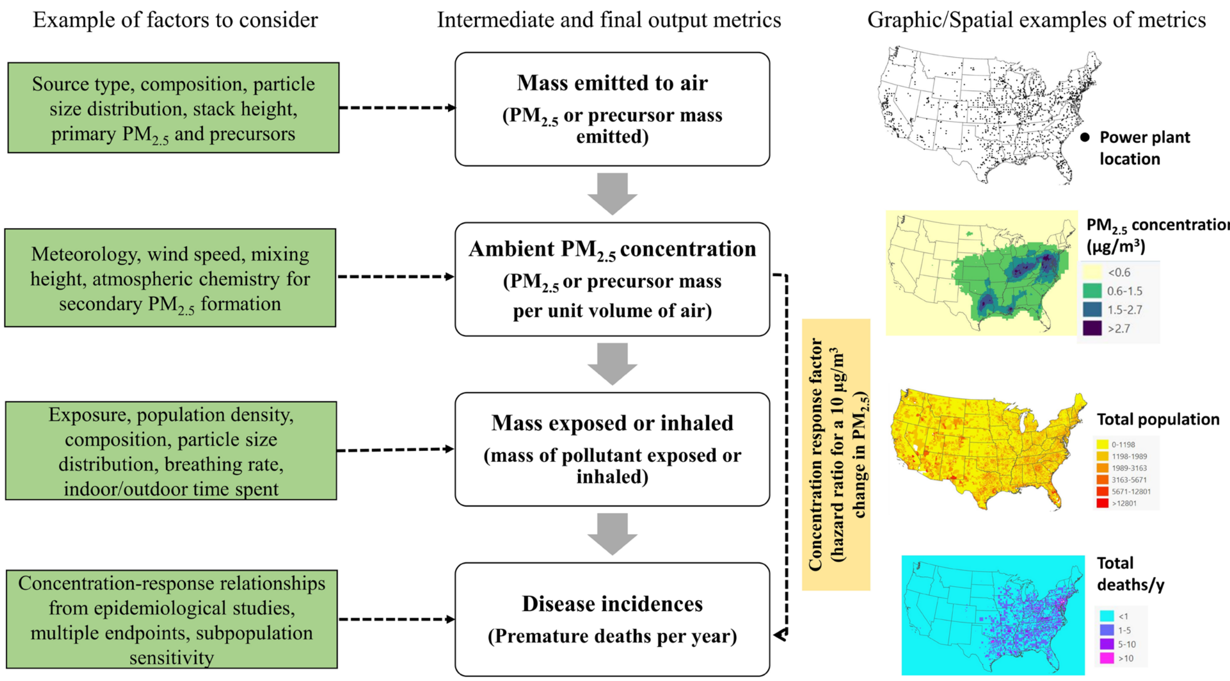

Figure 1.2 Emission-to-damage framework for $PM_{2.5}$ and factors affecting each metric in the framework. Adapted and modified from Apte et al. (2011)[49]

1.1.4 Air quality modeling

The atmosphere is a complex system in which numerous physical and chemical processes occur simultaneously. Ambient measurements using monitors provide conditions at a particular time and location. Scientists developed air quality (or "atmospheric") models in part to simulate concentrations at all locations and time when and where there are no comprehensive measurements available. These models are useful for solving air quality problems and making future policy decisions. Air quality models can be broadly classified into two types: (1) Statistical or Empirical models and (2) Mechanistic models.[10] Statistical models are based on observations and predictions (examples: land-use regression models). Mechanistic models are based on physics, chemistry, and meteorology parameters to simulate physical and chemical atmospheric processes in the atmosphere (examples: AERMOD, CMAQ).[50] Mechanistic models can be further classified into Lagrangian, where the reference frame moves with the wind, and Eulerian, where the reference frame is fixed. Eulerian Chemical Transport Models (CTMs; examples: CMAQ,[51] CAMx,[52] GEOSChem,[53] WRF-Chem[54]) are powerful tools that simulate atmospheric processes to predict concentrations and their spatiotemporal variability.

1.2 Goals and objectives

The overarching goals of this dissertation are to (i) quantify and compare metrics for greenhouse and noxious pollutants to evaluate environmental consequences from interventions, (ii) develop metrics and tools to quantify air quality and human health impacts from point and line sources, (iii) explore distributions of health impacts from air pollution by race, income, and geography, and (iv) demonstrate the use a reduced-complexity air quality model to quantify impacts from energy systems.

To reach these goals, I focus on two energy sectors in the contiguous U.S.: electricity generation and freight transportation. Electricity and transportation are important sources of $PM_{2.5}$ emissions and human health impacts, as discussed in previous sections. This dissertation addresses some important gaps in the literature within these sectors: (i) average and average marginal emission factors are common metrics for estimating emission benefits from energy efficiency interventions. Current research has not looked into comparison between these two metrics for U.S. electricity markets. (ii) A key knowledge gap is exploring exposure disparity among demographic groups from electricity generation and freight transportation sources. One of the assumptions in environmental injustice is the way infrastructure (power plants, roads/highways, rail tracks, airports) are laid out historically which impacts one community over others. (iii) Existing research has not investigated which freight mode – road, rail, water or air – has the least heath and climate impacts from transporting one unit mass of freight between an origin and destination. Each chapter discusses these gaps in more detail.

More specifically, the main objectives of this dissertation are to:

(1) Quantify and compare average and average marginal emissions factors for a greenhouse gas (CO_2) and two criteria pollutants (NO_x, SO_2) from electricity generation in a U.S. Regional Transmission Organization (RTO).

(2) Quantify health impacts from electricity generation by geography (national, RTO, state), race, and income.

(3) Quantify and compare health and climate impacts and exposure disparity among racial-ethnic groups from inter-state freight transportation by mode, route, and emission species.

(4) Conduct spatial air quality modeling using the Intervention Model for Air Pollution (InMAP) – a novel reduced-complexity air quality model.

To quantify health impacts and disparity between demographic groups, I use premature deaths as the health endpoint. I use data-driven empirical and mechanistic air quality modeling approaches in this work. For air quality modeling, I use the forward modeling approach: I input emissions and atmospheric data, and the model predicts concentrations; inputs and outputs may vary in space.

1.3 Approach

1.3.1 Air quality modeling using Intervention Model for Air Pollution (InMAP)

Many air quality models are used in regulatory and research communities, each with strengths and weaknesses. Complex chemical transport models (CTMs) represent state-of-the-science atmospheric models and provide the most robust estimates available when time and computational constraints are not limiting.[50-54] However, because complex CTMs are time and resource intensive, in some cases modelers may prefer reduced-complexity air quality models (RCMs) instead. RCMs can take a CTM-based,[55-63] Gaussian,[64-69] Lagrangian,[70-71] or chemical mass balance[72] approach. Although less accurate than complex CTMs, RCMs can have the flexibility to allow for a greater number of sensitivity analyses, Monte Carlo approaches, an understanding of source and receptor effects, use of smaller-sized grid cells, and longer simulated periods.[73-77] Three commonly used RCMs provide comprehensive estimates covering the contiguous U.S. at relatively high spatial resolution (county level or finer): the Air Pollution Emission Experiments and Policy (APEEP/AP2) model,[67] the Estimating Air pollution Social Impacts Using Regression (EASIUR) model,[60] and InMAP.[78] Gilmore et al. (2019) compare these three models.[79] Among the three, APEEP/AP2 has county-level spatial resolution, EASIUR uses a 36 km × 36 km grid covering the contiguous U.S., and InMAP employs smaller-sized grid cells at much finer-scale spatial resolution than the two other RCMs. While APEEP/AP2 can model concentrations from all $PM_{2.5}$ precursors, EASIUR cannot model formation of secondary organic aerosols (SOA) from VOC emissions; hence, EASIUR may not be suitable to estimate total $PM_{2.5}$. APEEP/AP2 has lower spatial resolution (county-level) than InMAP does, which is not desirable for addressing questions in this research.

InMAP is used for air quality modeling in this research. InMAP is designed to estimate the annual average $PM_{2.5}$ concentration and health impacts resulting from incremental changes in pollutant emissions.[78] It estimates average pollutant concentrations from emissions by estimating a steady-state solution to a mass-balance equation dependent on reaction, advection, and diffusion parameters. InMAP uses physics and chemistry parameters derived from a state-of-the-science CTM, WRF-Chem. Geographic locations in InMAP can be specified as polygon, line, or point sources (including stack-height and plume-rise attributes, where relevant). InMAP uses a variable spatial grid, where the grid cell size is a function of the gradient in population density and pollutant concentrations, varying from 1 km × 1 km (typically, in urban areas) to 48 km × 48 km (typically, in rural areas). InMAP output grid consists of ~26 layers. The bottom ("ground-level") layer extends from 0 m to an average height of ~56m. The height of the 26th layer is 19 km, i.e. well above the end of troposphere (~10-15 km).[10] For comparison, the typical height at which aircrafts fly is 11 km[80] and high clouds are formed at ~5-13 km altitude.[81] As described below in section 1.7.2, InMAP uses a Concentration-Response function to estimate health impacts from the resulting pollutant concentration. The output from InMAP provides pollutant concentration ($\mu g/m^3$) and number of premature deaths from long-term $PM_{2.5}$ exposure for each grid cell, based on underlying gridded population and mortality data. Details of InMAP are given elsewhere.[78,82]

I also use the InMAP Source-Receptor Matrix (ISRM) in this work.[12,48,82] ISRM is a series of matrices that describe linear relationships among multiple emission and impact locations. ISRM is created by running separate InMAP simulations that estimate the ground-level changes in $PM_{2.5}$

concentrations from emissions of SO_x, NO_x, VOCs, NH_3, and primary $PM_{2.5}$ in each of ~50,000 InMAP grid cells. The ISRM consists of 52,411 grid cells (Figure 1.3). The maximum height of the source modeled in ISRM is 1000 m. To model heights greater than 1000 m, the original InMAP model is used.

Concentrations within grid cells are assumed to be uniform. Air quality modeling in this work does not consider amount of time exposed population spends in indoor or outdoor environments. The modeling assumption here is that populations are exposed to outdoor ambient concentrations at their home locations at all times.

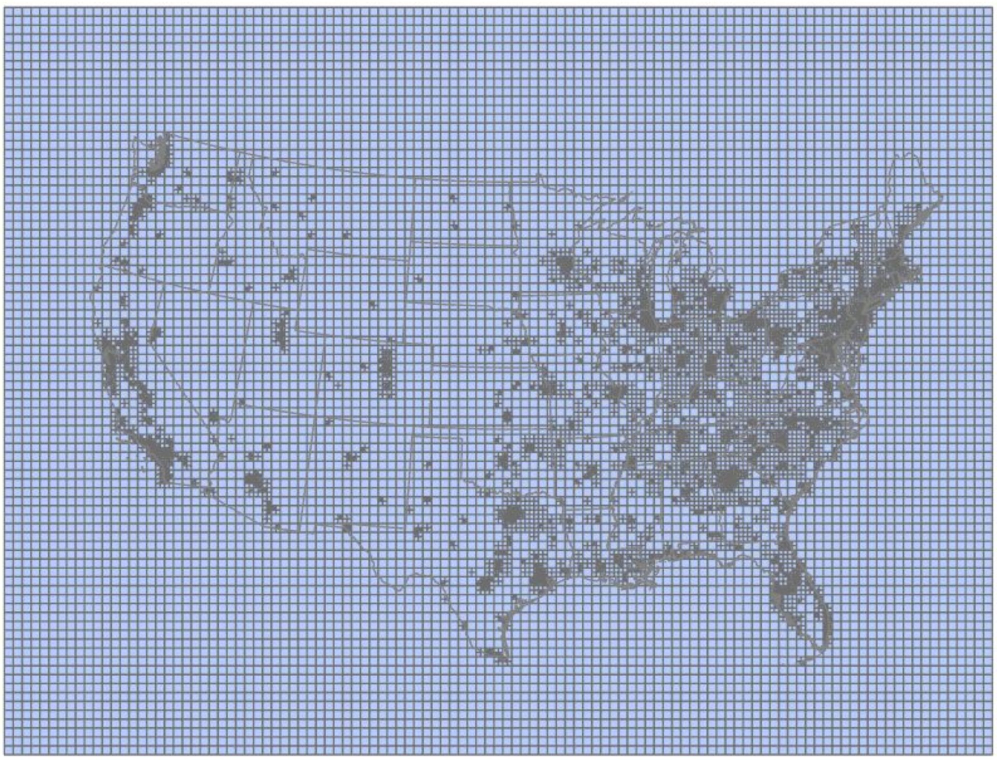

Figure 1.3 InMAP Source-Receptor Matrix (ISRM) grid

1.3.2 Concentration-Response (C-R) function

Consistent with prior research[83-85] and in keeping with EPA convention,[36,86,87] I assume that all particles are equally toxic in estimating health impacts from total $PM_{2.5}$. InMAP is capable of estimating health impacts from any user-defined C-R function. For this research, I employ the standard, commonly used expression in InMAP—from Krewski et al. (2009)[37]—for the $PM_{2.5}$ C-

R function, which is used to estimate $PM_{2.5}$-related health impacts as shown in Equation 1. The Krewski et al. (2009) equation is based on the standard Cox proportional-hazards model to calculate hazard ratios for various cause-of-death categories associated with the levels of air pollution exposure in the study cohort.[37] The default C-R equation in InMAP is a standard and is commonly used in regulatory[39] and academic air quality research.[40,41]

$$\text{Number of premature deaths} = \left(e^{(PM_{2.5}\ \text{Linear Coefficient} \times [PM_{2.5}])} - 1\right) \times P \times \frac{\text{All}-\text{Cause Mortality Rate}}{100{,}000}$$

(1)

Here, $PM_{2.5}$ Linear Coefficient = ln(1.078)/10 = 0.00751, i.e., a 7.8% increase in the number of premature deaths for every 10 μg/m^3 increase in the concentration of $PM_{2.5}$. [$PM_{2.5}$] is the concentration of $PM_{2.5}$. P is total population.

1.3.3 Main inputs to InMAP

The following are the three main inputs to InMAP for estimating health impacts of emissions from electricity and freight transportation sector:

(1) Annual emissions of VOCs, NO_x, NH_3, SO_2, and primary $PM_{2.5}$ as shapefiles. InMAP allocates emissions from shapefiles to the underlying grid cells using area weighting. Figure 1.4 provides example of locations of emission sources used in this dissertation.

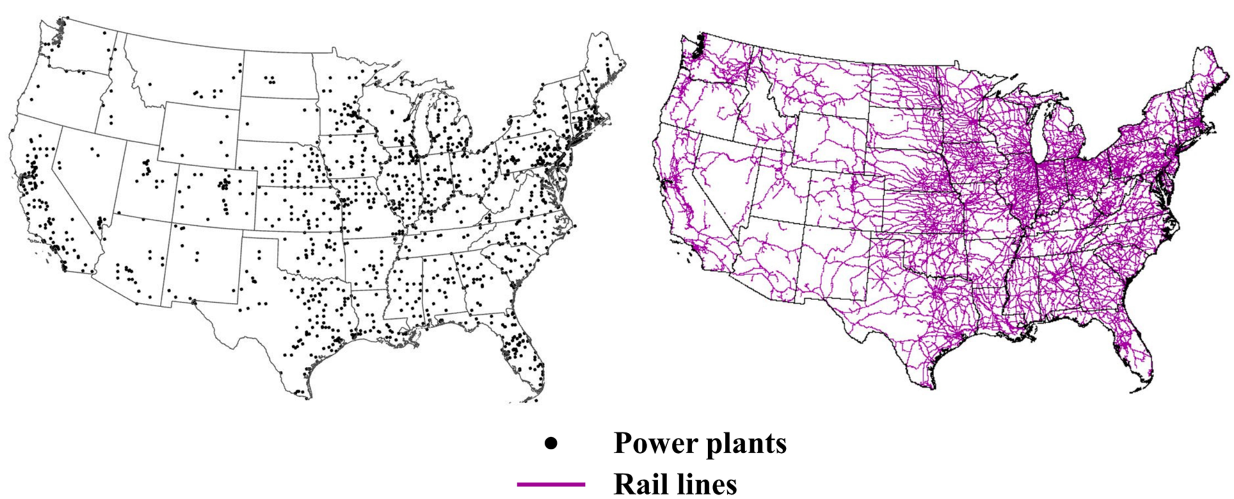

Figure 1.4 Examples of emission locations: power plants and rail lines

(2) Census data on population at the block group level from the American Community Survey (ACS).[88] Chapter 3 provides estimates for population of all age groups and Chapter 4 provides estimates for all age groups as well as for >35 years old. Figure 1.5 shows population estimates at the block group level for year 2016 using 2014-2018 ACS data.

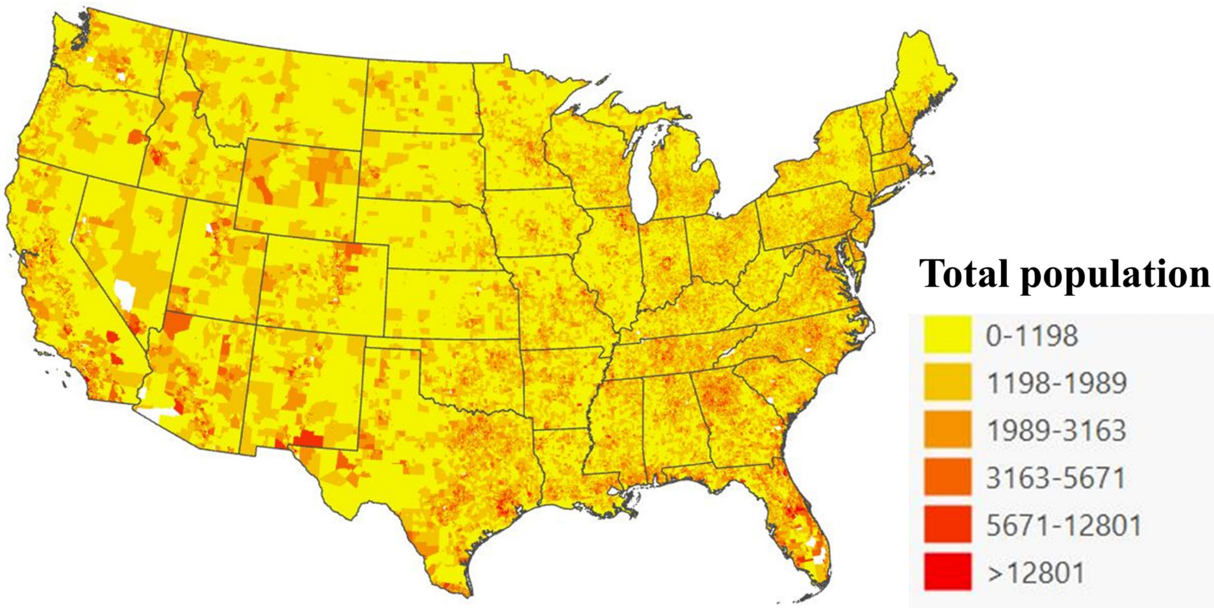

Figure 1.5 Total population for year 2016 at block group level from American Community Survey (ACS) data

(3) Baseline all-cause mortality data for all ages (and >35 years for chapter 4) at the county level from the National Center for Health Statistics Office of Analysis and Epidemiology at the Centers for Disease Control and Prevention (Figure 1.6).[89] Race-specific health impacts are calculated using all-cause mortality rates for the entire population of all age groups.

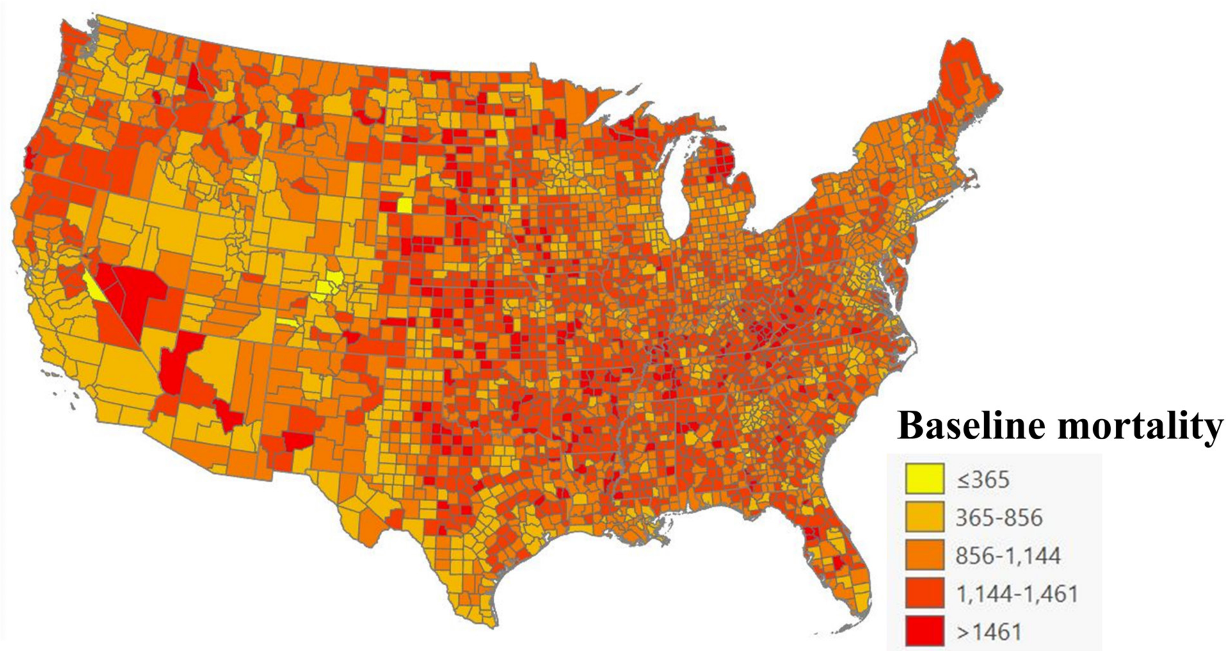

Figure 1.6 Baseline all-cause mortality data for all ages for year 2016

1.4 Structure

Chapter 2 uses the data-driven empirical approach using Ordinary Least Squares (OLS) linear regression. This chapter presents comparison between average emission factors and average marginal emission factors (AMEFs) for CO_2, NO_x, and SO_2 emissions from electricity generation in a coal-intensive U.S. power market (the "Midcontinent Independent System Operator (MISO)"). I perform this analysis at multiple spatial (all MISO; each of the 11 MISO states; each utility; each generator) and temporal scales (hour, day, month, and year). Using linear regression of hourly changes in generation and emissions, I estimate AEFs and AMEFs for CO_2, SO_2, and NO_x from fossil and non-fossil generators in the MISO region during years 2007−2016. This study uses hourly emissions and generation data from the Continuous Emissions Monitoring System (CEMS) database from the U.S. EPA.

Chapter 3 and **4** uses the mechanistic air quality modeling approach using Intervention Model for Air Pollution (InMAP). **Chapter 3** estimates exposures to and health impacts of $PM_{2.5}$ from electricity generation in the U.S., for each of the seven Regional Transmission Organizations

(RTOs), for each U.S. state, by income and by race. Using InMAP to model power plant emissions combined with a standard concentration-response function from Krewski et al. (2009), I estimate $PM_{2.5}$ concentrations and premature deaths at a fine spatial resolution across three geographical scales (U.S., RTO, State) by race and income. This study uses annual emissions data from the U.S. EPA's 2014 National Emission Inventory (NEI). **Chapter 4** explores health and climate impacts and exposure disparity among racial-ethnic groups from inter-state road, rail, water, and air freight transportation in the U.S. by mode, route, and emission species. Using InMAP, I estimate $PM_{2.5}$ concentrations and premature deaths for transporting 1 megaton of freight by heavy-duty truck, freight rail, barge, or aircraft, for each origin-destination pair. This study uses emission factors for each mode from the Greenhouse Gases, Regulated Emissions, and Energy Use in Transportation (GREET) model and tonnage data from the U.S. Department of Transportation (U.S. DOT)'s Freight Analysis Framework (FAF) data.

I present results in this dissertation through several metrics. Table 1.2 provides a summary of metrics identified and used in this work.

Table 1.2 Summary of metrics

Chapter	Metrics identified	Parameters	Description	Spatial scale
Chapter 2	Average marginal emission factor (AMEF) $= \frac{\Delta E_j}{\Delta G_j}$	ΔE = Change is system emissions at time interval j; ΔG = Change in system generation at interval j	Represents average change in emissions per unit increment in electricity generation from generators on the margin.	MISO, State, Utility, Generator
	Average emission factor (AEF) $= \frac{E}{G}$	E = Total sum of system emissions; G = Total sum of system generation	Represents average emissions per unit electricity generated in the system.	MISO, State, Utlility, Generator
Chapter 3	Total premature deaths = Sum of deaths in each InMAP grid cell		Represents total $PM_{2.5}$-related premature deaths from electricity generation using	Nation, RTO, State

			linear, non-threshold C-R function	
	Deaths per 100,000 people = $\frac{\text{Number of premature deaths}}{\text{Population}} \times 100{,}000$.		Represents health risk as normalized premature deaths per 100,000 people from electricity generation	Nation, RTO, State
	Deaths per unit electricity generation = $\frac{\text{Number of premature deaths}}{\text{Total generation (TWh)}}$		Represents average deaths per unit electricity generation	Nation, RTO, State
	Risk gap = Deaths per 100,000 people for most exposed group – Deaths per 100,000 people for least exposed group		Represents exposure disparity among racial-ethnic groups from electricity generation	State
	Population weighted average $PM_{2.5}$ concentration = $\frac{\sum_{i=1}^{n} P_i [PM_{2.5}]_i}{\sum_{i=1}^{n} P_i}$	P_i = Population in grid cell i $[PM_{2.5}]_i$ = $PM_{2.5}$ concentration in grid cell i n = total number of grid cells	Represents population-weighted average $PM_{2.5}$ concentration from electricity generation	Nation, RTO, State
Chapter 4	Deaths per megaton = sum of deaths in each ISRM grid cell		Represents total $PM_{2.5}$-related premature deaths per megaton from freight transportation using linear, non-threshold C-R function	Nation, Mode, Origin-destination (O-D) pair
	CO_2 emissions per megaton = CO_2 EF × Length of route	CO_2 EF = CO_2 Emission factor (kg/megaton-mile or kg per megaton)	Represents total CO_2 emissions from freight transportation	Nation, Mode, O-D pair
	Deaths per 100,000 people per megaton = $\frac{\text{Number of premature deaths}}{\text{Population}} \times 100{,}000$		Represents health risk as normalized premature deaths per 100,000 people from freight transportation	Nation, Mode, O-D pair

	Total deaths	Total deaths = Deaths per megaton × Tonnage	Represents total deaths from freight transportation	Nation, Mode, O-D pair
	Risk gap = Deaths per 100,000 people for most exposed group – Deaths per 100,000 people for total population		Represents exposure disparity among racial-ethnic groups from freight transportation	Mode, O-D pair
	$Z_{SA} = \frac{SA1}{SA2}$	SA1 = Simple average deaths or CO_2 emissions or risk gap per megaton from mode 1 SA2 = Simple average deaths or CO_2 emissions or risk gap per megaton from mode 2	Represents ratio of simple average of two modes. If $Z_{SA} > 1$, mode 1 has greater health or climate impacts per megaton than mode 2. This metric provides flexibility for use in future scenarios.	Mode combination (e.g. Rail [mode 1] and Truck [mode 2])
	$Z_{WA} = \frac{WA1}{WA2}$	WA1 = Tonnage-weighted average deaths or CO_2 emissions or risk gap per megaton from mode 1 WA2 = Tonnage-weighted average deaths or CO_2 emissions or risk gap per megaton from mode 2	Represents ratio of tonnage-weighted average of two modes. If $Z_{WA} > 1$, mode 1 has greater health or climate impacts per megaton than mode 2. Z_{WA} is tonnage weighted while Z_{SA} is the simple (i.e., unweighted) average. This metric reflects the current situation.	Mode combination (e.g. Rail [mode 1] and Truck [mode 2])
	Population weighted average $PM_{2.5}$ concentration = $\frac{\sum_{i=1}^{n} P_i [PM_{2.5}]_i}{\sum_{i=1}^{n} P_i}$	P_i = Population in grid cell i $[PM_{2.5}]_i$ = $PM_{2.5}$ concentration in grid cell i n = total number of grid cells	Population weighted $PM_{2.5}$ concentration from freight transportation	Nation, Mode, O-D pair

Chapter 2

Marginal Emissions Factors for Electricity Generation in the Midcontinent ISO

2.1 Abstract

Environmental consequences of electricity generation are often determined using average emission factors. However, as different interventions are incrementally pursued in electricity systems, the resulting marginal change in emissions may differ from what one would predict based on system-average conditions. Here, I estimate average emission factors and marginal emission factors for CO_2, SO_2, and NO_x from fossil and non-fossil generators in the Midcontinent Independent System Operator (MISO) region during years 2007 – 2016. I analyze multiple spatial scales (all MISO; each of the 11 MISO states; each utility; each generator) and use MISO data to characterize differences between the two emission factors (average; marginal). I also explore temporal trends in emissions factors by hour, day, month, and year, as well as the differences that arise from including only fossil generators versus total generation. I find, for example, that marginal emission factors are generally higher during late-night and early morning compared to afternoons. Overall, in MISO, average emission factors are generally higher than marginal estimates (typical difference: ~20%). This means that the true environmental benefit of an energy efficiency program may be ~20% smaller than anticipated if one were to use average emissions factors. This analysis can usefully be extended to other regions to support effective near-term technical, policy and investment decisions based on marginal rather than only average emission factors.

2.2 Introduction

In the United States, electricity generation is a major contributor to air pollution, with important consequences for health, the environment, and climate. The U.S. Environmental Protection Agency (EPA) estimates that in 2014, electricity generating units (EGUs) contributed 37% of CO_2, 67% of SO_2, 13% of NO_x, and 3% of primary $PM_{2.5}$ nation-wide emissions.[1,2] SO_x and NO_x emissions from EGUs contribute to secondary $PM_{2.5}$ formation, adding to the health and environmental consequences of EGUs. In 2014, coal-fired EGUs alone generated ~39% of the electricity in the U.S., and contributed to 77%, 97%, 86%, and 81%, respectively, of CO_2, SO_2, NO_x and $PM_{2.5}$ total electricity emissions.[1,3] Those pollutants contribute to acid rain, climate change, regional haze, crop damage, and health impacts from ambient air pollution.[4]

There are multiple approaches to estimating power plant emissions.[5] Different methods and data sources can generate substantially different estimates --- an important consideration for environmental policy. A simple and straightforward approach is to calculate average emissions factors (EFs) for a region and time-frame as the ratio between total emissions and total electricity generated. Another approach is to model marginal EFs based on bid-dispatch simulations of electricity generators;[6-11] such models use costs and engineering constraints to predict which EGU would increase/decrease output if the total energy demand at that time were marginally higher/lower. The degree of sophistication of these models varies. Models such as Integrated Planning Model (IPM), PROMOD, Electric Generation Expansion Analysis System (EGEAS) and PLEXOS are proprietary, complex, often provide little flexibility, and are time consuming to run; they require substantial input data, and like any model depend on assumptions and simplifications necessary to simulate a complex system.[12-16] Other approaches include the Fuel Type Assumed (FTA) method, Locational Marginal Price (LMP) based approaches and machine learning algorithms.[17-20] Here, I use an empirical approach for estimating average EF (AEF) and average marginal EF (AMEF). My approach, which was described in Siler-Evans *et al*. (2012),[21] is distinct in using data (historical observations) rather than models to estimate marginal EFs. The approach of using historical data has been applied in other studies as well.[22-25] EFs calculated using historical data are most appropriate for short to medium term analysis in electricity system, and are less appropriate for long term predictions for which fundamental aspects of the electricity system (e.g., fuel mix; infrastructure) may shift. Several applications of marginal emissions and impact factors have been used to determine the emissions saving and damage reductions associated with interventions in the electricity sector, such as solar and wind,[26,27] energy efficient buildings,[28,29] storage,[30] and vehicle charging,[31,32] and wastewater treatment from coal power plants.[33]

While several studies have investigated average and marginal EF[7-9,19,21,34,35], only one prior study has implemented the empirical approach employed here: Siler-Evans *et al*. (2012)[21] calculated AEF and AMEFs for the U.S. electricity system and for the eight North American Electric Reliability Corporation (NERC) regions. Those authors recommend that the method be applied to Regional Transmission Organizations (RTOs) rather than NERC regions, since RTOs provide a better representation of electricity dispatch; my approach follows that suggestion. I build on the Siler-Evans *et al.* (2012)[21] research, extending it in several ways: (1) I focus on an RTO rather than NERC regions. RTOs use bid-based markets to determine economic dispatch, and so are an appropriate scale for my analyses. (2) Siler-Evans *et al.* (2012)[21] consider fossil generation as proxy for total generation. That aspect is a limitation of their approach; with increasing amounts of renewables in the grid, renewables may be at the margin for some hours or levels of demand. I instead use total MISO generation (rather than fossil-only generation) when calculating EFs. (3) By focusing on a single RTO, I was able to assess with greater detail EFs's variability in time and space, thereby lending new insights into the environmental impacts of electricity generation. (4) I explore how EFs may vary by state, corporation, fuel-type, and EGU.

Average versus marginal EFs may differ for many reasons. In general, at a given time, the mix of fuels for the EGUs at the margin --- i.e., the last few units that will meet demand --- may differ from the average electricity mix in that hour. Furthermore, for a single EGU, AEF and AMEF may differ because the boiler is ramping up or down, or because the efficiency of emission control technologies may depend on the EGU's power output.

The results for MISO, years 2007-2013, reveal that AMEFs are often lower than the respective AEFs. The consequences of this finding for policy includes, for example, that the true emission reduction attributable to an energy efficiency program may be lower than the one a decision maker would assume using AEFs. Similarly, this result would indicate that an efficiency program may be less cost-effective than anticipated (since cost-effectiveness metrics are often computed as the ratio between the cost of the program and the emissions saved).

2.3 Methods and data

Here, I employ an empirical approach for estimating AEF and AMEF for the Midcontinent Independent System Operator (MISO). MISO is one of the seven U.S. RTOs. MISO includes 15 US states and serves ~42 million people (13% of U.S. population). In 2015, MISO included 176,600 MW of electric capacity, generating ~667,800 GWh (~16% of U.S. total electricity generation). In the Supplemental Information (SI), I provide the generation statistics for MISO for years 2007 through 2016 (Figure A1).

The geography of MISO changed in 2014: prior to 2014, MISO constituted 11 upper Midwest states and was called “Midwest ISO”. In 2014, a south region (4 additional states; see maps in Figure A2) was integrated to form “Midcontinent ISO”. For geographic consistency, most results presented here are only for years 2007–2013; that approach provides an assessment that includes well defined and consistent regional boundaries. Results for years 2014-2016, which include EGUs in the new regional boundaries, are in section 1 of the SI (Figure A3 and Table A1).

I use emission data from the Continuous Emissions Monitoring System (CEMS) database from the U.S. EPA.[36] CEMS provides hourly emissions of CO_2, SO_2, and NO_x, and energy generation for generators with nameplate capacity of 25 MW or larger. I complement this information with MISO databases that provide hourly imports, exports, total actual load, and wind generation.[37] Net imports account for ~6% of the total demand in MISO. The share for “other” generation sources (nuclear, hydroelectricity, and other renewable generation) is calculated by subtracting fossil and wind generation from total generation.

I calculate two EFs for a given time period or geography: AEFs and AMEFs. AEFs are the summation of hourly emissions (E_T) divided by the summation of hourly generation (G_T) for that time period and geography.

Marginal EFs vary by time and geography; AMEF represents the average of the marginal EF for a certain time period and over some spatial extent. AMEF are computed by calculating the hourly change in emissions (ΔE) and change in generation (ΔG), for each time step. Then, a linear regression is fitted to identify the relationship between those two variables (the change in emissions and in generation). The slope of linear regression (β_o) between those two values is the AMEF.

In addition to estimating AEF and AMEF for MISO during 2007 - 2016, I also investigate spatial and temporal variability in EFs at multiple temporal and spatial scales. I do so for the following scenarios: the 11 Midwest states in MISO; all corporations owning one or more generators in a case-study state (Minnesota) and, as a separate analysis, in the entire MISO (in SI); and, at the level of individual EGUs. I also estimate AEFs and AMEFs by fuel type, for coal and for natural gas, to understand the average marginal response of fuel-specific generators to changes in system demand. In general, I employ total generation when estimating AEFs and AMEFs. One exception, caused by limited data availability, is that state and utility-level EFs include fossil-only generation as a proxy for total generation. Net imports are subtracted from MISO total load to obtain net generation. Electricity exchanges and trading at the state and utility scales are not considered here because they are tracked and available only at the RTO level. Fuel specific AMEFs are calculated by aggregating emissions by fuel type at each time step and performing regression between change in fuel specific emissions and change in total generation. For each EGU bidding in the MISO grid, I calculate AMEFs via regression between unit specific hourly emissions and gross generation output. Coal and natural gas EGUs constitute most of the units that bid in MISO and hence are a focus of this analysis.

I also explore trends in AEFs and AMEFs in the MISO region as a function of total system demand. To do so, I bin the data from years 2007 through 2013 into 20 demand level bins. Each bin contains 5% of the data occurring at lowest to highest system demand hours. Separate regressions of ΔFuel Generation vs ΔTotal Generation are then performed for each bin. I also analyze trends in AEFs and AMEFs temporally by time-of-day, day-of-week, month and year (for years 2007 to 2016). To assess the differences between AEF and AMEF, I calculate their relative difference as:

$$\% \text{ difference} = \left(\frac{\text{AMEF}-\text{AEF}}{\text{AEF}}\right) * 100$$

2.4 Results

2.4.1 Comparison of AEF and AMEFs

Emissions estimates for MISO. Figure 1 presents data for years 2007 – 2013. Each data-point is an hourly change in MISO total pollutant emissions and power generation. The slope of the best-fit line is the AMEF. Figure 1 also displays the median data-point (red icon), the IQR ellipse (centered at the median data-point, displaying 25th and 75th percentiles parallel and perpendicular to the best-fit line; yellow ellipse), and the P10-P90 ellipse (centered at the median data-point, displaying 10th and 90th percentiles parallel and perpendicular to the best-fit line; dashed line). As expected, for data in Figure 1, ~25% of the data-points are inside the IQR ellipse, ~60% are inside the P10-P90 ellipse.

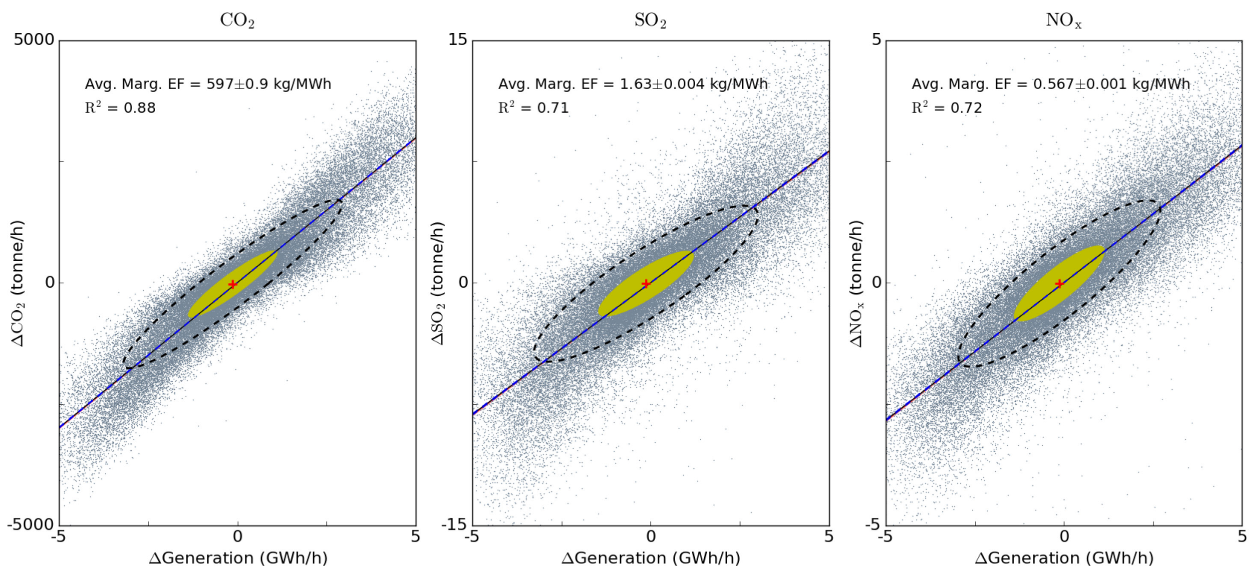

Figure 2.1 Linear regression for hourly changes in power generation and pollutant emissions, for Midcontinent ISO, years 2007 to 2013. Each dot represents a one-hour difference. I also show the median value (red icon), the interquartile (yellow) and P10-P90 ellipse (dashed line), the best-fit line (black line), and 95% confidence intervals on the best-fit line (dashed blue lines, nearly indistinguishable from the best-fit line).

Table 1 summarizes the results displayed in Figure 1. Figure A3 and Table A1 provides the results for years 2014-2016 (i.e., after the change in geography). Overall, and among pollutants, I find that AEFs are 17%-22% higher than the respective AMEF. This general pattern holds across pollutants and years (see Table A2).

For comparison, I also computed these estimates when including only fossil generation (which was the approach taken in Siler-Evans *et al*. (2012)[21]). When doing so, I find that the differences between EFs remain consistent (AMEFs 15%-19% lower than the respective AEF), but the AEFs are ~22% greater and AMEFs are ~27% greater than their values calculated using change in total generation.

I also estimate AEFs and AMEFs by fuel type, which I report in the SI, Tables S3, S4, and S5. I find that relative to other fuels, the AMEFs from coal-fired generators are generally closer to emission factors for entire MISO region. This result is likely because the average share of marginal generation from the coal fleet is greater than the natural gas fleet (~57% coal vs ~21%). For emissions from coal generators only, the AEF is 28% [CO_2], 18% [SO_2], and 27% [NO_x] larger than AMEF. For natural gas generators only, the AEF is 274% [CO_2], 78% [SO_2], and 182% [NO_x] lower than AMEF.

Table 2.1 Comparison between AEF and AMEF estimates for the MISO region using data from 2007 to 2013.

Pollutant	AEF (Kg/MWh)	AMEF (Kg/MWh)	EFs % Difference
CO_2	739	597	-19%
SO_2	1.97	1.63	-17%
NO_x	0.727	0.567	-22%

State emissions estimates. State Implementation Plans (SIPs) often require an accurate metric to assess emission benefits from different energy efficiency strategies. I have calculated AEF and AMEF for the state boundaries within MISO, as shown in Figure 2. For this portion of the analysis, I rely on total fossil generation when computing the emissions factors because there is no total generation data by state at the hourly level. For each state, this analysis considers only emissions and generation occurring within that state. I find that in most cases, AMEFs are lower than AEFs (which is consistent with results given above). Differences between AEF and AMEF are larger for states that have a large portion of their generation provided by natural gas (see Figure A4); not surprisingly, natural gas tends to be more on the margin in those states. Correlation between CO_2 AMEF, SO_2 AMEF and NO_x AMEF is shown in Figure A5.

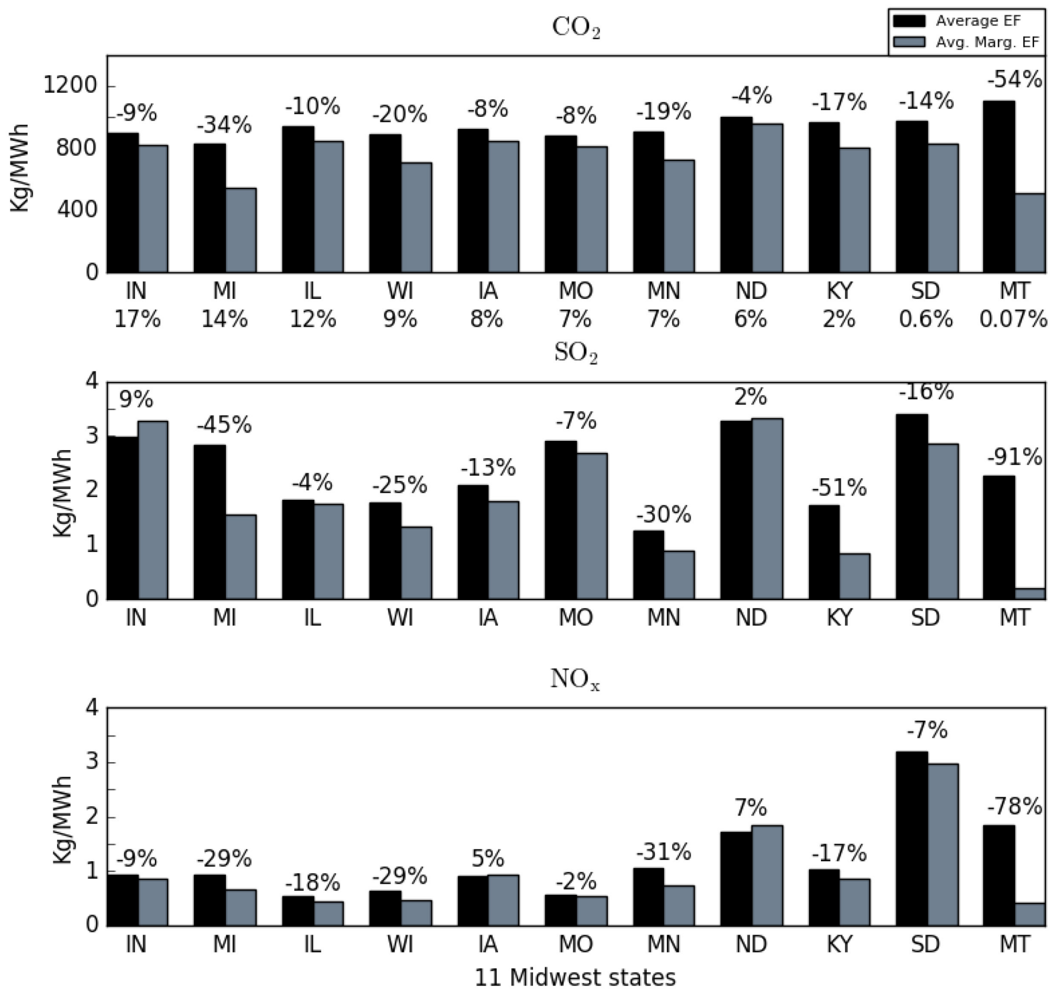

Figure 2.2 AEF and AMEF by state for CO_2, SO_2 and NO_x for years 2007–2013. The percentages reported show the relative difference between AEF and AMEF (positive values mean AMEF>AEF). States are displayed from highest to lowest electricity generation share of MISO's total generation. The electricity generation share for each state is shown along the x-axis for the CO_2 plot. In combination, fossil generation from these states accounted for 82% of MISO total generation.

Utility level estimates: I compute separate EFs for utilities that operate in MISO. At the utility scale, AEFs and AMEFs are important as they may be used to inform utilities' strategies to reduce their emissions (for example, on decisions of how to allocate emission allowances under cap & trade programs, or for monitoring and evaluation of climate mitigation or other emission reduction programs). Here, as a case-study, I calculate AEF and AMEF for utilities operating generators in Minnesota in year 2012. Differences between AEF and AMEFs for all utilities bidding in MISO in the year 2012 are presented in Figure A6. Minnesota's emission reduction goals include a 40% reduction in CO_2 emission rate; I use year 2012 as an illustrative example given that it was the baseline year for US EPA's former Clean Power Plan rule. Here too, owing to limitations in data availability, I employ the approach from Siler-Evans, and use total fossil generation instead of total generation. In Figure 3, I provide the resulting estimates for each utility operating generators in Minnesota. In this figure, the Minnesota Municipal Power Agency is atypical in that it has slightly negative AMEF for NO_x. It has the only must-run combined cycle natural gas unit with a large nameplate capacity (334.5 MW) and with installed NO_x control equipment. Non-linear emission changes attributable to shifting usage of NO_x control equipment could explain the negative AMEF for NO_x.

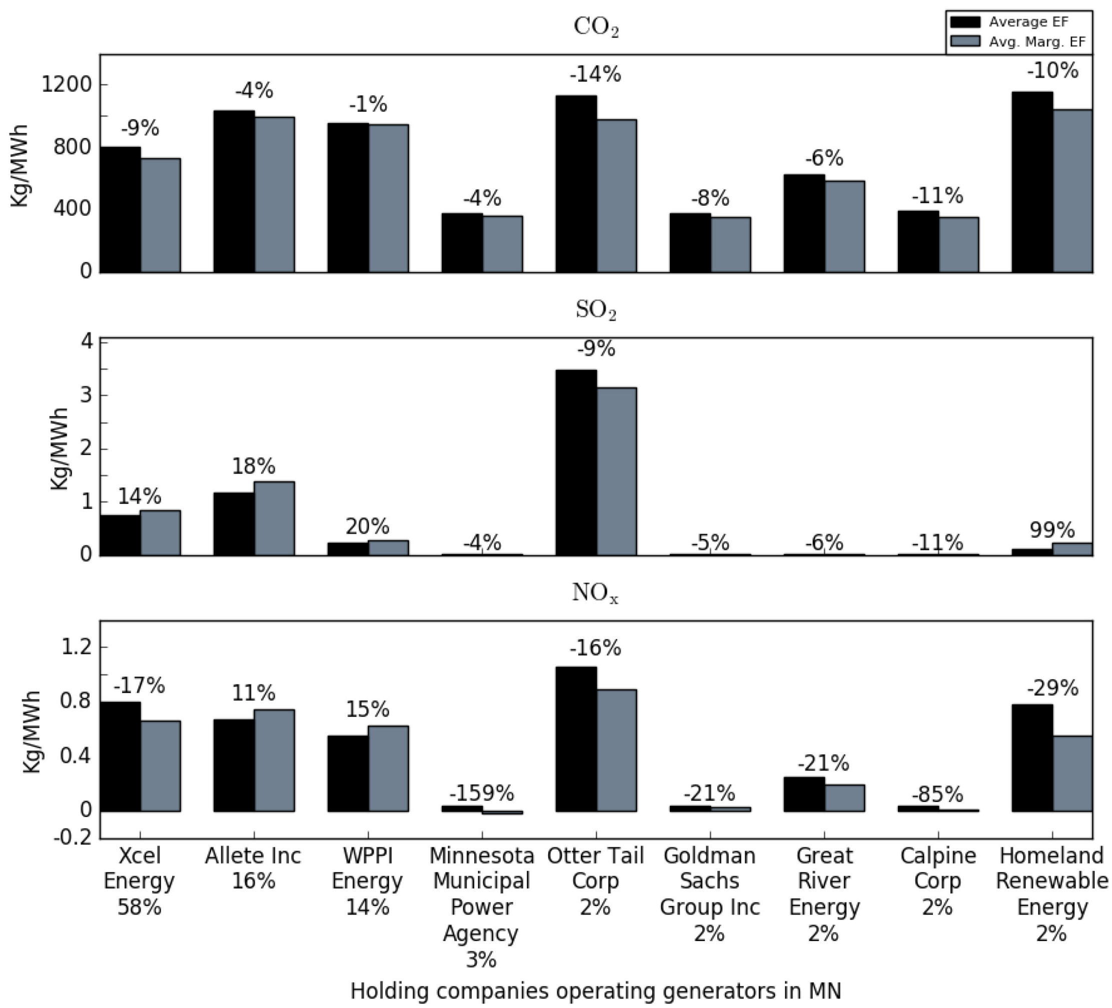

Figure 2.3 AEFs and AMEFs for utilities operating EGUs in Minnesota in 2012 that have a generation share > 1%. The percentages inside the figure represent the relative difference between

AEF and AMEF (positive values indicate AMEF>AEF). X-axis percentages (e.g., 58% for Xcel Energy) indicate percentage generation share of Minnesota's total generation; utilities are listed in order of that percentage.

Generator level analysis: I calculate AEF and AMEF for each generator bidding in MISO during years 2007 to 2013, which are shown in Figure 4. Over this time period, on average, 273 natural gas generators and 219 coal generators bid into MISO each year. In most cases, I find (consistent with results given above,) that AMEFs are smaller than AEFs: median differences between AEFs and AMEFs for coal are -4.9% for CO_2, -0.1% for SO_2, and -3.3% for NO_x; for natural gas, median differences are -6.3% for CO_2, -5.5% for SO_2 and -10.0% for NO_x. The AMEF-AEF percent difference is less than -20% (i.e., is more-negative than -20%) for CO_2 for 5% of coal generators and 6% of natural gas generators, for SO_2 for 7% (coal) and 10% (natural gas) generators, and for NO_x for 27% (coal) and 29% (natural gas) generators. Those results emphasize that there can be noteworthy differences between AEF and AMEF estimates when applied at the generator level.

On average, I find that AMEF-AEF differences are larger for SO_2 and NO_x than for CO_2 and are larger for coal than for natural gas. This result may reflect the nature of SO_2 and NO_x emission control equipment. Further analysis (see SI, section 4) reveals that for coal generators, the AEF and AMEF difference for CO_2 is larger for smaller generators than for larger generators (Figures S11 & S13). However, the reverse holds for natural gas (Figures S12 & S14). This observation likely reflects generator characteristics such as heat rate, capacity factor and age (Figure A15). An explanation for the coal units could be that old smaller (i.e., low capacity factor) units run at higher heat rates compared to their design heat rates, whereas new larger units (high capacity factor) typically run at heat rates at or below their design heat rates. As generators age, their heat rates degrade and the smaller units tend to cycle and follow load more. Hence, coal units with low capacity factors have higher AEF, and the larger difference between metrics. Additionally, EFs seem to be inversely correlated with share of electricity (see Figures S16 and S17), suggesting that share of electricity is greater for lower EF units than for higher EF units.

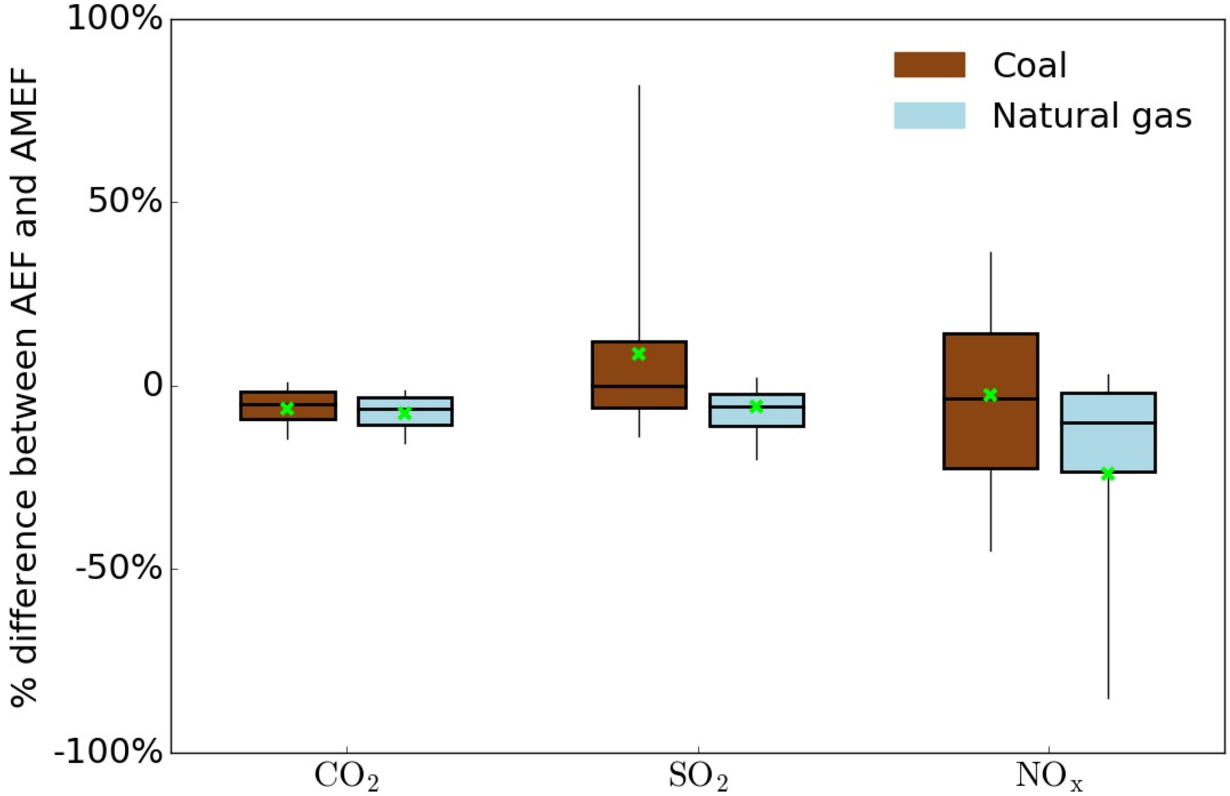

Figure 2.4 Boxplot showing distribution of EF differences among coal units (n=219, average per year, 2007-2013) and natural gas units (n=273 on average).

2.4.2 AEFs and AMEFs by system demand

In Figure 5 (A and B), I show the share of average and average marginal fuel source with respect to total generation in MISO. Coal is the dominant marginal fuel at low demand hours; natural gas is the dominant marginal fuel at high demand hours. The share of other fossil fuels to marginal generation is minor. Nuclear is generally not on the margin (which is consistent with output being ~constant and/or with changes in output being relatively uncorrelated with changes in demand). The share of generation from wind is greater during low demand hours (since wind blows significantly during night in the Midwest) than high demand hours, and the marginal generation from wind is negative (i.e., on average, wind generation decreases in hours when system total generation increases) during low demand hours. Two possible reasons for negative marginal generation could be: (1) load curtailment or (2) a decrease in generation because of less wind. I do not have hourly curtailment data needed to rigorously investigate the reason behind negative marginal generation. However, curtailment appears not to be a large issue for MISO: a U.S. Department of Energy report[38] estimates wind curtailment in MISO at <6% of potential wind energy generation. Curtailment was a larger issue for some other grids, notably the ERCOT grid, which experienced >15% curtailment in 2009 (but steps taken to address the issue reduced wind curtailment, to only 1% in 2015). Recent MISO programs have strived to make wind dispatchable like other fuels via, e.g., the Dispatchable Intermittent Resources program.[39,40]

Parts C and D of Figure 5 shows how AEF and AMEFs for CO_2, SO_2 and NO_x vary with MISO total generation. NO_x AMEF is relatively constant across demand. Figure A18 shows similar plot for year 2008 (wind data for year 2007 is not available) and 2013 for comparison; there is not much change in marginal generation from coal over the course of 6 years, and average share of wind has increased but its contribution to marginal load decreased substantially in the year 2013.

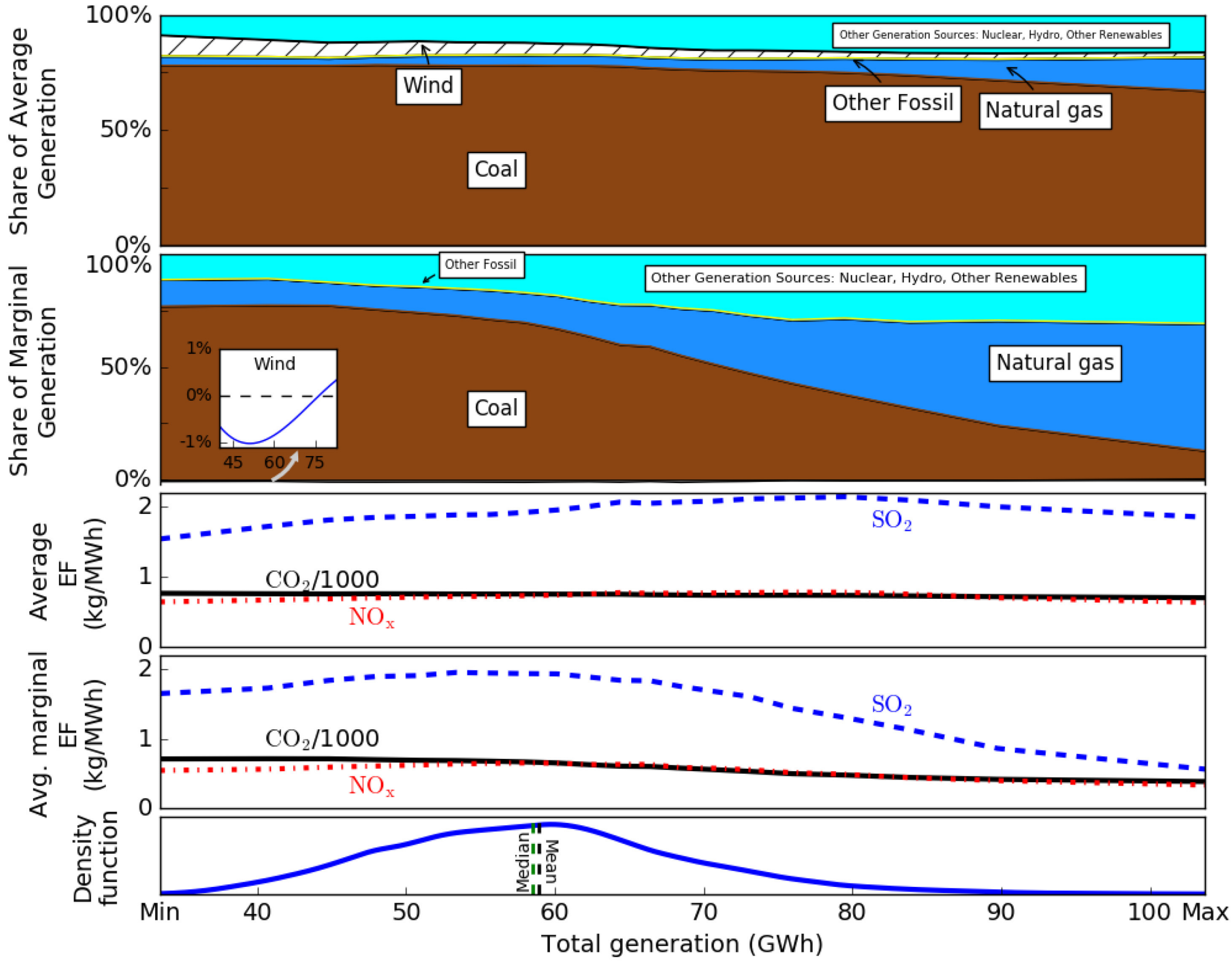

Figure 2.5 (A) Average generation by fuel. (B) Average marginal generation by fuel. (C) AEFs as a function of total generation (D) AMEFs as a function of total generation. (E) Kernel density distribution for total generation. All results are for MISO, for all data-points during years 2007–2013.

2.4.3 Temporal analysis

I explore variation of AMEFs (and AEF; Figure A19) by time of day, days of week, month and year (Figure 6). AMEF are higher-than-average during late-night and early morning hours when electricity demand is lower and coal is more often on the margin: AMEF is about 73% [CO_2], 125% [SO_2], and 55% [NO_x] higher at midnight compared to noon. The AMEFs are higher on the weekends compared to weekdays. AMEFs are highest in spring and fall, when demand is low and coal is more often on the margin. Time-of-day trends are more pronounced in summer (Figure

A20). Fuel-specific AEF and AMEFs by time-of-day are in Figure A21 and Table A6. From 2007 through 2013, AMEF for SO_2 decreased by 41%; changes were smaller for NO_x (26% decrease) and CO_2 (9% increase). From 2014-2016, AMEF for SO_2 decreased by 40%, NO_x decreased by 6% and CO_2 increased by 3%. Reduction in SO_2 and NO_x can be attributed in part to U.S. EPA regulations to reduce air pollution from the electricity sector. AEFs do not show pronounced variations by time of day, day of week and months (Figure A19). As seen in Figure 6, average MISO AMEFs were, for SO_2, lower after 2013 than before 2013; for CO_2, AMEFs were slightly higher after 2013 than before; for NO_x, they were mostly unchanged.

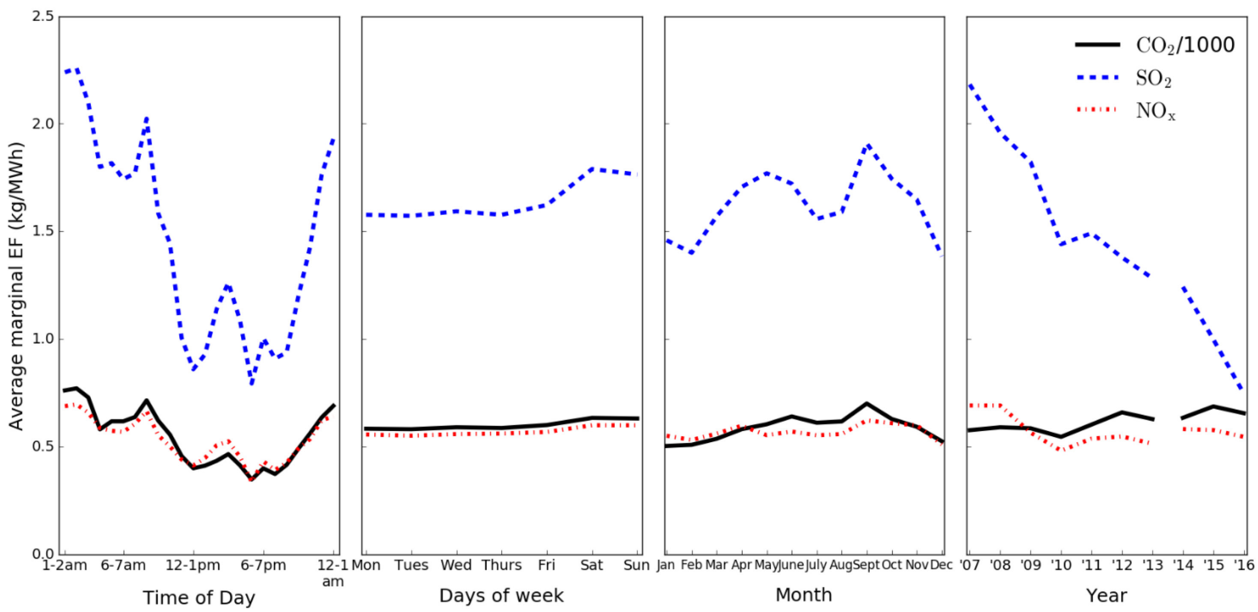

Figure 2.6 Time of day, days of week, and monthly trends in AMEFs for years 2007 through 2013. Yearly trends shown here for 2007 through 2016. The discontinuity in the yearly plot is to highlight the change of MISO geography after 2013.

2.5 Discussion and conclusions

I investigated differences between AEF and AMEFs at different spatial and temporal scales for MISO. In general, AEFs tend to overestimate emissions – and thus potential emissions benefits from interventions in the power sector - relative to AMEFs.

The deployment of renewable energy sources such as wind and solar will help reduce emissions by displacing energy from fossil-fired generators. However, if a decision-maker uses

AEF to understand the current contribution of renewables or other interventions in the electricity system, she will likely overestimate the emission benefits that are derived from such interventions. As noted above, for MISO, if emission-reduction benefits (e.g., from wind or solar generation, or from energy efficiency programs) are calculated using AEFs, the benefits are on average overestimated by 19% for CO_2, 17% for SO_2 and 22% for NO_x. Those values vary by time-of-day, fuel, company, and state. Results presented here could help energy efficiency programs become more cost-effective, for example, by consideration of how AMEF varies in time and space.

I show that AMEFs are higher during early morning and late evening hours – times of day when electricity demand is usually low and, historically for the Midwest, when wind energy is abundant. Further harnessing of the wind potential during these hours could provide substantial emission reductions and is of great importance for strategies such as Active Power Controls (APC)[41] for efficiently harnessing wind energy during those times. Further, following Siler Evans et al. (2012)[21], I calculated the daytime (8am – 5pm) and nighttime (7pm – 7am) AMEFs and compared them to system AMEF and AEF; I find that AEFs overestimate AMEFs by ~35% during daytime and by ~20% during nighttime (Table A7). For AMEF, differences between nighttime-average and daytime-average are ~14%.

This paper advances current understanding in a few key ways. I show that estimating recent AMEFs can be done using data rather than models. Siler Evans *et al*. (2012)[21] and Graff Zivin *et al*. (2014)[24] looked at the temporal and spatial differences between AEFs and AMEFs for NERC regions. I adopted Siler Evans' recommendation of focusing on RTOs, and in doing so uncovered important differences between AEF and AMEFs by time and geography (by state, corporation, and individual EGUs). In most cases, my analyses were based on total generation rather than using fossil generation as a proxy for total generation (exceptions include state and utility analyses, for which data limitations forced us to use fossil generation as a proxy for total generation). Electricity trading at the state and utility level could impact state and utility emission factor estimates,[42-44] but is not explicitly incorporated here.

Multiple methods exist for estimating AMEFs. My approach has the advantage of being based on empirical data rather than models. On the other hand, that means it may be inappropriate to use findings here unmodified if considering major shifts in the electricity infrastructure. Since results presented here are based on historical data, they likely would not be directly applicable for predicting long-term changes in the electricity grid.

Coal is frequently the marginal fuel source, especially during low-demand hours; it is not merely a base-load fuel that sits apart from marginal generation. In MISO, coal generators operate on margin and follow the load profile. In the future, if MISO continues to shift away from coal, that aspect could change.

Chapter 3

Fine Particulate Air Pollution from Electricity Generation in the US: Health Impacts by Race, Income, and Geography

3.1 Abstract

Electricity generation is a large contributor to fine particulate matter ($PM_{2.5}$) air pollution. However, the demographic distribution of its resulting exposure is largely unknown. I estimate exposures to and health impacts of $PM_{2.5}$ from electricity generation in the US, for each of the seven Regional Transmission Organizations (RTOs), for each US state, by income, and by race. I find that average exposures are highest for the Blacks, followed by Non-Latino Whites. Exposures for remaining groups (e.g., Asians, Native Americans, and Latinos) are somewhat lower. Disparities by race/ethnicity are observed for each income category, indicating that the racial/ethnic differences hold even after accounting for differences in income. Levels of disparity differ by state and RTO. Exposures are higher for lower-income than for higher-income, but disparities are larger by race than by income. Geographically, I observe large differences between where electricity is generated and where people experience the resulting $PM_{2.5}$ health consequences; some states are net exporters of health impacts, other are net importers. For 36 US states, most of the health impacts are attributable to emissions in other states. Most of the total impacts are attributable to coal rather than other fuels.

3.2 Introduction

Fine particulate matter ($PM_{2.5}$) is the largest environmental health risk in the United States (US) and globally.[1,2] $PM_{2.5}$ is associated with increased mortality rates from cardiovascular disease (ischemic heart disease and stroke), chronic obstructive pulmonary disease, and lung cancer.[3-5]

Fuel combustion emits $PM_{2.5}$ directly ("primary $PM_{2.5}$") as well as sulfur dioxide (SO_2) and oxides of nitrogen (NO_x), which can react with ammonia (NH_3) in the atmosphere to form $PM_{2.5}$ ("secondary $PM_{2.5}$").[6] The US Environmental Protection Agency (US EPA) estimates that in 2014, electricity generating units (EGUs) contributed 67% of SO_2, 13% of NO_x, and 3% of primary $PM_{2.5}$ emissions nation-wide.[7] In 2014, coal-fired EGUs generated ~39% of the electricity in the US, and contributed to 97%, 86%, and 81%, respectively, of SO_2, NO_x, and $PM_{2.5}$ total electricity emissions.[7] Although the health damages associated with these emissions continue to be important, EGU emissions have declined in recent decades[7,8] owing to environmental regulations[9] and a transition from coal to natural gas driven largely by market prices.

Existing estimates of annual $PM_{2.5}$-related mortality from EGUs in the US include the following: (i) for year 2005: 52,000 (Caiazzo et al. 2013),[10] 41,500 (Dedoussi et al. 2014),[11] 19,000 (Penn et al. 2017),[12] 38,000 (Fann et al. 2013);[13] (ii) for year 2010: 17,050 (Lelieveld et al. 2015);[14] (iii) for year 2014: 10,400 (Tessum et al. 2019);[15] and (iii) for year-2016 projected emissions: 17,000 (Fann et al. 2013).[13] Levy et al. (2009)[16] modeled the monetized damages associated with 407 coal-fired power plants in the United States. Buonocore et al. (2014)[17] estimated monetized health impacts of $PM_{2.5}$ from individual power plants and normalized to "per-ton emitted" using the Community Multiscale Air Quality (CMAQ) Model. Penn et al. (2017)[12] also quantified impacts from EGUs by state, finding 21,000 premature mortalities per year from EGU emissions ($PM_{2.5}$ and Ozone [O_3]). Mortality estimates vary among studies owing to differences in methods, models, concentration-response functions, and years considered (total EGU emissions are decreasing over time).

The consideration of how exposure to air pollution differs by demographic group is relevant to environmental justice (EJ).[18] Several studies have estimated health-impact disparities for air pollution from various source sectors,[19-27] but few studies have investigated EJ aspects of electricity generation in the US. Studying EGUs in the US, Levy et al. (2007)[28] quantified health benefits and the change in the spatial inequality of health risk for potential EGU pollution control strategies. They report 17,000–21,000 fewer premature deaths per year for hypothetical power-plant control scenarios in the US that aim to determine optimal control strategies. Martenies et al. (2017),[24] studying $PM_{2.5}$ health disparities in Detroit, Michigan, reported disproportionate burdens to Hispanics/Latinos owing to industrial emissions, and to low-income populations owing to traffic emissions. Tessum et al. (2019) reported that, while minorities are exposed to air pollution, they consume less and so therefore are less "responsible" for industry generating those emissions.[15] I are unaware of any prior national-scale investigation of EJ aspects of total $PM_{2.5}$ from electricity generation.

3.3 Materials and methods

I estimate $PM_{2.5}$-related health impacts from fossil-fuel fired EGUs at the national scale, for each Regional Transmission Organizations (RTO), and – in terms of emissions and impacts (i.e., as a source vs receptor for pollution) – for each US state. I use year 2014 as the reference year. I characterize impacts disaggregated by race and income.

US Regional Transmission Organizations (RTOs) are electricity power markets responsible for dispatching more than 60% of the net electricity generation in the US (eGRID 2014 & 2016).[29] The seven US RTOs are Midcontinent Independent System Operator (MISO), California Independent System Operator (CAISO), Electric Reliability Council of Texas (ERCOT), Southwest Power Pool (SPP), Pennsylvania-New Jersey-Maryland (PJM) Interconnection, New York Independent System Operator (NYISO), and New England Independent System Operator (NEISO). Coal intensity is greatest for MISO and SPP (>50% of generation comes from coal), followed by ERCOT and PJM (32% and 43%, respectively); the remaining RTOs (CAISO, NYISO, NEISO) are low-coal (<5%) (Figure B1; data from eGRID 2014).[29] RTO demographics (Table B1) also differ by region; CAISO and ERCOT have >50% Non-White population. I use RTOs as one of the units of analysis because they represent important geographic regions for electricity generation; they generally carry out electricity dispatch, which strongly impacts fuel-use and emissions; and, they typically operate and make decisions independently.[30]

Multiple air quality models are used in regulatory and research communities to link emissions with ambient concentrations, each with strengths and weaknesses.[17,31-53] Chemical Transport Models (CTMs) represent a state-of-the-science understanding of atmospheric chemistry and physics; they provide the most robust estimates available (i.e., the most robust representation of chemistry and physics) when time and computational constraints are not limiting.[49-53] CTMs are time and resource intensive. Reduced-complexity models (RCMs) are a less-intensive alternative.[17,31-48] RCMs are potentially less accurate than CTMs, but their reduced complexity allows for far greater number of runs, thereby opening the door to sensitivity analyses, Monte Carlo approaches, longer simulation duration, and new understandings of source-receptor relationships. The RCM employed here – the Intervention Model for Air Pollution (InMAP)[37] – employs smaller-sized grid cells than in conventional CTMs, thereby opening the door to the fine-scaled analysis generally thought to be important for EJ questions. Analyses carried out here would not be feasible using a conventional CTM, with current computational capacity. Other studies have demonstrated that InMAP and other RCMs can answer questions that could not be modeled using conventional CTMs.[28, 54-58]

Details of InMAP, including model design, operation, and validation, are available elsewhere.[37,59] Briefly, InMAP is an Eulerian grid model that predicts the change in annual-average $PM_{2.5}$ concentration attributable to a change in annual emissions, based on steady-state solutions to equations representing pollution emission, transport, transformation, and removal. InMAP's representation of chemistry and meteorology is simplified relative to a conventional CTM, but it incorporates spatially-varying parameters (e.g., rate constants) that are obtained from a CTM simulation. InMAP reflects the spatially-varying rates of formation of $PM_{2.5}$, based on the (spatially-varying) chemistry of the atmosphere (i.e., based on a CTM and a baseline [all-sources] emission inventory – here, the WRF-Chem model coupled with the National Emission Inventory [NEI]). Model runs carried out here focus only on emissions, concentrations, and health impacts from EGUs. The grid cell size in InMAP varies from 1 km × 1 km (typically in urban areas) to 48 km × 48 km (typically in rural areas), depending on the gradient in population density and pollutant concentrations. As configured here, InMAP also incorporates information about population, demographics, and concentration-response functions; I therefore use it to estimate concentrations and health impacts from EGU-attributable $PM_{2.5}$. Specifically, InMAP output for each grid cell includes annual-average $PM_{2.5}$ concentration ($\mu g/m^3$), number of premature deaths by race and household income category, population size, and baseline mortality.

For research questions considered here, InMAP requires three main inputs:

(1) Annual emissions of VOC, NO_x, NH_3, SO_2, and Primary $PM_{2.5}$ for each EGU; I employ US EPA's 2014 National Emission Inventory (NEI).[7] For point sources such as the EGUs, the NEI provides stack attributes including height, diameter, temperature, and exit velocity.

(2) Census data on population (by block group) and household income (tract) for 2014 from the 2014 American Community Survey (ACS).[60] Demographic groups given in the ACS are self-reported White Non-Latino, White Latino, Black Non-Latino, Black Latino, Asian Latino, Asian Non-Latino, Native American Non-Latino, Native American Latino, mixed/other Non-Latino, and mixed/other Latino. In my summaries, "Non-White" refers to all categories except White Non-Latino; "Black", "Asian", and "Native American" include both Latino and Non-Latino ethnicities. "Latino" refers to White Latinos, Black Latinos, Asian Latinos, Native American Latinos, and mixed/other Latinos (according to the Census, Latinos are 65% White, 31% mixed/other, 2% Black, 1% Native American, and 0.3% Asian). Census income data are divided into 16 income groups for each of six racial categories: White Non-Latino, White Latino, Black, Asian, Native American, and mixed/other race groups. Therefore, following the Census data, my summaries present income-based results for "White Latino" category and not all "Latinos". I calculate the percentage of households in each income category in a given census tract and apply those percentages to population counts at the block group level (matching census tracts to the block groups that they contain) to calculate an estimate of people in each income group.

(3) Baseline all-cause mortality data are for year 2014 from the National Center for Health Statistics (NCHS) Office of Analysis and Epidemiology (OAE) at the Centers for Disease Control and Prevention (CDC).[61] Race-specific health impacts are calculated using all-cause mortality rates for the entire population of all age groups. My analysis does not differentiate impacts by age-group. Literature-derived estimates of mortality rates and the concentration-response (C-R) function are not sufficiently robust to allow racial-ethnicity-specific values for those two parameters. Consistent with prior research[11-17, 27] and in keeping with EPA norms,[62-64] I assume that all $PM_{2.5}$ particles are equally toxic.

I employ an expression derived from Krewski et al. (2009)[65] for my $PM_{2.5}$ concentration-response function, which is used to estimate $PM_{2.5}$-related health impacts (Cox proportional hazards model):

Number of premature deaths = $\left(e^{(PM_{2.5}\ \text{Linear Coefficient} \times [PM_{2.5}])} - 1\right) \times P \times \frac{\text{All-Cause Mortality Rate}}{100{,}000}$.

Here, $PM_{2.5}$ Linear Coefficient is assumed to be ln(1.078)/10 = 0.00751, i.e., a 7.8% increase in the number of premature deaths for every 10 g/m^3 increase in the concentration of $PM_{2.5}$. $[PM_{2.5}]$ is the concentration of $PM_{2.5}$; P is total population. Mortality is then estimated as:

Deaths per 100,000 people = $\frac{Number\ of\ premature\ deaths}{Population} \times 100{,}000$.

I estimate premature mortality at the national scale, for each RTO, for each US state, and for each race/ethnicity and race/ethnicity-income group. I run InMAP for all EGUs to estimate impacts at the national scale. I also run InMAP separately for coal-fired EGUs, natural gas-fired EGUs, and all other fuel-type EGUs, to estimate impacts by fuel-type at the national scale. Finally, I apportion health impacts by constituents of $PM_{2.5}$ at the national scale: primary $PM_{2.5}$, particulate SO_4 (pSO_4), particulate NO_3 (pNO_3), particulate NH_4 (pNH_4) and secondary organic aerosol (SOA; caused by VOC emissions). I run InMAP separately for each RTO. For each of 49 geographies in the contiguous US (i.e., the 48 states plus the District of Columbia – for brevity I refer here to these 49 geographies as "states"), I use the InMAP Source-Receptor Matrix (ISRM) to estimate impacts from EGUs within and across state boundaries.[66] Total number of premature deaths – by race & income – are aggregated by RTO and by state. In some cases, analyses are constrained by available Census data. For example, Census data on ethnicity are available for Whites, Blacks, Asian, Native Americans, and mixed/other groups – i.e., each racial group is differentiated by ethnicity (Hispanic-origin status). In contrast, for combined race & income data, demographic data is differentiated by Hispanic origin for Whites only, not for other races; results by income categories are available for six racial/ethnic categories (White Non-Latino, White Latino, Black, Asian, Native American, and mixed/other race groups), reflecting the race-income data available from the US Census. If robust, more-detailed demographic information were publicly available, it would be straightforward to update my estimates.

Population-weighted concentrations are calculated as follows:

$$\text{Population weighted average PM}_{2.5}\text{ concentration} = \frac{\sum_{i=1}^{n} P_i [PM_{2.5}]_i}{\sum_{i=1}^{n} P_i}$$

Here, P_i is the number of people of a specific demographic group in grid cell i, $[PM_{2.5}]_i$ is concentration in grid cell i, and n is total number of grid cells.

Damages are presented in terms of three types of metrics:

a) I compute total damages in terms of deaths by aggregating deaths (from total $PM_{2.5}$) in each grid cell for each state, RTO, and nationally, and each race/ethnicity and race/ethnicity-income group in each spatial scale. For mortality rate in terms of deaths per 100,000 people, health impacts are normalized to the respective population in each geographic scale, race/ethnicity and race/ethnicity-income groups.
b) I estimate "risk gap" for state-level mortality estimates to quantify the difference in environmental health risk (deaths per 100,000 people per year) between the most and least exposed group in a state. The advantage of this metric is that it does not force a preselection of specific groups to compare (e.g., Blacks relative to Whites, Asians relative to population-average, lowest-income relative to highest-income) but instead is flexible across geographies to which groups are most and least exposed in that location (i.e., only in that US state).
c) I compute the deaths per unit of electricity service provided (deaths per TWh) for state, RTO, and nationally. This metric facilitates nationwide comparisons of the impacts of EGUs.

3.4 Results

3.4.1 Total premature deaths and deaths per unit of electricity: nationally, regionally, and by state

Total national damages: For 2014, I estimate ~16,400 $PM_{2.5}$-related premature deaths attributable to EGUs, for an average of ~4 deaths/TWh electricity generated, corresponding to a total national population weighted estimate of ~0.82 μg/m^3 of EGU-$PM_{2.5}$. Most of the deaths

(~14,200 deaths, or ~86%; see Table 1) are attributable to EGUs that are in an RTO (the rest are caused by EGUs that are not in an RTO).

Deaths per unit energy generated (Table 1) vary substantially among regional grids – by up to a factor of ~30 (MISO vs CAISO) – with higher values in coal-heavy grids (MISO, SPP). Total attributable premature deaths vary even more by state (Table B2), from ~1,850 deaths/year (Pennsylvania) to ~1 death/year (Montana). Among states, deaths per unit electricity generation (units: deaths/TWh) for each state (Table B3) varies, from 0.02 (Vermont) to 14 (Indiana).

Table 3.1 Estimated deaths per unit electricity generation, by RTO.

RTO	Annual net generation (TWh)†	Total deaths attributable to RTO's emissions		Percent of generation by fuel†		
		Total deaths	Deaths per TWh	Coal	Natural gas	Oil, biomass, and other fossil fuels
CAISO	170	45	0.3	0.5%	59%	4%
ERCOT	365	1788	4.9	32%	46%	0.7%
MISO	691	5649	8.2	56%	19%	4%
NEISO	110	48	0.4	5%	43%	10%
NYISO	140	162	1.2	3%	42%	4%
PJM	809	4868	6.0	43%	17%	2%
SPP	238	1599	6.7	59%	19%	0.8%

† From year-2014 in eGRID.[30]

Of the ~16,400 premature deaths from EGUs nationwide, I estimate that the vast majority (~15,200, or ~93%) are from coal EGUs, ~800 (5%) from natural gas EGUs, and ~460 from other fuel EGUs (Figure B2). Similar patterns hold in most states: coal-fired EGUs are the largest contributor to total EGU-$PM_{2.5}$ deaths (Table B4). Nationally, most EGU-$PM_{2.5}$ impacts (~73%)

are from pSO_4, which is dominated by sulfur emissions from coal EGUs; contributions by other species (Figure B3) are 15% (pNO_3), 11% (primary $PM_{2.5}$), 1% (pNH_4), and ~0% (SOA).

3.4.2 Differences in damages by demographic group

Race. I find that year-2014 mortality rates from EGU-$PM_{2.5}$ are largest for Black people, second-largest for White Non-Latino people, and lower-than-average for Asians, Native Americans, and Latinos (Figure 1). Differences by race vary by RTO (Figure B4) and species (Figure B5).

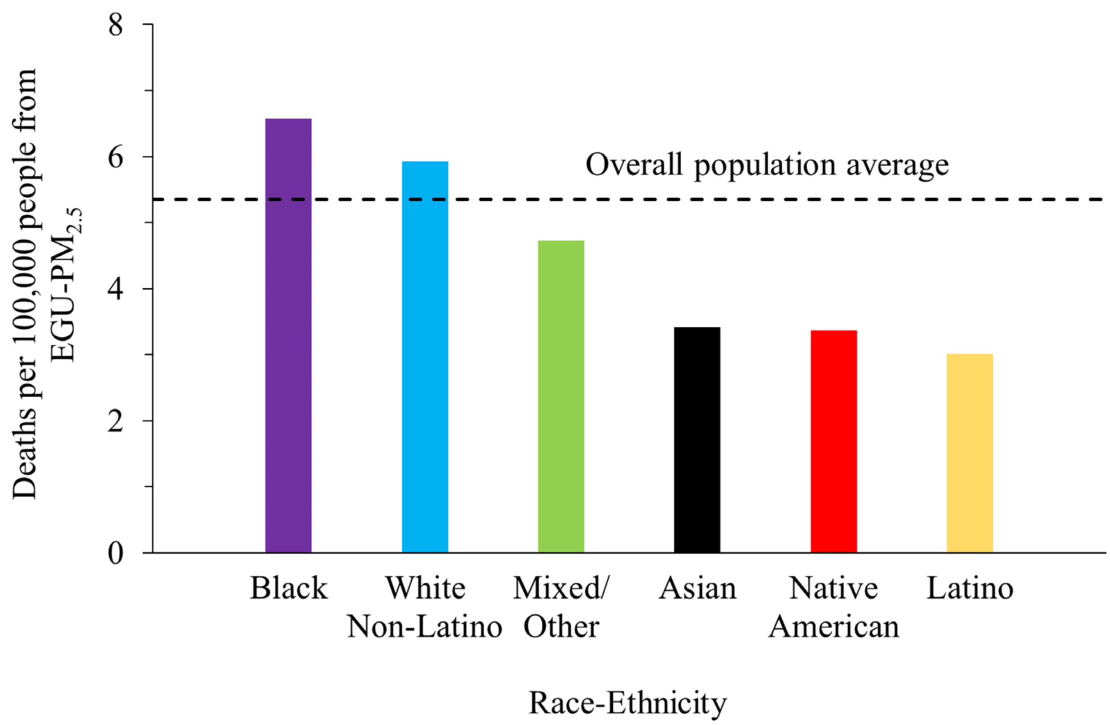

Figure 3.1 Deaths per 100,000 people, attributable to $PM_{2.5}$ from electricity generation in the US in 2014.

The overall average mortality rates from EGU-$PM_{2.5}$ are 5.3 for all people, 6.6 for Blacks, 5.9 for White Non-Latinos, and 3.6 averaged across the remaining groups (Figure 1). I assessed the spatial distribution of EGU-caused premature deaths per km^2 across the US by race-ethnicity groups (Figure B6 [A, B, C]) and find areas where groups have largest impacts. For example, for

Native Americans, the largest premature deaths per km^2 are, e.g., in western Oklahoma. Subdividing by fuel-type (Figure B7) reveals that Blacks are the most-exposed group for all three fuel categories. For natural gas emissions, exposures are higher than average for Blacks, Asians, and Latinos, and lower than average for White Non-Latinos. For coal emissions, relative exposures are similar to Figure 1 except Native Americans are slightly more exposed to coal emissions than Asians are.

Income & Race. Differences by race are observed across all income categories (Figure 2). Thus, differences by race/ethnicity (Figure 1) are not "merely" income differences; race/ethnicity differences are present even after accounting for differences in income (Figure 2).

On average, exposures are higher for lower-income households than for higher-income households. Considering Figure 2 (deaths per 100,000 people attributable to EGU-$PM_{2.5}$), the difference between most- and least-exposed income group is ~1.0 for the overall population; the same difference is 1.5 for White Non-Latino, 0.9 [Black], 0.3 [White Latino], 0.5 [Asian], 0.9 [Native American], and 0.8 [mixed/other]. The difference between most- and least-exposed race is 3.6 for the overall population, 4.0 for lowest-income, and 2.8 for highest-income. Thus, differences by race are larger than differences by income.

Based on results in Figure 2, if I calculate the risks by race, but making the adjustment that all race/ethnicity groups have an income distribution equal to the national average distribution, then mortality rates from EGU-$PM_{2.5}$ (deaths per 100,000 people) would be 5.3 for all people, 6.4 for Blacks, 5.9 for White Non-Latinos, and 3.2 averaged across the remaining groups. Here too, analyses reveal that exposure differences by race are observed even after accounting for income differences.

Race-income results differ substantially by RTO (Figure B8); for example, exposures are higher for White Non-Latino income-groups than for Black income groups for CAISO, MISO, NEISO, and SPP, but not ERCOT, NYISO, and PJM.

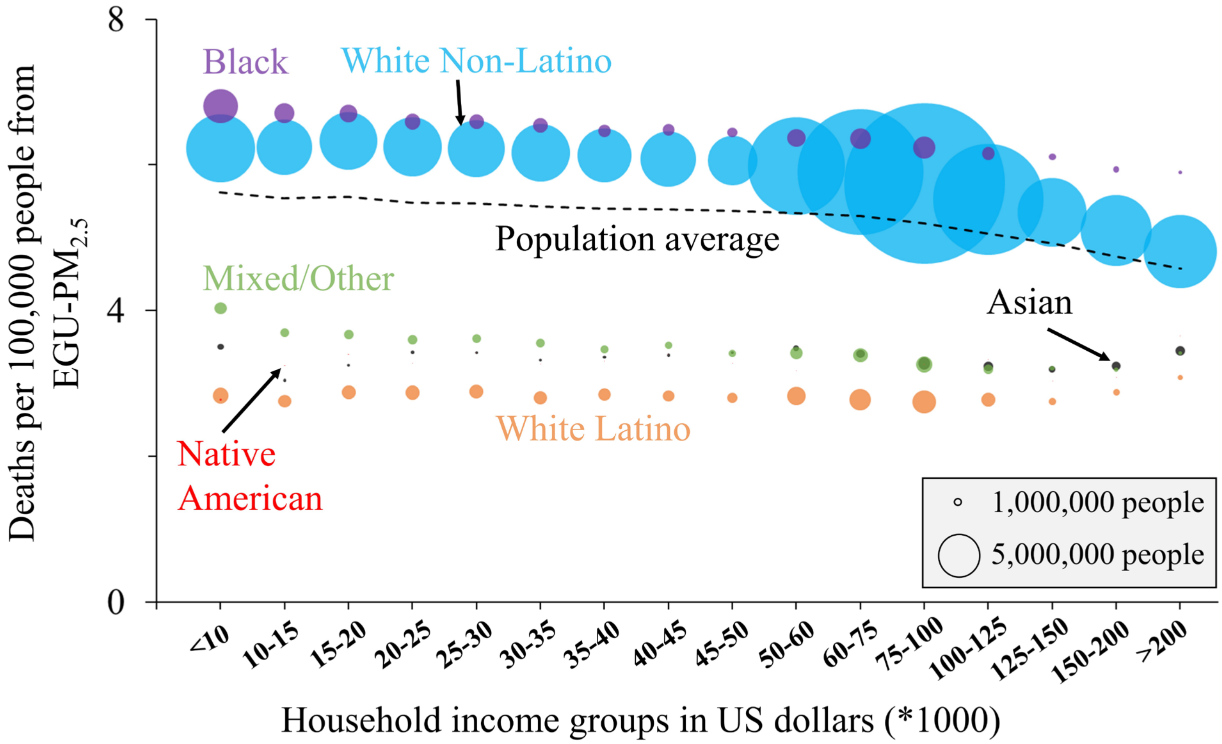

Figure 3.2 Deaths per 100,000 people by income groups among White Non-Latino, White Latino, Black, Asian, Native Americans, and mixed/others. Icon area is proportional to the population size.

I estimate exposures for the household income groups in each state from EGU-$PM_{2.5}$ emissions in the entire US; Figure 3 shows the most-exposed income category in each state and the risk gap (premature deaths per 100,000 people) between most and least exposed household income group. The "$10,000 - $15,000 per year" household income category is the most-exposed category for 19 out of 49 states (risk gap varies between 0.06 – 3.6 for these 19 states). Overall, low-income categories are most exposed in a majority of the states [38 states], followed by middle-income [5 states], and upper-income [6 states]. The gap between most- and least-exposed household income category is sizeable (>2 premature deaths per 100,000 people) in only three states (Maryland [3.5], Virginia [3.6], Indiana [2.9]; total population = 21 million).

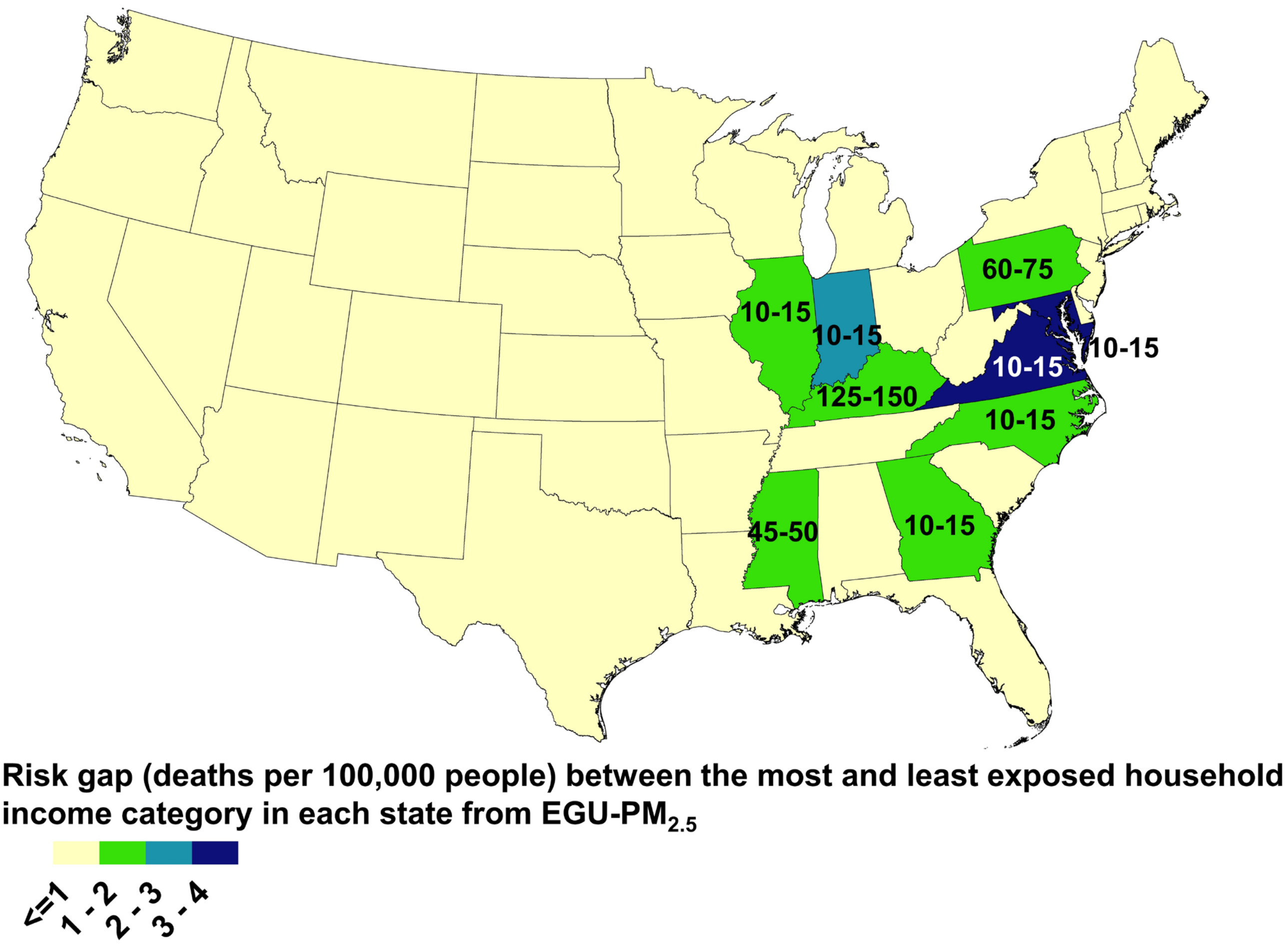

Figure 3.3 Most exposed household income group in thousand US dollars (for overall population) and risk gap (units: deaths per 100,000 people, attributable to EGU-$PM_{2.5}$ from all EGUs in the US) between the most and least exposed household income group in each US state. The income group that is the most exposed is shown for states where the gap in mortality rate is greater than 1 death per 100,000 people. The remaining states are unlabeled because the gap between most- and least-exposed income group is small (less than 1 per 100,000 people). A version of the map displaying labels for all states is in Figure B9. Risk gap is shown by color gradation.

3.4.3 Health damages by state

My results estimate EGU-$PM_{2.5}$ health impacts, with each state as a source and a receptor of pollution (Figure 4). The maps reveal geographic differences between where EGU emissions are produced and where exposures and health impacts are experienced. For example, Texas experienced an estimated total of ~1360 EGU-$PM_{2.5}$ premature deaths in 2014 (Figure 4A), most of which (~1160, or >80%) are attributable to EGU emissions occurring inside Texas (Figure 4B);

the remainder (~200/y deaths in Texas) were attributable to $PM_{2.5}$ in Texas caused by EGU emissions outside of Texas. EGU emissions in Texas caused an additional ~524 deaths/y in states other than Texas (Figure 4C). Thus, Texas is a net exporter of EGU-$PM_{2.5}$ deaths: the number of premature deaths/y caused by Texas EGU emissions (~1684; the sum of ~1160 in-state plus ~524 out-of-state) exceeds the number of EGU-$PM_{2.5}$ premature deaths in Texas (~1360) by ~325 (Figure 4D). For some states (e.g., Arizona), damages from their EGU emissions are large in many downwind states; for other states (e.g., Washington), damages are more local (Figure B10 A). As expected, many of the net importing states are on the East Coast (Figure 4D). A bar chart of Figure 4 (Figure B11) reveals comparison between health impacts among different states.

States with the largest EGU-$PM_{2.5}$ mortality are Pennsylvania, Texas, Ohio, New York, Indiana, Virginia, Maryland, Kentucky, North Carolina, New Jersey, Illinois, and Florida; states with the smallest values are New Hampshire, South Dakota, Nevada, New Mexico, Maine, Arizona, Utah, North Dakota, Vermont, Wyoming, Oregon, Idaho, and Montana. The states with the largest import-export mortality imbalance are New York, Virginia, Maryland, New Jersey, North Carolina, and Ohio, which are net importers, i.e., the impacts from other states exceed impacts onto other states; Missouri, Texas, Kentucky, Illinois, West Virginia, and Indiana are the largest net exporters (i.e., the impacts to other states exceed impacts from other states). Among the largest net importing states, New York, Maryland, and New Jersey import the largest share of out-of-state impacts from Pennsylvania [29%, 36%, and 49% respectively], North Carolina's largest share of out-of-state impacts comes from Kentucky [16%], Ohio from Indiana [37%], and Virginia from West Virginia [20%]. A similar number of states are net importers versus net exporters of EGU-$PM_{2.5}$ mortality (24 states and 24 states, respectively); importers (exporters) are more likely to be found in the Eastern (Western) portion of the US.

My results reflect that EGU emissions travel great distances. For example, when considering states as receptors, in 39 states, a majority (>50%) of EGU-$PM_{2.5}$ mortality is attributable to EGU emissions in other states (Figure B12). When considering states as sources, in 35 states, a majority (>50%) of the state's EGU-$PM_{2.5}$ mortality impacts occur outside of that state (Figure B10 B).

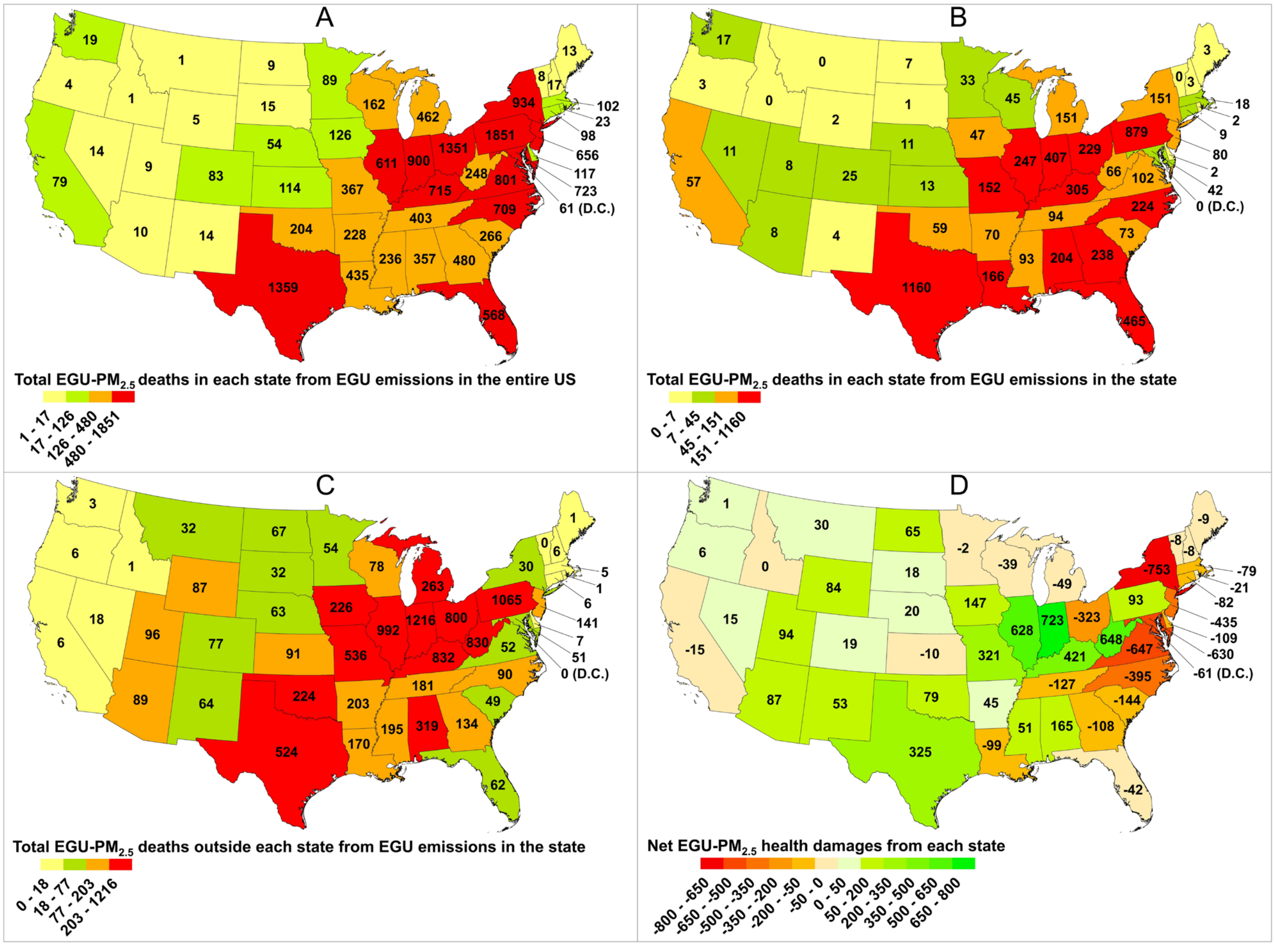

Figure 3.4 Deaths from EGU-$PM_{2.5}$ by state. (A) Total deaths in each state from EGUs throughout the US, (B) total deaths in-state from EGUs in that state, (C) total deaths out-of-state from EGUs in that state, (D) Net imports (negative values) or exports (positive values) of deaths. Values in D are calculated as B + C – A. Range limits for color bars in A, B, and C are by quantiles.

3.4.4 Variations by geography and race

Regional Transmission Organizations. The most-impacted race/ethnicity varies by RTO (Figure B13): White Non-Latino for NEISO; Asian [CAISO and NYISO]; White Latino [ERCOT]; Black [PJM and MISO]; and Native American [SPP]. MISO and SPP (the two RTOs with >50% of generation from coal; Table 1) are the only RTOs where more than 50% of total premature deaths occur outside RTO boundaries (Figures S14 and S15).

States. Environmental justice aspects of EGU-$PM_{2.5}$ vary by state and by EJ metric employed (Figure 5, Figure B16, Table B5). For example, the impacts in Texas from nationwide emissions are greater for Blacks than any other race-ethnicity group, with a gap of ~2.4 deaths/100,000 people between the most (Black) and least exposed group (White Latino). In contrast, in Oklahoma impacts are greatest for Native Americans, with a gap of ~2.1 deaths/100,000 people between the most (Native American) and least exposed group (Asian). Among the seven states with the largest gaps by race (Figure 5 value >2 premature deaths per 100,000 people), one can find examples where the most-exposed group is White Non-Latino (Maryland, Pennsylvania, Virginia), Black (Kentucky, Texas), White Latino (Mississippi), and Native American (Oklahoma); in total, these seven states comprise 64 million people (compared to 21 million people in the three analogous states from Figure 3 [i.e., the three states in Figure 3 with risk gap >2]). A map, analogous to Figures 3 and 5, but combining race/ethnicity and income, is in the SI (Figure B17). Impacts within each state by fuel-type and race-ethnicity are in Table B6.

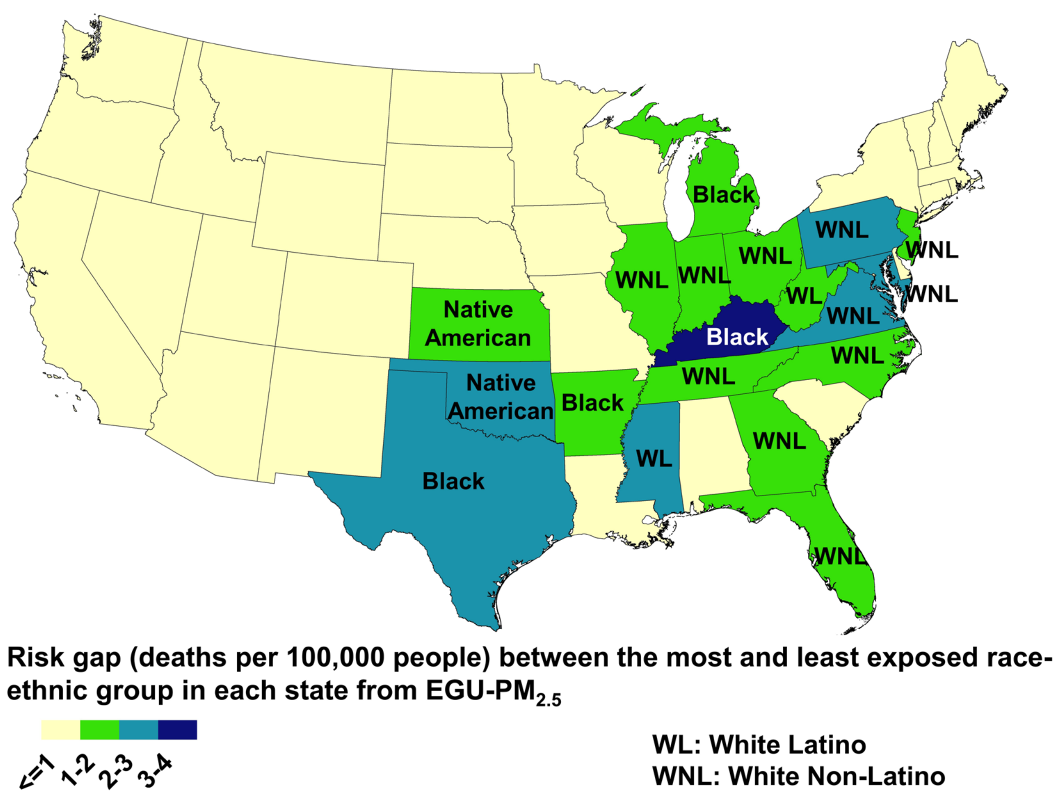

Figure 3.5 Most exposed racial-ethnic group and risk gap (units: deaths per 100,000 people) between the most and least exposed racial-ethnic group in each US state from total EGU-PM$_{2.5}$ emissions in the entire US. Race-ethnicity labels are displayed for states with a gap in mortality rate greater than 1 death per 100,000 people. The remaining states are unlabeled because the gap between most- and least-exposed race-ethnicity group is relatively small (less than 1 per 100,000

people). A version of the map displaying labels for all states is in Figure B17. Risk gap is shown by color gradation.

3.5 Discussion and conclusions

Previous studies have estimated the total damages associated with $PM_{2.5}$ from the US electricity sector. This work complements those findings by systematically analyzing the damages for different geographical boundaries (RTOs and states) and for different demographic groups (race and income).

I find that Blacks are disproportionately affected by EGU $PM_{2.5}$ nationally, but most-exposed race/ethnicity varies by state and by RTO. Differences by race/ethnicity hold across all income groups. Exposures are higher for lower-income than for higher-income households, but differences by race/ethnicity are larger than differences by income.

A substantial portion of the health risks in most states is attributable to out-of-state emissions, reflecting that EGU-$PM_{2.5}$ is a long-range pollutant. Some states are net imports of harm, others are net exporters. Regarding issues related to cross-state damages, EPA regulations such as the Cross-State Air Pollution Rule (CSAPR)[67] address air pollution from upwind states that crosses state lines and affect air quality in downwind states. My findings highlight the inter-state nature of EGU-$PM_{2.5}$ impacts: $PM_{2.5}$ mortality impacts in a state often are highly impacted by out-of-state EGU emissions.

My estimate of total premature deaths (~16,400 EGU-$PM_{2.5}$ premature deaths in 2014) is on low end of the range given in the literature (see above); reasons include (1) reduced emissions in 2014 relative to 2005, and (2) differences in concentration response functions used in other studies (see below).

My investigation considers exposure and health impacts from EGU-$PM_{2.5}$, instead of proximity to EGUs as considered by previous studies.[68] Previous work[68] reported that the proportion of the population living within 30 miles of a power plant is greater for blacks than whites. Power plants are mostly located in rural areas, but the long-range transport of emissions can impact downwind population groups at varying magnitudes and distances. In considering effective policy for reducing EGU impacts and disparities in impacts, it is important to consider the spatial distribution of emissions and populations, and the long-range transport of $PM_{2.5}$ and its emission precursors.

Future research could usefully explore the impact on results of (1) alternative models and modeling approaches, (2) grid-cell size, (3) alternative concentration-response functions (e.g., a supra-linear C-R), or allowing the C-R to vary by source, geography, or chemical components,[69-72] (4) health impacts of tropospheric (i.e., ground-level) ozone (O_3) formation from NO_x and VOCs emissions from EGUs, and (5) updated emissions for more recent year, such as 2017 NEI emissions.

Paolella et al. (2018)[73] demonstrated the importance of fine spatial resolution for identifying and quantifying exposure disparities. My approach employs a reduced-complexity air quality model (InMAP; ISRM) that uses variable resolution grid (i.e., spatially fine grid in high population density areas). Thus, while my approach addresses the needs identified by Paolella et al. (2018)[73] (i.e., smaller-scale grid cells), I hypothesize that grid-cell size is less important for issues considered here because (1) EGUs typically have tall stacks, which spread pollution and reduce the relative importance of local conditions, and (2) EGU-$PM_{2.5}$ is a long-range pollutant (secondary $PM_{2.5}$ formation is dominated by emissions of SO_2, which typically takes several days to transform into $PM_{2.5}$). Future research could test whether results seen here are also observed using other RCMs[74] or a conventional CTM.

My study employs the mortality hazard ratio of 1.078 for all-cause mortality from the American Cancer Society (ACS) re-analysis study (Krewski et al. 2009)[65] to estimate premature deaths using a linear C-R function with no threshold. This C-R function is considered a US EPA standard and is commonly used in regulatory and academic air quality research.[54,75,76] To understand the impact of alternative mortality hazard ratios on the premature deaths calculated in this work, as a sensitivity analysis I use values from Lepeule et al. (2012) (i.e., reanalysis of the Harvard Six Cities (H6C) study) [1.14, 95% CI=1.07-1.22],[77] Vodonos et al. (2018) [1.129, 95% CI=1.109–1.150],[78] and Pope et al. (2019) [1.12, 95% CI=1.08–1.15].[79] These alternative hazard ratios increase the national premature deaths estimated in this work substantially: by 75% [Lepeule et al. (2012)], 62% [Vodonos et al. (2018)], and 51% [Pope et al. (2019)]. Future research in the $PM_{2.5}$ C-R functions may benefit from relationships that are specific to source sector, geographical region, or chemical constituents. Straightforward interpretation of the values individually reported by those three studies suggests an uncertainty of up to a factor of 2 (i.e., for Lepeule, the lower CI relative to the central estimate) if considering the 95% CIs, an uncertainty of 17% if considering just the three central-tendency estimates used in this sensitivity analysis, and an uncertainty of up to 75% if comparing those three studies against my base-case predictions. Detailed quantification of uncertainty in the C-R, via meta-analysis or other techniques, is outside the scope of research for this article, however, these comparisons suggest that my results are conservative, i.e., likely underestimate the true health impacts from air pollution.

Health impacts of ozone from electricity generation have been previously modeled for the year 2005 and are estimated to be much smaller (~1-10% of the total impacts from EGUs in the US) than $PM_{2.5}$-related impacts.[10,12,13] I studied year-2014 because it reflects the most current, well-vetted NEI dataset available. Emissions and population patterns may differ for year-2014 than for more-recent (and, future) years, which would impact results here. In general, electricity generation has lower emissions and uses less coal today than in 2014.[80] For that reason, total deaths/y from EGU-$PM_{2.5}$ are likely lower for present-year than for 2014.

My analysis could be extended to other specific sectors of the economy. I hope that results here are useful for scientists and policymakers to understand and address disparities in air pollution exposure by race, income, and geography. Reductions in EGU emissions and EGU-$PM_{2.5}$ would not only save lives, but also can reduce environmental and health inequalities.

Chapter 4

Health and climate impacts from inter-state road, rail, water, and air freight transportation in the United States. Accessing $PM_{2.5}$ and CO_2 impacts by mode, route, and emission species

4.1 Abstract

Fine particulate matter ($PM_{2.5}$) and carbon dioxide (CO_2) emissions from on-road (e.g., heavy-duty trucks) and non-road (e.g., freight rail, barge, and freight (cargo) aircraft) modes of freight transportation contribute to human health and climate impacts. In this research, I quantify and compare health ($PM_{2.5}$) and climate (CO_2) impacts from inter-state freight transportation in the contiguous United States (U.S.) by four modes: heavy-duty truck ("truck"), freight rail ("rail"), barge, and freight aircraft ("aircraft"). I explore exposure disparity between different racial-ethnic groups resulting from inter-state freight movement. This is a first comprehensive study to compare overall health, climate, and economic impacts and exposure disparity from all four freight modes in the U.S. I find that, overall, aircraft poses the greatest health, climate, and economic damages and exposure disparity per unit mass of freight moved. Among the non-aircraft modes, rail has the greatest health impacts and exposure disparity and lowest climate impacts per unit freight mass. Truck has the lowest health impacts and exposure disparity (and barge) among all modes and greatest climate impacts among the non-aircraft modes. Barge has slightly greater health impacts than truck and greater climate damages than rail. Among the non-aircraft modes, total combined health and climate-related economic damages are greatest for truck followed by rail and lowest for barge. I find that average exposures from truck and rail are the highest for white non-Latinos, barge exposure is highest for blacks, and aircraft exposure is highest for mixed/other race groups. Level

of exposure and disparity among racial-ethnic groups vary in urban and rural areas. This research can be useful to shipping companies, transportation planners, and policymakers to incentivize freight choices in the future based on combined overall impacts from freight modes rather than only climate impacts.

4.2 Introduction

Freight transportation plays an important role in the economy of the United States (U.S.) by moving goods across regions.[1,2] In 2018, the U.S. transportation system moved a daily average of about 51 million tons of freight valued at more than $52 billion.[1] U.S. Department of Transportation projects significant growth in freight ton-miles by truck [48%], rail [9%], water [19%], and air [110%] between 2018 and 2045.[3] With rise in the e-commerce industry in the recent years, reliance on freight modes is expected to increase substantially now and in the near future. Shipping and e-commerce companies usually incentivize the mode selection based on the climate impacts and usually do not consider air quality and health impacts of freight modes.[4,5,6] A 2013 report by the U.S. Department of Energy (DOE)'s highlighted potential of truck-to-rail modal shift due to higher efficiency of rail than truck.[7] It is important to compare the overall impact of freight modes by considering both health and climate impacts.

About 40% of total U.S. transport energy consumption in 2018 was used for transporting freight from one place to another by commercial and freight trucks [24%], aviation [9%], marine [4%], and trains and buses [3%].[8] These freight modes are mostly driven by diesel engines except the aircrafts for which energy is provided by combustion of kerosene (also called, "petroleum jet fuel"). Diesel and kerosene exhaust emissions contribute to the formation of fine particulate matter ($PM_{2.5}$) – a regulated pollutant known to have the largest air quality health impacts in the U.S. and globally by causing increased mortality from respiratory and cardiovascular diseases among human population.[9,10] The exhaust emissions comprise of "primary" $PM_{2.5}$ (emitted directly) and precursor pollutants – sulfur dioxide (SO_2), oxides of nitrogen (NO_x), and volatile organic compounds (VOCs) that react in the atmosphere to form "secondary" $PM_{2.5}$. Ammonia (NH_3) is emitted through "ammonia-slip" from emission control equipment fitted in the vehicles. The U.S. Environmental Protection Agency (U.S. EPA) estimates that in 2014, transportation sector contributed 58% of NO_x, 7% of VOCs, 7% of primary $PM_{2.5}$, 5% of SO_2, and 3% of NH_3 emissions nationwide.[11] In 2014, diesel heavy-duty vehicles, rail, commercial marine vessels, and aircraft combined contributed to 87%, 50%, and 43%, respectively, of SO_2, NO_x, and primary $PM_{2.5}$ total mobile emissions.[11] Freight transportation also impacts climate by emitting greenhouse gas carbon dioxide (CO_2) and is responsible for 29% of the total greenhouse gas emissions from the U.S. transportation sector of which CO_2 accounts for nearly all the share.[1]

Previously, health impacts of combustion emissions from U.S. transportation sector have been significantly studied by research community at different scales: global, regional, and local.[12-23] Table 4.1 shows the summary of research articles. Little research has linked freight emissions with health impacts. Only three articles (7, 11, and 12) in the Table 4.1 have specifically studied freight transportation but limited to only land freight transport. Studies like Caiazzo et al. (2013)[16] presents aggregate impact of annual emissions from land, marine, and rail transport (based on county-level 2005 NEI data) irrespective of their usage (freight/passenger). Two studies focused on quantifying exposure from freight-related emissions, Liu et al. (2019)[22] and Pan et al. (2019)[23] quantifies health impacts from heavy-duty truck and freight rail an do not analyze all freight modes (including barge and freight aircraft). These studies do not perform individual route analysis but present aggregate impacts from heavy-duty truck and freight rail.

No single study makes complete assessment of comparison between health and climate impacts of all four modes of freight transport: road, rail, water, and air. Additionally, existing knowledge of air quality and climate impacts from freight transportation is limited to total impacts and have not been explored impacts for each route. Environmental justice impacts of pollutants originating from transportation sources have been previously studied but not specific to freight transportation. Clark et al. (2017) explore disparities in exposure to outdoor NO_2 concentrations the U.S. and found that non-whites are exposed to higher NO_2 concentrations than whites.[24] Houston et al. (2016)'s study focused in California finds that minority and high-poverty neighborhoods bear over two times the level of traffic density compared to the rest of the Southern California region, which may associate them with a higher risk of exposure to vehicle-related pollutants.[25] There has been no effort to quantify $PM_{2.5}$ health disparities specifically arising from freight transportation.

Table 4.1 Summary of research articles looking at impacts from transportation sector by mode

	Research article	Spatial modeling domain	Modes or sub-sectors analyzed	Summary of total $PM_{2.5}$ impacts	Specific freight modes analyzed?
1.	Corbett et al. (2007)[12]	Global, continents	Oceangoing ships	Shipping-related PM emissions are responsible for approximately 60,000 annual cardiopulmonary and lung cancer deaths globally	No
2.	Barrett et al. (2010)[13]	Global, selected countries	Aircraft	Full-flight aircraft emissions result in ~10,000 premature mortalities per year globally, out of which ~8000 premature mortalities per year are attributable to aircraft cruise emissions (i.e. remaining are from landing and takeoff cycle [LTO] emissions)	No
3.	Fann et al. (2012)[14]	U.S.	Combined aircraft, locomotives, and marine vessels	Showed benefits of $210,000, $41,000, and $4,400 for reducing a ton of primary $PM_{2.5}$, SO_2, and NO_x respectively from combined aircraft, locomotives, and marine vessels sector in year 2005	No
4.	Fann et al. (2013)[15]	U.S.	Mobile sources combined	$PM_{2.5}$ and O_3 related deaths attributable to mobile sources were ~29,000 and ~19,300 in modeled year 2016	No
5.	Caiazzo et al. (2013)[16]	U.S.	Road, marine, and rail	$PM_{2.5}$-related annual deaths in 2005 were 52,800 from road, 8,300 from marine, and 4,500 from rail transportation	No
6.	Dedoussi et al. (2014)[17]	U.S.	Road, marine, and rail	Attributed $PM_{2.5}$ exposure and premature deaths from road, marine, and rail transportation to emissions species, time of emission, and location of emissions.	No
7.	Bickford et al. (2014)[18]	Midwestern U.S.	Truck and rail freight	Presented air quality benefits (in terms of changes in concentration) of shifting freight from truck to rail in the upper Midwestern U.S.	Yes
8.	Yim et al. (2015)[19]	Global, continents, and airports	Civil aviation	2,150 premature deaths per year in North America due to the population exposure to aviation attributable $PM_{2.5}$ and ozone, from which 43% were found to be attributable to the LTO portion of emissions.	No

9.	Galvis et al. (2015)[21]	Region: Atlanta, Georgia	Rail	Quantified the impact on local air quality from two rail yards in Atlanta before and after conversion to a low emission technology using AERMOD modeling	No
10.	Liu et al. (2019)[22]	U.S.	Freight truck and rail	Presented $PM_{2.5}$-related health impacts from urban short-haul trucks, rural short-haul trucks, long-haul trucks, and long-haul rail across U.S. using InMAP	Yes
11.	Pan et al. (2019)[23]	U.S.	Freight truck and rail	Studied air quality and public health impacts of projected freight-related emissions in year 2050 under three scenarios	Yes

Present state of knowledge does not answer a policy question: which freight mode has the least health and climate impacts and exposure disparity from transporting a unit mass of freight from origin to destination? Given the complexity of various factors among different modes such as emission intensity, spatial pattern of routes for each mode, mileage, and variable population density across space, it is not clear which freight mode has least impact on human health, climate, and exposure disparity. Using freight data from U.S. DOT and air quality modeling capabilities of a novel air quality model, Intervention Model for Air Pollution (InMAP),[26] I compare health and climate impacts and exposure disparities between all four modes of freight transportation: road, rail, water, and air.

4.3 Methods and data

In this work, I compare impacts from four freight modes: Combination long-haul heavy-duty truck, freight rail, barge, and freight aircraft. For brevity, I refer here to combination long-haul heavy-duty truck as “truck”, freight rail as “rail”, and freight aircraft as “aircraft”. My methods are based on origin-destination (O-D) pairs from the U.S. DOT’s Freight Analysis Framework (FAF) data,[3] modal network data from National Transportation Atlas Databases (NTAD),[27] emission factors for each mode derived from the Argonne National Laboratory’s Greenhouse Gases, Regulated Emissions, and Energy Use in Transportation (GREET) model [28] and U.S. EPA’s Motor Vehicle Emission Simulator (MOVES) model[29] (except ammonia emissions, which are derived from literature), mode routing using ArcGIS software,[30] and air quality modeling using Intervention Model for Air Pollution (InMAP).[26]

4.3.1 Freight Analysis Framework (FAF) data

The Freight Analysis Framework (FAF) data, produced through a partnership between US Bureau of Transportation Statistics (BTS) and Federal Highway Administration (FHWA), provides a comprehensive picture of freight movement between major metropolitan areas (also called FAF regions) and states by all modes of transportation.[2,3] I use the FAF version 4 (FAF4) data for year 2017 which provides estimates for tonnage, ton-miles, and value by FAF regions and mode.[3] Data is provided for freight movement between 132 FAF regions. In this work, I only focus on the inter-regional (FAF) freight transport due to non-availability of origin and destination locations of freight transport within FAF zones. But I find that majority of ton-miles movement within FAF zones is inter-regional (most are mostly inter-state) rather than intra (within) regional: percentage of total ton-miles movement between different FAF zones is 84% for truck, 99% for rail, 97% for water, and 98% for air.

The FAF4 database provides ton-miles of freight transported between specific origin-destination pairs, by mode. For analysis in this research, I select all inter-FAF origin-destination (O-D) pairs across contiguous U.S. for truck, rail, water, and air transport; there are 16,293 inter-state FAF O-D pairs for truck, 4,875 for rail, 732 for water, and 7,913 for air.

4.3.2 Geospatial data from the National Transportation Atlas Databases (NTAD)

The geospatial route data for O-D pairs is not available from the FAF data. I use the spatial data for roads and highway network, railways, waterways, and runways from National Transportation Atlas Databases (NTAD) developed by the Bureau of Transportation Statistics, U.S. Department of Transportation.[27] NTAD provides spatial information for transportation modal networks – highways & roadways, rail, navigable waterways, and airport runways, Freight Analysis Framework (FAF) regions, and Intermodal Terminal Facilities. FAF regions consist of portions of large metropolitan areas based on their size (in terms of business activity) or their importance as a transportation hub. Intermodal Terminal Facilities are the locations where freight can be transferred between modes of transportation. Figure C1 in appendix shows the geospatial network data used in this work. NTAD does not provide flight path data for aviation transport – it only provides spatial data (polyline) for airport runways.

4.3.3 Modal routing

I use ArcGIS's network analyst tool to perform routing of truck, rail, and barge to find the shortest route between origin and destination for an O-D pair on roads and highways, rail lines, and waterway network, respectively. For routing aircrafts, shortest flight path between airports is assumed to be a great-circle distance (i.e., length of flight = great-circle distance).[31] I assume a great circle path at an average cruise height of 11 km (~35,000 ft) for a flight path.[32] A simplified landing and take-off (LTO) cycle is used for an aircraft based on the LTO cycle in the International Civil Aviation Organization (ICAO)'s air quality manual (Figure 4.1).[33] ICAO's full LTO cycle is included in the appendix in Figure C2. I use minimum landing and take-off slope assumptions from the U.S. DOT's Federal Aviation Administration (FAA)'s Aeronautical Information Manual.[34] LTO cycle is typically assumed 0.914 km above ground level which also corresponds to a typical planetary boundary layer height, within which pollutants mix rapidly (also called "mixing height").[33,35] The shapefile input to InMAP for aircraft includes airport runway, LTO cycle, and great-circle path from origin to destination. My assumptions for shortest paths for truck, rail, barge, and aircraft result in total miles that are in approximate range of total miles estimated in the FAF data (Table C1).

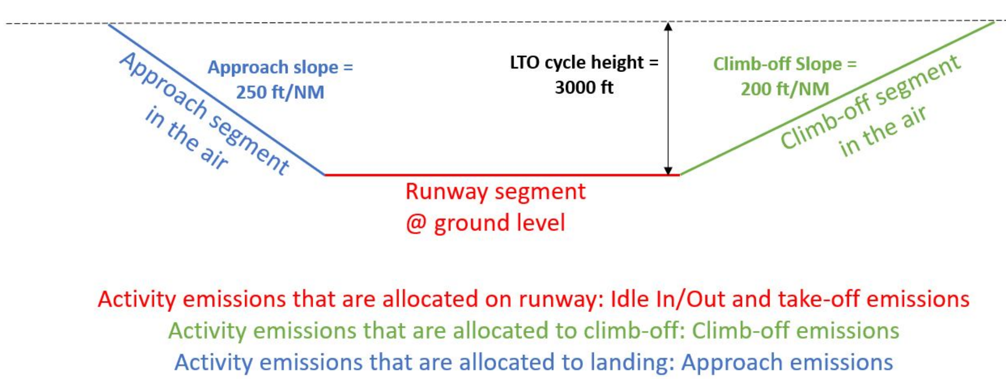

Figure 4.1 Side view projection of a simplified LTO Cycle used in this analysis

4.3.4 Emission factors for truck, rail, barge, and aircraft

I use NO_x, SO_2, VOC, primary $PM_{2.5}$, and CO_2 emission factors in terms of kg per ton per mile from the Argonne National Laboratory's GREET model for each mode (Figure 4.2).[28] Fuel assumptions for each mode in accordance to current U.S. EPA's sulfur standards (ultra-low sulfur diesel for highway vehicles and non-road engines) are:[36]

(1) Heavy-duty truck: Low-sulfur diesel (sulfur (S) content = 11 ppm)

(2) Freight rail: Diesel for non-road engines (S content = 11 ppm)

(3) Barge: Diesel for non-road engines (S content = 11 ppm)

(4) Aircraft: Conventional jet fuel (S content = 700 ppm)

NH_3 emission factor for truck is estimated using U.S. EPA's MOVES model[29] and for rail and barge from other U.S. EPA studies.[37,38]

Aircraft emission factors are used from GREET model (GREET model procures aircraft emission factors from U.S. DOT Volpe Center's Aviation Environmental Design Tool (AEDT))[39]. GREET provides cruise and LTO emission factors for four AEDT aircraft types, categorized based on distance travelled by each type: Single Aisle, Small Twin Aisle, Large Twin Aisle, and Large Quad (Figure 4.2 and 4.3). NH_3 emissions from aircraft are assumed to be zero (2014 NEI data shows zero emissions from Mobile-Aircraft data). Cruise emissions are assumed at the aircraft's cruise altitude of 11 km. LTO emission factors are for estimated for each activity type: idle/taxi-in, idle/taxi-out, take-off, climb-out, and approach (landing) using emission factors from GREET model and fuel rate from the ICAO databank (Table 4.2).[40] Aircraft LTO emissions are allocated at four stages of LTO cycle: idle/taxi-in, idle/taxi-out and take-off emissions on the runway (height = 0), climb-out emissions along the climb-out slope, and approach emissions along the approach slope. For an O-D pair, idle/taxi-out, take-off, and climb-out emissions are considered at the origin airport and approach and idle/taxi-in emissions are considered at the destination airport.

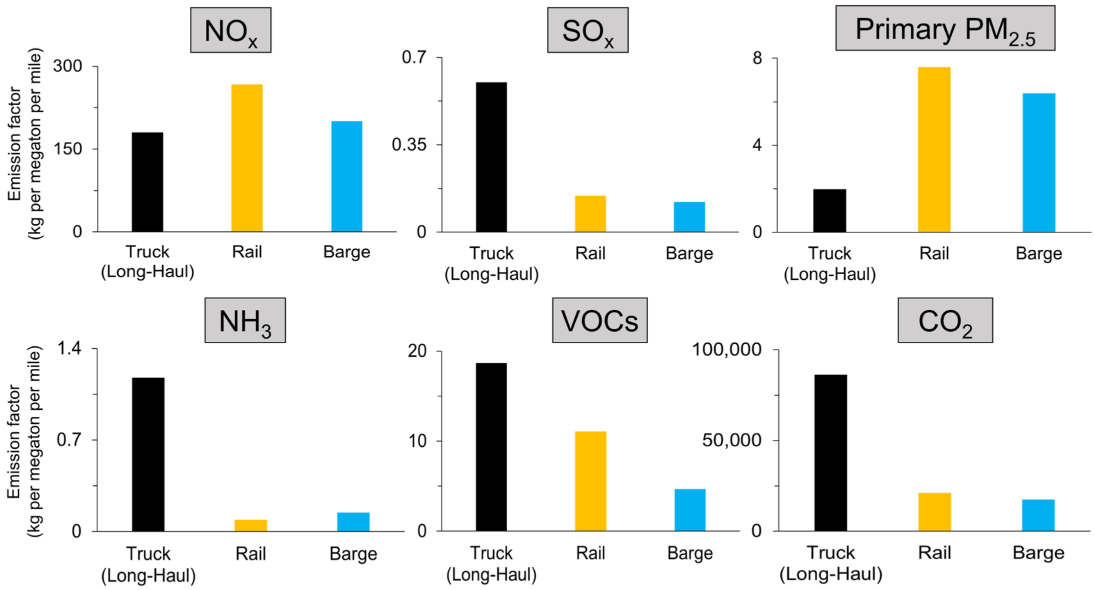

Figure 4.2 Emissions factors (kg per megaton per mile) for truck, rail, and barge

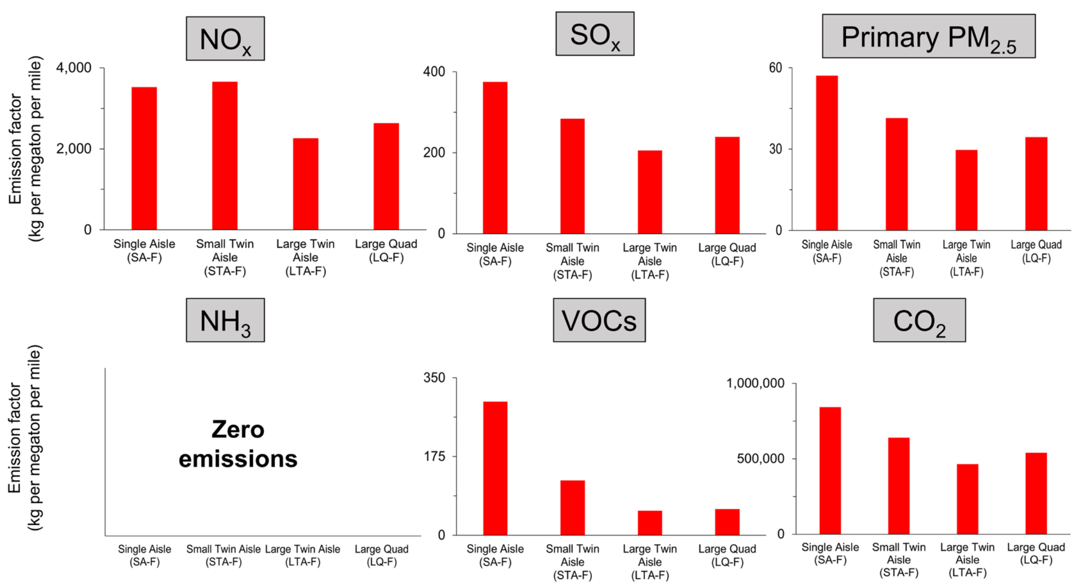

Figure 4.3 Cruise emission factors (kg per megaton per mile) for aircraft by aircraft types

Table 4.2 Aircraft Landing and Take-off (LTO) cycle emission factors

Pollutant	Activity	Single Aisle (kg/megaton)	Small Twin Aisle (kg/megaton)	Large Twin Aisle (kg/megaton)	Large Quad (kg/megaton)
CO_2	Take-off	9,698,826	7,209,271	5,697,412	7,782,233
	Climb-out	24,802,095	18,435,738	14,569,573	19,900,931
	Landing	14,827,780	11,021,693	8,710,330	11,897,649
	Idle/Taxi in	8,532,050	6,341,990	5,012,009	6,846,024
	Idle/Taxi out	23,165,367	17,219,136	13,608,105	18,587,638
VOCs	Take-off	6,282	4,998	3,346	4,387
	Climb-out	16,064	12,780	8,557	11,217
	Landing	9,604	7,640	5,115	6,706
	Idle/Taxi in	5,526	4,396	2,943	3,859
	Idle/Taxi out	15,004	11,936	7,992	10,477
NO_x	Take-off	37,478	41,272	39,759	54,340
	Climb-out	95,841	105,542	101,672	138,959
	Landing	57,298	63,098	60,784	83,076
	Idle/Taxi in	32,970	36,307	34,976	47,803
	Idle/Taxi out	89,516	98,577	94,963	129,789
$PM_{2.5}$	Take-off	190	90	85	88
	Climb-out	486	229	217	224
	Landing	291	137	130	134
	Idle/Taxi in	167	79	75	77
	Idle/Taxi out	454	214	203	209
SO_x	Take-off	4,325	3,216	2,539	3,465
	Climb-out	11,059	8,223	6,492	8,860
	Landing	6,612	4,916	3,881	5,297
	Idle/Taxi in	3,804	2,829	2,233	3,048
	Idle/Taxi out	10,329	7,681	6,064	8,275

4.3.5 Air quality modeling, health impact, and economic analysis

I use Source−Receptor (S−R) matrices built from Intervention Model for Air Pollution (InMAP) called ISRM to estimate changes in annual average concentrations of $PM_{2.5}$.[41] I use hazard ratio from Krewski et al. (2019) in the log-linear concentration-response function for estimating premature deaths.[42] More details are discussed in the introduction section of this dissertation.

For estimating monetary damages, social cost of CO_2 is assumed as 42 per tonne CO_2 (i.e., \$0.042/kg CO_2) in year-2020 dollars, from the National Academy of Sciences report: Valuing Climate Damages Updating Estimation of the Social Cost of Carbon Dioxide (2017).[43] Value of statistical life (VSL) in year-2020 dollars is assumed as \$9.7 million per death which is based on \$8.3 million per death from Goodkind et al. (2019),[41] then inflation adjusted to year-2020 using U.S. Bureau of Labor Statistics's CPI inflation calculator.[44]

4.3.6 Metrics

Premature deaths, CO_2 emissions, and exposure disparities are estimated for each O-D pair and then aggregated and averaged for each mode. Averages are estimated for all O-D pairs for a mode and for same O-D pairs for any two modes to provide pairwise comparison.

Metrics presented in this chapter are:

1. Deaths per megaton = sum of deaths in each ISRM grid cell

2. CO_2 emissions per megaton = CO_2 EF × Length of route (CO_2 EF = kg per megaton per mile)

3. Deaths per 100,000 people per megaton = $\frac{\text{Number of premature deaths}}{\text{Population}} \times 100{,}000$

4.Total deaths = Deaths per megaton × Tonnage

5. Risk gap = Deaths per 100,000 people for most exposed group – Deaths per 100,000 people for total population

6. $Z_{SA} = \frac{SA1}{SA2}$

Where, SA1 = Simple average deaths or CO_2 emissions or risk gap per megaton from mode 1

SA2 = Simple average deaths or CO_2 emissions or risk gap per megaton from mode 2

7. $Z_{WA} = \frac{WA1}{WA2}$

WA1=Tonnage-weighted average deaths or CO_2 emissions or risk gap per megaton from mode 1

WA2=Tonnage-weighted average deaths or CO_2 emissions or risk gap per megaton from mode 2

8. Population weighted average $PM_{2.5}$ concentration = $\frac{\sum_{i=1}^{n} P_i [PM_{2.5}]_i}{\sum_{i=1}^{n} P_i}$

Here, P_i is the number of people of a specific demographic group in grid cell i, $[PM_{2.5}]_i$ is concentration in grid cell i, and n is total number of grid cells.

4.4 Results

4.4.1 Health and climate impacts and exposure disparity by mode and origin-destination (O-D) pair

Figure 4.3 shows deaths per megaton (Part A), kg CO_2 emissions per megaton (Part B), and risk gap per megaton between most exposed racial-ethnic group and population average exposure (Part C) for each O-D pair that is common between two modes (six lower left plots) and all modes (six upper right yellow subplots). Z_{SA} and Z_{WA} metrics are shown in the Figure 4.4. Figure 4.5 is the summary of Figure 4.3 showing average premature deaths, average CO_2 emissions, and risk gap per megaton by mode for common O-D pairs between any two modes (Part A) and all modes (Part B).

For aircrafts, there is lack of publicly available data that provides direction of landing or climb-out relative to runway. To account for both possibilities, I estimate premature mortalities from LTO using both orientations: original and reversed (where landing and climb-off segment of the LTO cycle for the aircraft emissions is reversed between ends of runway). The results show an average absolute difference of 0.04 deaths per megaton (or 4% relative to original) between reversed and original among all O-D pairs. Range of differences between two orientations among all O-D pairs is -0.15 to 0.16 deaths per megaton (or -22% to 31% relative to original among O-D pairs). For the aircraft results here, I used average of the two orientations. Premature mortality from cruise emissions from all O-D pairs is estimated to be very low and are not included in the aircraft impacts. Though findings from Barrett et al. (2010) show that globally ~8000 premature mortalities per year are attributable to aircraft cruise emissions, 458 of which occur in the U.S.[35] ISRM results showing low mortality from cruise emissions in this work requires further investigation.

Health impacts. I find that, on an average, shipping 1 megaton of freight by aircraft has the greatest health damages per megaton from $PM_{2.5}$ followed by rail, barge, and lowest for truck. If O-D pairs are weighted by 2017 tonnage, I find the same order but relative difference changes.

Average [tonnage-weighted] health damages per megaton from rail are 2 [3] times greater than truck, barge 1.1 [1.3] times greater than truck (almost same), rail 2 [2] times greater than barge, and aircraft 2 [5], 1.4 [2], 2 [5] times greater than truck, rail, and barge, respectively. Among the 214 O-D pairs, I find the same order. Overall, among all O-D pairs, average aircraft damages originate from runway [63%] (taxi-in, taxi-out, and take-off), climb off [23%], and landing [14%]. In Figure 4.4 (A), for aircraft, there are certain O-D pairs that have significantly greater deaths per megaton (and risk gap in Figure 4.3 (B)) than the rest of O-D pairs (>2.2 deaths per megaton shown by the horizontal patch of points in part A of Figure 4.4) – most of those O-D pairs have Los Angeles as the origin or destination.

Average health damages from each $PM_{2.5}$ precursor by mode and O-D pairs are shown in the appendix, Figures C3-C7. Figure C8 and C9 show the average metrics for each $PM_{2.5}$ precursor by mode-combinations and all O-D pairs for each mode. Tonnage-weighted estimates by precursor type are provided in excel sheet in the SI. Health damages across modes are dominated by particulate nitrate (pNO_3). Damages from particulate sulfate (pSO_4) are only significant from aircraft. Table C3 provides Z_{SA} by precursor type for each mode combination. Primary $PM_{2.5}$-related average premature deaths per megaton from aircraft are lower than truck, rail, and barge. Overall, for truck, contributions by each species are 6% (primary $PM_{2.5}$), 87% (pNO_3), 1% (pSO_4), 4% (SOA), and 3% (NH_3); for rail the contribution is 15% (primary $PM_{2.5}$), 83% (pNO_3), 0% (pSO_4), 1% (SOA), and 0% (NH_3), for barge the contribution is 15% (primary $PM_{2.5}$), 84% (pNO_3), 0% (pSO_4), 1% (SOA), and 0% (NH_3), and for aircraft the contribution is 3% (primary $PM_{2.5}$), 77% (pNO_3), 13% (pSO_4), 7% (SOA), and 0% (NH_3).

Climate impacts. Climate damages from CO_2 emissions per megaton are greatest from aircraft, followed by truck, barge, and lowest for rail. If O-D pairs are weighted by 2017 tonnage, I find a slightly different order and different relative difference: Air>Truck>Rail>Barge. Average [tonnage-weighted] CO_2 emissions (kg) per megaton from truck are 3 [2] times greater than rail, truck 3 [2.5] times greater than barge, barge 1.4 [0.8] times of rail, and aircraft 6 [17], 25 [34], 21 [42] times greater than truck, rail, and barge, respectively. Among the 214 O-D pairs, I find the same conclusions. For barge, there are O-D pairs that have significantly larger CO_2 emissions per megaton (>75 kg per ton) that rest of the pairs, the routes between those O-D pairs cross via

Panama Canal. The length of routes via Panama Canal is significantly larger than other inland waterways which increases CO_2 emissions per megaton.

Exposure disparity. Risk gap per megaton between most exposed and population average exposure is greatest in aircraft follows by rail, truck, and barge. Truck and barge show almost same disparity. Average [tonnage-weighted] risk gap per megaton from rail is 2 [3] times greater than truck, truck 1.1 [1.1] times of barge (almost same), rail 2 [2.2] times greater than barge, and aircraft 3 [8], 3 [4], 5 [11] times greater than truck, rail, and barge, respectively. Among the 214 O-D pairs, I find the same conclusions.

National estimates. Using U.S. DOT's FAF data, I estimate total premature deaths and CO_2 emissions from each mode in year 2017: 660 premature deaths and 124 million kg of CO_2 from truck, 663 and 23 million kg [rail], 65 and 3 million kg [barge], and 2 and 1 million kg [aircraft]. Total premature deaths for population age≥35 years is shown in Table C2 of appendix.

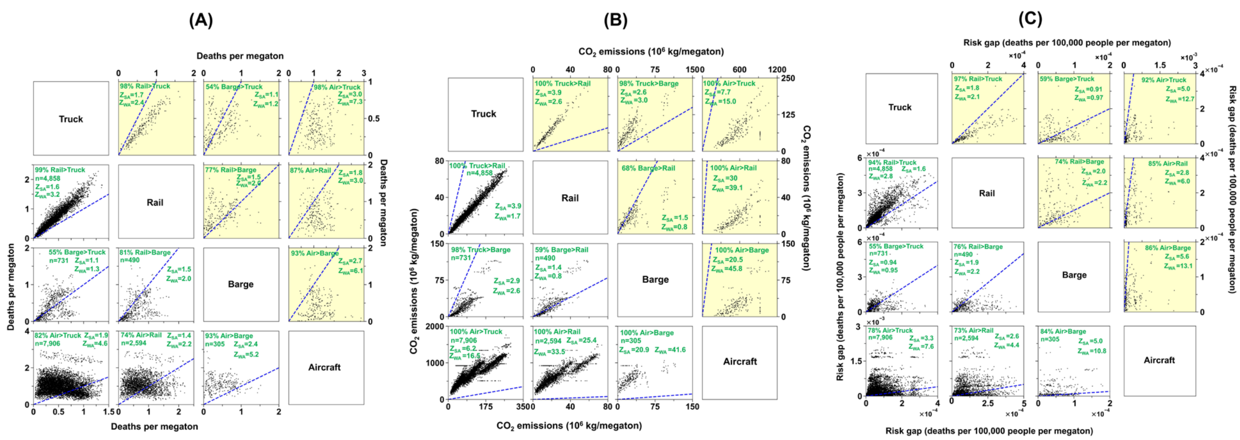

Figure 4.4 Health and climate impacts and risk gap among racial-ethnic groups by freight mode and each origin-destination (O-D) pair. (A) Deaths from $PM_{2.5}$ per megaton of freight shipped, (B) Carbon dioxide (CO_2) emissions per megaton of freight shipped, (C) risk gap between most exposed racial-ethnic group and population average (deaths per 100,000 people per megaton of freight shipped). Each dot represents an O-D pair. Lower six plots contains data points for all O-D pairs ("n") that are common between two modes and upper six plots (yellow color) have data points for 214 O-D pairs that are common across all modes. The blue dashed line signifies y=x line. Percentages in each plot shows percent of data points above y=x line for the mode that has the greater metric in the respective plot A, B, and C. For example, 99% of all O-D pairs that are common among truck and rail have greater health impacts from rail than truck. Z_{SA} [Z_{WA}] represents ratio of simple average [2017 tonnage-weighted average] of a metric for the mode with greater percentage to the mode with lower percentage. For example, for Rail-Truck, Z_{SA}=1.6 means average deaths per megaton for rail is 1.6 times of truck. Z_{WA}=3.2 means tonnage-weighted average deaths per megaton for rail is 3.2 times of truck.

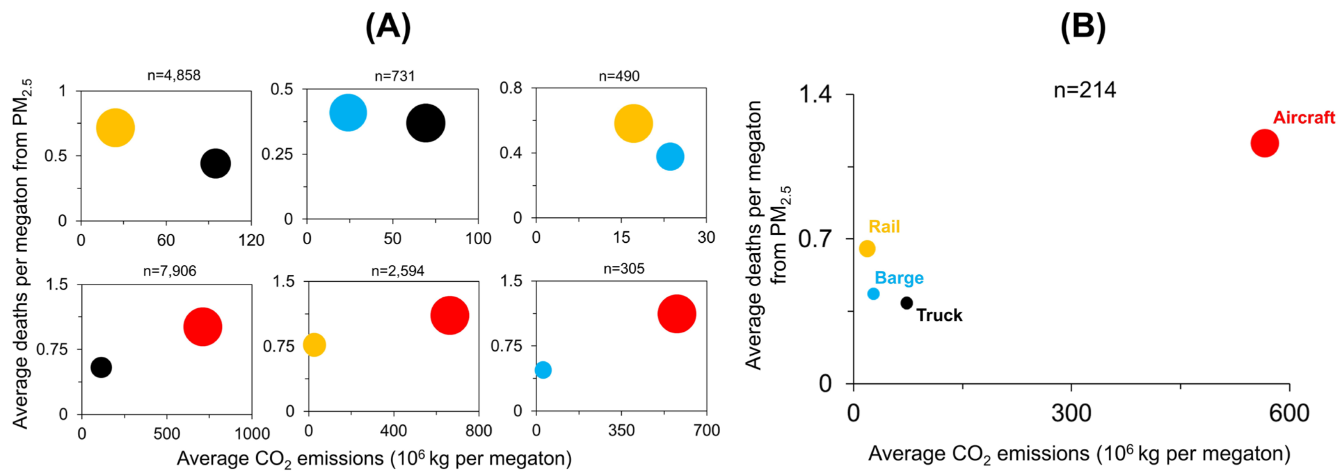

Figure 4.5 Average deaths from $PM_{2.5}$ and CO_2 emissions per megaton of freight by mode. Icon area is proportional to risk gap per megaton (deaths per 100,000 people per megaton). "n" represents number of common routes between two modes. (A) Summary for same O-D pairs between two modes and (B) Summary for same O-D pairs among all modes.

4.4.2 Health impacts in urban and rural areas

Table 4.3 shows health impacts in urban and rural areas for all O-D pairs by mode. I find that truck, rail, and barge has larger impacts in rural than urban areas whereas aircraft has larger impacts in urban than rural areas.

Table 4.3 Health impacts in urban and rural areas

Mode	n	Total (average deaths per megaton)	Urban (average deaths per megaton)	Rural (average deaths per megaton)	% of O-D pairs which have greater impacts in urban than rural areas
Truck	16,293	0.52	0.25	0.28	32%
Rail	4,875	0.72	0.34	0.38	32%
Barge	732	0.41	0.17	0.24	19%
Aircraft	7,913	1.01	0.65	0.36	85%

4.4.3 Differences in damages by racial-ethnic Groups

Overall, inter-state freight movement in the U.S. disproportionately impacts white non-Latinos relative to other racial-ethnic groups (Figure 4.6 A). However, blacks are the most exposed group than others in the urban areas. Analyzing by mode, overall, in the U.S, truck and rail damages are largest for white non-Latinos, barge damages are largest for blacks, and aircraft damages are largest for mixed/other groups (Figure 4.6 B). However, impacts differ in urban and rural areas for each mode. In urban areas, truck, rail, and barge damages are largest for blacks than other racial-ethnic groups (aircraft damages are largest for mixed/other group as in the whole U.S.). In rural areas, aircraft damages are largest for blacks (white non-Latinos is second most exposed group in rural areas and risk gap is small between the two groups) than other racial-ethnic groups. Barge has greater risk gap between blacks and white non-Latinos in the rural areas than urban and whole U.S.

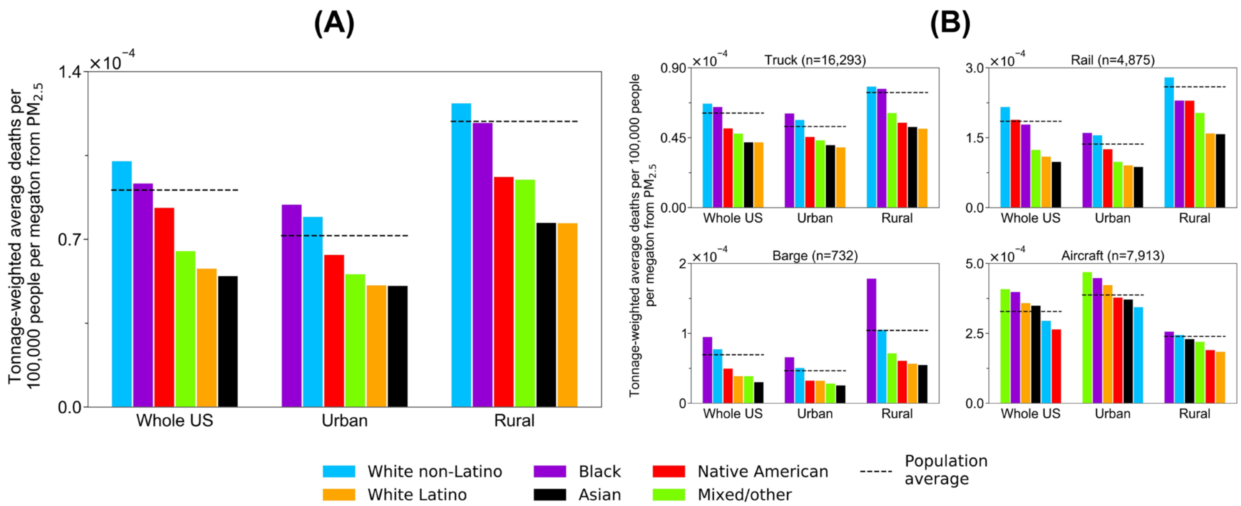

Figure 4.6 (A) Impacts by racial-ethnic group in the whole U.S., only urban areas, and only rural areas from freight transportation (B) Impacts by racial-ethnic group in the whole U.S., only urban areas, and only rural areas from freight modes.

4.4.4 Monetary damages

I estimate health and climate monetary damages from each mode (Figure 4.7) and find that total average monetary damages are largest from aircraft followed by truck, rail, and barge. Average health-related ($PM_{2.5}$) monetary damages are largest from aircraft followed by rail, barge, and truck. Average climate-related (CO_2) monetary damages are largest from aircraft followed by truck, barge, and rail. Figure C10 in the appendix shows health and climate monetary damages from each mode for all O-D pairs. I find that truck, rail, and barge have higher health-related monetary damages [5, 7, and 4 million US dollars (USD) per megaton] than climate-related monetary damages [4.6, 1, and 1 million USD per megaton]. Aircraft has higher climate-related monetary damages [30 million USD per megaton] than health-related monetary damages [10 million USD per megaton].

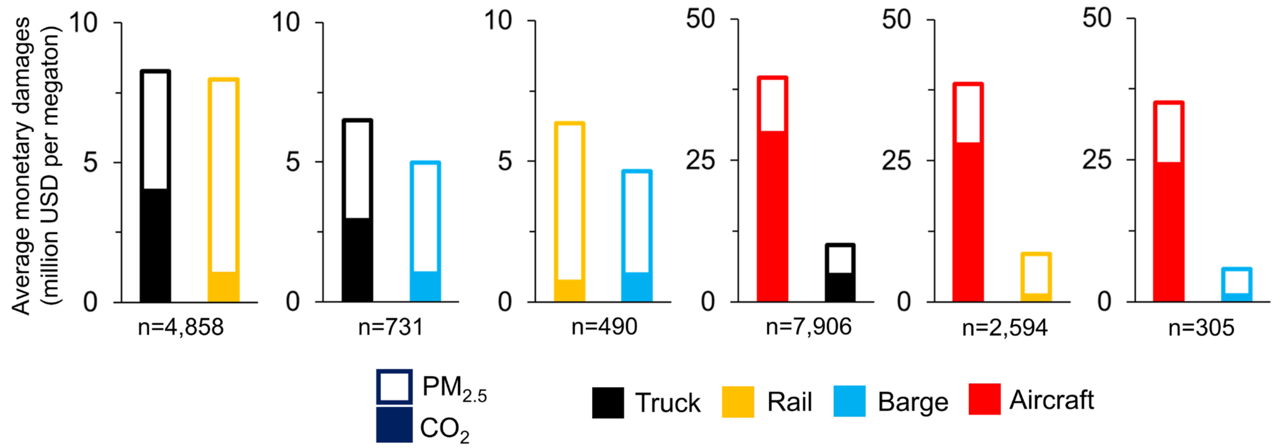

Figure 4.7 Average monetary damages from $PM_{2.5}$ and CO_2 emissions in million USD per megaton of freight by mode.

4.5 Discussion

This work quantifies and compares health impacts, climate impacts, and exposure disparity from transporting a unit mass of freight from origin to destination. This work is also first to explore exposure disparity between different racial-ethnic groups from inter-state freight transportation.

I find that aircraft poses the greatest health and climate damages among all other modes. My assumptions use conventional jet fuel (sulfur content: 700 ppm) for aircraft as it is currently used in practice. Future efforts in the aviation industry are pushing Ultra Low Sulfur Petroleum Jet Fuel (ULSJ) to fuel the aircrafts.[45] ULSJ has lower sulfur content (sulfur content: 11 ppm) but higher $PM_{2.5}$ emissions (approximately twice as much as conventional jet fuel). CO_2 emissions remain same in ULSJ and conventional jet fuel. I did sensitivity analysis to quantify health impacts from ULSJ. I find that overall, the average deaths per megaton decreased by ~10% compared to original (conventional jet fuel). Even with ULSJ fuel, aircraft still has higher impacts than rail, barge, truck (though the gap is lowered by 18%-31%; largest for rail; Table 4.4). This is an expected result because most of the aircraft health impacts are from pNO_3 (which remains unchanged for ULSJ).

Table 4.4 Difference between health impacts from conventional jet fuel and ULSJ aircraft and truck, rail, and barge

Mode combination (Air – Mode 2)	Difference in health impacts from conventional jet fuel aircraft and mode 2 (deaths per megaton)	Difference in health impacts from ULSJ aircraft and mode 2 (deaths per megaton)
Air-Truck	0.47	0.37
Air-Rail	0.34	0.24
Air-Barge	0.65	0.53

Health impact estimates for barge do not include part of route that goes via Panama Canal due to ISRM grid domain constraint (Figure C11). As a sensitivity analysis, I find that part of the barge routes that are in the ocean or near the U.S. coastline have average impacts of 6.7×10^{-5} deaths per megaton per mile (range: 3.2×10^{-5} to 16.8×10^{-5} deaths per megaton per mile among routes). Routes that go via Panama Canal have a length = 3506 miles outside the InMAP grid. This results an average of 0.23 deaths per megaton from in-ocean segment of barge route via Panama Canal.

Among the non-aircraft modes, rail has the greatest health impacts and lowest climate impacts per megaton of freight movement. Truck has the lowest health impacts among all modes and greatest climate impacts among the non-aircraft modes. Barge has slightly greater health impacts than truck and greater climate damages than rail. Efforts from shipping companies and policymakers to incentivize rail due to its high efficiency and lower carbon emissions per ton-mile may also consider health impacts that arise from rail transportation.

For estimating truck exposures, I used long-haul heavy-duty truck for all the O-D pairs irrespective of their length. GREET and MOVES model assumes that combination trucks with a range greater than 200 miles per day are considered as long-haul and less than 200 miles are considered as short-haul. In this work, O-D pairs less than 200 miles carry 19% of the total truck ton-miles. As a sensitivity analysis, I estimated health impacts from short-haul trucks for the routes less than 200 miles. I find that health impacts from short-haul truck are 51-61% (average is 58%) lower than long-haul trucks for the routes less than 200 miles.

I find that health impacts from $PM_{2.5}$ are dominated by NO_x emissions for all modes. This complements previous findings and hence efforts should be directed towards lowering NO_x emissions from freight modes.

I investigated exposure disparity among racial-ethnic groups from freight movement across states and regions by four modes and find that impacts from truck and rail are greatest for white non-Latinos, impacts from barge are greatest for blacks, and impacts from aircraft are greatest for mixed/other groups. Health impacts and disparity among groups differ in urban and rural areas. These findings add to the efforts of exploring environmental inequality and injustice from the transportation systems. Future research can benefit from exploring disparity within cities and regions (intra-regional) from the transportation systems.

The findings presented in this work are based on a novel reduced-complexity air quality model, InMAP (offering high spatial resolution estimates at low computational requirements) and a standard C-R function (log linear, non-threshold) for the concentrations found in the U.S. Like any other air quality modeling study is based on model assumptions, my results are sensitive to InMAP's assumptions and limitations. These results can be replicated using other air quality models including RCMs (APEEP/AP4, EASIUR) and complex chemical transport models (CAMx, CMAQ) and C-R functions such as supralinear or allowing the C−R to vary by source, geography, or chemical components. Additionally, availability and access to precise data such as specific origin and destination locations in the U.S. DOT's FAF4 database can be useful for better estimates. Aircraft routing (LTO and cruise) can be improved using data from FlightAware, a digital aviation company that operates the world's largest flight tracking and data platform.[46] Future work can also explore health and climate impacts by commodity type (coal, cereal grains, gasoline, fertilizers, electronics, furniture, etc.) and value of commodity shipped (USD) – data for which is available through FAF4 database.

Emissions from transportation systems in the U.S. have decreased through the years especially through fuel and vehicle technology regulations (e.g., sulfur content in the fuels, NO_x control equipment), but it is still one of the largest source of health impacts among any other energy sectors.[47] With the expanding e-commerce industry, reliance on freight modes is expected to increase dramatically in the future leading to increased emissions that impact human health and climate. The findings from this work can be used by shipping companies, e-commerce industry, transportation planners, and policymakers to make decisions on modal choices that have least impact on human health, climate, and exposure disparity.

Chapter 5

Conclusions and future work

5.1 Summary of findings

This dissertation investigates air quality, human health and climate impacts, and human health disparities from emissions originating from two source sectors: electricity generation (point sources) and freight transportation (line or mobile sources). Pollutants investigated in this work are $PM_{2.5}$ (air quality, health impacts, and health disparity) and CO_2 (climate impacts) as they are known to have the largest impacts on human health and climate among any other pollutants.

The following are the main research findings in the order of the research objectives of this dissertation:

Objective 1: Quantify and compare average and average marginal emissions factors for a greenhouse gas (CO_2) and two criteria pollutants (NO_x, SO_2) from electricity generation in a U.S. Regional Transmission Organization (RTO).

1. I find that overall, in the Midcontinent Independent System Operator (MISO), average emission factors are generally higher than marginal estimates (typical difference: ~20%). For example, average marginal emission factor for CO_2 is 19% lower than the average emission factors. This finding means that the true climate benefits of an energy efficiency program may be ~19% smaller than anticipated if one were to base expectations on average emissions factors.
2. The relative difference between average and average marginal emission factor varies by state, utility, and each generator, though average emission factor is generally greater than average marginal emission factor at all scales.
3. For MISO, coal is the dominant marginal fuel at low demand hours; natural gas is the dominant marginal fuel at high demand hours.

4. Average marginal emission factors are higher-than-average during late-night and early morning hours when electricity demand is lower and coal is more often on the margin: AMEF is about 73% [CO_2], 125% [SO_2], and 55% [NO_x] higher at midnight compared to noon.
5. I show that estimating recent average marginal emission factors can be done using data rather than models.

Objective 2: Quantify health impacts from electricity generation by geography (national, RTO, state), race, and income.

1. I find that blacks are disproportionately affected by power plant emissions nationally, but most-exposed race/ethnicity varies by state and by RTO.
2. I find that exposures are higher for lower-income than for higher-income, but disparities are larger by race than by income.
3. I estimate ~16,400 deaths nationally, 86% of which occur in RTOs. Within states, total deaths vary from ~1,850 deaths/year (Pennsylvania) to ~1 death/year (Montana).
4. Deaths per unit energy generated vary substantially among regional grids, by up to a factor of ~30 (MISO vs CAISO), with higher values in coal-heavy grids (MISO, SPP).
5. Geographically, I observe differences between where electricity is generated and where people experience the resulting $PM_{2.5}$ health consequences; some states are net exporters of health impacts, other are net importers. For 36 U.S. states, most of the health impacts are attributable to emissions in other states.

Objective 3: Quantify and compare health and climate impacts and exposure disparity among racial-ethnic groups from inter-state freight transportation by mode, route, and emission species.

1. Overall, the order of average impacts by mode is:
    - Health impacts from $PM_{2.5}$ (premature deaths per megaton): Aircraft>Rail>Barge>Truck.
    - Climate impacts from CO_2 (kg CO_2 emissions per megaton): Aircraft>Truck>Barge>Rail.

- Exposure disparity between most exposed racial-ethnic group and population average exposure (premature deaths per 100,000 people per megaton): Aircraft>Rail>Truck>Barge.

2. Overall, the order of average monetary damages (million USD per megaton) by mode is:
    - Total average monetary damages: Aircraft>Truck>Rail>Barge.
3. $PM_{2.5}$ monetary damages are greater than CO_2 monetary damages per megaton for truck (within 10%), rail, and barge and CO_2 monetary damages are greater than $PM_{2.5}$ monetary damages per megaton for aircraft.
4. $PM_{2.5}$-related health impacts per megaton from truck, rail, and barge are larger in rural areas than in urban areas whereas aircraft impacts per megaton are larger in urban than in rural areas. Those results reflect that inter-state travel is mostly in rural areas for truck, rail, and barge, whereas for aircraft the ground-level emissions are often in urban areas.
5. Inter-state freight movement in the U.S. disproportionately impacts white non-Latinos more than other racial-ethnic groups.
6. Truck and rail $PM_{2.5}$ exposure is greater for white non-Latinos than blacks whereas barge $PM_{2.5}$ exposure is greater for blacks than white non-Latinos. Aircraft $PM_{2.5}$ exposure is greater for mixed/other and black race groups than for white non-Latinos.

Objective 4: Conduct spatial air quality modeling using the Intervention Model for Air Pollution (InMAP) – a novel reduced-complexity air quality model.

1. InMAP is used to model $PM_{2.5}$ concentrations from two $PM_{2.5}$ emitting source sectors: electricity generation (point) and freight transportation (mobile).
2. InMAP offers capability to model several scenarios with less computational resources and time.
3. InMAP provides output concentrations at a very fine resolution from 1km×1km in urban areas to as large as 48 km×48 km in rural areas.

Interestingly, I observe that $PM_{2.5}$ health impacts from interstate freight is, like electricity generation, larger in rural areas, which likely skews the damages towards white people.

5.2 Limitations

Specific limitations are discussed in each chapter. I highlight here the broader limitations of this research work.

The data-driven empirical approach for estimating average and average marginal emission factors is based on historical data. That means it may be inappropriate to use average and average marginal emission factor findings from Chapter 2 unmodified if considering major shifts in the electricity infrastructure. Since results presented in Chapter 2 are based on historical data, they likely would not be directly applicable for predicting long-term changes in the electricity grid.

The health impact analysis presented in this dissertation is based on one reduced-complexity air quality model – InMAP. InMAP offers many strengths over other complex CTMs and RCMs: high spatial resolution is useful for investigating environmental disparity questions, high computational efficiency offers greater ability to test many scenarios and cases, and ability to model long-range transport of $PM_{2.5}$ and spatially variable secondary $PM_{2.5}$ formation from all $PM_{2.5}$ precursors. However, reduced computational intensity in InMAP comes at a cost which leads to some limitations of the model: (1) InMAP is better at predicting population-weighted changes in primary $PM_{2.5}$, pSO_4, and SOA concentrations ($R^2 \geq 0.9$) than it is in predicting changes in pNO_3 and pNH_4 concentrations ($R^2 \geq$ 0.4-0.8), (2) in general, InMAP tends to underpredict observed total $PM_{2.5}$ concentrations, and (3) a temporally-explicit analysis is not possible with current version of InMAP. Additionally, current InMAP version uses 2005 data for physics and chemistry parameters and baseline concentrations – future analysis can benefit from updated data for the most recent year such as 2014 NEI emissions dataset. The results from chapter 3 and 4 can be reproduced using different models such as complex chemical transport models (CAMx, CMAQ, WRF-Chem), other reduced-complexity air quality models (APEEP/AP2, EASIUR), and land-use regression models. This dissertation does not model health impacts from ozone (though other research suggests that impacts from ozone only comprise a small proportion of total air pollution health impacts) because the current version of InMAP cannot model ozone. Future efforts can integrate ozone impacts into the health impact estimates of this study.

A linear, non-threshold concentration-response function is used to link $PM_{2.5}$ concentration to health risk. Future research can explore impact on results from the alternative concentration−response functions (e.g., a supralinear C−R) or allowing the C−R to vary by source, geography, or chemical components. Additionally, considering differential impacts from indoor versus outdoor exposure is another aspect of research that needs to be addressed in current health impact modeling tools and methods.

For nearly all research, up-to-date data is preferable to outdated data. For example, in Chapter 2, future analysis can benefit from availability of total generation (including renewables) and electricity import and exports data at the state and utility levels. Updated emissions for a more-recent year, such as 2017 National Emissions Inventory (NEI) emissions and tonnage data from most recent version of Freight Analysis Framework (FAF) data can be used to explore the impact on results presented in Chapter 3 and 4. Availability of FAF data for specific origin and destination (O-D) locations (not by zones or regions) and release of GIS data on routes modeled under FAF assumptions for each O-D pair may improve estimates presented in Chapter 4.

5.3 Policy implications

The empirical and mechanistic modeling methods described in this dissertation could be extended to other energy sectors. Reducing air pollution and its impacts is an important policy goal of federal, state, and local agencies. InMAP is a useful tool to help answer policy questions related to air quality. InMAP's ability to produce high spatial resolution outputs in a computationally inexpensive way makes it more accessible to scientists, policymakers, planners, and people.

The analysis presented in the Chapter 2 can usefully be extended to other regions to support effective near-term technical, policy and investment decisions based on marginal rather than only average emission factors. In Chapter 2, I point out that average marginal emission factors are generally lower than average emission factors for electricity generation in Midcontinent Independent System Operator (MISO). The deployment of renewable energy sources in MISO region such as wind and solar will help reduce emissions by displacing energy from fossil-fired generators. However, if a decision-maker uses average emission factor to understand the current contribution of renewables or other interventions in the electricity system, she/he will likely overestimate the emission benefits that are derived from such interventions. Electric vehicles (EVs) however are the opposite – using more electricity from the grid but reducing emissions in the transportation sector. So, if a decision-maker uses average emission factors to estimate the emission change from EVs, she/he is overestimating the prospective new electricity emissions, and therefore underestimating the emission benefit that would be attributable to EVs.

The results presented in the Chapter 3 are useful for scientists and policymakers to understand and address disparities in air pollution exposure by race, income, and geography. The metrics and data presented can be useful to scientists to apply to new energy scenarios to understand the health damages caused or avoided.

The results from chapter 4 answer a major policy question in the freight transportation sector: which freight mode has least health and climate impacts? This research adds a major contribution to the literature of freight transportation on comparison of environmental impacts between all four major modes (truck, rail, barge, aircraft) of freight transportation. Results can be useful to scientists, policymakers and transportation planners to develop future strategies that not only focus on climate impacts but also health impacts of freight transportation choices.

The environmental justice findings educate policymakers, planners, and people on environmental disparity issues prevailing in the electricity and freight sector and fuels efforts to address the environmental injustice issues.

5.4 Intellectual impact so far

Table 5.1 shows the impact so far of two published research papers from this dissertation (Chapter 2 and 3).

Table 5.1 Intellectual impact of this dissertation so far

Research paper	Intellectual impact so far
Thind, M.P.S.; Tessum, C.W; Azevedo, I.L.; Marshall, J.D. **Fine Particulate Air Pollution from Electricity Generation in the US: Health Impacts by Race, Income, And Geography**. *Environ. Sci. Technol.* 2019, 53, 14010−14019. DOI: https://doi.org/10.1021/acs.est.9b02527	• Education: covered by several news outlets to disperse environmental justice-related findings from this work • Data used and cited in the University of California, Berkeley's 2035 report: "Plummeting solar, wind, and battery costs can accelerate our clean electricity future" • Cited by two other research publications as of July 25, 2020 • Data requests by organizations working towards environmental justice issues
Thind, M.P.S.; Wilson, E.J.; Azevedo, I.L.; Marshall, J.D. **Marginal Emissions Factors for Electricity Generation in the Midcontinent ISO**. *Environ. Sci. Technol.* 2017, 51, 14445–14452. DOI: https://doi.org/10.1021/acs.est.7b03047	• Barr Engineering company used emission factor data developed in this work for marketing under U.S. EPA's former Clean Power Plan • Cited by eight other research publications as of July 25, 2020 • The manager for the environmental policy department at the Xcel Energy Inc. (an electric utility) found the results useful and discussed some interesting implications of temporal results for electric vehicle charging and other time-flexible and potentially controllable loads.

5.5 Future areas of research

This dissertation explores air quality, health and climate impacts, and disparities from air pollution sources using empirical and air quality model approaches. Paolella et al. (2018) demonstrated the importance of fine spatial resolution for identifying and quantifying exposure disparities.[1] InMAP provides a computationally inexpensive way to model air quality impacts at a fine spatial resolution useful to quantify exposure disparities and answer research questions that require running different scenarios and cases multiple times. I discuss here possible future directions of research that are based on methods and new findings from this dissertation.

Marginal emission factors play an important role in understanding emission benefits from electrifying transportation and other sectors. If a scenario is imagined in the future with hundreds of thousands or millions of electric vehicles (EVs) in a utility's service territories, the time of EV charging matters. The results from chapter 2 show that average marginal emission factors are higher during early morning and late evening hours (than during the day) for the grid operating in the Midwest states (MISO). Does that mean plugging EVs for charging during work or afternoon hours are likely to have maximum emission benefits? This is an important policy question to incentivize EV owners regarding when to charge their EVs to have maximum environmental benefits. Future research can explore this question and quantify environmental benefits of EV charging scenarios by studying interactions of increased electric vehicle fleet with the electric grid, utilizing marginal emission factors for estimating emission benefits.

Chapter 3 shows exposure disparities in the power sector as well as cross-state $PM_{2.5}$ impacts. This work doesn't explore cross-state contribution of fine particulate matter pollution to exposure disparity in the U.S. Future research can explore that as an extended work to understand cross-state aspects of environmental justice in more detail.

Agriculture is another source of $PM_{2.5}$ emissions that impacts human health. Thakrar et al. (2020) estimated that the food and agriculture sector is attributable to thousands more deaths each year than the electricity sector.[2] Replacing petroleum-based vehicle fuels with biofuels is considered an important strategy to mitigate greenhouse gas emissions.[3,4] Increased biomass production to meet the future demands of biofuel can also lead to increased emissions of $PM_{2.5}$. Future research can use InMAP capabilities to quantify and compare impacts of $PM_{2.5}$ emissions from different approaches to biomass feedstock production (corn, corn stover, miscanthus). The U.S. Department of Transportation (DOT)'s 2016 Billion-Ton Report Volume 2 is a great source of emissions and production data for different biomass feedstock sources (food crops and lignocellulosic biomass).[5]

Within the freight transportation sector, health and climate impacts can be further attributed to different commodity types and value of commodity shipped. U.S. DOT's FAF4 database provides tonnage, ton-miles, and value estimated by commodity type (coal, cereal grains, gasoline, fertilizers, electronics, furniture, etc.) and value of commodity shipped in U.S. dollars. Health disparities from exposure to emissions from local transport within U.S. cities is also an important environmental justice question that needs to be addressed. Finally, analyzing air quality impacts of different transportation choices by technology and fuel type is another interesting area to explore.

InMAP can be utilized to understand air quality and health benefits of future energy scenarios such as increased electric vehicles fleet and wind penetration in the electric grid. Further, InMAP can be integrated to Life Cycle Assessment (LCA) models such as National Renewable Energy Laboratory (NREL)'s Feedstock Production Emission to Air Model (FPEAM)[6] model to perform air quality and health impact assessment for LCA-related research questions. InMAP's capability to model high spatial resolution estimates can be used to do local-scale analysis; this will be useful to validate InMAP's performance to model local-scale impacts. A global version of InMAP is currently in the process of being released ; that version of the model could be used to replicate objectives and methods of this dissertation to other parts of the world, specially to explore environmental justice aspects of air pollution.

5.6 Closing remarks

It was an enjoyable and wonderful experience working on different research questions addressed in this dissertation. This dissertation investigates air quality, health and climate impacts, and exposure disparities from air pollution from two energy sectors: electricity generation and freight transportation. I hope the results from this dissertation not only educate scientists, policymakers, planners, and environmental justice advocates on the impacts of air pollution but also lead them to take necessary actions to tackle air pollution problems.

Citations

(by chapter)

Chapter 1

1. *The Earth as a System*; University Corporation for Atmospheric Research (UCAR) – Center for Science Education: Boulder, CO, 2020. https://scied.ucar.edu/longcontent/earth-system (accessed July 27, 2020).

2. Jacobson, M.Z. *Air Pollution And Global Warming: History, Science, And Solutions*, 2nd, ed.; Cambridge University Press: New York, NY, 2012.

3. *Criteria Air Pollutants*; U.S. Environmental Protection Agency: Washington, DC, 2018. https://www.epa.gov/criteria-air-pollutants (accessed July 27, 2020).

4. *What are Hazardous Air Pollutants?*; U.S. Environmental Protection Agency: Washington, DC, 2017. https://www.epa.gov/haps/what-are-hazardous-air-pollutants (accessed July 27, 2020).

5. *Overview of Greenhouse Gases*; U.S. Environmental Protection Agency: Washington, DC, 2020. https://www.epa.gov/ghgemissions/overview-greenhouse-gases (accessed July 27, 2020).

6. *NAAQS Table;* U.S. Environmental Protection Agency: Washington, DC, 2016. https://www.epa.gov/criteria-air-pollutants/naaqs-table (accessed July 27, 2020).

7. *Health and Environmental Effects of Particulate Matter (PM)*; US Environmental Protection Agency: Washington, DC, 2016; https://www.epa.gov/pm-pollution/health-and-environmental-effects-particulate-matter-pm (accessed July 27, 2020).

8. *Particulate Matter (PM) Basics;* US Environmental Protection Agency: Washington, DC, 2018; https://www.epa.gov/pm-pollution/particulate-matter-pm-basics#PM (accessed July 27, 2020).
9. *Health Effects of Ozone Pollution*; US Environmental Protection Agency: Washington, DC, 2019; https://www.epa.gov/ground-level-ozone-pollution/health-effects-ozone-pollution (accessed July 27, 2020).
10. Seinfeld, J.H.; Pandis, S.N. *Atmospheric Chemistry and Physics: From Air Pollution to Climate Change*, 2nd, ed.; John Wiley & Sons, Inc.: Hoboken, New Jersey, 2006.
11. Watson, J.G.; Chow, J.C.; DuBois, D.; Green, M.; Frank, N.; Pitchford, M.; *Guidance For Network Design and Optimum Site Exposure For $PM_{2.5}$ And PM_{10}*; EPA-454/R-99-022; U.S. Environmental Protection Agency: Washington, DC, December 1997; https://www3.epa.gov/ttnamti1/files/ambient/pm25/network/r-99-022.pdf (accessed July 27, 2020).
12. Goodkind, A.L.; Tessum, C.W.; Coggins, J.S.; Hill, J.D.; Marshall, J.D. Fine-Scale Damage Estimates of Particulate Matter Air Pollution Reveal Opportunities for Location-Specific Mitigation of Emissions. *Proc. Natl. Acad. Sci. U.S.A.* **2019**, 116, 8775-8780.
13. *Sources of Greenhouse Gas Emissions;* U.S. Environmental Protection Agency: Washington, DC, 2020. https://www.epa.gov/ghgemissions/sources-greenhouse-gas-emissions (accessed July 27, 2020).
14. Dockery, D. W.; Pope, C. A.; Xu, X. P.; Spengler, J. D.; Ware,J. H.; Fay, M. E.; Ferris, B. G.; Speizer, F. E. An association between air- pollution and mortality in six US cities. *N. Engl. J. Med.* **1993**, 329, 1753–1759.
15. Dockery, D. W.; Pope, C. A. Acute respiratory effects of particulate pollution. *Annu. Rev. Pub. Health* **1994**, 15, 107–132.
16. Pope, C. A.; Thun, M. J.; Namboodiri, N. M.; Dockery, D. W.; Evans, J. S.; Speizer, F. E.; Heath, C. W., Jr. Particulate air-pollution as a predictor of mortality in a prospective-study of US adults. *Am. J. Respir. Crit. Care Med.* **1995**, 151, 669–674.

17. Pope, C. A.; Burnett, R. T.; Thun, M. J.; Calle, E. E.; Krewski, D.; Ito, K.; Thurston, G. D. Lung cancer, cardiopulmonary mortality, and long-term exposure to fine particulate air pollution. *J. Am. Med. Assoc.* **2002**, 287, 1132–1141.

18. Pope, C. A.; Ezzati, M.; Dockery, D. W. Fine-particulate air pollution and life expectancy in the United States. *N. Engl. J. Med.* **2009**, 360, 376–386.

19. Kuenzli, N.; Kaiser, R.; Medina, S.; Studnicka, M.; Chanel, O.; Filliger, P.; Herry, M.; Horak, F., Jr.; Puybonnieux-Texier, V.; Quenel, P.; Schneider, J.; Seethaler, R.; Vergnaud, J.-C.; Sommer, H. Public-health impact of outdoor and traffic-related air pollution: a European assess- ment. *Lancet* **2000**, 356, 795–801.

20. Laden, F.; Neas, L. M.; Dockery, D. W.; Schwartz, J. Association offine particulate matter from different sources with daily mortality in six U.S. cities. *Environ. Health Perspect.* **2000**, 108, 941–947.

21. Bell, M. L.; Ebisu, K.; Belanger, K. The relationship between air pollution and low birth weight: effects by mother's age, infant sex, co- pollutants, and pre-term births. *Environ. Res. Lett*. **2008**, 3,1–7.

22. Schwartz, J.; Coull, B.; Laden, F.; Ryan, L. The effect ofdose and timing ofdose on the association between airborne particles and survival. *Environ. Health Perspect.* **2008**, 116,64–69.

23. Siddiqui, A. R.; Lee, K.; Bennett, D.; Yang, X.; Brown, K. H.; Bhutta, Z. A.; Gold, E. B. Indoor carbon monoxide and $PM_{2.5}$ concentrations by cooking fuels in Pakistan. *Indoor Air* **2008**, 19,75–82.

24. Jerrett, M.; Shankardass, K.; Berhane, K.; Gauderman, W. J.; K€unzli, N.; Avol, E.; Gilliland, F.; Lurmann, F.; Molitor, J. N.; Molitor, J. T.; Thomas, D. C.; Peters, J.; McConnell, R. Traffic-related air pollution and asthma onset in children: a prospective cohort study with individual exposure measurement. *Environ. Health Perspect.* **2008**, 116,1433–1438.

25. Schwartz, J.D.; Wang, Y.; Kloog, I.; Yitshak-Sade, M.; Dominici, F.; Zanobetti, A. Estimating the Effects of $PM_{2.5}$ on Life Expectancy Using Causal Modeling Methods. *Environ. Health Perspect.* **2018**, 126, 127002.
26. Muller, N.Z.; Mendelsohn, R.; Measuring the damages of air pollution in the United States. J Environ. Econ. Manage. **2007**, 54, 1–14.
27. *Ambient air pollution;* World Health Organization: Geneva, Switzerland, 2020; https://www.who.int/gho/phe/outdoor_air_pollution/en/ (accessed July 27, 2020).
28. Cohen, A.J.; Brauer, M.; Burnett, R.; Anderson, H.R.; Frostad, J.; Estep, K.; Balakrishnan, K.; Brunekreef, B.; Dandona, L.; Dandona, R.; Feigin, V.; Freedman, G.; Hubbell, B.; Jobling, A.; Kan, H.; Knibbs, L.; Liu, Y.; Martin, R.; Morawska, L.; Pope, C.A. III; Shin, H.; Straif, K.; Shaddick, G.; Thomas, M.; van Dingenen, R.; van Donkelaar, A.; Vos, T.; Murray, C.J.L.; Forouzanfar, M.H. Estimates and 25-Year Trends of the Global Burden of Disease Attributable to Ambient Air Pollution: An Analysis of Data from the Global Burden of Diseases Study 2015. *Lancet* **2017**, 389, 1907-1918.
29. Apte, J.S.; Brauer, M.; Cohen, A.J.; Ezzati, M.; Pope III, C.A. Ambient $PM_{2.5}$ Reduces Global and Regional Life Expectancy. *Environ. Sci. Technol. Lett.* **2018**, 5, 9, 546–551.
30. Lelieveld, J.; Evans, J.S.; Fnais, M.; Giannadaki; D.; Pozzer, A. The contribution of outdoor air pollution sources to premature mortality on a global scale. Nature **2015**, 525, 367–371.
31. Fann, N.; Fulcher, C. M.; Baker, K. The Recent and Future Health Burden of Air Pollution Apportioned Across US Sectors. *Environ. Sci. Technol.* **2013**, 47, 3580−3589.
32. Thakrar, S.K.; Balasubramanian, S.; Adams, P.J.; Azevedo, I.M.L.; Muller, N.Z.; Pandis, S.N.; Polasky, S.; Pope, C.A.; Robinson, A.L.; Apte, J.S.; Tessum, C.W.; Marshall, J.D.; Hill, J.D. Reducing Mortality from Air Pollution in the United States by Targeting Specific Emission Sources. *Environ. Sci. Technol. Lett.* **2020**, In Press. DOI: https://doi.org/10.1021/acs.estlett.0c00424.
33. Frischknecht R, Jolliet O. Global Guidance for Life Cycle Impact Assessment Indicators, Vol. 1. Paris, France: UNEP/SETAC Life Cycle Initiative **2016**.
34. Apte J.S.; Marshall J;D;, Cohen A;J;, Brauer M. Addressing global mortality from ambient $PM_{2.5}$. Environ Sci Technol. **2015**, 49, 8057-8066.

35. Pope III, C.A.; Coleman, N.; Pond, Z.A.; Burnett, R.T. Fine particulate air pollution and human mortality: 25+ years of cohort studies. Environmental Research **2020**, 183, 2020.
36. U.S. EPA. Integrated Science Assessment (ISA) for Particulate Matter (Final Report, 2019). U.S. Environmental Protection Agency, Washington, DC, EPA/600/R-19/188, 2019.
37. Krewski, D.; Jerrett, M.; Burnett, R.T.; Ma, R.; Hughes, E.; Shi, Y.; Turner, M.C.; Pope III, C.A.; Thurston, G.; Calle, E.E.; Thun, M.J. *Extended Follow-Up and Spatial Analysis of the American Cancer Society Study Linking Particulate Air Pollution and Mortality*; Research Report 140, Health Effects Institute, Boston, MA, May **2009**; https://www.healtheffects.org/system/files/Krewski140.pdf (assessed July 27, 2020)
38. Lepeule, J.; Laden, F.; Dockery, D.; Schwartz, J. Chronic exposure to fine particles and mortality: an extended follow-up of the Harvard six cities study from 1974 to 2009. *Environ. Health Persp.* **2012**, 120, 965–970.
39. *Quantitative Health Risk Assessment for Particulate Matter*; U.S. Environmental Protection Agency, Research Triangle Park, NC 2010; EPA-452/R-10-005.
40. Thakrar, S.K. ; Goodkind, A.L. ; Tessum, C.W. ; Marshall, J.D. ; Hill, J.D. Life Cycle Air Quality Impacts on Human Health from Potential Switchgrass Production in the United States. *Biomass and Bioenergy* **2017**,114, 73-82.
41. Hill, J.; Goodkind, A.; Tessum, C.; Thakrar, S.; Tilman, D.; Polasky, S.; Smith, T.; Hunt, N.; Mullins, K.; Clark, M.; Marshall, J. Air-quality-related health damages of maize. *Nature Sustainability* **2019**, 2, 397–403.
42. Vodonos, A.; Awad, Y. A.; & Schwartz, J. The concentration-response between long-term PM2.5 exposure and mortality; A meta-regression approach. *Environmental Research* **2018**, 166, 677–689.
43. Pope III, C.A.; Lefler, J.S.; Ezzati, M.; Higbee, J.D.; Marshall, J.D.; Kim, S.Y.; Bechle, M.; Gilliat, K.S.; Vernon, S.E.; Robinson, A.L.; Burnett, R.T. Mortality Risk and Fine Particulate Air Pollution in a Large, Representative Cohort of U.S. Adults. *Environ. Health Perspect.* **2019.** In Press. DOI 10.1289/EHP4438.
44. *Environmental Justice*; U.S. Environmental Protection Agency, Washington, DC 2020; https://www.epa.gov/environmentaljustice (accessed July 27, 2020).

45. Clark, L.P.; Millet, D.B.; Marshall, J.D. Changes in Transportation-Related Air Pollution Exposures by Race-Ethnicity and Socioeconomic Status: Outdoor Nitrogen Dioxide in the United States in 2000 and 2010. Environmental Health Perspectives **2017**, 125, CID: 097012.
46. Clark, L.P. Air quality, urban form, and environmental justice. PhD Dissertation, **2018**, University of Minnesota, Twin Cities.
47. Clark, L.P.; Millet, D.B.; Marshall, J.D. National patterns in environmental injustice and inequality: outdoor NO_2 air pollution in the United States. PLOS ONE. **2014**, 9, e94431.
48. Tessum, C.W.; Apte, J.S.; Goodkind, A.L.; Muller, N.Z.; Mullins, K.A.; Paolella, D.A.; Polasky, S.; Springer, N.P.; Thakrar, S.K.; Marshall, J.D.; Hill, J.D. Inequity in consumption of goods and services adds to racial-ethnic disparities in air pollution exposure. Proc. Natl. Acad. Sci. U.S.A. **2019**, 116, 6001–6006.
49. Humbert, S.; Marshall, J.D.; Shaked, S.; Spadaro, J.V.; Nishioka, Y.; Preiss, P.; McKone, T.E.; Horvath, A.; Jolliet, O. Intake Fraction for Particulate Matter: Recommendations for Life Cycle Impact Assessment. *Environ. Sci. Technol.* **2011**, 45, 4808-4816.
50. *Photochemical Air Quality Modeling*; U.S. Environmental Protection Agency: Washington, DC, 2017; https://www.epa.gov/scram/photochemical-air-quality-modeling (accessed July 27, 2020).
51. *CMAQ: The Community Multiscale Air Quality Modeling System*; U.S. Environmental Protection Agency, Washington, DC, 2018; https://www.epa.gov/cmaq (accessed July 27, 2020).
52. *Comprehensive Air Quality Model with Extensions (CAMx)*; Environ International Corporation, Novato, CA, 2016; http://www.camx.com/home.aspx (accessed July 27, 2020).
53. *GEOS-Chem Model*; Atmospheric Chemistry Modeling Group, Harvard University, Cambridge, MA, 2018; http://acmg.seas.harvard.edu/geos/index.html (accessed July 27, 2020).
54. *WRF-CHEM*; National Center for Atmospheric Research, University Corporation for Atmospheric Research, Boulder, CO, 2018; https://www2.acom.ucar.edu/wrf-chem (July 27, 2020).

55. Buonocore, J. J.; Dong, X.; Spengler, J. D.; Fu, J. S.; Levy, J. I. Using the Community Multiscale Air Quality (CMAQ) Model to Estimate Public Health Impacts of $PM_{2.5}$ from Individual Power Plants. *Environ. Int.* **2014**, 68, 200-208.
56. Carnevale, C.; Finzi, G.; Pisoni, E.; Volta, M. Neuro-Fuzzy and Neural Network Systems for Air Quality Control. *Atmos. Env.* **2009**, 43, 4811-4821.
57. GEOS-Chem Adjoint Model: Dedoussi, I. C.; Barrett, S. R. H. Air Pollution and Early Deaths in the United States. Part II: Attribution of $PM_{2.5}$ Exposure to Emissions Species, Time, Location and Sector. *Atmos. Environ*. **2014**, 99, 610-617.
58. DDM/ RSM Model: Foley, K. M.; Napelenok, S. L.; Jang, C.; Phillips, S.; Hubbell, B. J.; Fulcher, C. M. Two Reduced Form Air Quality Modeling Techniques for Rapidly Calculating Pollutant Mitigation Potential Across Many Sources, Locations and Precursor Emission Types. *Atmos. Environ*. **2014**, 98, 283-289.
59. Hakami, A.; Henze, D. K.; Seinfeld, J. H.; Singh, K.; Sandu, A.; Kim, S.; Byun, D.; Li, Q. The Adjoint of CMAQ. *Environ. Sci. Technol*. **2007**, 41, 7807-7817.
60. EASIUR Model: Heo, J.; Adams, P.J.; Gao, H.O. Reduced-Form Modeling of Public Health Impacts of Inorganic $PM_{2.5}$ and Precursor Emissions. *Atmos. Env*. **2016**, 137, 80-89.
61. *Technical Support Document for the Proposed PM NAAQS Rule: Response Surface Modeling*, Tech. Rep. U.S. Environmental Protection Agency, Research Triangle Park, NC, 2006; http://www.epa.gov/scram001/reports/pmnaaqs_tsd_rsm_all_021606.pdf (accessed July 27, 2020).
62. Particle Source Apportionment Tool (PSAT): Wagstrom, K. M.; Pandis, S. N.; Yarwood, G.; Wilson, G. M.; Morris, R. E. Development and Application of a Computationally Efficient Particulate Matter Apportionment Algorithm in a Three-Dimensional Chemical Transport Model. *Atmos. Environ.* **2008**, 42, 5650-5659.
63. Zhang, W.; Capps, S. L.; Hu, Y.; Nenes, A.; Napelenok, S. L.; Russell, A. G. Development of the High- Order Decoupled Direct Method in Three Dimensions for Particulate Matter: Enabling Advanced Sensitivity Analysis in Air Quality Models. *Geosci. Model Dev*. **2012**, 5, 355-368.
64. Cimorelli, A. J.; Perry, S. G.; Venkatram, A.; Weil, J. C.; Paine, R. J.; Wilson, R. B.; Lee, R. F.; Peters, W. D.; Brode, R.W. AERMOD: A Dispersion Model for Industrial Source

Applications. Part I: General Model Formulation and Boundary Layer Characterization. *J. Appl. Meteorol.* **2005**, 44, 682-693.

65. Guttikunda, S. K. *SIM-Air Modeling Tools*. UrbanEmissions.info, 2009; http://www.urbanemissions.info/tools/ (accessed July 27, 2020).
66. Logue, J. M.; Small, M. J.; Robinson, A. L. Evaluating the National Air Toxics Assessment (NATA): Comparison of Predicted and Measured Air Toxics Concentrations, Risks, and Sources in Pittsburgh, Pennsylvania. *Atmos. Environ*. **2011**, 45, 476-484.
67. APEEP Model: Muller, N. Z. Boosting GDP growth by accounting for the environment. *Science* **2014**, 345 (6199), 873−874. DOI: 10.1126/science.1253506
68. *User's Manual for the Co-Benefits Risk Assessment Health Impacts Screening and Mapping Tool (COBRA)*. Tech. rep. U.S. Environmental Protection Agency, Washington, DC, 2012; https://www.epa.gov/sites/production/files/2017-10/documents/cobra_user_manual_september2017_508_v2.pdf (accessed July 27, 2020).
69. *Revision to the Guideline on Air Quality Models: Enhancements to the AERMOD Dispersion Modeling System and Incorporation of Approaches to Address Ozone and Fine Particulate Matter.* Tech. rep., U.S. Environmental Protection Agency, Washington, DC, 2015 #2060-AS54; http://www.epa.gov/ttn/scram/11thmodconf/9930-11-OAR_AppendixW_Proposal.pdf (accessed July 27, 2020).
70. Draxler, R. R.; Hess, G. D. *Description of the HYSPLIT 4 Modeling System*. Tech. rep. NOAA Technical Memorandum ERL ARL-224: Silver Spring, MD, 1997; https://www.arl.noaa.gov/documents/reports/arl-224.pdf (accessed July 27, 2020).
71. Scire, J. S.; Strimaitis, D. G.; Yamartino, R. J. *A User's Guide for the CALPUFF Dispersion Model.* Tech. Rep. Earth Tech, Inc., Concord, MA, 2000; http://www.src.com/calpuff/download/CALPUFF_UsersGuide.pdf (accessed July 27, 2020).
72. *CMB8.2 Users Manual*. Tech. Rep. U.S. Environmental Protection Agency, Washington, DC, 2004 #EPA-452/R-04-011; http://www3.epa.gov/ttn/scram/models/receptor/EPA-CMB82Manual.pdf (accessed July 27, 2020).
73. Levy, J.I.; Wilson, A.M.; Zwack, L.M. Quantifying the Efficiency and Equity Implications of Power Plant Air Pollution Control Strategies in the United States, *Environ Health Perspect.* **2007**, 115, 5, 743-750.

74. Keeler, B.L.; Gourevitch, J.D; Polasky, S.; Isbell, F.; Tessum, C.W.; Hill, J. D; Marshall, J. D. The Social Costs of Nitrogen. *Science Advances* **2016**, 2, e1600219.
75. Gourevitch, J.D.; Keeler, B.L.; Ricketts, T.H. Determining Socially Optimal Rates of Nitrogen Fertilizer Application. *Agric. Ecosyst. Environ.* **2018**, 254, 292–299.
76. Millstein, D.; Wiser, R.; Bolinger, M.; Barbose, G. The climate and air-quality benefits of wind and solar power in the United States. *Nature Energy* **2017**, 2, 17134.
77. Holland, S.P.; Mansur, E.T.; Muller, N.Z.; Yates, A.J. Damages and Expected Deaths Due to Excess NOx Emissions from 2009 to 2015 Volkswagen Diesel Vehicles. *Environ. Sci. Technol*. **2016**, 50, 1111–1117.
78. Tessum, C.W.; Hill, J.D.; Marshall, J.D. InMAP: A Model for Air Pollution Interventions. *Plos One* **2017**, 12, e0176131.
79. Gilmore, E.A.; Heo, J.; Muller, N.Z.; Tessum, C.W.; Hill, J.; Marshall, J.; Adams, P.J. An inter-comparison of air quality social cost estimates from reduced-complexity models. *Environ. Res. Lett.* **2019**, 14, 074016.
80. Whitt, D.B.; Jacobson, M.Z.; Wilkerson, J.T.; Naiman, A.D.; Lele, S.K. Vertical mixing of commercial aviation emissions from cruise altitude to the surface. *Journal of Geophysical Research* **2011**, 116, https://doi.org/10.1029/2010JD015532.
81. Cloud Types; University Corporation for Atmospheric Research (UCAR): Boulder, CO, 2020. https://scied.ucar.edu/learning-zone/clouds/cloud-types (accessed July 27, 2020)
82. Tessum, C. W.; Hill, J. D.; Marshall, J. D. Intervention Model for Air Pollution (InMAP). http://spatialmodel.com/inmap/ (accessed July 27, 2020).
83. Fann, N.; Fulcher, C. M.; Baker, K. The Recent and Future Health Burden of Air Pollution Apportioned Across US Sectors. *Environ. Sci. Technol.* **2013**, 47, 3580−3589.
84. Penn, S.L.; Arunachalam, S.; Woody, M.; Heiger-Bernays, W.; Tripodis, Y.; Levy, J.I. Estimating State-Specific Contributions to $PM_{2.5}$- and O_3-Related Health Burden from Residential Combustion and Electricity Generating Unit Emissions in the United States. *Environ. Health Perspect.* **2017**, 125, 324-332.
85. Levy, J.I.; Baxter, L. K.; Schwartz, J. Uncertainty and Variability in Health-Related Damages from Coal-Fired Power Plants in the United States. *Risk Anal.* **2009**, 29, 1000-1014.

86. *Expanded Expert Judgment Assessment of the Concentration-Response Relationship Between $PM_{2.5}$ Exposure and Mortality (Final Report)*, Office of Air Quality Planning and Standards, U.S. Environmental Protection Agency, Research Triangle Park, NC, September 2006. Prepared by: Industrial Economics, Incorporated, Cambridge, MA; https://www3.epa.gov/ttnecas1/regdata/Uncertainty/pm_ee_report.pdf (assessed July 27, 2020).
87. *Health Benefits of the Second Section 812 Prospective Study of the Clean Air Act,* Review of EPA's DRAFT; Science Advisory Board, U.S. Environmental Protection Agency, Washington, DC, 2010.
88. *The IPUMS National Historical Geographic Information System (NHGIS)*, University of Minnesota, Minneapolis, MN, 2018; https://data2.nhgis.org/main (accessed July 27, 2020).
89. *CDC Wonder*; Center for Disease Control and Prevention, Atlanta, GA, 2018; https://wonder.cdc.gov/ (assessed July 27, 2020).

Chapter 2

1. *2014 National Emissions Inventory (NEI) Data*; U.S. Environmental Protection Agency: Washington, DC, 2016. https://www.epa.gov/air-emissions-inventories/2014-national-emissions-inventory-nei-data (accessed December 18, 2016).

2. *Overview of Greenhouse Gases*; U.S. Environmental Protection Agency: Washington, DC, 2016. https://www.epa.gov/ghgemissions/overview-greenhouse-gases (accessed December 18, 2016).

3. *Sources of Greenhouse Gas Emissions*; U.S. Environmental Protection Agency: Washington, DC, 2016. https://www.epa.gov/ghgemissions/sources-greenhouse-gas-emissions#electricity (accessed December 18, 2016).

4. Seinfeld, J.H.; Pandis, S.N. *Atmospheric Chemistry and Physics: From Air Pollution to Climate Change*, 2nd, ed.; John Wiley & Sons, Inc.: Hoboken, New Jersey, 2006.

5. Ryan, N.A.; Johnson, J.X.; Keoleian, G.A. Comparative Assessment of Models and Methods to Calculate Grid Electricity Emissions. *Environ. Sci. Technol*. **2016**, 50(17), 8937-8953.

6. *Environmental Impacts of Wind-Energy Projects*; National Research Council, National Academies Press, Washington, D.C., 2007; https://www.nap.edu/catalog/11935/environmental-impacts-of-wind-energy-projects (assessed February 18, 2017).

7. Mamay, C.; Fisher, D.; Murtishaw, S.; Phadke, A.; Price, L.; Sathaye, J. *Estimating Carbon Dioxide Emissions Factors for the California Electric Power Sector*; Lawrence Berkeley National Laboratory report LBNL-49945: Berkeley, CA, 2002.

8. *2003 NEPOOL Marginal Emission Rate Analysis*; ISO New England Inc., December 2004; https://www.iso-ne.com/static-assets/documents/genrtion_resrcs/reports/emission/Marginal_Emissions_Analysis_2003.pdf.

9. Zheng, Z.; Han, F.; Li, F.; Zhu, J. Assessment of Marginal Emissions Factor in Power Systems Under Ramp-Rate Constraints. *CSEE J. Pow. Ener. Sys*. **2015**, *1(4)*, 37-49.
10. Bettle, R.; Pout, C. H.; Hitchin, E. R. Interactions Between Electricity-Saving Measures and Carbon Emissions from Power Generation in England and Wales. *Energy Policy*. **2006**, 34, 3434−3446.
11. Voorspools, K. R.; D'haeseleer, W. D. An Evaluation Method for Calculating the Emission Responsibility of Specific Electric Applications. *Energy Policy*. **2000**, 28, 967−980.
12. *Clean Air Markets - Power Sector Modeling*; U.S. Environmental Protection Agency: Washington, DC, 2016; https://www.epa.gov/airmarkets/clean-air-markets-power-sector-modeling (assessed November 11, 2017).
13. *MTEP16: MISO Transmission Expansion Plan*; Midcontinent Independent System Operator, Inc., Carmel, IN, 2017; https://www.misoenergy.org/Library/Repository/Study/MTEP/MTEP16/MTEP16%20Full%20Report.pdf.
14. *Analysis of EPA's Proposal to Reduce CO_2 Emissions from Existing Electric Generating Units*; Midcontinent Independent System Operator, Inc., Carmel, IN, 2017; https://www.misoenergy.org/Library/Repository/Communication%20Material/EPA%20Regu

lations/AnalysisofEPAsProposaltoReduceCO2EmissionsfromExistingElectricGeneratingUnits.pdf.

15. Brinkman, G.; Jorgenson, J.; Ehlen, A.; Caldwell, J. *Low Carbon Grid Study: Analysis of a 50% Emission Reduction in California*; NREL/TP-6A20-64884; National Renewable Energy Laboratory (NREL), Golden, CO, January 2016; http://www.nrel.gov/docs/fy16osti/64884.pdf.
16. Foley, A.; Tyther, B.; Calnan, P.; Ó Gallachóir, B. Impacts of Electric Vehicle Charging Under Electricity Market Operations. *Applied Energy*. **2013**, 101, 93-102.
17. *2013 ISO New England Electric Generator Air Emissions Report*; ISO New England Inc., December 2014; https://www.iso-ne.com/static-assets/documents/2014/12/2013_emissions_report_final.pdf.
18. *2014 ISO New England Electric Generator Air Emissions Report*; ISO New England Inc., January 2016; https://www.iso-ne.com/static-assets/documents/2016/01/2014_emissions_report.pdf.
19. Rogers, M.M.; Wang, Y.; Wang, C.; McElmurry, S. P.; Miller, C.J. Evaluation of a Rapid LMP-Based Approach for Calculating Marginal Unit Emissions. *Applied Energy*. **2013**, 111, 812-820.
20. Wang, C.; Wang, Y.; Miller, C.J.; Lin, J. *Estimating Hourly Marginal Emission in Real Time for PJM Market Area Using a Machine Learning Approach*. 2016 IEEE Power and Energy Society General Meeting (PESGM), Boston, MA, USA, 17-21 July 2016; IEEE Xplore, 2016; http://ieeexplore.ieee.org/document/7741759/?reload=true (accessed January 19, 2017).
21. Siler-Evans, K.; Azevedo, I.L.; Morgan, M.G. Marginal Emissions Factors for the U.S. Electricity System. *Environ. Sci. Technol.* **2012**, 46, 4742−4748.
22. Holland, S. P.; Mansur, E. T. Is Real-Time Pricing Green?: the Environmental Impacts of Electricity Demand Variance. Rev. Econ. Stat. **2008**, 90 (3), 550–561.
23. Jansen, K. H.; Brown, T. M.; Samuelsen, G. S. Emissions Impacts of Plug-in Hybrid Electric Vehicle Deployment on the U.S. Western Grid. *J. Power Sources*. **2010**, 195 (16), 5409–5416.
24. Graff Zivin, J. S.; Kotchen, M. J.; Mansur, E. T. Spatial and Temporal Heterogeneity of Marginal Emissions: Implications for Electric Cars and Other Electricity-Shifting Policies. *J. Econ. Behav. Organ.* **2014**, 107, 248–268.

25. Li, M.; Smith, T.M.; Yang, Y.; Wilson, E.J. Marginal Emissions Factors Considering Renewables: A Case Study of the U.S. Midcontinent Independent System Operator (MISO) System. *Environ. Sci. Technol*. **2017**, 51, 11215-11223.
26. Siler-Evans, K., Azevedo, I.L., Morgan, M.G, Apt, J. Regional variations in the health, environmental, and climate benefits from wind and solar generation. *Proc. Natl. Acad. Sci. U.S.A.* **2013**, 110, 11768-11773.
27. Vaishnav, P.; Horner, N.; Azevedo, I.L. Was It Worthwhile? Where Have the Benefits of Rooftop Solar Photovoltaic Generation Exceed the Cost? *Environ. Res. Lett.* **2017**, 12: 094015, 1-13.
28. Min, J.; Azevedo, I.L.; Hakkarainen, P. Net Carbon Emissions Savings and Energy Reductions from Lighting Energy Efficiency Measures when Accounting for Changes in Heating and Cooling Demands: A Regional Comparison. *Applied Energy*. **2015**, 141, 12–18.
29. Gilbraith, N.; Azevedo, I.L.; Jaramillo, P. Regional Energy and GHG Savings from Building Codes Across the United States. *Environ. Sci. Technol.* **2014**, 48, 14121–14130.
30. Hittinger, E.; Azevedo, I.L. Bulk Energy Storage Increases US Electricity System Emissions. *Environ. Sci. Technol.* **2015**, 49, 3203-3210.
31. Tamayao, M.; Michalek, J.; Hendrickson, C.; Azevedo I.L. Regional Variability and Uncertainty of Electric Vehicle Life Cycle CO_2 Emissions Across the United States. *Environ. Sci. Technol.* **2015**, 49, 8844–8855.
32. Yuksel, T.; Tamayao, M-A.; Hendrickson, C.; Azevedo, I.L.; Michalek, J. Effect of Regional Grid Mix, Driving Patterns and Climate on the Comparative Carbon Footprint of Gasoline and Plug-In Electric Vehicles in the United States. *Environ. Res. Lett.* **2016**, 11, 044007.
33. Gingerich, D.; Sun, X.; Behrer, P.; Azevedo, I.L.; Mauter, M. Air Emissions Implications of Expanded Wastewater Treatment at Coal-Fired Generators. *Proc. Natl. Acad. Sci. U.S.A.* **2017**, doi: 10.1073/pnas.1524396114.
34. Hawkes, A. Estimating Marginal CO_2 Emissions Rates for National Electricity Systems. *Energy Policy*. **2010**, 38, 5977−5987.
35. Hawkes, A.D. Long-Run Marginal CO_2 Emissions Factors in National Electricity Systems. *Applied Energy.* **2014**, 125, 197–205.
36. *Air Markets Program Data*; U.S. Environmental Protection Agency: Washington, DC, 2016. https://ampd.epa.gov/ampd/ (assessed January 19, 2017).

37. *Market Reports*; Midcontinent Independent System Operator, Inc., Carmel, IN, 2017; https://www.misoenergy.org/Library/MarketReports/Pages/MarketReports.aspx (assessed January 19, 2017).
38. Wiser, R.; Bolinger, M. *2015 Wind Technologies Market Report*; LBNL-1005951; Lawrence Berkeley National Lab, Berkeley, CA, August 2016; https://emp.lbl.gov/publications/2015-wind-technologies-market-report.
39. Stafford, B.A.; Wilson, E.J. Winds of Change in Energy Systems: Policy Implementation, Technology Deployment, and Regional Transmission Organizations. *Energy Res. Soc. Sci*. **2016**, 21, 222-236.
40. *Wind Integration*; Midcontinent Independent System Operator, Inc., Carmel, IN, 2017; https://www.misoenergy.org/WhatWeDo/StrategicInitiatives/Pages/WindIntegration.aspx (assessed September 15, 2017).
41. Ela, E.; Gevorgian, V.; Fleming, P.; Zhang, Y.C.; Singh, M.; Muljadi, E.; Scholbrook, A.; Aho, J.; Buckspan, A.; Pao, L.; Singhvi, V.; Tuohy, A.; Pourbeik, P.; Brooks, D.; Bhatt, N. *Active Power Controls from Wind Power: Bridging the Gaps*; NREL/TP-5D00-60574; National Renewable Energy Laboratory (NREL), Golden, CO, January 2014; https://www.nrel.gov/docs/fy14osti/60574.pdf.
42. Kim, J.D.; Rahimi, M. Future Energy Loads for a Large-Scale Adoption of Electric Vehicles in the City of Los Angeles: Impacts on greenhouse gas (GHG) emissions. *Energy Policy*. **2014**, 73, 620–630.
43. Marriot, J and Matthews, H.S. Environmental Effects of Interstate Power Trading on Electricity Consumption Mixes. *Environ. Sci. Technol*. **2005**, 39, 8584-8590.
44. Weber, C.L.; Jaramillo, P.; Marriot, J.; Samaras, C. Life Cycle Assessment and Grid Electricity: What Do We Know and What Can We Know? *Environ. Sci. Technol*. **2010**, 44, 1895-1901.

Chapter 3

1. Cohen, A.J.; Brauer, M.; Burnett, R.; Anderson, H.R.; Frostad, J.; Estep, K.; Balakrishnan, K.; Brunekreef, B.; Dandona, L.; Dandona, R.; Feigin, V.; Freedman, G.; Hubbell, B.; Jobling, A.; Kan, H.; Knibbs, L.; Liu, Y.; Martin, R.; Morawska, L.; Pope, C.A. III; Shin, H.; Straif, K.; Shaddick, G.; Thomas, M.; van Dingenen, R.; van Donkelaar, A.; Vos, T.; Murray, C.J.L.; Forouzanfar, M.H. Estimates and 25-Year Trends of the Global Burden of Disease Attributable to Ambient Air Pollution: An Analysis of Data from the Global Burden of Diseases Study 2015. *Lancet* **2017**, 389, 1907-1918.
2. *Health and Environmental Effects of Particulate Matter (PM)*; US Environmental Protection Agency: Washington, DC, 2016; https://www.epa.gov/pm-pollution/health-and-environmental-effects-particulate-matter-pm (accessed April 11, 2018).
3. Dockery, D.W.; Pope, C.A.; Xu, X.; Spengler, J.D.; Ware, J.H.; Fay, M.E.; Ferris, B.G. Jr; Speizer, F.E. An Association Between Air Pollution and Mortality in Six US Cities. *New Engl J Med.* **1993**, 329, 1753-1759.
4. Pope, C.A. 3rd; Thun, M.J.; Namboodiri, M.M.; Dockery, D.W.; Evans, J.S.; Speizer, F.E.; Heath, C.W. Jr. Particulate Air Pollution as a Predictor of Mortality in a Prospective Study of US Adults. *Am J Resp Crit Care* **1995**, 151, 669-674.
5. Hoek, G.; Krishnan, R.M.; Beelen, R.; Peters, A.; Ostro, B.; Brunekreef, B.; Kaufman, J.D. Long-Term Air Pollution Exposure and Cardio-Respiratory Mortality: A Review. *Environ Health* **2013**, 12, 43-57.
6. Seinfeld, J.H.; Pandis, S.N. *Atmospheric Chemistry and Physics: From Air Pollution to Climate Change*, 2nd, ed.; John Wiley & Sons, Inc.: Hoboken, New Jersey, 2006.
7. *2014 National Emissions Inventory (NEI) Data*; US Environmental Protection Agency: Washington, DC, 2016; https://www.epa.gov/air-emissions-inventories/2014-national-emissions-inventory-nei-data (accessed April 11, 2018).
8. Thind, M.P.S.; Wilson, E.J.; Azevedo, I.L.; Marshall, J.D. Marginal Emissions Factors for Electricity Generation in the Midcontinent ISO. *Environ. Sci. Technol.* **2017**, 51 (24), 14445–14452.
9. *Electric Power Generation, Transmission and Distribution (NAICS 2211): Laws and Regulations*; US Environmental Protection Agency: Washington, DC, 2018;

https://www.epa.gov/regulatory-information-sector/electric-power-generation-transmission-and-distribution-naics-2211 (accessed November 14, 2018).

10. Caiazzo, F.; Ashok, A.; Waitz, I.A.; Yim, S.H.L.; Barrett, S.R.H. Air Pollution and Early Deaths in the United States. Part I: Quantifying the Impact of Major Sectors in 2005. *Atmos. Environ.* **2013**, 79, 198-208.
11. Dedoussi, I.C.; Barrett, S.R.H. Air Pollution and Early Deaths in the United States. Part II: Attribution of $PM_{2.5}$ Exposure to Emissions Species, Time, Location and Sector. *Atmos. Environ.* **2014**, 99, 610-617.
12. Penn, S.L.; Arunachalam, S.; Woody, M.; Heiger-Bernays, W.; Tripodis, Y.; Levy, J.I. Estimating State-Specific Contributions to $PM_{2.5}$- and O_3-Related Health Burden from Residential Combustion and Electricity Generating Unit Emissions in the United States. *Environ. Health Perspect.* **2017**, 125, 324-332.
13. Fann, N.; Fulcher, C. M.; Baker, K. The Recent and Future Health Burden of Air Pollution Apportioned Across US Sectors. *Environ. Sci. Technol.* **2013**, 47, 3580−3589.
14. Lelieveld, J.; Evans, J.S.; Fnais, M.; Giannadaki, D.; Pozzer, A. The Contribution of Outdoor Air Pollution Sources to Premature Mortality on a Global Scale. *Nature* **2015**, 525, 367-371.
15. Tessum, C.W.; Apte, J.S.; Goodkind, A.L; Muller, N.Z.; Mullins, K.A.; Paolella, D.A.; Polasky, S.; Springer, S.P.; Thakrar, S.K.; Marshall, J.D.; Hill, J.D. Inequity in Consumption of Goods and Services Adds to Racial–Ethnic Disparities in Air Pollution Exposure. *Proc. Natl. Acad. Sci. U.S.A.* **2019**, 116, 6001-6006.
16. Levy, J.I.; Baxter, L. K.; Schwartz, J. Uncertainty and Variability in Health-Related Damages from Coal-Fired Power Plants in the United States. *Risk Anal.* **2009**, 29, 1000-1014.
17. Buonocore, J. J.; Dong, X.; Spengler, J. D.; Fu, J. S.; Levy, J. I. Using the Community Multiscale Air Quality (CMAQ) Model to Estimate Public Health Impacts of $PM_{2.5}$ from Individual Power Plants. *Environ. Int.* **2014**, 68, 200-208.
18. *Environmental Justice*; US Environmental Protection Agency: Washington, DC, 2018; https://www.epa.gov/environmentaljustice (accessed March 11, 2018).
19. Collins, M.B.; Munoz, I.; JaJa, J. Linking ‘Toxic Outliers’ to Environmental Justice Communities. *Environ. Res. Lett.* **2016**, 11, 1-9.
20. Zwickl, K.; Ash, M.; Boyce, J.K. Analysis Regional Variation in Environmental Inequality: Industrial Air Toxics Exposure in US Cities. *Ecol. Econ.* **2014**, 107, 494-509.

21. Benmarhnia, T.; Huang, J.; Basu, R.; Wu, J.; Bruckner, T. A. Decomposition Analysis of Black–White Disparities in Birth Outcomes: The Relative Contribution of Air Pollution and Social Factors in California. *Environ Health Perspect*. **2017**, 125, 107003-1 - 107003-7.
22. Ard, K. Trends in Exposure to Industrial Air Toxins for Different Racial and Socioeconomic Groups: A Spatial and Temporal Examination of Environmental Inequality in the US from 1995 to 2004. *Soc. Sci. Res*. **2015**, 53, 375-390.
23. Ottinger, G. The Winds of Change: Environmental Justice in Energy Transitions. *Sci. Cult.* **2013**, 22, 222−229.
24. Martenies, S.E.; Milando, C.W.; Williams, G.O.; Batterman, S.A. Disease and Health Inequalities Attributable to Air Pollutant Exposure in Detroit, Michigan. *Int. J. Environ. Res. Public Health* **2017**, 14, 1-24.
25. Clark, L.P.; Millet, D.B.; Marshall, J.D. National Patterns in Environmental Injustice and Inequality: Outdoor NO_2 Air Pollution in the United States. *Plos One* **2014**, 9, e94431, 1-8.
26. Rosofsky, A.; Levy, J.I.; Zanobetti, A.; Janulewicz, P.; Fabian, M.P. Temporal Trends in Air Pollution Exposure Inequality in Massachusetts. *Environ. Res.* **2018**, 161, 76-86.
27. Maguire, K.; Sheriff, G. Comparing Distributions of Environmental Outcomes for Regulatory Environmental Justice Analysis. *Int. J. Environ. Res. Public Health* **2011**, 8, 1707-1726.
28. Levy, J.I.; Wilson, A.M.; Zwack, L.M. Quantifying the Efficiency and Equity Implications of Power Plant Air Pollution Control Strategies in the United States, *Environ Health Perspect.* **2007**, 115, 5, 743-750.
29. *Emissions & Generation Resource Integrated Database (eGRID)*; US Environmental Protection Agency: Washington, DC, 2018; https://www.epa.gov/energy/emissions-generation-resource-integrated-database-egrid (assessed July 9, 2018).
30. *Regional Transmission Organizations (RTO)/Independent System Operators (ISO)*; Federal Energy Regulatory Commission (FERC): Washington, DC, 2018; https://www.ferc.gov/industries/electric/indus-act/rto.asp (assessed January 1, 2019).
31. Carnevale, C.; Finzi, G.; Pisoni, E.; Volta, M. Neuro-Fuzzy and Neural Network Systems for Air Quality Control. *Atmos. Env.* **2009**, 43, 4811-4821.
32. GEOS-Chem Adjoint Model: Dedoussi, I. C.; Barrett, S. R. H. Air Pollution and Early Deaths in the United States. Part II: Attribution of $PM_{2.5}$ Exposure to Emissions Species, Time, Location and Sector. *Atmos. Environ*. **2014**, 99, 610-617.

33. DDM/ RSM Model: Foley, K. M.; Napelenok, S. L.; Jang, C.; Phillips, S.; Hubbell, B. J.; Fulcher, C. M. Two Reduced Form Air Quality Modeling Techniques for Rapidly Calculating Pollutant Mitigation Potential Across Many Sources, Locations and Precursor Emission Types. *Atmos. Environ*. **2014**, 98, 283-289.
34. Hakami, A.; Henze, D. K.; Seinfeld, J. H.; Singh, K.; Sandu, A.; Kim, S.; Byun, D.; Li, Q. The Adjoint of CMAQ. *Environ. Sci. Technol*. **2007**, 41, 7807-7817.
35. EASIUR Model: Heo, J.; Adams, P.J.; Gao, H.O. Reduced-Form Modeling of Public Health Impacts of Inorganic $PM_{2.5}$ and Precursor Emissions. *Atmos. Env*. **2016**, 137, 80-89.
36. *Technical Support Document for the Proposed PM NAAQS Rule: Response Surface Modeling*, Tech. Rep. US Environmental Protection Agency, Research Triangle Park, NC, 2006; http://www.epa.gov/scram001/reports/pmnaaqs_tsd_rsm_all_021606.pdf (accessed February 5, 2018).
37. Tessum, C.W.; Hill, J.D.; Marshall, J.D. InMAP: A Model for Air Pollution Interventions. *Plos One* **2017**, 12, e0176131.
38. Wagstrom, K. M.; Pandis, S. N.; Yarwood, G.; Wilson, G. M.; Morris, R. E. Development and Application of a Computationally Efficient Particulate Matter Apportionment Algorithm in a Three-Dimensional Chemical Transport Model. *Atmos. Environ.* **2008**, 42, 5650-5659.
39. Zhang, W.; Capps, S. L.; Hu, Y.; Nenes, A.; Napelenok, S. L.; Russell, A. G. Development of the High- Order Decoupled Direct Method in Three Dimensions for Particulate Matter: Enabling Advanced Sensitivity Analysis in Air Quality Models. *Geosci. Model Dev*. **2012**, 5, 355-368.
40. Cimorelli, A. J.; Perry, S. G.; Venkatram, A.; Weil, J. C.; Paine, R. J.; Wilson, R. B.; Lee, R. F.; Peters, W. D.; Brode, R.W. AERMOD: A Dispersion Model for Industrial Source Applications. Part I: General Model Formulation and Boundary Layer Characterization. *J. Appl. Meteorol.* **2005**, 44, 682-693.
41. Guttikunda, S. K. *SIM-Air Modeling Tools*. UrbanEmissions.info, 2009; http://www.urbanemissions.info/tools/ (accessed February 5, 2018).
42. Logue, J. M.; Small, M. J.; Robinson, A. L. Evaluating the National Air Toxics Assessment (NATA): Comparison of Predicted and Measured Air Toxics Concentrations, Risks, and Sources in Pittsburgh, Pennsylvania. *Atmos. Environ*. **2011**, 45, 476-484.

43. Muller, N. Z.; Mendelsohn, R; *The Air Pollution Emission Experiments and Policy Analysis Model (APEEP): Technical Appendix*. Tech. rep. 2006; https://www.researchgate.net/publication/253359043_The_Air_Pollution_Emission_Experiments_and_Policy_Analysis_Model_APEEP_Technical_Appendix (accessed February 5, 2018).
44. *User's Manual for the Co-Benefits Risk Assessment Health Impacts Screening and Mapping Tool (COBRA)*. Tech. rep. US Environmental Protection Agency, Washington, DC, 2012; https://www.epa.gov/sites/production/files/2017-10/documents/cobra_user_manual_september2017_508_v2.pdf (accessed February 5, 2018).
45. *Revision to the Guideline on Air Quality Models: Enhancements to the AERMOD Dispersion Modeling System and Incorporation of Approaches to Address Ozone and Fine Particulate Matter*. Tech. rep., US Environmental Protection Agency, Washington, DC, 2015 #2060-AS54; http://www.epa.gov/ttn/scram/11thmodconf/9930-11-OAR_AppendixW_Proposal.pdf (accessed February 5, 2018).
46. Draxler, R. R.; Hess, G. D. *Description of the HYSPLIT 4 Modeling System*. Tech. rep. NOAA Technical Memorandum ERL ARL-224: Silver Spring, MD, 1997; https://www.arl.noaa.gov/documents/reports/arl-224.pdf (accessed February 5, 2018).
47. Scire, J. S.; Strimaitis, D. G.; Yamartino, R. J. *A User's Guide for the CALPUFF Dispersion Model.* Tech. Rep. Earth Tech, Inc., Concord, MA, 2000; http://www.src.com/calpuff/download/CALPUFF_UsersGuide.pdf (accessed February 5, 2018).
48. *CMB8.2 Users Manual*. Tech. Rep. US Environmental Protection Agency, Washington, DC, 2004 #EPA-452/R-04-011; http://www3.epa.gov/ttn/scram/models/receptor/EPA-CMB82Manual.pdf (accessed February 5, 2018).
49. *GEOS-Chem Model* ; Atmospheric Chemistry Modeling Group, Harvard University, Cambridge, MA, 2018; http://acmg.seas.harvard.edu/geos/index.html (accessed February 20, 2018).
50. *Comprehensive Air Quality Model with Extensions* ; Environ International Corporation, Novato, CA, 2016; http://www.camx.com/home.aspx (accessed February 20, 2018).

51. Jacobson, M.Z. GATOR-GCMM: A Global-Through Urban-Scale Air Pollution and Weather Forecast Model: 1. Model Design and Treatment of Subgrid Soil, Vegetation, Roads, Rooftops, Water, Sea Ice, and snow. *J Geophys Res.* 2001; 106, 5385–5401.
52. *WRF-CHEM*; National Center for Atmospheric Research, University Corporation for Atmospheric Research, Boulder, CO, 2018; https://www2.acom.ucar.edu/wrf-chem (accessed February 20, 2018).
53. *CMAQ: The Community Multiscale Air Quality Modeling System*; US Environmental Protection Agency, Washington, DC, 2018; https://www.epa.gov/cmaq (accessed February 20, 2018).
54. Thakrar, S.K.; Goodkind, A.L.; Tessum, C.W.; Marshall, J.D.; Hill, J. D. Life Cycle Air Quality Impacts on Human Health from Potential Switchgrass Production in the United States. *Biomass and Bioenergy* **2017**, 114, 73-82.
55. Keeler, B.L.; Gourevitch, J.D; Polasky, S.; Isbell, F.; Tessum, C.W.; Hill, J. D; Marshall, J. D. The Social Costs of Nitrogen. *Science Advances* **2016**, 2, e1600219.
56. Gourevitch, J.D.; Keeler, B.L.; Ricketts, T.H. Determining Socially Optimal Rates of Nitrogen Fertilizer Application. *Agric. Ecosyst. Environ.* **2018**, 254, 292–299.
57. Millstein, D.; Wiser, R.; Bolinger, M.; Barbose, G. The Climate and Air-Quality Benefits of Wind and Solar Power in the United States. *Nature Energy* **2017**, 2, 17134.
58. Holland, S.P.; Mansur, E.T.; Muller, N.Z.; Yates, A.J. Damages and Expected Deaths due to Excess NOx Emissions from 2009 to 2015 Volkswagen Diesel Vehicles. *Environ. Sci. Technol*. **2016**, 50, 1111–1117.
59. Tessum, C.W.; Hill, J.D.; Marshall, J.D. *Intervention Model for Air Pollution (InMAP)*; http://spatialmodel.com/inmap/ (assessed January 18, 2019).
60. *The IPUMS National Historical Geographic Information System (NHGIS)*, University of Minnesota, Minneapolis, MN, 2018; https://data2.nhgis.org/main (accessed August 18, 2018).
61. *CDC Wonder*; Center for Disease Control and Prevention, Atlanta, GA, 2018; https://wonder.cdc.gov/ (assessed August 18, 2018).
62. *Integrated Science Assessment for Particulate Matter (Final Report)*; US Environmental Protection Agency, Research Triangle Park, NC, December 2009; https://cfpub.epa.gov/ncea/isa/recordisplay.cfm?deid=216546 (accessed August 18, 2018).

63. *Expanded Expert Judgment Assessment of the Concentration-Response Relationship Between $PM_{2.5}$ Exposure and Mortality (Final Report)*, Office of Air Quality Planning and Standards, US Environmental Protection Agency, Research Triangle Park, NC, September, 2006. Prepared by: Industrial Economics, Incorporated, Cambridge, MA; https://www3.epa.gov/ttnecas1/regdata/Uncertainty/pm_ee_report.pdf (assessed August 18, 2018).
64. *Health Benefits of the Second Section 812 Prospective Study of the Clean Air Act,* Review of EPA's Draft; Science Advisory Board, US Environmental Protection Agency, Washington, DC, 2010.
65. Krewski, D.; Jerrett, M.; Burnett, R.T.; Ma, R.; Hughes, E.; Shi, Y.; Turner, M.C.; Pope III, C.A.; Thurston, G.; Calle, E.E.; Thun, M.J. *Extended Follow-Up and Spatial Analysis of the American Cancer Society Study Linking Particulate Air Pollution and Mortality*; Research Report 140, Health Effects Institute, Boston, MA, May 2009; https://www.healtheffects.org/system/files/Krewski140.pdf (assessed July 8, 2018).
66. Goodkind, A.L.; Tessum, C.W.; Coggins, J.S.; Hill, J.D.; Marshall, J.D. Fine-Scale Damage Estimates of Particulate Matter Air Pollution Reveal Opportunities for Location-Specific Mitigation of Emissions. *Proc. Natl. Acad. Sci. U.S.A.* **2019**, 116, 8775-8780.
67. *Overview of the Cross-State Air Pollution Rule (CSAPR);* US Environmental Protection Agency, Washington, DC, 2018; https://www.epa.gov/csapr/overview-cross-state-air-pollution-rule-csapr (assessed July 10, 2018).
68. Keating, M.H.; Davis, F. *Air of Injustice*; LaBerge Printers, Inc, Orlando, FL, October 2002; http://www.energyjustice.net/files/coal/Air_of_Injustice.pdf (assessed August 16, 2018).
69. Nasari, M. M.; Szyszkowicz, M.; Chen, H.; Crouse, D.; Turner, M. C.; Jerrett, M.; Pope III, C.A.; Hubbell, B.; Fann, N.; Cohen, A.; Gapstur, S.M.; Diver, W.R.; Stieb, D.; Forouzanfar, M.H.; Kim, S.; Olives, C.; Krewski, D.; Burnett, R.T. A Class of Non-Linear Exposure-Response Models Suitable for Health Impact Assessment Applicable to Large Cohort Studies of Ambient Air Pollution. *Air Qual Atmos Health* **2016**, 9, 961–972.
70. Pope III, C.A.; Cropper, M.; Coggins, J.; Cohen, A. Health Benefits of Air Pollution Abatement Policy: Role of the Shape of the Concentration–Response Function. *J Air Waste Manag Assoc.* **2015**, 65, 516-522.

71. Levy, J.I.; Diez, D.; Dou, Y.; Barr, C.D.; Dominici, F. A Meta-Analysis and Multisite Time-Series Analysis of the Differential Toxicity of Major Fine Particulate Matter Constituents. *Am J Epidemiol.* **2012**, 175, 1091–1099.
72. Marshall, J.D.; Apte, J.S.; Coggins, J.S.; Goodkind, A.L. Blue Skies Bluer? Environ. Sci. Technol. **2015**, 49, 13929–13936.
73. Paolella, D.A.; Tessum, C.W.; Adams, P.J.; Apte, J.S; Chambliss, S.; Hill, J.; Muller, N.Z.; Marshall, J.D. Effect of Model Spatial Resolution on Estimates of Fine Particulate Matter Exposure and Exposure Disparities in the United States. *Environ. Sci. Technol. Lett.* **2018**, 5, 436–441.
74. Gilmore, E. A.; Heo, J.; Muller, N. Z.; Tessum, C. W.; Hill, J.D.; Marshall, J. D.; Adams, P. J. An inter-comparison of the social costs of air quality from reduced-complexity models. *Environ. Res. Lett.* **2019**, 14, 074016.
75. *Integrated Science Assessment (ISA) for Particulate Matter (Final Report, Dec 2009)*; US Environmental Protection Agency, Washington, DC, EPA/600/R-08/139F, 2009; https://cfpub.epa.gov/ncea/isa/recordisplay.cfm?deid=216546 (accessed August 8, 2019).
76. Hill, J.; Goodkind, A.; Tessum, C.; Thakrar, S.; Tilman, D.; Polasky, S.; Smith, T.; Hunt, N.; Mullins, K.; Clark, M.; Marshall, J. Air-Quality-Related Health Damages of Maize. *Nat. Sustain.* **2019**, 2, 397-403.
77. Lepeule, J.; Laden, F.; Dockery, D.; Schwartz, J. Chronic Exposure to Fine Particles and Mortality: An Extended Follow-Up of the Harvard Six Cities Study from 1974 to 2009. *Environ. Health Persp.* **2012**, 120, 965–970.
78. Vodonos, A.; Awad, Y. A.; & Schwartz, J. The Concentration-Response Between Long-Term $PM_{2.5}$ Exposure and Mortality; A Meta-Regression Approach. *Environmental Research* **2018**, 166, 677–689.
79. Pope III, C.A.; Lefler, J.S.; Ezzati, M.; Higbee, J.D.; Marshall, J.D.; Kim, S.Y.; Bechle, M.; Gilliat, K.S.; Vernon, S.E.; Robinson, A.L.; Burnett, R.T. Mortality Risk and Fine Particulate Air Pollution in a Large, Representative Cohort of U.S. Adults. *Environ. Health Perspect.* **2019**. In Press. DOI 10.1289/EHP4438.
80. *Electricity Data Browser;* US Energy Information Administration, Washington, DC, 2018; https://www.eia.gov/electricity/data/browser/ (assessed August 8, 2019).

Chapter 4

1. *Freight Facts and Figures*; U.S. Department of Transportation, Bureau of Transportation Statistics: Washington, DC, 2019. https://datahub.transportation.gov/stories/s/45xw-qksz (accessed 18 August 2020).
2. *Transportation Statistics Annual Report 2019: The State of Statistics*; U.S. Department of Transportation, Bureau of Transportation Statistics: Washington, DC, 2019. https://doi.org/10.21949/1502602 (accessed August 18, 2020).
3. *Freight Analysis Framework Version* 4; U.S. Department of Transportation: Washington, DC, 2019. https://faf.ornl.gov/fafweb/ (accessed November 20, 2019).
4. *OTR vs Intermodal: Which Shipping Strategy is Right for You?*; ZIPLINE Logistics: Columbus, OH, 2020; https://ziplinelogistics.com/blog/converting-truck-rail/ (accessed August 18, 2020).
5. *Protect the Environment and Your Bottom Line*; Flexport: San Francisco, CA, 2020. https://www.flexport.com/services/carbon-offset/ (accessed August 18, 2020).
6. Is one-day shipping really more eco-friendly? Fact-checking Jeff Bezos as Amazon speeds up delivery; Geekwire, 2019; https://www.geekwire.com/2019/one-day-shipping-really-eco-friendly-fact-checking-bezos-amazon-speeds-delivery/ (accessed August 18, 2020).
7. Brogan, J.J.; Aeppli, A.E.; Beagan, D.F; Brown, A.; Fischer, M.J.; Grenzeback, L.R.; McKenzie, E.; Vimmerstedt, L.; Vyas, A.D.; Witzke, E.; Freight Transportation Modal Shares: Scenarios for a Low-Carbon Future. Transportation Energy Futures Series. Prepared by Cambridge Systematics, Inc. (Cambridge, MA), and the National Renewable Energy Laboratory (Golden, CO) for the U.S. Department of Energy, Washington, DC. DOE/GO-102013-3705, 2013. 80 pp.
8. *Use of energy explained: Energy use for transportation*; U.S. Energy Information Administration: Washington, DC, 2018. https://www.eia.gov/energyexplained/use-of-energy/transportation-in-depth.php (accessed August 18, 2020).
9. Cohen, A. J.; Brauer, M.; Burnett, R.; Anderson, H. R.; Frostad, J.; Estep, K.; Balakrishnan, K.; Brunekreef, B.; Dandona, L.; Dandona, R.; Feigin, V.; Freedman, G.; Hubbell, B.; Jobling, A.; Kan, H.; Knibbs, L.; Liu, Y.; Martin, R.; Morawska, L.; Pope, C. A.; Shin, H.; Straif, K.; Shaddick, G.; Thomas, M.; van Dingenen, R.; van Donkelaar, A.; Vos, T.; Murray, C. J. L.;

Forouzanfar, M. H. Estimates and 25-Year Trends of the Global Burden of Disease Attributable to Ambient Air Pollution: An Analysis of Data from the Global Burden of Diseases Study 2015. *Lancet* **2017**, 389, 1907−1918.

10. Pope III, C.A.; Coleman, N.; Pond, Z.A.; Burnett, R.T. Fine particulate air pollution and human mortality: 25+ years of cohort studies. Environmental Research **2020**, 183, 2020.
11. *2014 National Emissions Inventory (NEI) Data*; US Environmental Protection Agency: Washington, DC, 2020; https://www.epa.gov/air-emissions-inventories/2014-national-emissions-inventory-nei-data (accessed August 19, 2020).
12. Corbett, J.J.; Winebrake, J.J.; Green, E.H.; Kasibhatla, P.; Eyring, V.; Lauer, A. Mortality from ship emissions: A Global Assessment. *Environmental Science & Technology* **2007**, 41, 8512–8518.
13. Barrett, S.R.H.; Britter, R.E.; Waitz, I.A. Global Mortality Attributable to Aircraft Cruise Emissions. *Environmental Science & Technology* **2010**, 44, 7736–7742.
14. Fann, N.; Baker, K.R.; Fulcher, C.M. Characterizing the $PM_{2.5}$-related health benefits of emission reductions for 17 industrial, area and mobile emission sectors across the U.S. *Environment International* **2012**, 49, 141–151.
15. Fann, N.; Fulcher, C.M.; Baker, K. The recent and future health burden of air pollution apportioned across U.S. sectors. *Environmental Science & Technology* **2013**, 47, 3580-3589.
16. Caiazzo, F.; Ashok, A.; Waitz, I.A.; Yim, S.H.L.; Barrett, S.R.H. Air pollution and early deaths in the United States. Part I: Quantifying the impact of major sectors in 2005. *Atmospheric Environment* **2013**, 79, 198-208.
17. Dedoussi, I.C.; Barrett, S.R.H. Air pollution and early deaths in the United States. Part II: Attribution of $PM_{2.5}$ exposure to emissions species, time, location and sector. *Atmospheric Environment* **2014**, 99, 610-617.
18. Bickford, E.; Holloway, T.; Karambelas, A.; Johnston, M.; Adams, T.; Janssen, M.; Moberg, C. Emissions and air quality impacts of truck-to-rail freight modal shifts in the Midwestern United States. *Environ. Sci. Technol.* **2014**, 48, 446–454.
19. Yim, S.H.L.; Lee, G.L.;Lee, I.H.; Allroggen, F.; Ashok, A.; Caiazzo, F.; Eastham, S.D.; Malina, R.; Barrett, S.R.H. Global, regional and local health impacts of civil aviation emissions. *Environmental Research Letters* **2015**, 10, 1-12.

20. Harrison, R.M.; Masiol, M.; Vardoulakis, S. Civil aviation, air pollution and human health. *Environmental Research Letters* **2015**, 10, 1-3.
21. Galvis, B.; Bergin, M.; Boylan, J.; Huang, Y.; Bergin, M.; Russell, A.G. Air quality impacts and health-benefit valuation of a low-emission technology for rail yard locomotives in Atlanta Georgia. *Science of the Total Environment* **2015**, 533, 156–164.
22. Liu, L.; Hwang, T.; Lee, S.; Ouyang, Y.; Lee, B.; Smith, S.J.; Tessum, C.W.; Marshall, J.D.; Yan, F.; Daenzer, K.; Bond, T.C. Health and climate impacts of future United States land freight modelled with global-to-urban models. *Nature Sustainability* **2019**, 2, 105–112.
23. Pan, S.; Roy, A.; Choi, Y.; Sun, S.; Gao, H.O. The air quality and health impacts of projected long-haul truck and rail freight transportation in the United States in 2050. *Environment International* ***2019,*** 130, 104922.
24. Clark, L.P.; Millet, D.B.; Marshall, J.D. Changes in Transportation-Related Air Pollution Exposures by Race-Ethnicity and Socioeconomic Status: Outdoor Nitrogen Dioxide in the United States in 2000 and 2010. Environmental Health Perspectives **2017**, 125, CID: 097012.
25. Houston, D.; Wu, J.; Ong, P.; Winer, A. Structural Disparities of Urban Traffic in Southern California: Implications for Vehicle-Related Air Pollution Exposure in Minority and High-Poverty Neighborhoods, Journal of Urban Affairs **2004,** 26, 565-592, DOI: 10.1111/j.0735-2166.2004.00215.x
26. Tessum, C.W.; Hill, J.D.; Marshall, J.D. InMAP: A Model for Air Pollution Interventions. *Plos One* **2017**, 12, e0176131.
27. *National Transportation Atlas Databases*; U.S. Department of Transportation, Bureau of Transportation Statistics: Washington, DC, 2019; https://www.bts.gov/geospatial/national-transportation-atlas-database (accessed August 19, 2020).
28. *GREET Model*; Argonne National Laboratory: Argonne, IL, 2018; https://greet.es.anl.gov/ (accessed August 19, 2020).
29. *Latest Version of Motor Vehicle Emission Simulator (MOVES)*; US Environmental Protection Agency: Washington, DC, 2019; https://www.epa.gov/moves/latest-version-motor-vehicle-emission-simulator-moves (accessed August 19, 2020).
30. *ArcGIS Desktop*; Environmental Systems Research Institute (ESRI): Redlands, CA, 2019. http://desktop.arcgis.com/en/ (accessed August 19, 2020).

31. *Great circle*; Environmental Systems Research Institute (ESRI): Redlands, CA, 2020. https://support.esri.com/en/other-resources/gis-dictionary/term/e20b3375-490b-4ba6-ba65-b33ce0f96b48 (accessed August 19, 2020).
32. Whitt, D.B.; Jacobson, M.Z.; Wilkerson, J.T.; Naiman, A.D.; Lele, S.K. Vertical mixing of commercial aviation emissions from cruise altitude to the surface. *Journal of Geophysical Research* **2011**, 116, https://doi.org/10.1029/2010JD015532.
33. *Airport Air Quality Manual*; International Civil Aviation Organization: Montreal, Canada, ISBN 978-92-9231-862-8, 2011; https://www.icao.int/publications/Documents/9889_cons_en.pdf (accessed August 19, 2020).
34. *Aeronautical Information Manual*: Official Guide to Basic Flight Information and ATC Procedures; U.S. Department of Transportation, Federal Aviation Administration: Washington, DC, 2019. https://www.faa.gov/air_traffic/publications/media/aim_basic_chg_1_1-30-20.pdf (accessed August 19, 2020).
35. Barrett, S.R.H.; Britter, R.E.; Waitz, I.A. Global Mortality Attributable to Aircraft Cruise Emissions. Environ. Sci. Technol. **2010**, 44, 7736–7742.
36. Diesel Fuel Standards and Rulemakings; US Environmental Protection Agency: Washington, DC, 2020; https://www.epa.gov/diesel-fuel-standards/diesel-fuel-standards-and-rulemakings#onroad-diesel (accessed August 19, 2020).
37. Bergin, M.S.; Harrell, M.; Janssen, M. Locomotive Emission Inventories for the United States from ERTAC Rail; US Environmental Protection Agency: Washington, DC, 2020. https://www3.epa.gov/ttnchie1/conference/ei20/session8/mbergin.pdf (accessed August 19, 2020).
38. Estimating ammonia emissions from anthropogenic nonagricultural sources - draft final report; US Environmental Protection Agency: Washington, DC, 2004. https://www.epa.gov/sites/production/files/2015-08/documents/eiip_areasourcesnh3.pdf (accessed August 19, 2020).
39. Aviation Environmental Design Tool (AEDT) Training; U.S. Department of Transportation, Vope Center: Washington, DC, 2020. https://www.volpe.dot.gov/policy-planning-and-

environment/environmental-measurement-and-modeling/aviation-environmental-design (accessed August 19, 2020).

40. *ICAO Aircraft Engine Emissions Databank*; International Civil Aviation Organization (ICAO): Montreal, Canada, 2020. https://www.easa.europa.eu/domains/environment/icao-aircraft-engine-emissions-databank (accessed August 19, 2020).
41. Goodkind, A.L.; Tessum, C.W.; Coggins, J.S.; Hill, J.D.; Marshall, J.D. Fine-Scale Damage Estimates of Particulate Matter Air Pollution Reveal Opportunities for Location-Specific Mitigation of Emissions. *Proc. Natl. Acad. Sci. U.S.A.* **2019**, 116, 8775-8780.
42. Krewski, D.; Jerrett, M.; Burnett, R.T.; Ma, R.; Hughes, E.; Shi, Y.; Turner, M.C.; Pope III, C.A.; Thurston, G.; Calle, E.E.; Thun, M.J. *Extended Follow-Up and Spatial Analysis of the American Cancer Society Study Linking Particulate Air Pollution and Mortality*; Research Report 140, Health Effects Institute, Boston, MA, May **2009**; https://www.healtheffects.org/system/files/Krewski140.pdf (assessed August 19, 2020)
43. National Academies of Sciences, Engineering, and Medicine, *Valuing Climate Damages: Updating Estimation of the Social Cost of Carbon Dioxide*. The National Academies Press: Washington, DC, 2017. DOI: https://doi.org/10.17226/24651.
44. *CPI Inflation Calculator*; U.S. Bureau of Labor Statistics: Washington, D.C. https://www.bls.gov/data/inflation_calculator.htm (accessed August 19, 2020).
45. Gilmore et al. *Environmental Cost-Benefit Analysis of Ultra Low Sulfur Jet Fuel;* U.S. Federal Aviation Administration Office of Environment and Energy: Washington, D.C. 2011. https://ascent.aero/documents/2020/02/environmental-costbenefit-analysis-of-ultra-low-sulfur-jet-fuel.pdf/ (accessed August 19, 2020).
46. About FlightAware; FlightAware: Houston, TX. https://flightaware.com/about/ (accessed August 19, 2020).
47. Thakrar, S.K.; Balasubramanian, S.; Adams, P.J.; Azevedo, I.M.L.; Muller, N.Z.; Pandis, S.N.; Polasky, S.; Pope, C.A.; Robinson, A.L.; Apte, J.S.; Tessum, C.W.; Marshall, J.D.; Hill, J.D. Reducing Mortality from Air Pollution in the United States by Targeting Specific Emission Sources. *Environ. Sci. Technol. Lett.* **2020**, In Press. DOI: https://doi.org/10.1021/acs.estlett.0c00424.

Chapter 5

1. Paolella, D.A.; Tessum, C.W.; Adams, P.J.; Apte, J.S; Chambliss, S.; Hill, J.; Muller, N.Z.; Marshall, J.D. Effect of Model Spatial Resolution on Estimates of Fine Particulate Matter Exposure and Exposure Disparities in the United States. *Environ. Sci. Technol. Lett.* **2018**, 5, 436–441.
2. Thakrar, S.K.; Balasubramanian, S.; Adams, P.J.; Azevedo, I.M.L.; Muller, N.Z.; Pandis, S.N.; Polasky, S.; Pope, C.A.; Robinson, A.L.; Apte, J.S.; Tessum, C.W.; Marshall, J.D.; Hill, J.D. Reducing Mortality from Air Pollution in the United States by Targeting Specific Emission Sources. *Environ. Sci. Technol. Lett.* **2020**, In Press. DOI: https://doi.org/10.1021/acs.estlett.0c00424.
3. *Bioenergy*; U.S. Department of Energy: Washington, DC, 2018; https://www.energy.gov/science-innovation/energy-sources/renewable-energy/bioenergy (accessed November 21, 2018).
4. *IPCC, 2014: Climate Change 2014: Synthesis Report*. Contribution of Working Groups I, II and III to the Fifth Assessment Report of the Intergovernmental Panel on Climate Change [Core Writing Team, R.K. Pachauri and L.A. Meyer (eds.)]. IPCC, Geneva, Switzerland, 151 pp.
5. Efroymson, R.A.; Langholtz, M.H.; Johnson, K.E.; and Stokes, B.J. (Eds.); U.S. Department of Energy, 2017; *2016 Billion-Ton Report: Advancing Domestic Resources for a Thriving Bioeconomy, Volume 2: Environmental Sustainability Effects of Select Scenarios from Volume 1*; Chapter 9, ORNL/TM-2016/727; Oak Ridge National Laboratory, Oak Ridge, TN; 640p; https://bioenergykdf.net/sites/default/files/BillionTonDownloads/BillionTon_Report_2016_vol2_Chapter9.pdf (accessed April 30, 2019).
6. *Bioenergy Models: Feedstock Production Emissions to Air Model (FPEAM)*; National Renewable Energy Laboratory (NREL), Golden, CO, 2020; https://bioenergymodels.nrel.gov/models/24/ (assessed August 28, 2020).

Appendix A

Supplemental information for Chapter 2

Sections:

1) Regional MISO analysis
2) State analysis
3) Utility analysis
4) Generator analysis
5) Variation of share of average and average marginal generation and AEFs and AMEFs by system demand
6) Temporal analysis

1. Regional MISO analysis

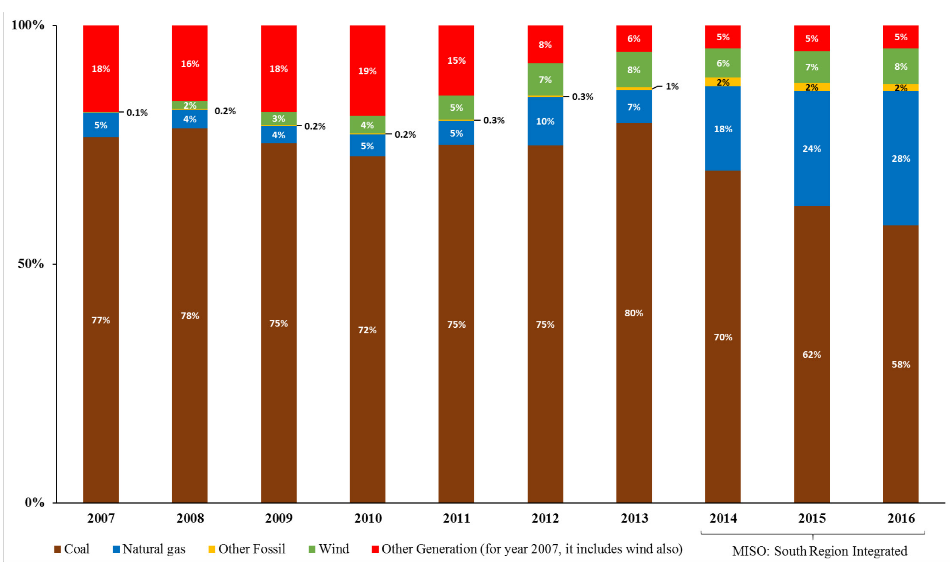

Figure A1. Generation statistics of MISO (Other generation includes nuclear, hydro and other renewables. For the year 2007, 'Other generation' includes wind as well because MISO wind data for year 2007 is not available).

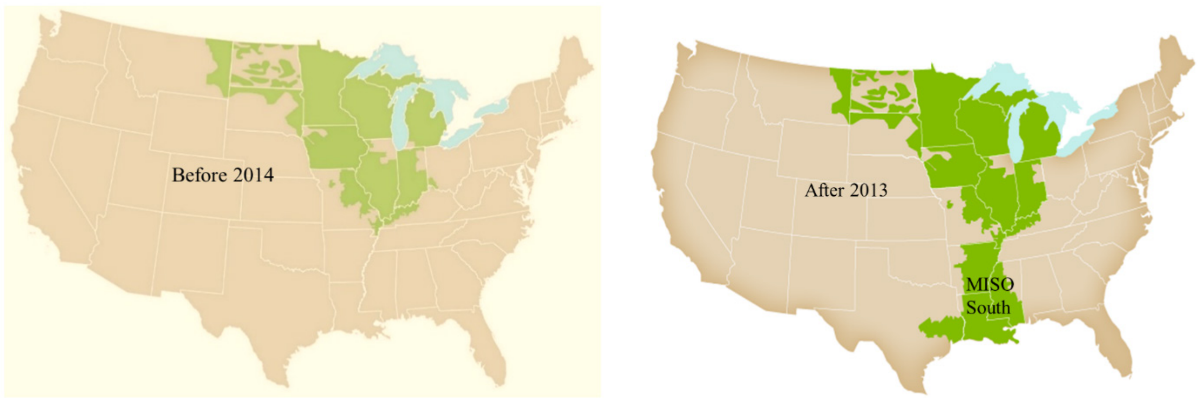

Figure A2. Midcontinent ISO footprint (Source: https://www.misoenergy.org/Planning/InterregionalCoordination/PublishingImages/IPSAC_MISO_Map.png)

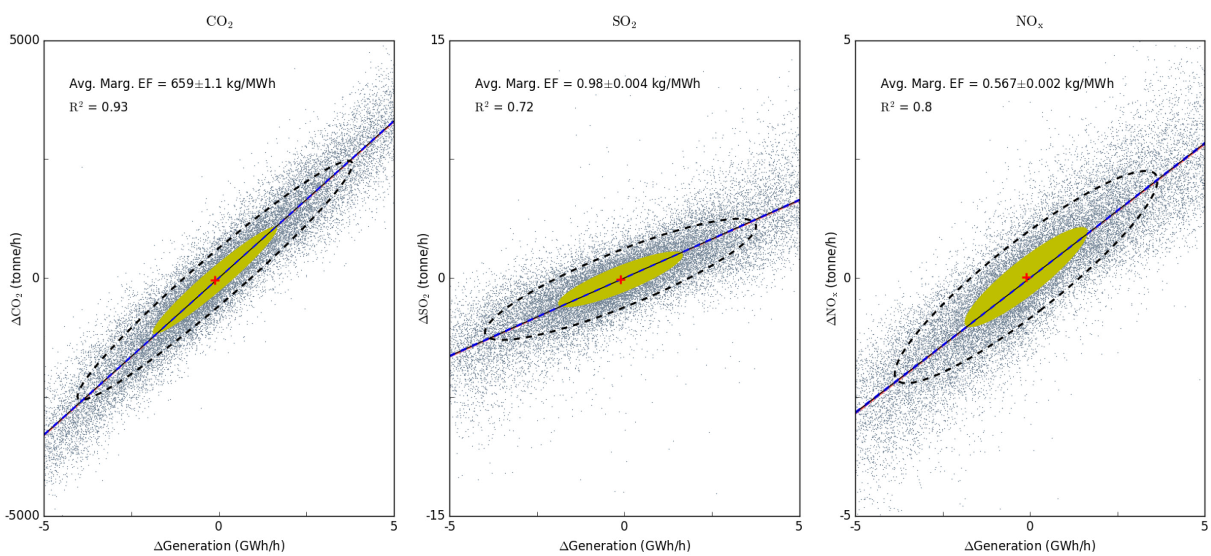

Figure A3. Linear regression for hourly changes in power generation and pollutant emissions, for Midcontinent ISO, years-2014 through 2016, after south region was integrated to Midwest ISO.

Table A1. Comparison between AEF and AMEF at regional scale for years 2014-2016

Pollutant	AEF (Kg/MWh)	AMEF (Kg/MWh)	EFs % Difference
CO_2	704	659	-6.4%
SO_2	0.953	0.984	3%
NO_x	0.521	0.567	9%

Table A2. MISO Regional AEF and AMEFs differences by year

Year	CO_2 AEF	CO_2 AMEF	CO_2 AMEF R^2	CO_2 AMEF -AEF	SO_2 AEF	SO_2 AMEF	SO_2 AMEF R^2	SO_2 AMEF -AEF	NO_x AEF	NO_x AMEF	NO_x AMEF R^2	NO_x AMEF -AEF
2007	747	576	0.87	-23%	2.71	2.18	0.71	-20%	0.963	0.691	0.63	-28%
2008	756	590	0.84	-22%	2.48	1.96	0.70	-21%	0.936	0.691	0.74	-26%
2009	722	585	0.89	-19%	2.06	1.82	0.80	-12%	0.678	0.565	0.76	-17%
2010	703	545	0.88	-22%	1.83	1.44	0.73	-21%	0.618	0.481	0.77	-22%
2011	732	602	0.88	-18%	1.68	1.49	0.70	-11%	0.626	0.537	0.76	-14%
2012	745	659	0.90	-12%	1.44	1.38	0.78	-4%	0.616	0.547	0.77	-11%
2013	772	628	0.88	-19%	1.43	1.28	0.72	-10%	0.628	0.513	0.73	-18%
All years	739	597	0.88	-19%	1.97	1.63	0.71	-17%	0.727	0.567	0.72	-22%

Table A3. MISO Regional AEF and AMEFs by fuel type for years 2007 through 2013

Coal-fired EGUs				
	AEF	AMEF	AMEF R^2	AMEF - AEF
CO_2	712	511 ± 1.085	0.78	-28%
SO_2	1.96	1.61 ± 0.0042	0.70	-18%
NO_x	0.708	0.518 ± 0.0015	0.67	-27%
Natural gas-fired EGUs				
	AEF	AMEF	AMEF R^2	AMEF - AEF
CO2	22.9	85.7 ± 0.391	0.44	274%

SO2	0.0096	0.017 ± 0.0003	0.06	78%
NOx	0.016	0.046 ± 0.0003	0.24	182%

*% difference is calculated as ((AMEF – AEF)/AEF) *100

Table A4. MISO Regional AEF and AMEFs for coal fleet by year

Year	CO_2 AEF	CO_2 AMEF	CO_2 AMEF R^2	CO_2 AMEF -AEF	SO_2 AEF	SO_2 AMEF	SO_2 AMEF R^2	SO_2 AMEF -AEF	NO_x AEF	NO_x AMEF	NO_x AMEF R^2	NO_x AMEF -AEF
2007	720	450	0.71	-37%	2.68	2.10	0.68	-21%	0.927	0.619	0.56	-33%
2008	737	507	0.73	-31%	2.46	1.91	0.69	-22%	0.908	0.632	0.70	-30%
2009	704	530	0.83	-25%	2.06	1.81	0.79	-12%	0.668	0.533	0.73	-20%
2010	680	467	0.78	-31%	1.83	1.43	0.73	-22%	0.605	0.432	0.71	-29%
2011	706	526	0.80	-25%	1.68	1.49	0.70	-11%	0.612	0.494	0.71	-19%
2012	702	557	0.83	-21%	1.44	1.38	0.78	-4%	0.596	0.496	0.72	-17%
2013	740	538	0.79	-27%	1.42	1.28	0.72	-10%	0.614	0.471	0.68	-23%
All years	712	511	0.78	-28%	1.96	1.61	0.70	-18%	0.708	0.518	0.67	-27%

Table A5. MISO Regional AEF and AMEFs for natural gas fleet by year

Year	CO_2 AEF	CO_2 AMEF	CO_2 AMEF R^2	CO_2 AMEF -AEF	SO_2 AEF	SO_2 AMEF	SO_2 AMEF R^2	SO_2 AMEF -AEF	NO_x AEF	NO_x AMEF	NO_x AMEF R^2	NO_x AMEF -AEF
2007	26.4	126	0.53	375%	0.034	0.075	0.22	118%	0.034	0.071	0.34	106%
2008	16.9	82.6	0.42	389%	0.024	0.044	0.15	84%	0.024	0.052	0.21	114%
2009	14.5	54.8	0.39	278%	0.002	0.007	0.05	220%	0.008	0.028	0.15	275%
2010	19.2	78.3	0.41	307%	0.002	0.006	0.08	219%	0.010	0.045	0.28	341%
2011	20.8	75.7	0.41	265%	0.001	0.002	0.03	52%	0.010	0.040	0.26	291%
2012	38.2	102	0.52	167%	0.0003	0.001	0.03	149%	0.016	0.048	0.31	208%
2013	26.6	89.3	0.47	235%	0.0002	0.001	0.14	256%	0.010	0.040	0.19	303%
All years	22.9	85.7	0.44	274%	0.0096	0.017	0.06	78%	0.016	0.046	0.24	182%

2) State analysis

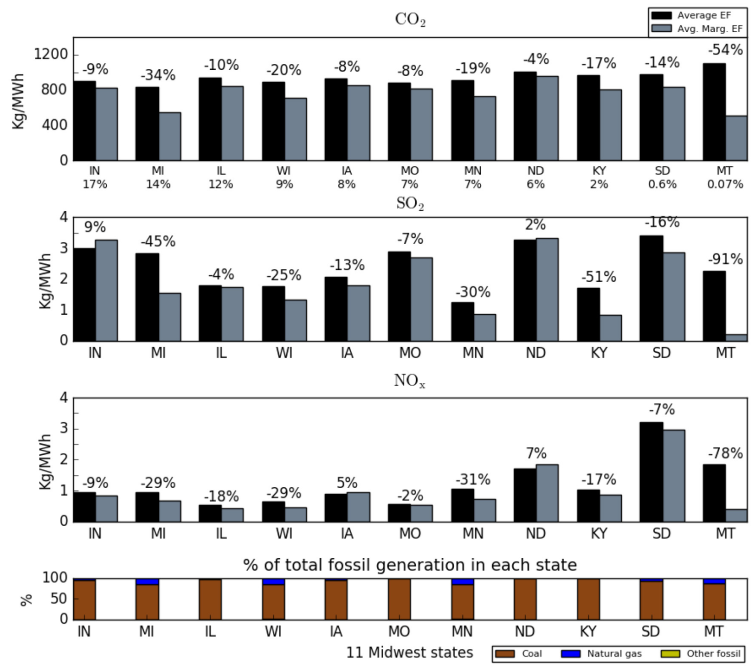

Figure A4. State wise AEF and AMEF for three pollutants from year 2007 through 2013. Percentages at top of bars show the difference between AEF and AMEF. States are sorted by increasing % share of total MISO generation (shown at bottom of x-axis for CO2 plot, sum of percentages ~83%). Bottommost plot shows % generation by fuel in each state.

(A.)

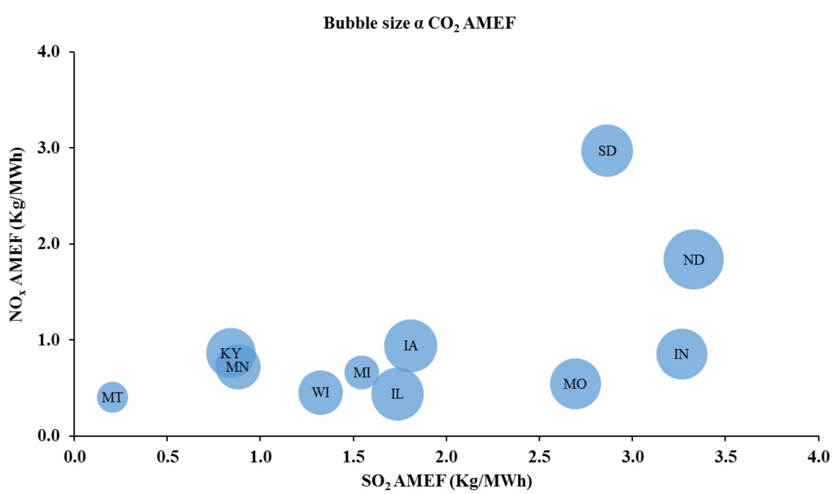

B.)

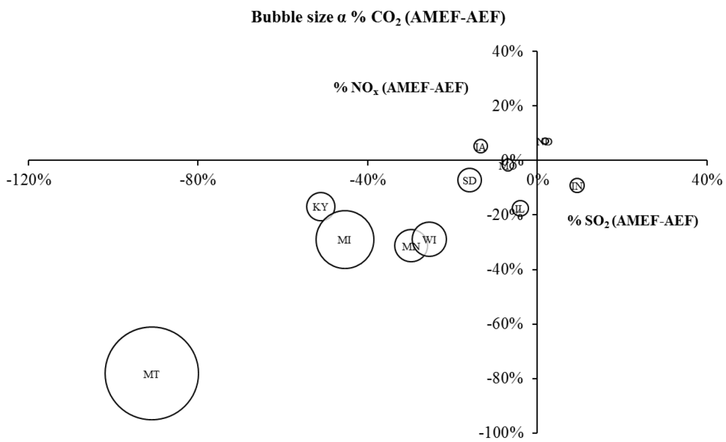

Figure A5. (A) Plots showing inter-relation between three variables: CO_2 AMEF, SO_2 AMEF and NO_x AMEF. (B) Plot showing inter-relation between % difference between AEF and AMEF for three pollutants.

Plot (A) shows low correlation between NO_x AMEF and SO_2 AMEF with insignificant change in CO_2 AMEF.

3) Utility Analysis

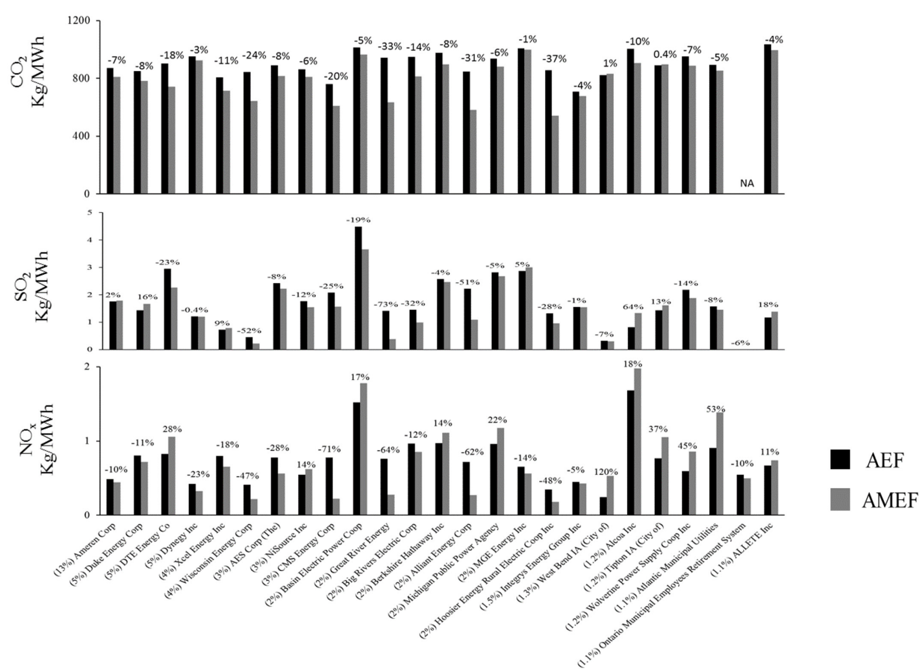

Figure A6. AEFs and AMEFs for utilities bidding in MISO in the year 2012 (having generation share > 1%). Percentages shown at top of bars are difference between AEF and AMEF. Utilities are sorted by decreasing % generation share of total generation (shown in brackets on x-axis).

4) Generator Analysis

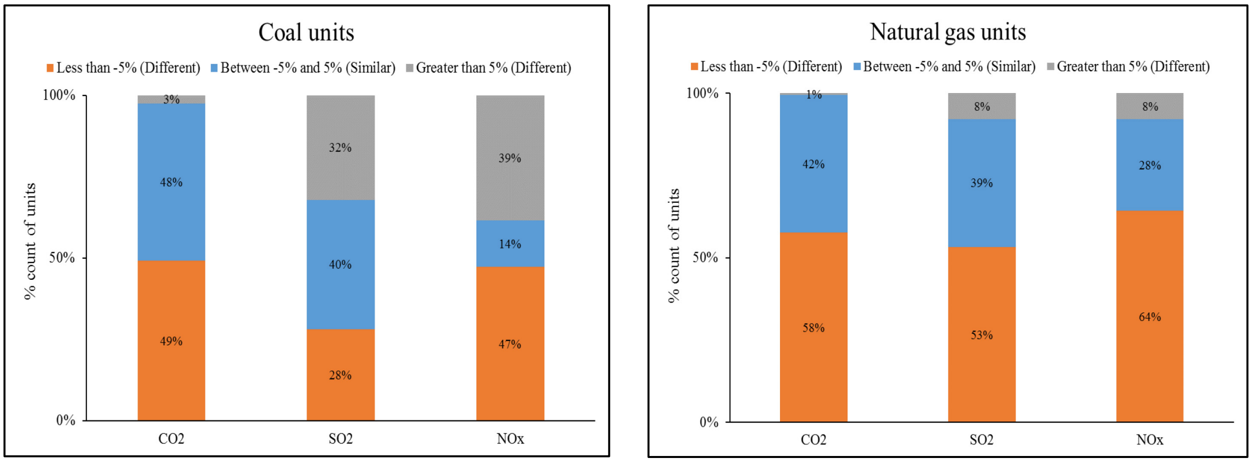

Figure A7. Figure showing significance of difference between AEF and AMEF for three pollutants among coal and natural gas units using ±5% range for all years 2007 through 2013 combined

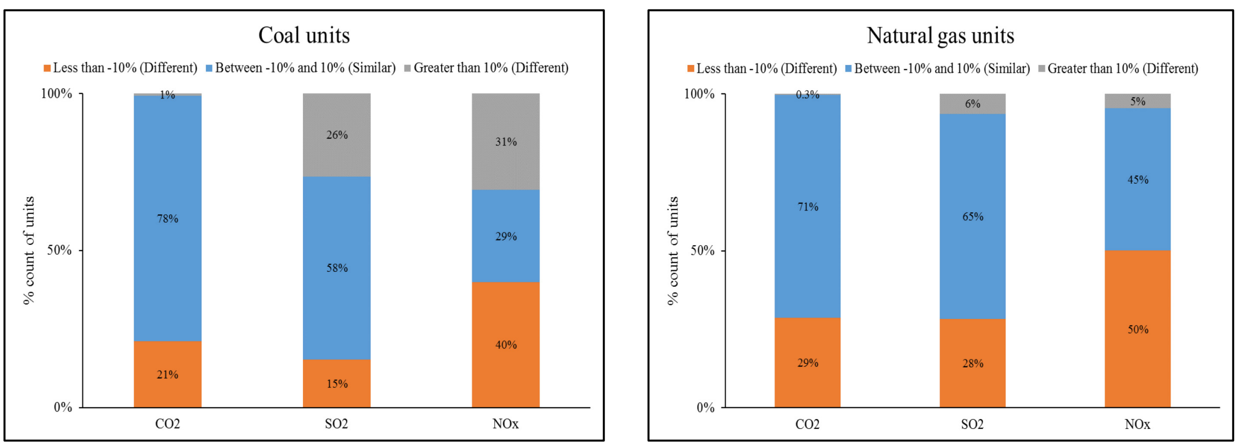

Figure A8. Figure showing significance of difference between AEF and AMEF for three pollutants among coal and natural gas units using ±10% range for all years 2007 through 2013 combined

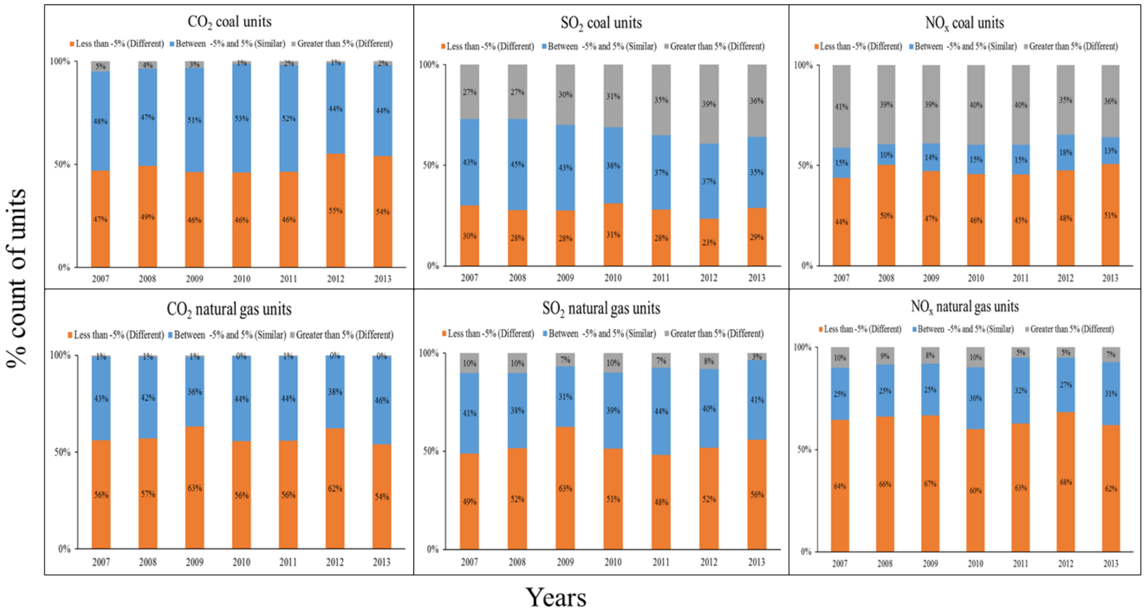

Figure A9. Significance of differences between EFs using ±5% range by year

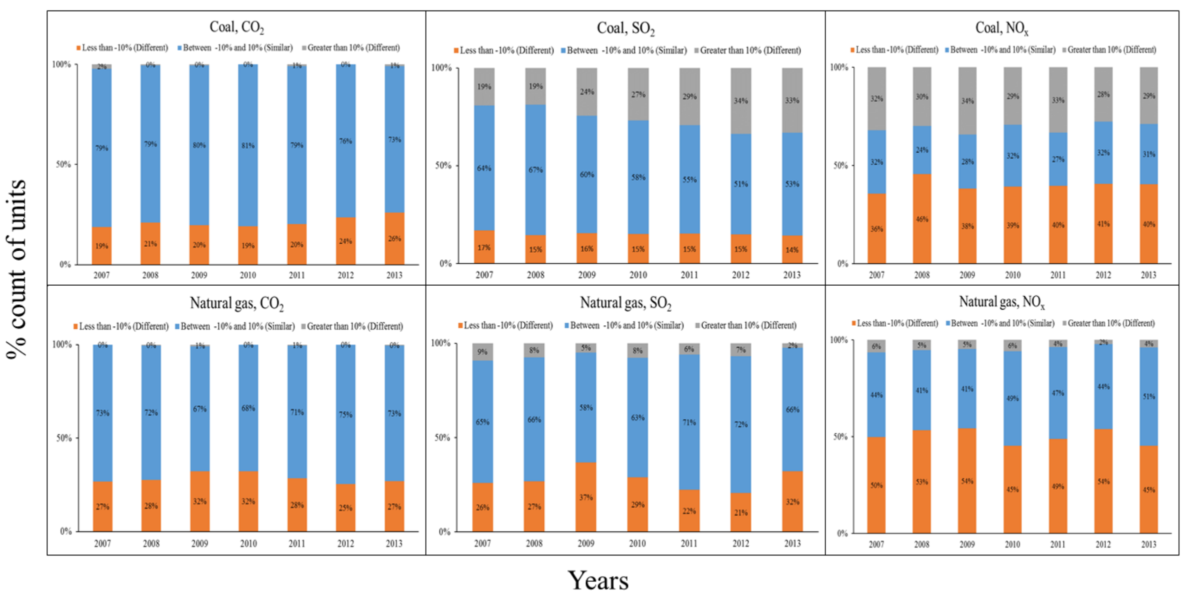

Figure A10. Significance of differences between EFs using ±10% range by year

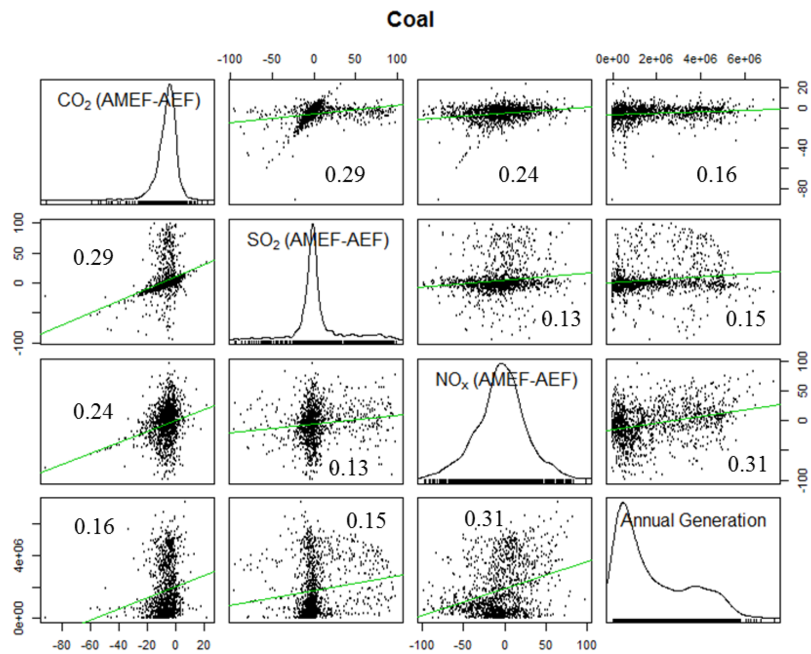

Figure A11. Scatterplot matrix showing correlation among % difference between AEF and AMEF for CO_2, SO_2 and NO_x, and Annual Generation (MWh) for coal generators. Numbers in each plot is correlation coefficient.

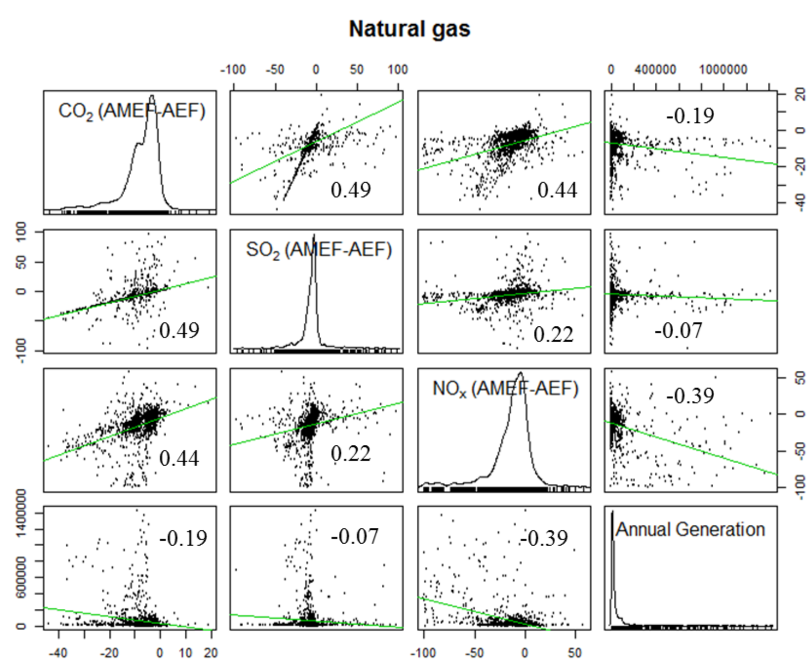

Figure A12. Scatterplot matrix showing correlation among % difference between AEF and AMEF for CO_2, SO_2 and NO_x, and Annual Generation (MWh) for natural gas generators. Numbers in each plot is correlation coefficient.

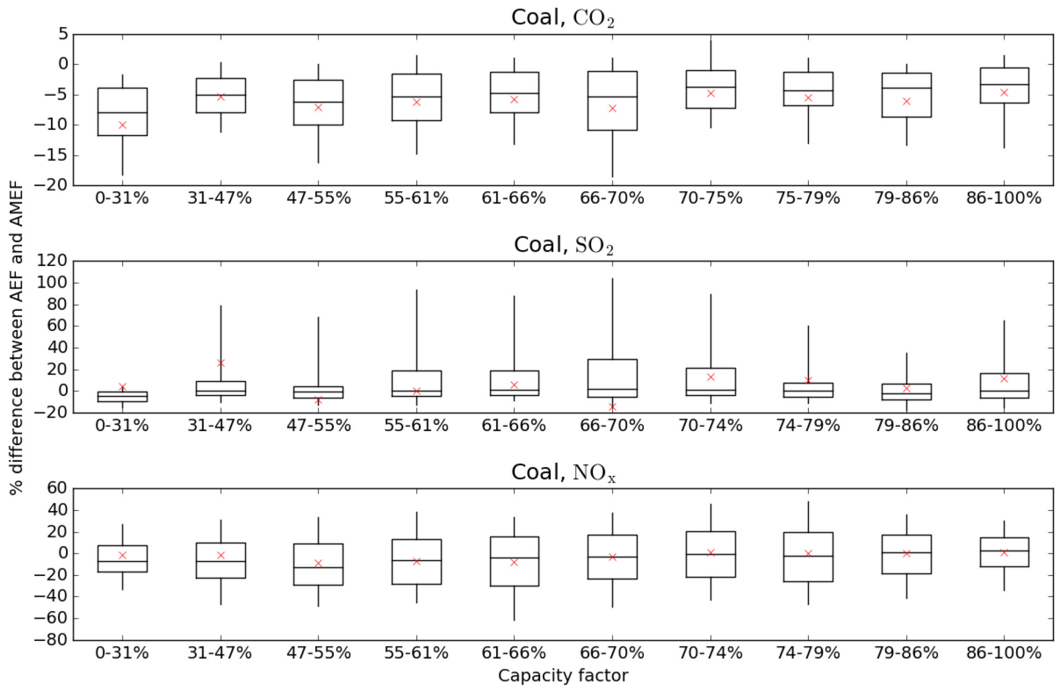

Figure A13. % difference between generator AEF and AMEF as a function of capacity factor for CO_2, SO_2 and NO_x emissions from coal units.

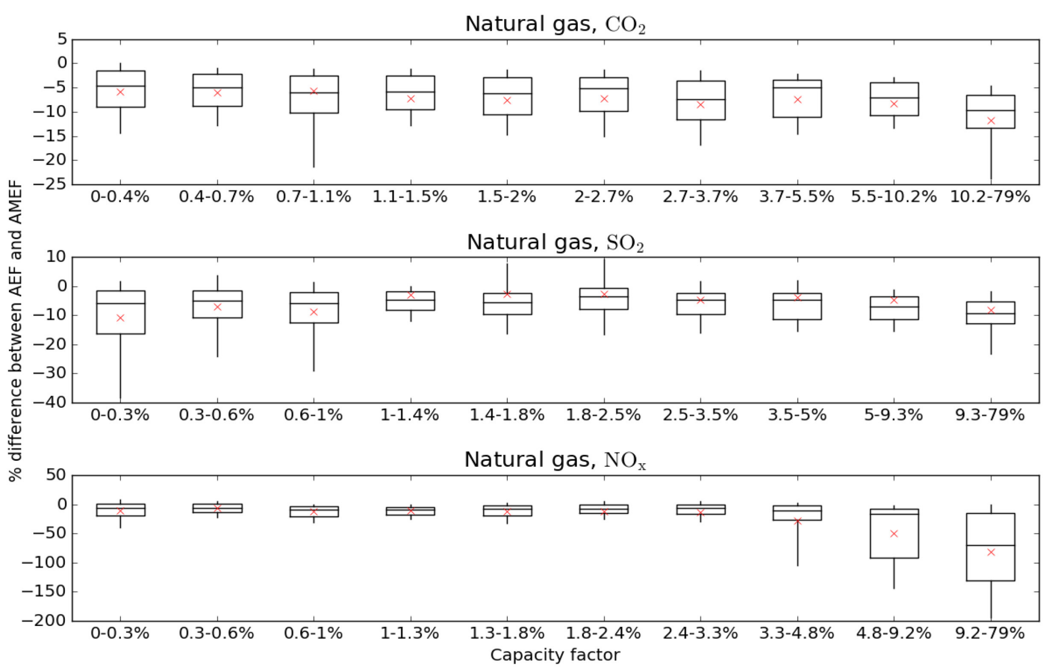

Figure A14. % difference between generator AMEF and AEF as a function of capacity factor for CO_2, SO_2, and NO_x emissions from natural gas units.

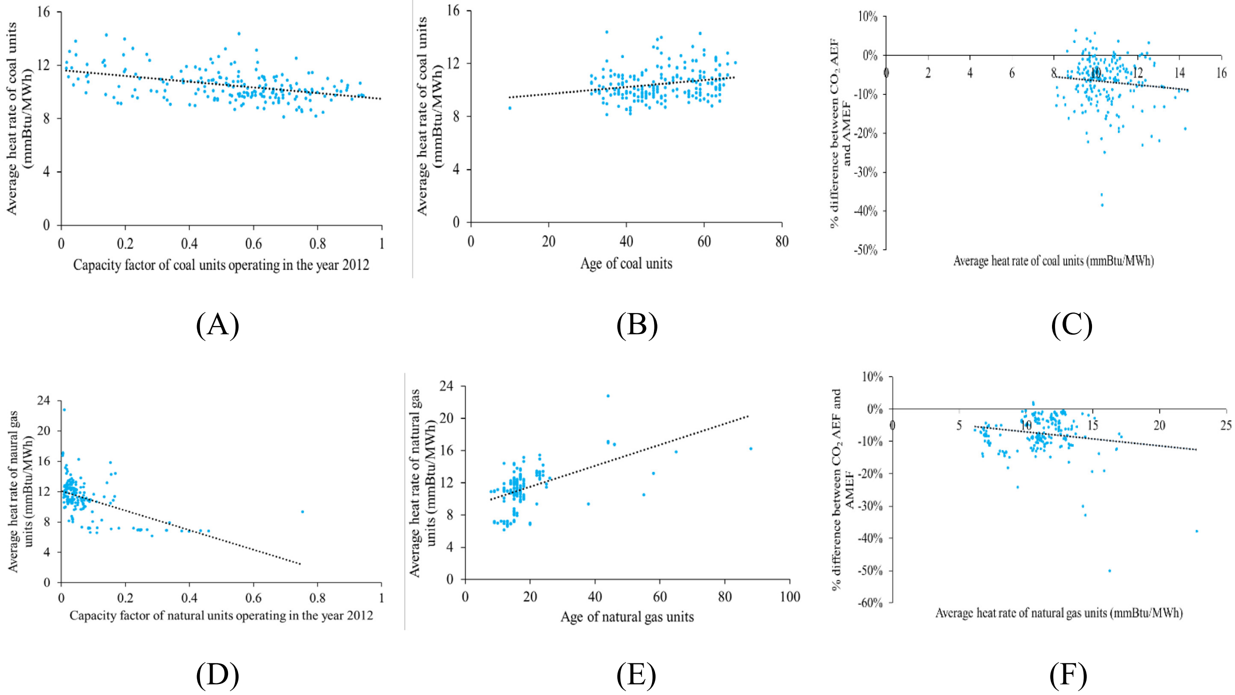

Figure A15. (A,B,C) Dependence of average heat rate of coal units operating in year 2012 on capacity factor, age of coal units; and relation between % CO_2 (AEF-AMEF) difference and average heat rate of coal units. (D,E,F) Dependence of average heat rate of natural gas units operating in year 2012 on capacity factor, age of natural gas units; and relation between % CO_2 (AEF-AMEF) difference and average heat rate of natural gas units.

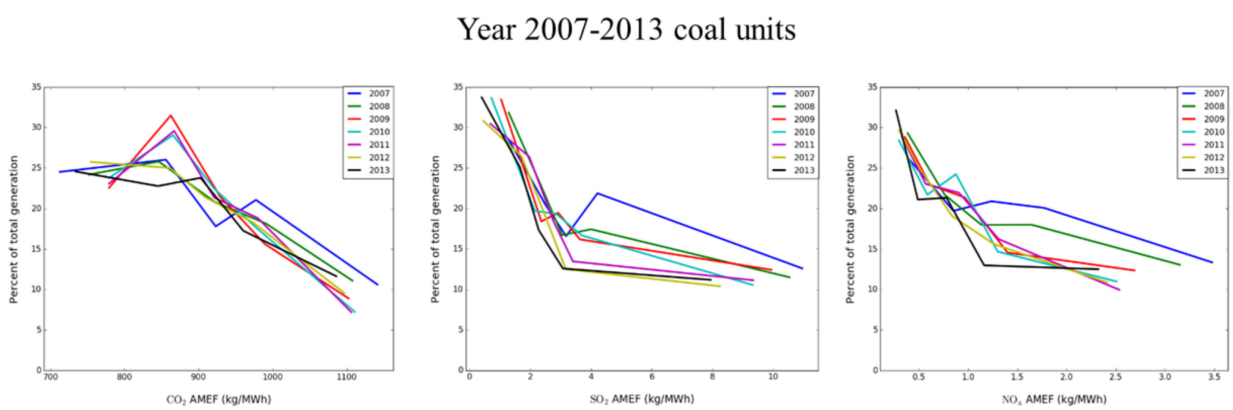

Figure A16. % of generation as a function of AMEFs for coal units

Year 2007-2013 natural gas units

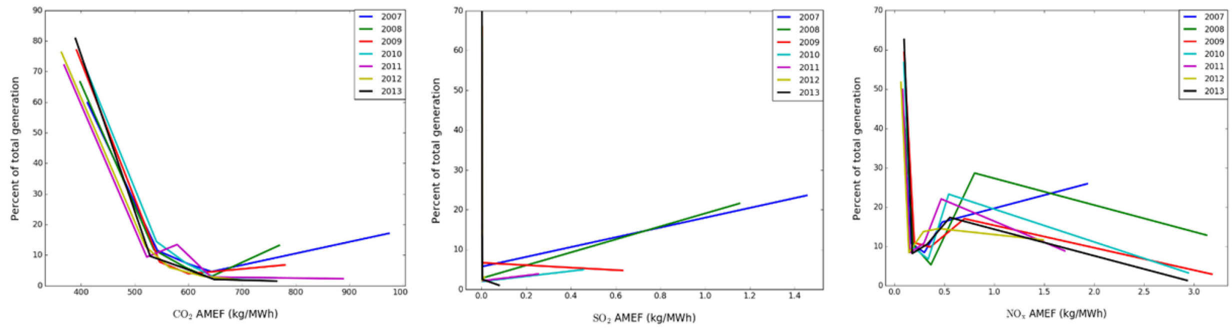

Figure A17. % of generation as a function of AMEFs for natural gas units

5. Variation of share of average and average marginal generation and AEFs and AMEFs by system demand

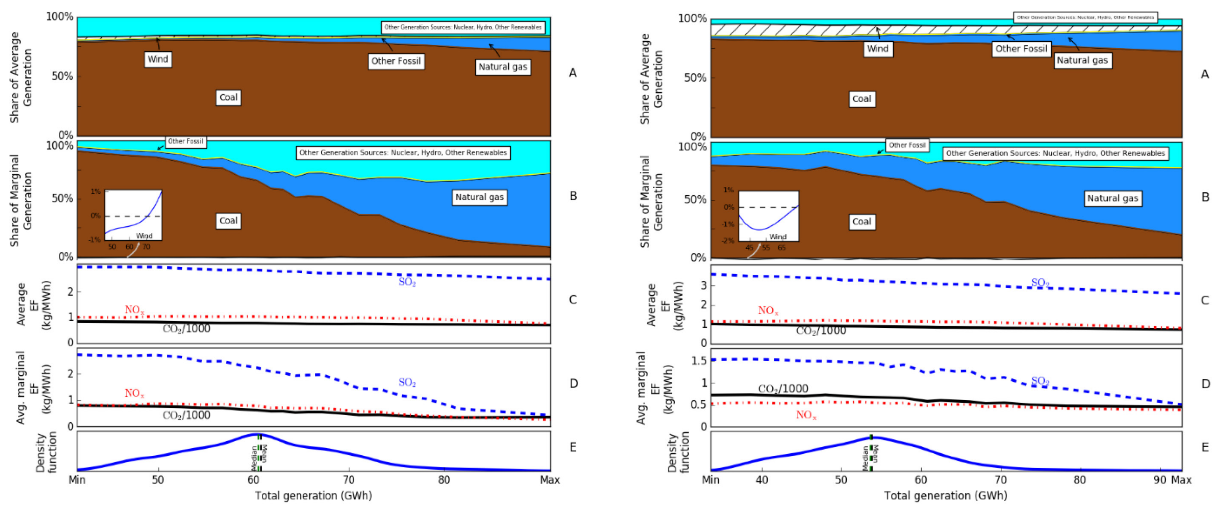

(I) 2008 (II) 2013

Figure A18. Results by total generation for MISO for year 2008 (I) and 2013 (II). (A) Average generation by fuel. (B) Average marginal generation by fuel. (C) AEFs as a function of total generation (D) AMEFs as a function of total generation. (E) Kernel density distribution for total generation.

6. Temporal analysis

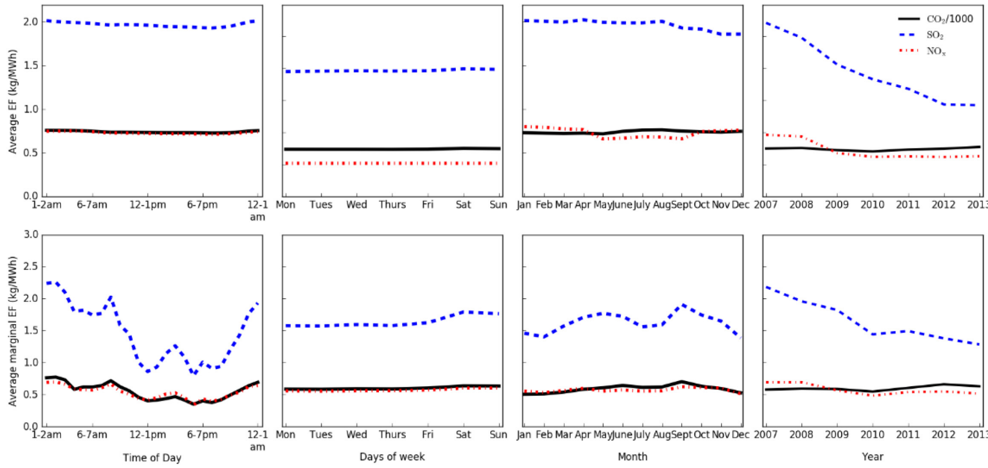

Figure A19. Comparison of time of day, days of week, monthly and yearly trends in AEF and AMEFs for MISO from year 2007 through 2013

CO_2 AMEF is ~64% higher at low demand hours than at high demand hours, because coal is the dominant marginal fuel at low demand hours. Similarly, AMEF for SO_2 is 84% higher (for NO_x: 38% higher) at low demand hours than at high demand hours.

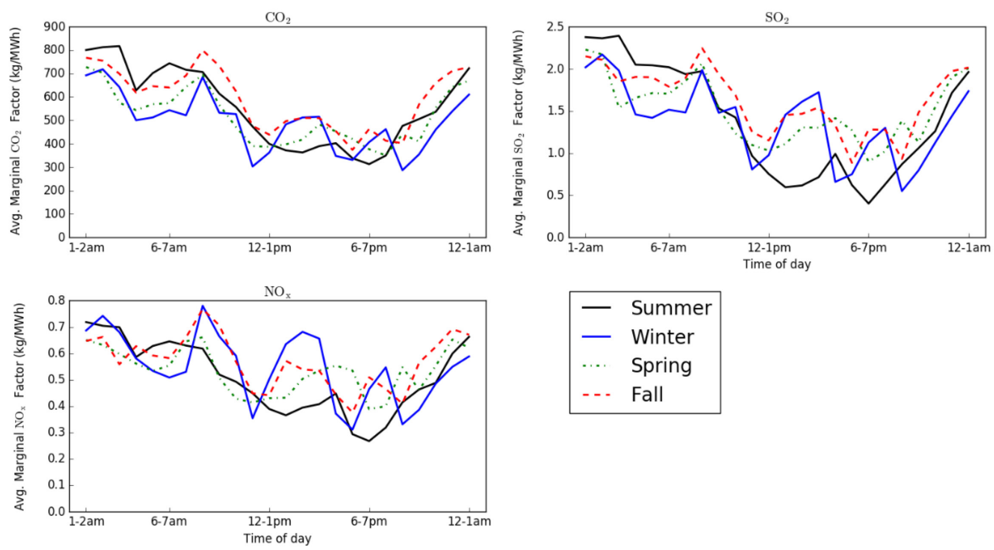

Figure A20. AMEFs by season for combined all years, 2007-2013

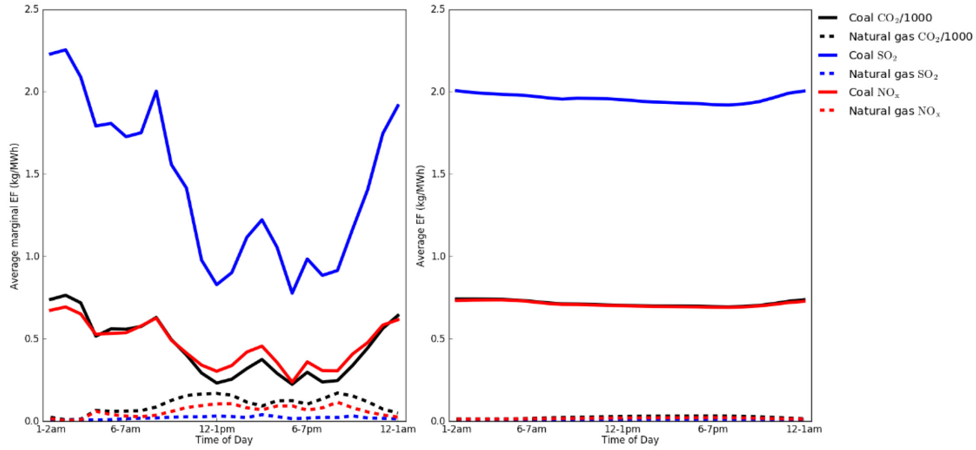

Figure A21. AMEF and AEFs by time of day and fuel source: coal and natural gas (2007-2013)

Table A6. Percent difference between system (MISO region) AEF and AMEF by time of day for all fuels, coal-specific and natural-gas specific emissions

	System (all fuel) AEF/AMEF % difference			Coal-specific system AEF/AMEF % difference			Natural gas-specific system AEF/AMEF % difference		
Time/Pollutants	CO_2	SO_2	NO_x	CO_2	SO_2	NO_x	CO_2	SO_2	NO_x
1 AM	0.45%	11%	-8%	-0.4%	11%	-8%	79%	10%	31%
2 AM	2%	13%	-7%	3%	13%	-6%	-43%	-53%	-74%
3 AM	-4%	5%	-12%	-3%	5%	-12%	-13%	4%	-40%
4 AM	-23%	-10%	-22%	-30%	-10%	-28%	401%	-20%	407%
5 AM	-18%	-9%	-23%	-24%	-9%	-27%	310%	3%	209%
6 AM	-17%	-12%	-23%	-23%	-13%	-26%	270%	75%	111%
7 AM	-14%	-10%	-17%	-20%	-11%	-19%	235%	100%	70%
8 AM	-3%	3%	-9%	-12%	2%	-12%	306%	100%	128%
9 AM	-16%	-20%	-24%	-30%	-21%	-31%	448%	152%	253%
10 AM	-24%	-27%	-31%	-43%	-28%	-41%	530%	162%	384%
11 AM	-38%	-49%	-39%	-59%	-50%	-52%	523%	152%	424%
12 PM	-46%	-56%	-43%	-67%	-58%	-57%	507%	190%	464%
1 PM	-44%	-53%	-38%	-64%	-54%	-52%	447%	158%	457%
2 PM	-41%	-42%	-29%	-54%	-42%	-40%	292%	98%	316%
3 PM	-36%	-35%	-27%	-46%	-37%	-35%	209%	256%	254%
4 PM	-44%	-44%	-37%	-59%	-45%	-49%	314%	149%	365%
5 PM	-52%	-59%	-53%	-68%	-60%	-66%	315%	35%	363%
6 PM	-45%	-48%	-40%	-57%	-49%	-48%	240%	66%	228%
7 PM	-49%	-53%	-45%	-66%	-54%	-56%	355%	112%	304%
8 PM	-43%	-52%	-40%	-65%	-53%	-56%	507%	109%	515%
9 PM	-33%	-39%	-32%	-52%	-40%	-42%	489%	202%	375%
10 PM	-24%	-28%	-26%	-38%	-28%	-33%	430%	90%	269%
11 PM	-15%	-12%	-15%	-23%	-12%	-19%	319%	80%	185%
12 AM	-9%	-4%	-14%	-13%	-4%	-15%	236%	62%	108%

Table A7. MISO-wide daytime and nighttime AMEFs for years 2007 through 2013. Column 2 and 3 represents AMEF considering daytime (8am to 5pm everyday) and nighttime hours (7pm to 7am everyday). Column 4 and 5 represents AMEF and AEF not accounting for temporal differences. Daytime and Nighttime AMEFs are calculated by regressing hourly changes in emissions during respective times over hourly changes in generation during respective times.

	Daytime AMEF	Nighttime AMEF	System AMEF	System AEF
CO_2 (Kg/MWh)	557	618	597	739
SO_2 (Kg/MWh)	1.44	1.71	1.63	1.97
NO_x (Kg/MWh)	0.526	0.585	0.567	0.727

Appendix B

Supplemental information for Chapter 3

In this SI, all mortality figures refer to deaths from $PM_{2.5}$ attributable to EGU emissions.

Sections:

1) US Regional Transmission Organizations (RTOs)
2) Total damages
3) Damages by demographic group
4) Health damages by state
5) Variations by geography and race
6) Other relevant plots

1. US Regional Transmission Organizations (RTOs)

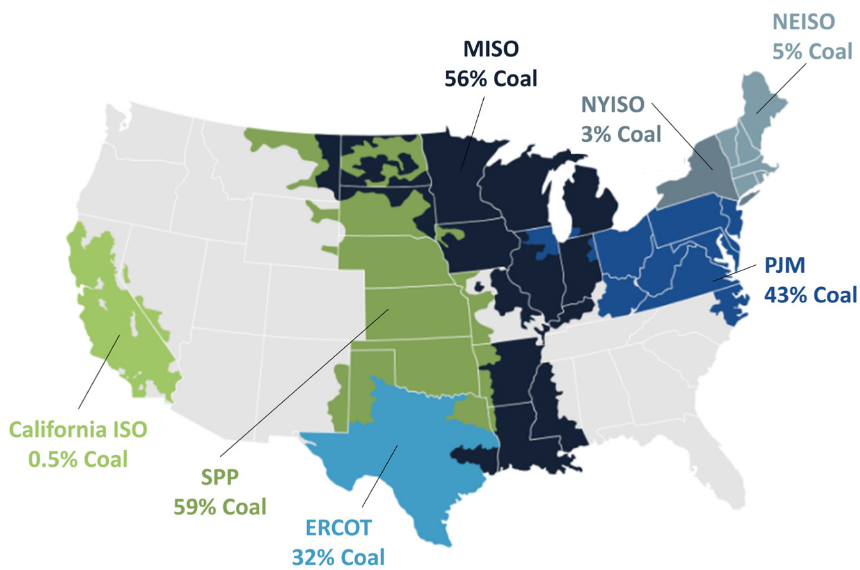

Figure B1. US RTOs with their percentage coal generation (eGRID 2014 data). Map of US RTOs obtained from https://isorto.org/.

Table B1. Demographics of US RTOs.

RTO	Total Population	% White Non-Latino	% Non-White
CAISO	30,375,993	39%	61%
ERCOT	22,999,033	44%	56%
MISO	46,039,213	77%	23%
NEISO	13,904,726	78%	22%
NYISO	18,641,324	57%	43%
PJM	63,096,305	69%	31%
SPP	16,859,226	75%	25%

2. Total damages

Table B2. Total premature deaths and deaths per 100,000 people in and out of each state from EGU-$PM_{2.5}$ emissions originating from the state and from electricity generation in the entire US.

State	Total deaths in each state from electricity generation in the entire US	Deaths per 100,000 people in each state from electricity generation in the entire US	Total deaths in the entire US from EGU-$PM_{2.5}$ emissions originating in the state	Deaths per 100,000 people (entire US) from EGU-$PM_{2.5}$ emissions originating in the state	Total deaths inside the state from in-state EGU-$PM_{2.5}$ emissions	In-state deaths per 100,000 people in the state from in-state EGU-$PM_{2.5}$ emissions	Total deaths outside each state from in-state EGU-$PM_{2.5}$ emissions	Out-of-state deaths per 100,000 people outside state from in-state EGU-$PM_{2.5}$ emissions
AL	357	7.39	522	0.167	204	4.215	319	0.104
AR	228	7.69	273	0.088	70	2.372	203	0.066
AZ	10	0.16	98	0.031	8	0.128	89	0.029
CA	79	0.21	64	0.020	57	0.150	6	0.002
CO	83	1.59	102	0.033	25	0.483	77	0.025
CT	98	2.73	15	0.005	9	0.263	6	0.002
DC	61	9.61	0	0.000	0	0.000	0	0.000
DE	117	13.01	8	0.003	2	0.199	7	0.002
FL	568	2.94	526	0.169	465	2.402	62	0.021
GA	480	4.85	373	0.119	238	2.408	134	0.044
IA	126	4.12	273	0.087	47	1.533	226	0.073
ID	1	0.09	1	0.000	0	0.003	1	0.000
IL	611	4.73	1240	0.397	247	1.914	992	0.332
IN	900	13.84	1623	0.520	407	6.257	1216	0.398
KS	114	3.99	104	0.033	13	0.454	91	0.029
KY	715	16.16	1137	0.364	305	6.891	832	0.270
LA	435	9.46	336	0.108	166	3.611	170	0.055
MA	102	1.55	23	0.007	18	0.278	5	0.002
MD	723	12.20	93	0.030	42	0.714	51	0.017
ME	13	1.00	4	0.001	3	0.240	1	0.000
MI	462	4.67	413	0.132	151	1.522	263	0.087
MN	89	1.66	88	0.028	33	0.623	54	0.018
MO	367	6.09	688	0.220	152	2.514	536	0.175
MS	236	7.99	287	0.092	93	3.137	195	0.063
MT	1	0.15	32	0.010	0	0.032	32	0.010
NC	709	7.29	314	0.101	224	2.303	90	0.030
ND	9	1.28	73	0.023	7	0.975	67	0.021
NE	54	2.97	75	0.024	11	0.616	63	0.020
NH	17	1.34	10	0.003	3	0.250	6	0.002
NJ	656	7.39	221	0.071	80	0.902	141	0.047
NM	14	0.69	67	0.022	4	0.188	64	0.021
NV	14	0.53	29	0.009	11	0.397	18	0.006
NY	934	4.75	181	0.058	151	0.767	30	0.010

OH	1351	11.71	1028	0.330	229	1.983	800	0.266
OK	204	5.29	283	0.091	59	1.537	224	0.073
OR	4	0.09	9	0.003	3	0.074	6	0.002
PA	1851	14.48	1944	0.623	879	6.871	1065	0.356
RI	23	2.23	2	0.001	2	0.156	1	0.000
SC	266	5.57	122	0.039	73	1.530	49	0.016
SD	15	1.80	32	0.010	1	0.095	32	0.010
TN	403	6.26	275	0.088	94	1.456	181	0.059
TX	1359	5.21	1684	0.540	1160	4.449	524	0.183
UT	9	0.33	103	0.033	8	0.265	96	0.031
VA	801	9.77	154	0.049	102	1.248	52	0.017
VT	8	1.21	0	0.000	0	0.013	0	0.000
WA	19	0.28	20	0.007	17	0.249	3	0.001
WI	162	2.82	123	0.040	45	0.783	78	0.026
WV	248	13.63	896	0.287	66	3.632	830	0.268
WY	5	0.89	89	0.028	2	0.338	87	0.028

Table B3. Total premature deaths per unit electricity generation from EGU-$PM_{2.5}$ emissions in each US state.

State	State annual net generation (TWh)	Deaths per TWh	% Coal share	% NG share
AL	149	3.5	32	32
AR	62	4.4	54	16
AZ	109	0.9	38	24
CA	197	0.3	0.4	60
CO	54	1.9	60	22
CT	34	0.5	2	44
DC	0.07	0.0	0	100
DE	8	1.1	11	81
FL	230	2.3	23	61
GA	126	3.0	36	33
IA	57	4.8	59	2
ID	15	0.1	1	17
IL	202	6.1	43	3
IN	115	14.1	85	8
KS	50	2.1	58	3
KY	91	12.5	92	3
LA	104	3.2	18	54

MA	31	0.7	9	60
MD	38	2.5	47	7
ME	13	0.3	1	33
MI	107	3.9	50	12
MN	57	1.5	49	7
MO	88	7.8	82	5
MS	55	5.2	19	59
MT	30	1.1	51	2
NC	126	2.5	38	22
ND	36	2.0	75	1
NE	39	1.9	63	1
NH	20	0.5	7	22
NJ	67	3.3	4	45
NM	32	2.1	63	28
NV	36	0.8	18	64
NY	134	1.4	3	40
OH	134	7.6	67	18
OK	70	4.0	43	38
OR	60	0.2	5	21
PA	221	8.8	36	24
RI	6	0.4	0	95
SC	97	1.3	30	12
SD	11	2.9	24	4
TN	80	3.5	45	8
TX	438	3.8	34	47
UT	44	2.4	76	19
VA	77	2.0	27	27
VT	7	0.02	0	0.04
WA	116	0.2	6	10
WI	61	2.0	61	13
WV	80	11.2	96	1
WY	50	1.8	87	1

Table B4. Total premature deaths and risk in each state from electricity generation in the entire US by fuel-type.

	Coal EGUs		**Natural gas EGUs**		**Other fossil fuel EGUs**	
State	Total deaths	Deaths per 100,000 people in state	Total deaths	Deaths per 100,000 people in state	Total deaths	Deaths per 100,000 people in state

AL	342	7.1	12	0.3	3	0.1
AR	217	7.3	9	0.3	2	0.1
AZ	7	0.1	3	0.04	0	0.004
CA	17	0.04	53	0.1	9	0.02
CO	79	1.5	3	0.1	1	0.01
CT	79	2.2	9	0.2	10	0.3
DC	59	9.3	0	0.1	1	0.2
DE	109	12.1	3	0.3	6	0.6
FL	439	2.3	95	0.5	34	0.2
GA	448	4.5	28	0.3	4	0.04
IA	122	4.0	3	0.1	1	0.04
ID	1	0.1	0	0.01	0	0.01
IL	597	4.6	11	0.1	3	0.02
IN	886	13.6	10	0.1	4	0.1
KS	106	3.7	7	0.2	1	0.05
KY	710	16.0	4	0.1	1	0.02
LA	375	8.2	39	0.8	21	0.4
MA	79	1.2	10	0.1	14	0.2
MD	692	11.7	7	0.1	24	0.4
ME	10	0.7	1	0.04	3	0.2
MI	439	4.4	12	0.1	11	0.1
MN	81	1.5	2	0.04	6	0.1
MO	356	5.9	9	0.2	2	0.03
MS	223	7.5	10	0.3	4	0.1
MT	1	0.1	0	0.01	0	0.02
NC	678	7.0	15	0.2	16	0.2
ND	9	1.3	0	0.01	0	0.01
NE	52	2.8	1	0.1	1	0.05
NH	15	1.1	1	0.1	1	0.1
NJ	554	6.2	52	0.6	49	0.6
NM	12	0.6	2	0.1	0	0.02
NV	3	0.1	11	0.4	0	0.02
NY	681	3.5	176	0.9	75	0.4
OH	1329	11.5	14	0.1	8	0.1
OK	179	4.6	23	0.6	2	0.1
OR	1	0.02	0	0.01	2	0.1
PA	1763	13.8	30	0.2	57	0.4
RI	17	1.6	4	0.4	3	0.3
SC	252	5.3	7	0.1	7	0.1
SD	14	1.7	0	0.03	0	0.03
TN	393	6.1	8	0.1	2	0.03

TX	1201	4.6	129	0.5	28	0.1
UT	7	0.2	2	0.1	0	0.002
VA	758	9.3	12	0.2	30	0.4
VT	7	1.1	0	0.03	0	0.1
WA	13	0.2	2	0.03	4	0.1
WI	154	2.7	5	0.1	4	0.1
WV	245	13.5	2	0.1	1	0.04
WY	5	0.9	0	0.02	0	0.02

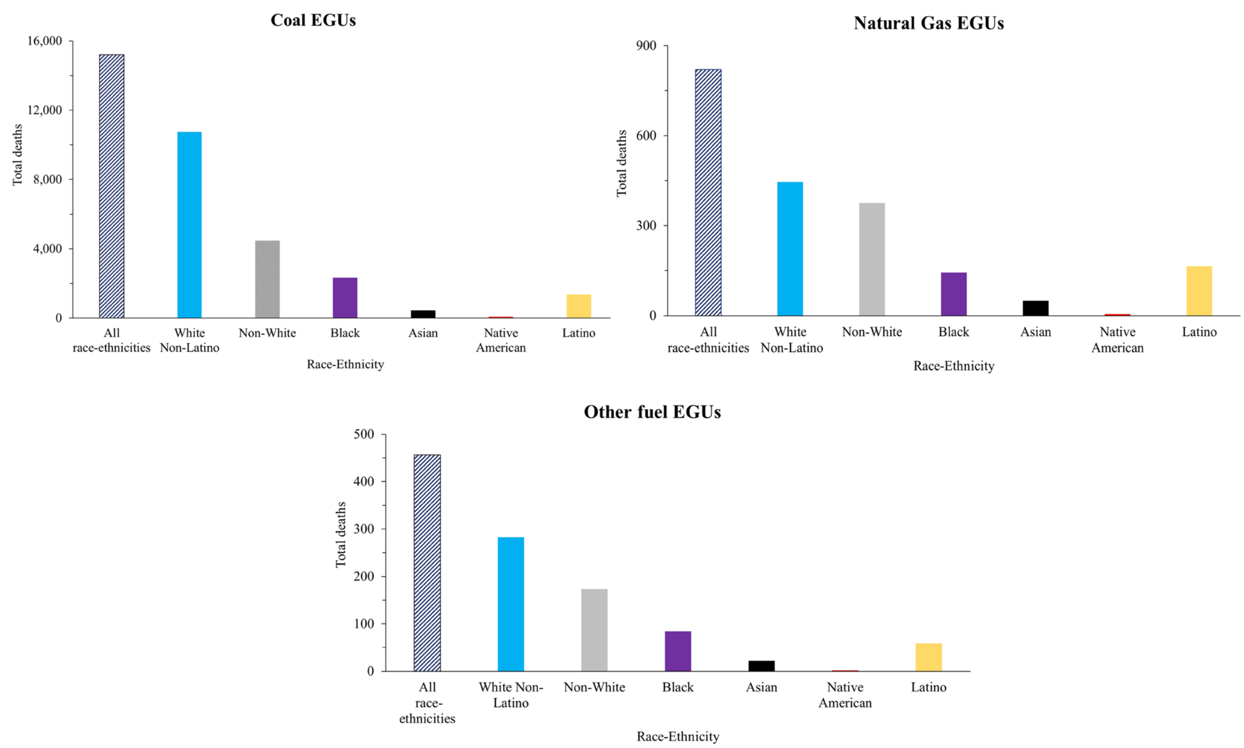

Figure B2. Total premature deaths by fuel-type and race from electricity generation in the US for the year 2014. “Non-White” refers to all categories except White Non-Latino; “Black”, “Asian”, “Native” and other categories include both Latino and Non-Latino ethnicities.

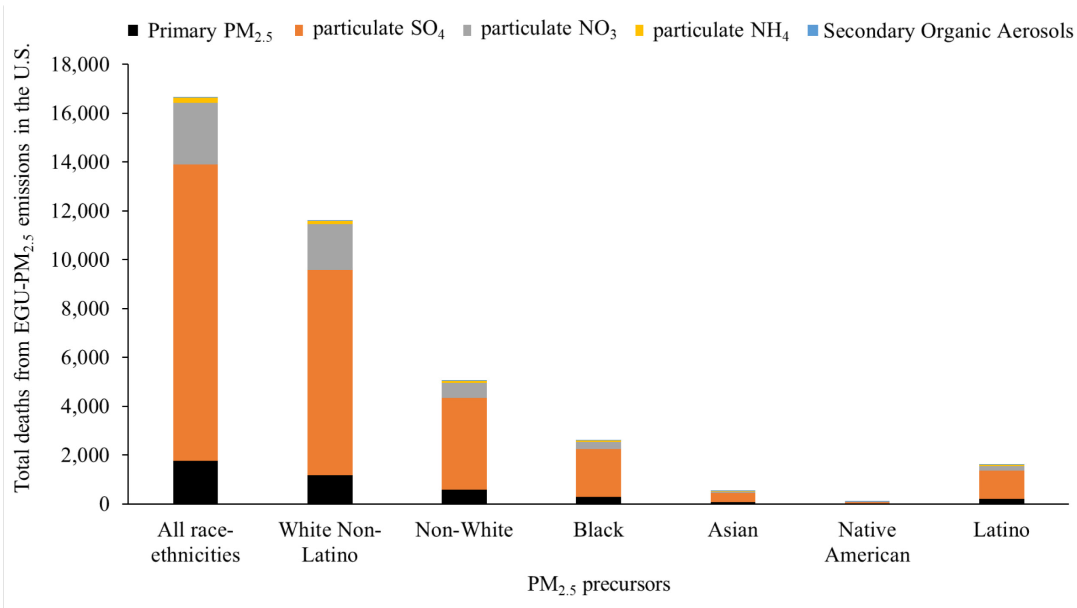

Figure B3. Total premature deaths by PM2.5 species-type and race from electricity generation in the entire US for the year 2014.

3. Damages by demographic group

3.1 Race

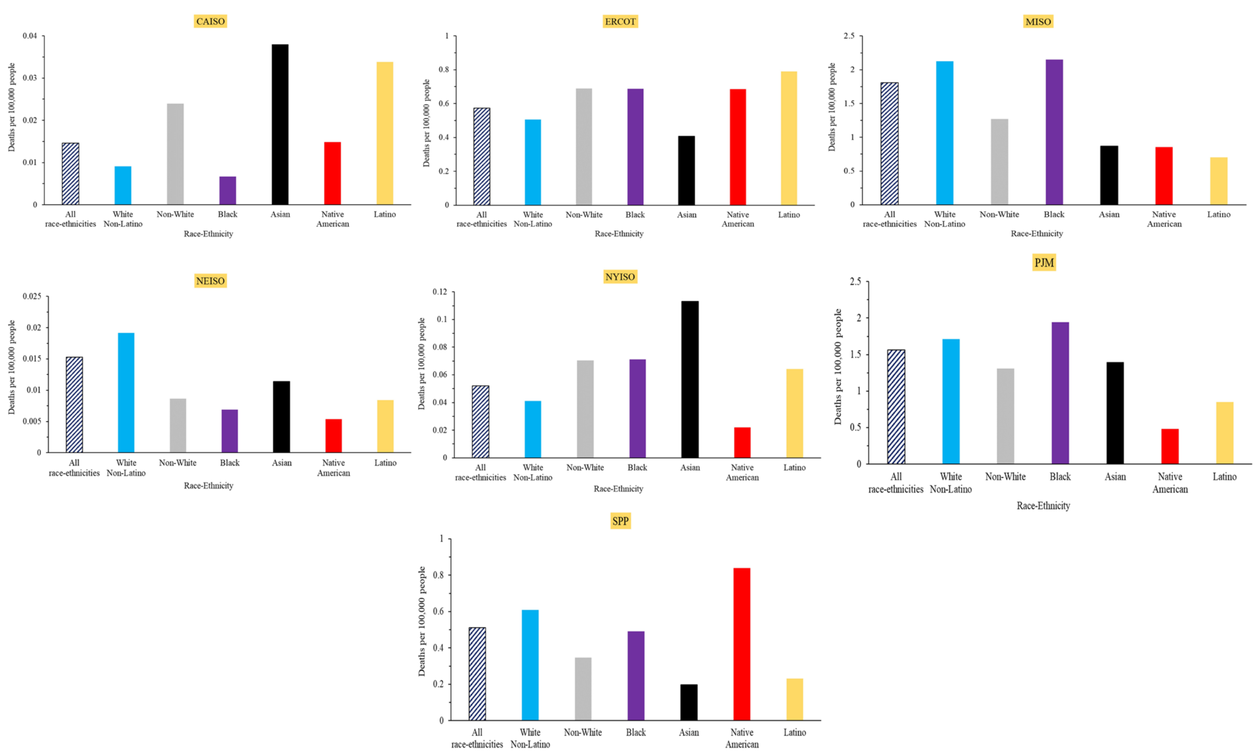

Figure B4. Deaths per 100,000 people, attributable to $PM_{2.5}$ from electricity generation in each RTO for the year 2014. “Non-White” includes all races except White Non-Latino.

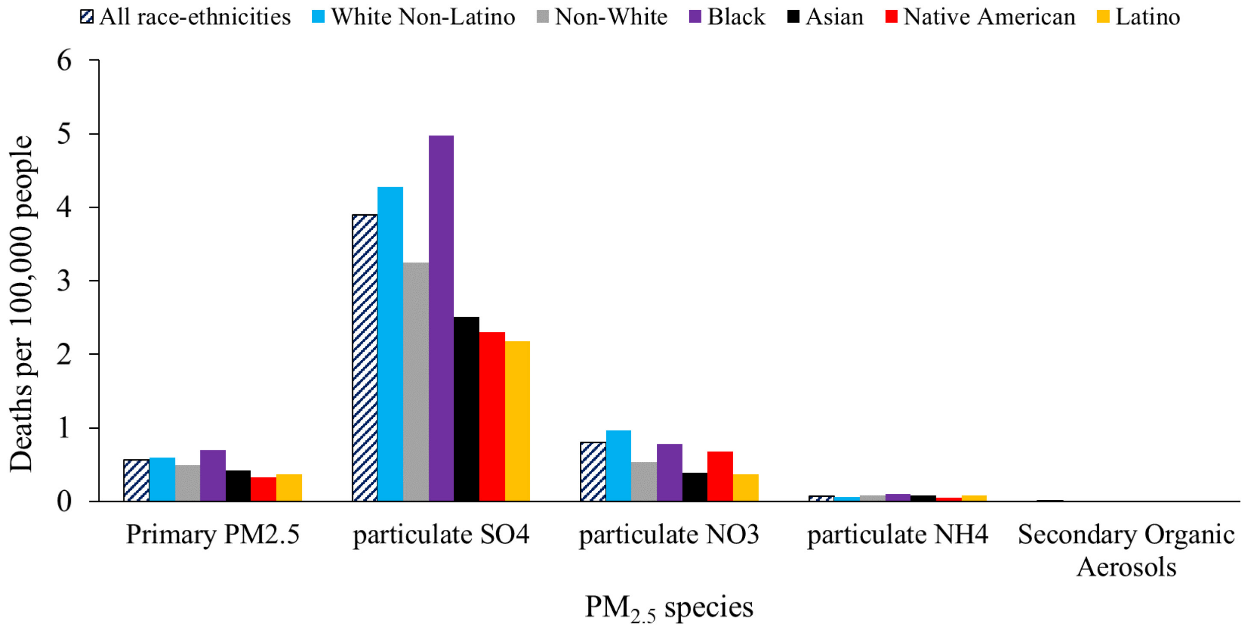

Figure B5. Deaths per 100,000 people by $PM_{2.5}$ specie-type and race from electricity generation in the entire US for the year 2014. “Non-White” refers to all categories except White Non-Latino; “Black”, “Asian”, “Native” and other categories include both Latino and Non-Latino ethnicities.

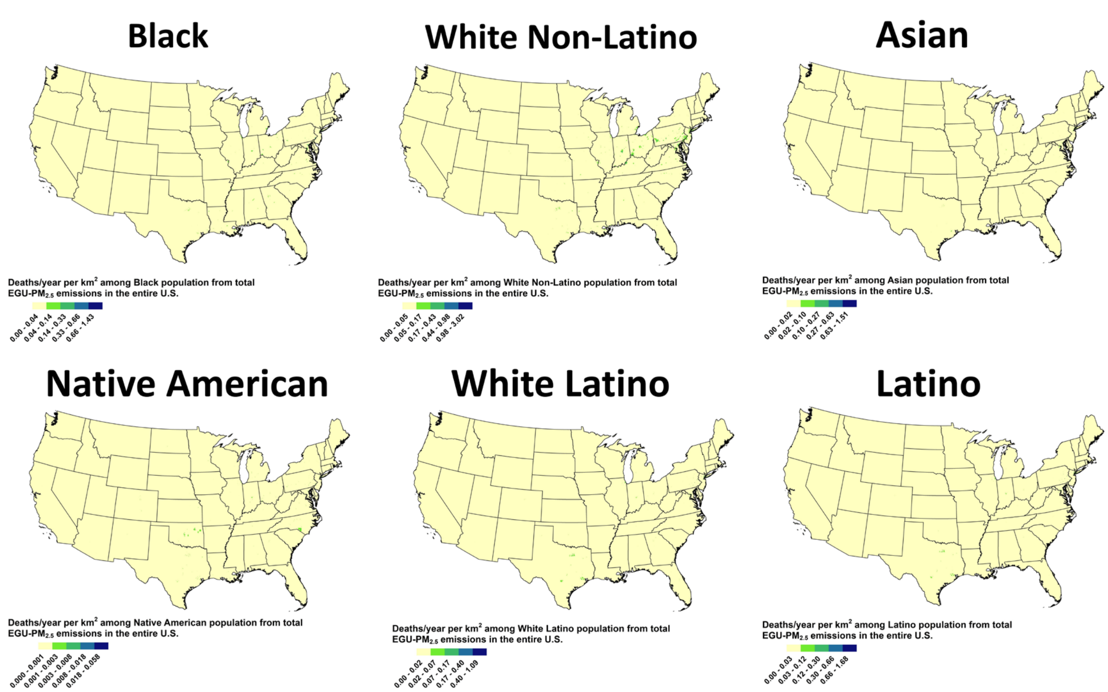

Figure B6 (A). Spatial distribution of premature deaths/year per km^2 by race-ethnicity across US at the scale of InMAP's grid cell size. Mortalities shown are from total $PM_{2.5}$ emissions from EGUs across the entire US.

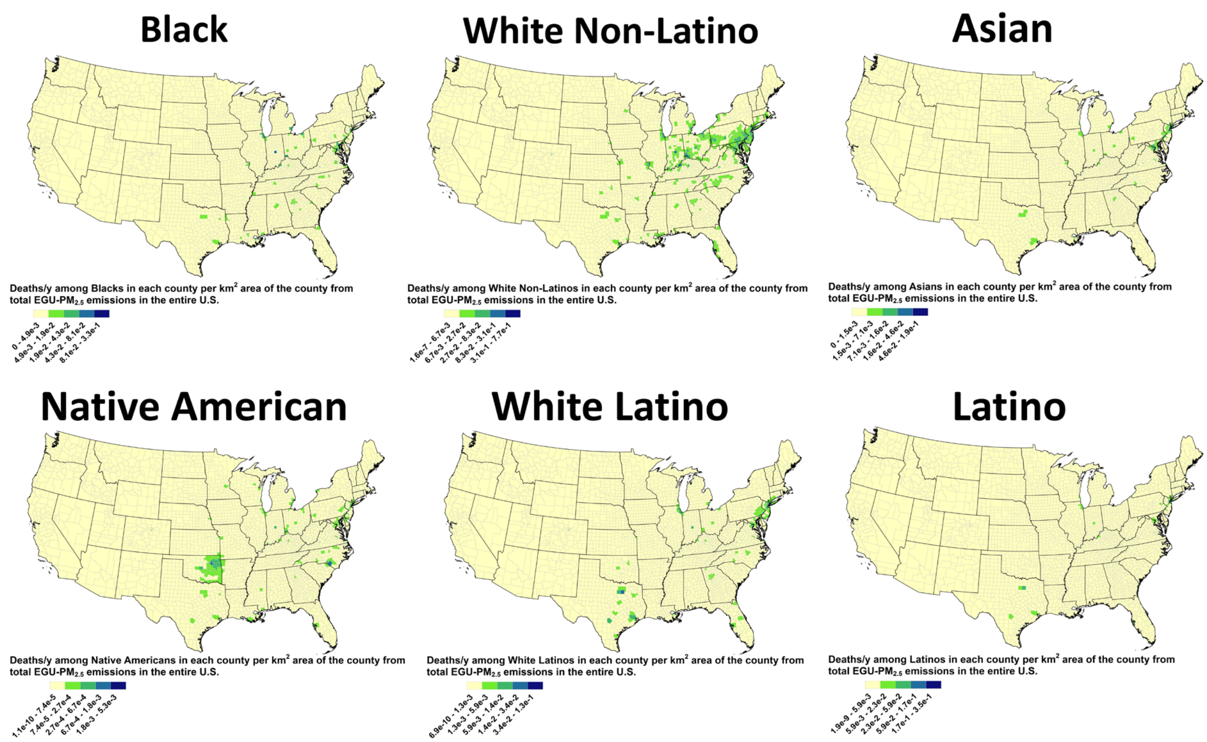

Figure B6 (B). Spatial distribution of premature deaths/year per km^2 by race-ethnicity across US counties. Premature deaths in each county is estimated by aggregating deaths from grid cells within the county. Mortalities shown are from total $PM_{2.5}$ emissions from EGUs across the entire US.

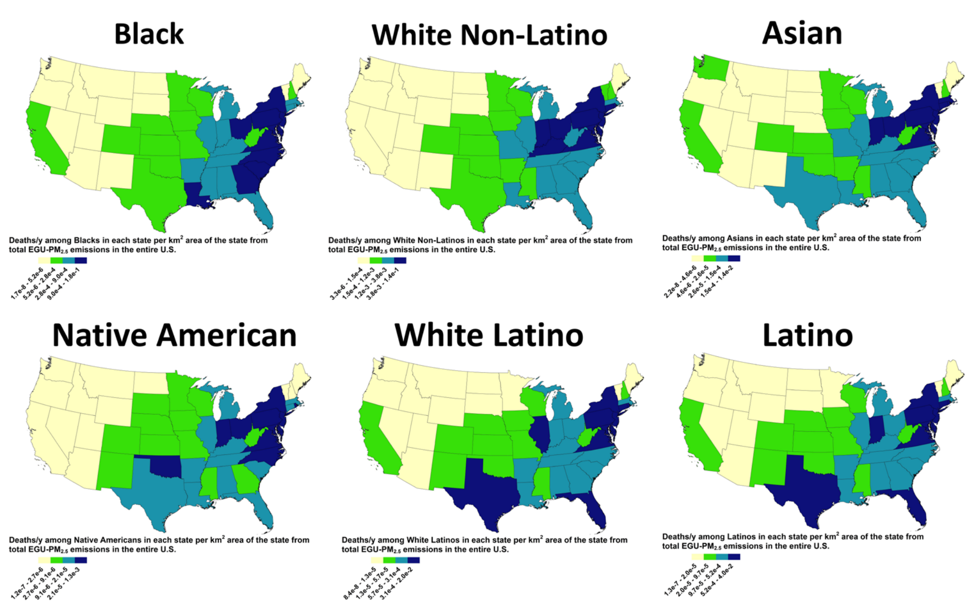

Figure B6 (C). Spatial distribution of premature deaths/year per km^2 by race-ethnicity across US states. Premature deaths in each state is estimated by aggregating deaths from grid cells within state. Mortalities shown are from total $PM_{2.5}$ emissions from EGUs across the entire US. Color gradation in the legend is shown by four quantiles.

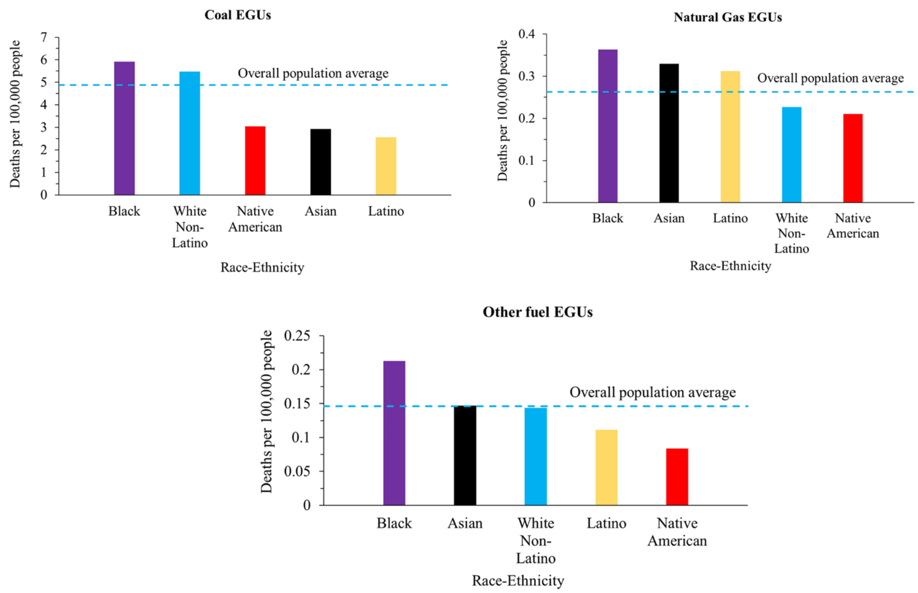

Figure B7. Deaths per 100,000 people by fuel-type and race from electricity generation in the entire US for the year 2014. Note that y-axis of each plot has different scaling.

3.2 Income and Race

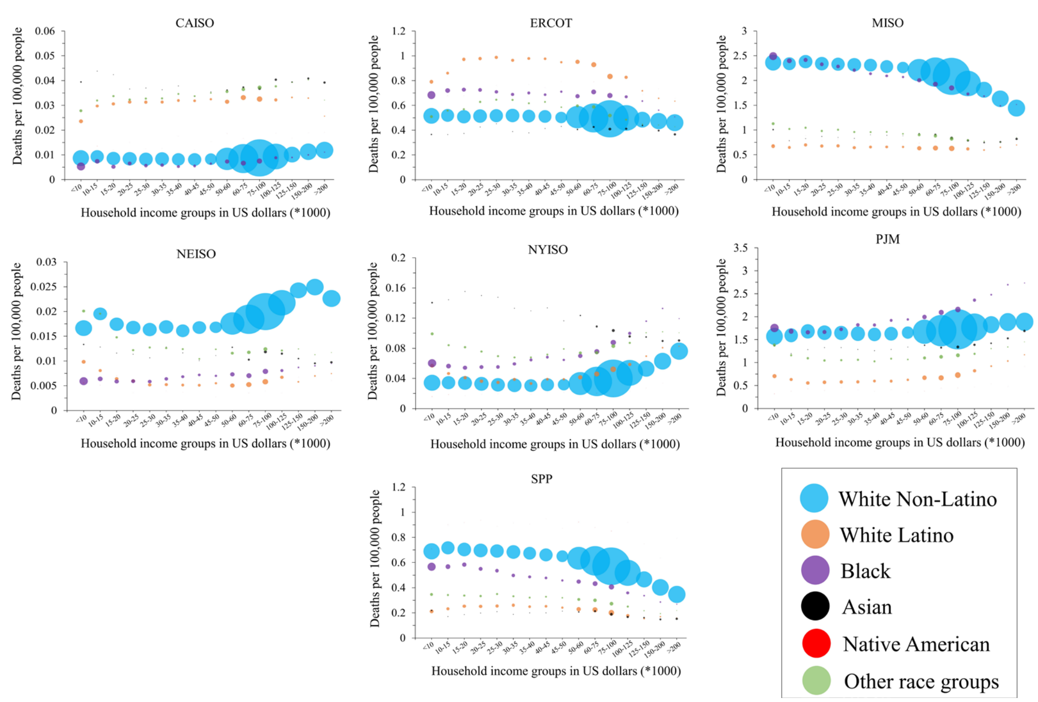

Figure B8. Deaths per 100,000 people by race-income groups from each RTO. Here, risk indicates impact of an RTO on the race-income groups in the entire US. Size of bubbles is proportional to the population in each income group.

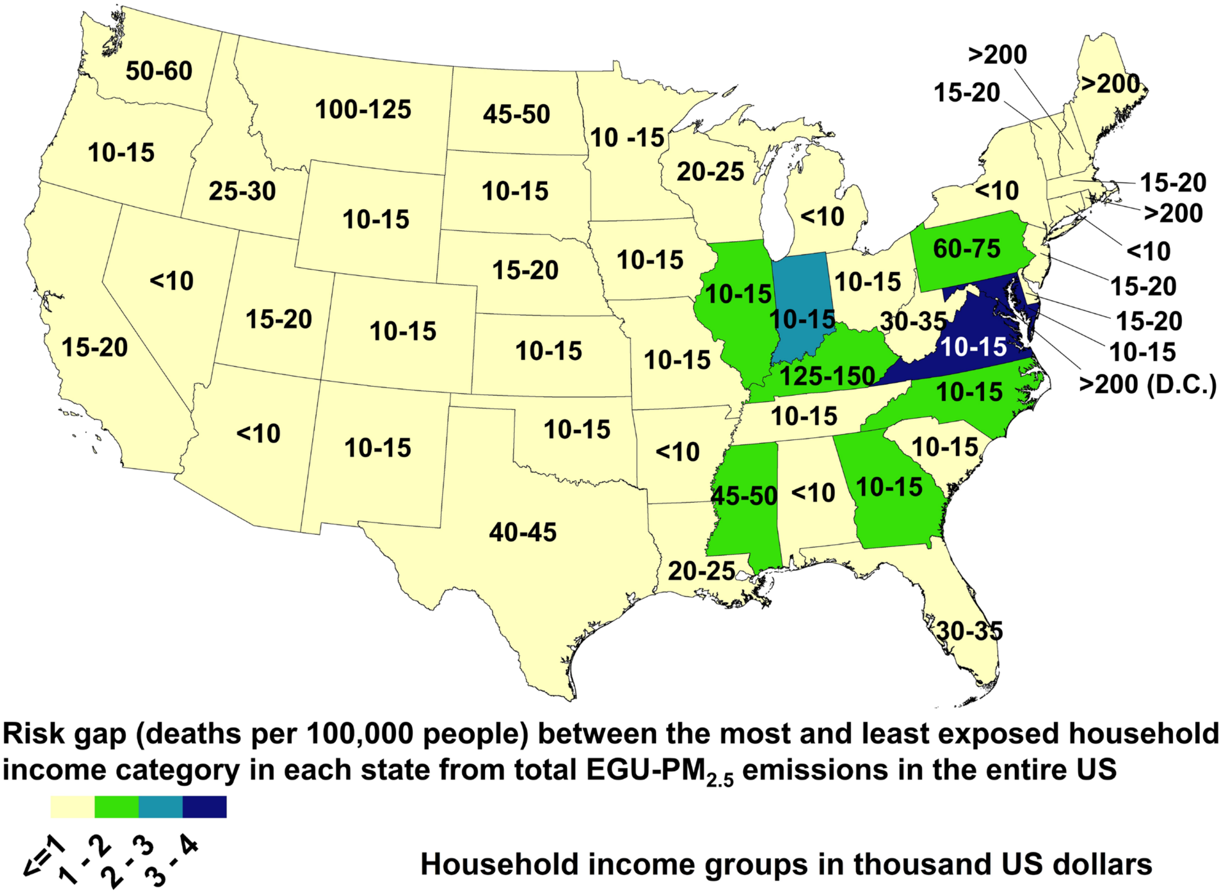

Figure B9. Most exposed household income group in thousand US dollars (for overall population) and risk gap (deaths per 100,000 people) between the most and least exposed household income group in each US state from EGU-PM$_{2.5}$ emissions in the entire US. Most exposed household income group in a state is shown by labels in each state and risk gap is shown by color gradation.

4. Heath Damages by State

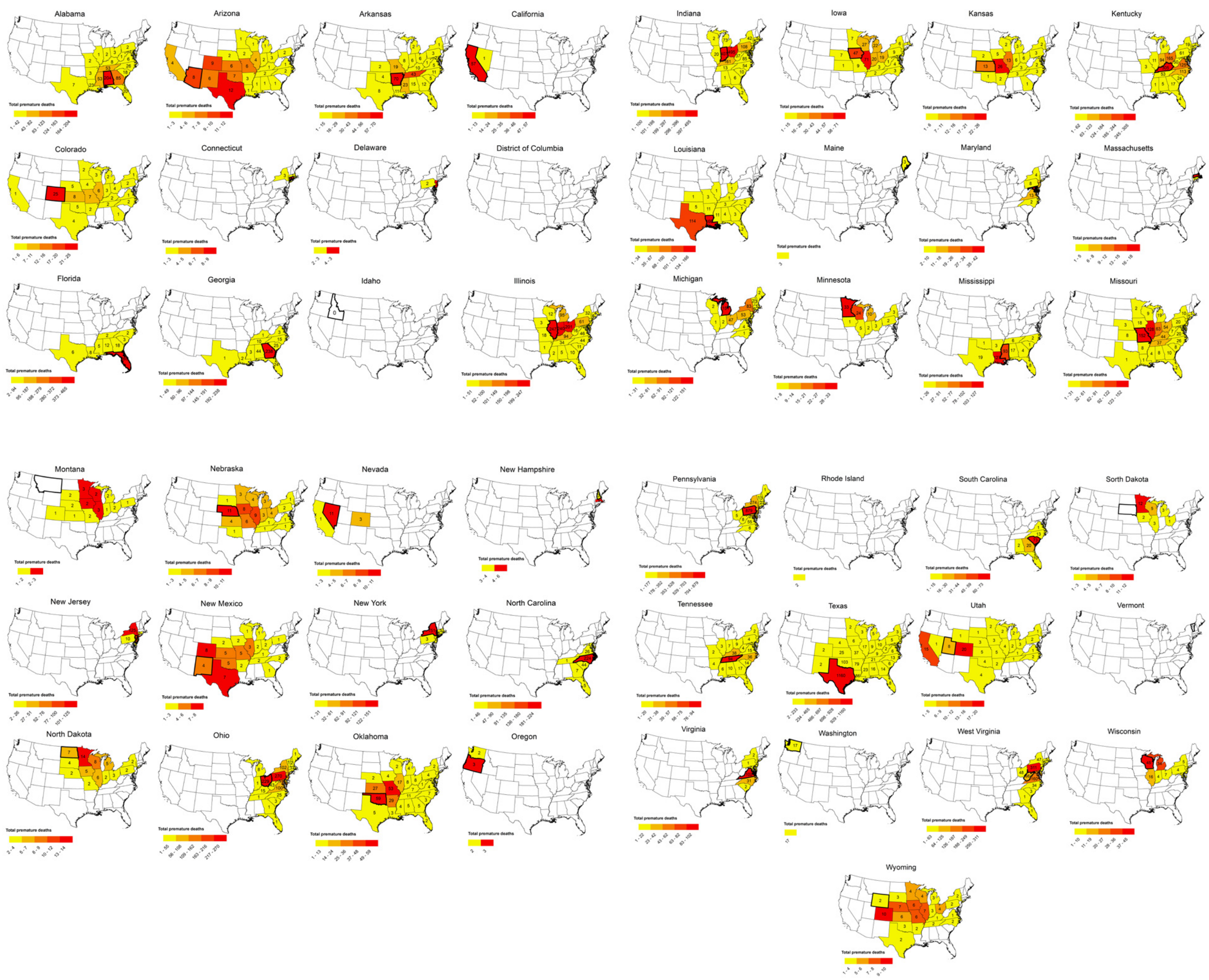

Figure B10 (A). Total deaths in each of US state from electricity generation in each 48 US states (highlighted as bold black boundary) and District of Columbia. Equal interval bins are used for each state's color ramp. For example, considering EGU-$PM_{2.5}$ emissions in Indiana, this figure shows that those emissions cause 407 deaths in Indiana, 495 deaths in Ohio, 161 deaths in Kentucky, 108 deaths in Pennsylvania, and 20 deaths in Illinois.

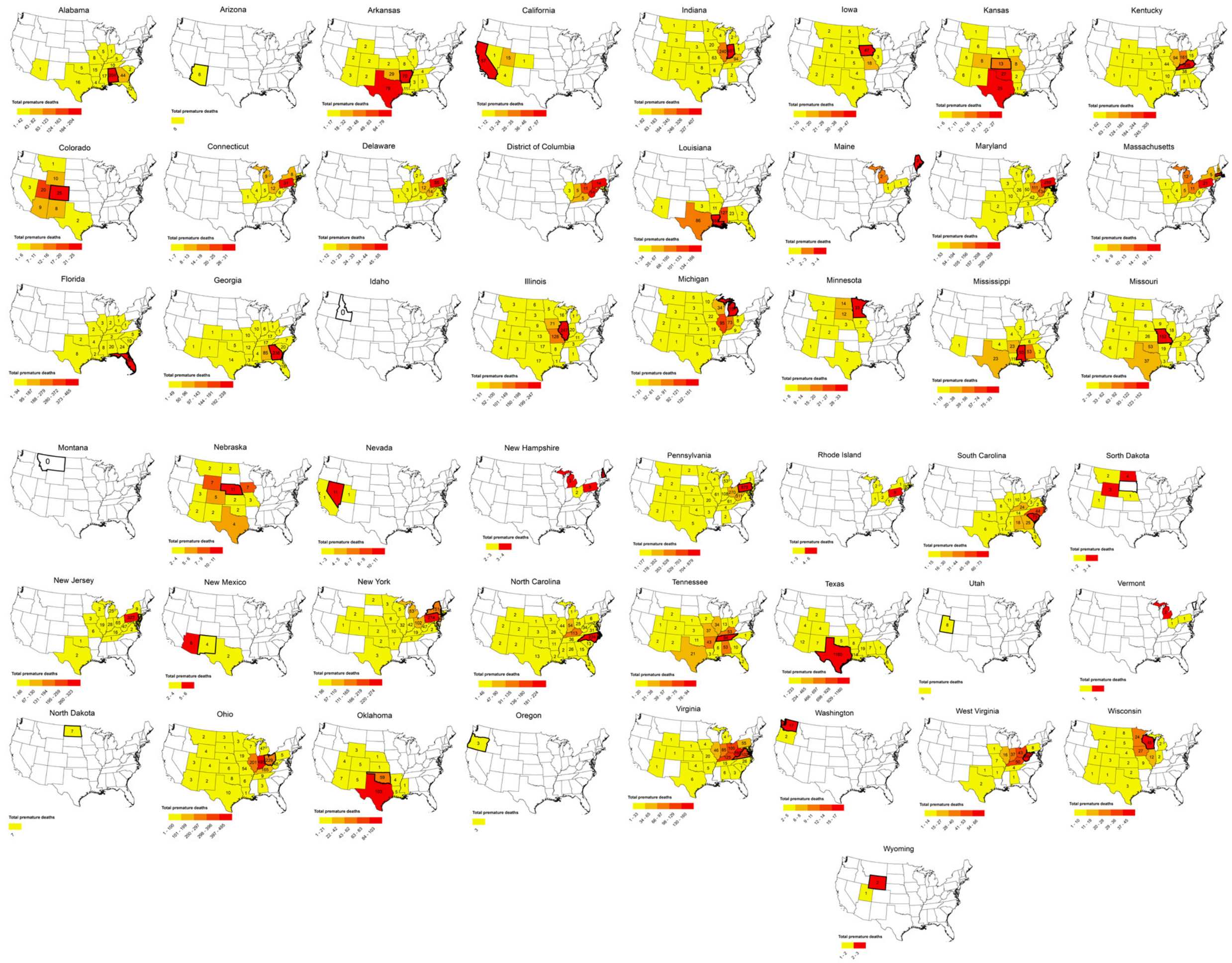

Figure B10 (B). Total deaths contributed by other states in each of 48 US states (highlighted as bold black boundary) and District of Columbia. Equal interval bins are used for each state's color ramp. For example, considering EGU-$PM_{2.5}$ deaths in Indiana, this figure shows that 407 deaths in Indiana are from EGU emissions in Indiana, 240 deaths in Indiana are from EGU emissions in Illinois, and 94 deaths in Indiana are from EGU emissions in Kentucky.

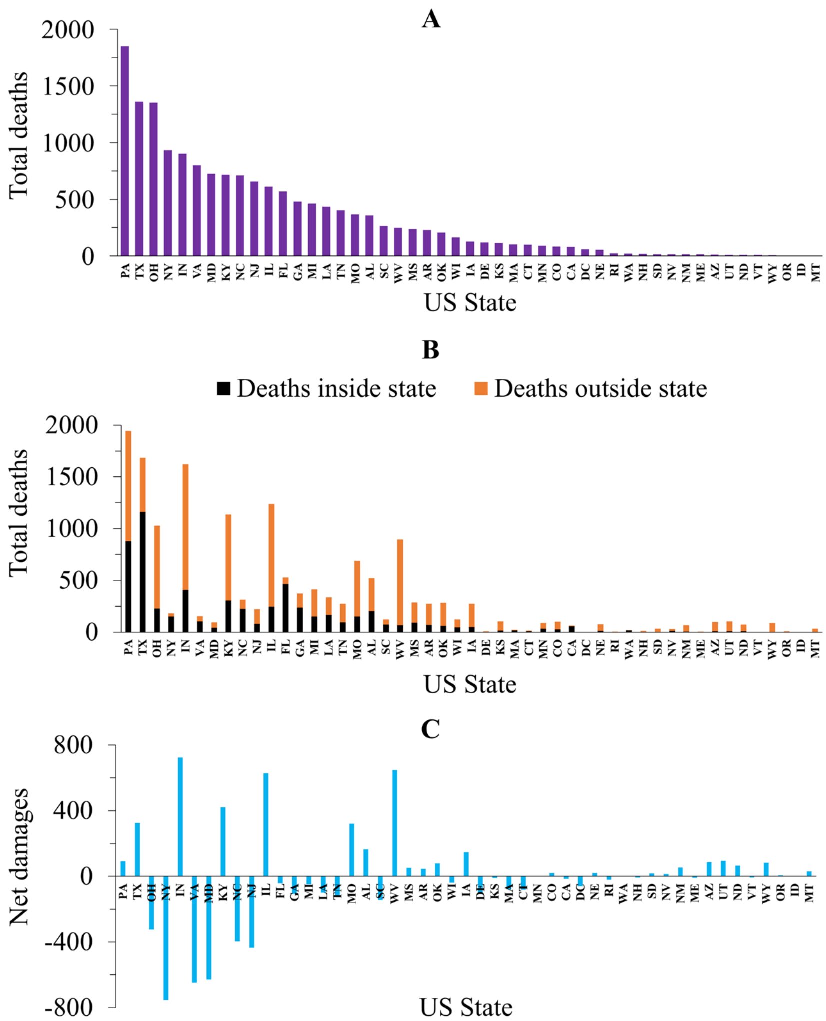

Figure B11. Figure 4. $PM_{2.5}$-related premature annual deaths from emissions from electricity generation units (EGUs). (A) Total estimated annual deaths in each state from EGUs throughout the US, (B) Total estimated annual deaths in-state and out-of-state from EGUs in that state, (C) Net imports (negative values) or exports (positive values) of estimated annual deaths. Values in C are calculated as B – A. X-axes in all three plots are sorted by decreasing total premature deaths.

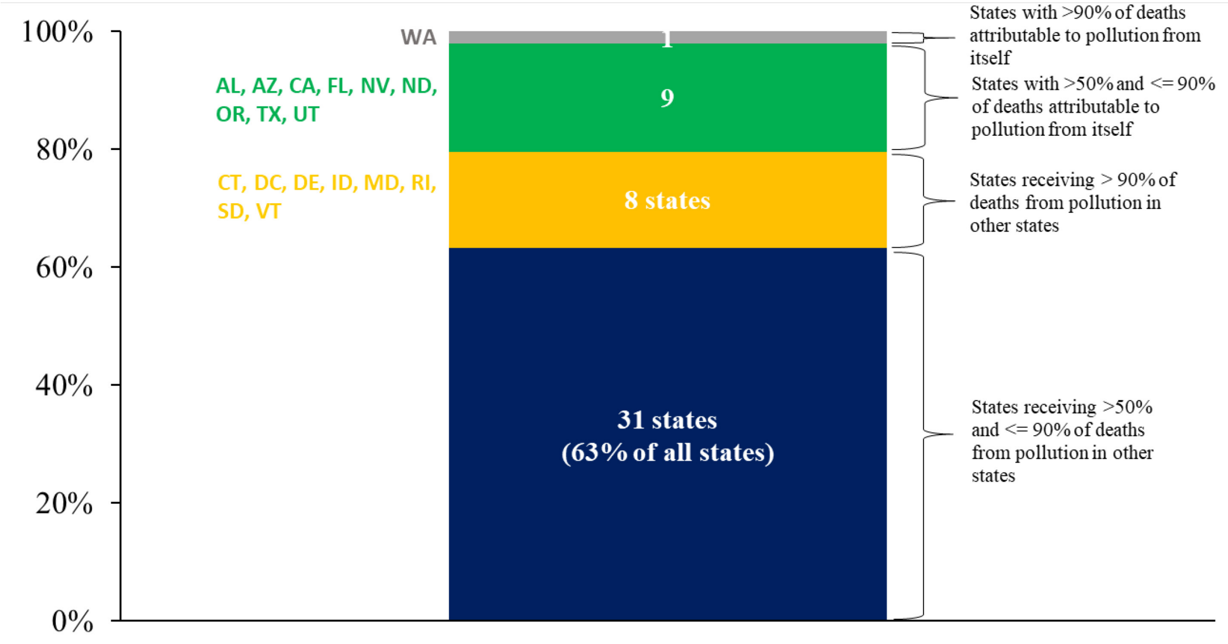

Figure B12. Inter-state health damages from EGU-$PM_{2.5}$ emissions in each state and District of Columbia.

5. Variations by geography and race

5.1 Regional Transmission Organizations (RTOs)

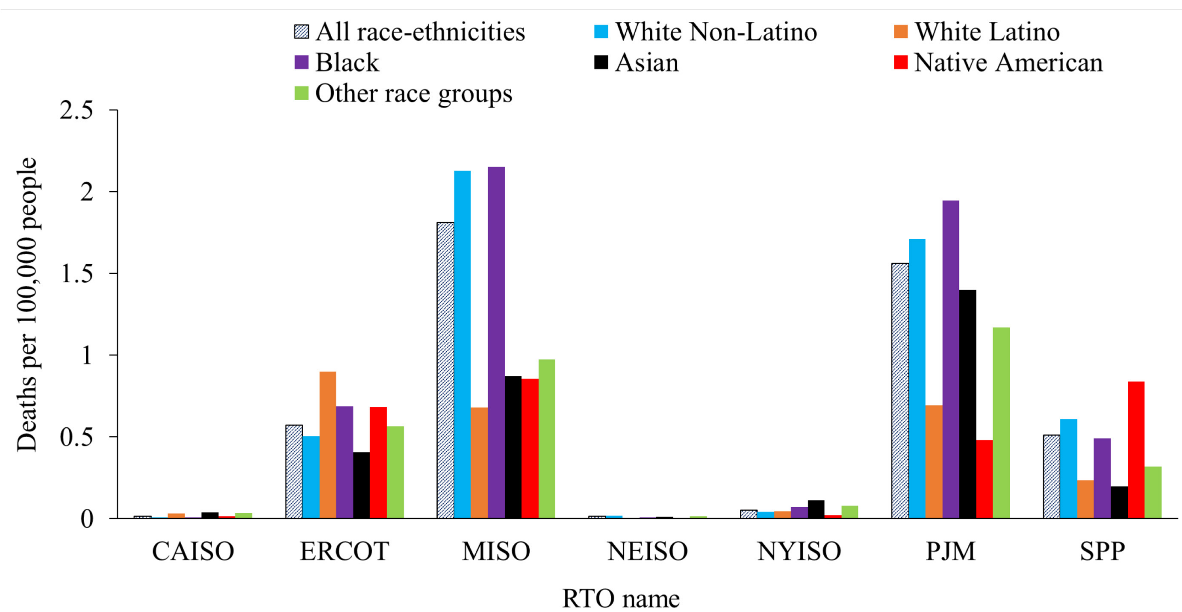

Figure B13. Deaths per 100,000 people by race-ethnicity in the entire US from EGU-$PM_{2.5}$ emissions in each RTO.

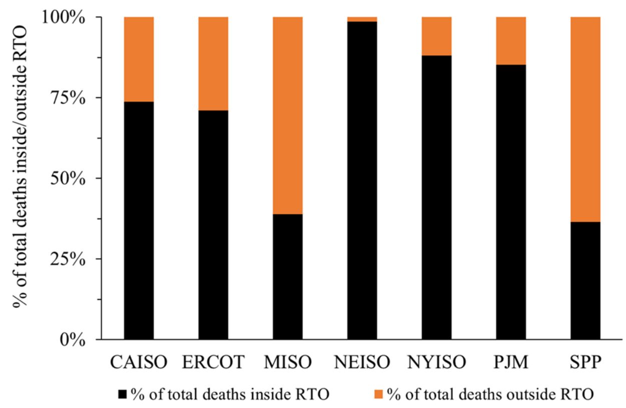

Figure B14. Percentage of total health damages inside and outside of RTO boundaries.

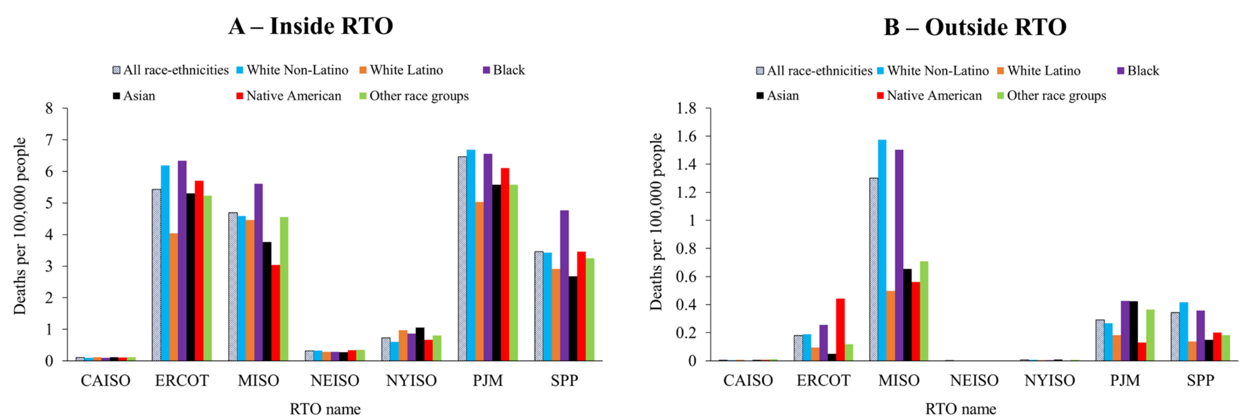

Figure B15. (A) Deaths per 100,000 people inside the RTO from EGU-$PM_{2.5}$ emissions in each RTO, (B) Deaths per 100,000 people outside the RTO from EGU-$PM_{2.5}$ emissions in each RTO.

5.2 States

Table B5. Deaths per 100,000 people by race-ethnicity in each state and population-weighted average risk by race-ethnicity from electricity generation in the entire US.

State	Deaths per 100,000 White Non-Latino	Deaths per 100,000 White Latino	Deaths per 100,000 Black	Deaths per 100,000 Asian	Deaths per 100,000 Native American	Deaths per 100,000 Mixed/Other	White Non-Latino Population	White Latino Population	Black Population	Asian Population	Native American Population	Mixed/Other Population
Alabama	7.4	7.0	7.4	6.8	7.4	7.1	3,209,159	122,254	1,274,583	58,621	24,959	138,584
Arizona	0.1	0.2	0.1	0.1	0.3	0.2	3,709,118	1,427,031	274,056	190,752	288,992	621,828
Arkansas	7.6	7.0	8.4	6.7	7.4	7.1	2,181,425	127,095	466,886	37,949	21,407	128,322
California	0.2	0.2	0.2	0.2	0.2	0.2	14,956,566	8,757,216	2,263,160	5,131,592	289,723	6,746,582
Colorado	1.6	1.6	1.4	1.5	1.6	1.6	3,602,669	758,100	209,029	146,569	51,155	426,878
Connecticut	2.7	2.9	2.8	2.7	2.9	2.8	2,497,255	279,992	364,192	144,984	8,063	281,751
District of Columbia	9.8	9.8	9.5	9.7	9.7	9.7	226,495	31,712	305,997	23,317	2,087	40,507
Delaware	13.1	13.1	12.8	12.6	13.3	13.0	580,268	48,986	193,539	30,052	3,195	44,186
Florida	3.5	1.6	2.8	3.1	3.2	2.7	10,947,069	3,787,662	3,110,450	490,250	59,166	948,899
Georgia	5.0	4.2	4.9	3.6	4.7	4.3	5,435,139	540,719	3,058,613	343,022	24,980	491,514
Idaho	0.1	0.1	0.1	0.1	0.1	0.1	1,325,346	134,943	9,448	21,758	20,066	80,185
Illinois	5.1	3.6	4.7	3.3	4.6	3.8	8,153,155	1,242,851	1,841,070	628,058	28,755	1,035,274
Indiana	14.0	12.1	13.8	12.7	13.2	13.1	5,240,695	233,641	608,988	113,306	15,208	291,953
Iowa	4.2	3.9	3.9	3.4	4.2	3.9	2,663,501	116,269	104,180	60,649	11,653	102,566
Kansas	4.1	3.5	3.6	3.4	4.9	3.8	2,222,031	222,012	164,103	72,240	25,939	158,340
Kentucky	15.9	17.3	18.4	16.5	15.0	16.4	3,797,972	85,580	347,760	53,993	9,323	132,177
Louisiana	9.3	9.4	9.8	9.5	9.0	9.6	2,749,527	143,673	1,476,096	75,757	28,141	128,001
Maine	1.0	1.0	1.1	1.1	0.7	1.0	1,261,041	13,636	15,138	15,088	7,111	29,148
Maryland	12.9	10.4	12.0	10.1	11.8	10.4	3,170,622	266,536	1,748,760	347,404	16,317	371,467
Massachusetts	1.6	1.5	1.4	1.3	1.6	1.5	4,958,336	333,463	465,141	384,467	13,551	465,299
Michigan	4.6	4.8	5.0	4.4	3.8	4.7	7,540,317	303,542	1,385,669	259,434	54,900	363,613
Minnesota	1.7	1.7	1.6	1.6	1.5	1.6	4,413,906	161,096	289,424	229,918	57,391	219,190
Mississippi	8.5	10.0	7.1	9.7	8.5	9.2	1,700,113	50,565	1,104,758	28,226	13,182	58,284
Missouri	6.1	5.8	6.4	5.6	6.2	5.7	4,851,726	141,180	696,348	101,824	24,859	214,024
Montana	0.1	0.1	0.1	0.1	0.2	0.1	872,221	21,744	4,545	6,643	64,818	30,487
Nebraska	3.0	2.9	3.1	2.5	2.7	2.9	1,500,659	125,131	78,053	35,147	20,296	75,030
Nevada	0.5	0.6	0.6	0.5	0.4	0.6	1,442,740	479,656	229,024	206,947	29,473	358,352
New Hampshire	1.3	1.4	1.3	1.4	1.3	1.3	1,192,302	28,038	15,930	28,248	2,405	31,534
New Jersey	7.7	6.6	7.3	6.5	7.5	7.1	5,138,224	962,374	1,199,194	779,757	18,823	779,806
New Mexico	0.7	0.7	0.6	0.6	0.8	0.7	812,390	691,900	40,776	28,422	187,103	294,662
New York	4.5	5.1	5.0	5.3	4.6	4.8	11,258,424	1,514,975	3,060,672	1,524,799	74,578	2,205,509
North Carolina	7.5	6.8	7.1	6.3	6.7	7.0	6,291,871	489,881	2,086,726	230,183	111,382	525,392
North Dakota	1.3	1.1	0.9	0.9	1.2	1.1	597,049	10,084	10,521	7,841	36,612	19,812
Ohio	11.9	10.5	11.3	10.7	11.4	11.0	9,292,730	237,642	1,405,796	208,971	21,124	372,590
Oklahoma	5.3	4.6	4.6	4.4	6.5	5.5	2,622,370	221,605	280,162	72,669	265,927	398,190
Oregon	0.1	0.1	0.1	0.0	0.1	0.1	3,039,058	287,759	70,894	152,999	47,228	310,993
Pennsylvania	14.9	13.0	12.5	12.6	13.5	13.6	10,040,338	428,957	1,402,554	378,251	23,155	515,022
Rhode Island	2.3	2.1	2.1	2.2	2.2	2.1	782,101	64,793	66,071	32,732	4,909	91,079
South Carolina	5.5	5.2	5.7	5.2	5.9	5.4	3,048,733	156,089	1,314,230	66,291	16,968	168,698
South Dakota	1.8	1.8	1.6	1.7	1.8	1.7	688,548	15,602	12,777	9,350	64,651	28,752
Tennessee	6.4	5.9	5.6	5.4	6.3	6.0	4,831,414	188,939	1,075,388	97,712	18,136	223,785
Texas	6.1	3.8	6.2	4.9	5.4	4.7	11,546,339	7,936,603	3,090,641	1,066,268	130,601	2,307,295
Utah	0.3	0.4	0.3	0.3	0.4	0.3	2,279,933	236,797	31,183	60,558	33,218	219,244
Vermont	1.2	1.2	1.2	1.2	1.1	1.2	611,151	8,257	7,278	9,733	2,140	15,032
Virginia	10.2	8.1	10.0	7.3	9.3	8.5	5,241,618	439,351	1,580,182	473,512	23,518	439,496
Washington	0.3	0.3	0.3	0.3	0.3	0.3	4,924,781	473,709	250,278	517,513	95,909	643,901
West Virginia	13.6	14.4	13.1	12.7	12.4	13.5	1,687,265	16,796	57,796	12,745	3,096	42,054
Wisconsin	2.8	3.1	3.1	2.7	2.6	2.9	4,765,136	231,580	358,717	137,983	49,733	215,627
Wyoming	0.9	0.9	1.3	1.0	0.7	1.1	481,744	34,046	5,932	5,267	13,720	27,634
Total population by race-ethnicity							196,382,590	34,632,066	39,512,708	15,139,771	2,459,647	23,858,548
US Population weighted average risk	5.7	2.8	6.3	3.3	3.2	3.5						

Table B6. Deaths per 100,000 people by race-ethnicity and fuel type in each state from electricity generation in the entire US.

Coal EGUs

State	White Non-Latino deaths	Deaths per 100,000 White Non-Latinos	White Latino deaths	Deaths per 100,000 White Latinos	Black deaths	Deaths per 100,000 Blacks	Asian deaths	Deaths per 100,000 Asians	Native American deaths	Deaths per 100,000 Native Americans	Latino deaths	Deaths per 100,000 Latinos
AL	228	7.1	8	6.8	90	7.1	4	6.6	2	7.0	13	6.9
AR	159	7.3	8	6.6	37	8.0	2	6.4	2	7.0	13	6.7
AZ	4	0.1	2	0.1	0	0.1	0	0.1	1	0.2	2	0.1
CA	7	0.0	4	0.0	1	0.0	2	0.0	0	0.0	6	0.0
CO	55	1.5	12	1.5	3	1.4	2	1.4	1	1.5	17	1.5
CT	55	2.2	6	2.3	8	2.2	3	2.2	0	2.2	11	2.2
DC	22	9.5	3	9.5	28	9.2	2	9.5	0	9.4	6	9.5
DE	71	12.2	6	12.1	23	11.8	3	11.6	0	12.4	9	12.0
FL	299	2.7	42	1.1	65	2.1	11	2.3	2	2.5	54	1.2
GA	257	4.7	21	3.9	137	4.5	11	3.3	1	4.4	35	3.9
IA	107	4.0	4	3.8	4	3.8	2	3.3	0	4.1	7	3.8
ID	1	0.1	0	0.1	0	0.1	0	0.1	0	0.1	0	0.1
IL	410	5.0	43	3.5	84	4.6	20	3.3	1	4.5	72	3.5
IN	723	13.8	28	11.9	82	13.5	14	12.6	2	13.0	49	12.0
KS	84	3.8	7	3.3	6	3.4	2	3.1	1	4.6	10	3.3
KY	600	15.8	15	17.1	64	18.3	9	16.4	1	14.9	23	16.5
LA	220	8.0	12	8.0	124	8.4	6	8.1	2	7.7	17	8.1
MA	60	1.2	4	1.2	5	1.1	4	1.0	0	1.2	8	1.1
MD	392	12.4	27	10.0	201	11.5	34	9.7	2	11.3	50	9.7
ME	9	0.7	0	0.8	0	0.8	0	0.8	0	0.6	0	0.8
MI	331	4.4	14	4.5	65	4.7	11	4.2	2	3.6	21	4.5
MN	68	1.5	3	1.6	4	1.4	3	1.4	1	1.3	4	1.5
MO	285	5.9	8	5.7	44	6.3	6	5.5	1	5.9	12	5.4
MS	137	8.0	5	9.5	73	6.6	3	9.3	1	7.9	7	8.8
MT	1	0.1	0	0.1	0	0.1	0	0.1	0	0.2	0	0.1
NC	450	7.1	32	6.5	140	6.7	14	6.1	7	6.3	56	6.6
ND	8	1.3	0	1.1	0	0.9	0	0.9	0	1.1	0	1.0
NE	43	2.9	3	2.8	2	3.0	1	2.4	1	2.6	5	2.8
NH	13	1.1	0	1.1	0	1.1	0	1.1	0	1.1	0	1.1
NJ	341	6.6	52	5.4	73	6.1	42	5.4	1	6.2	91	5.5
NM	5	0.6	4	0.5	0	0.5	0	0.5	1	0.8	5	0.6
NV	2	0.1	1	0.1	0	0.1	0	0.1	0	0.1	1	0.1
NY	401	3.6	51	3.4	103	3.4	51	3.4	3	3.5	118	3.3
OH	1084	11.7	24	10.3	156	11.1	22	10.6	2	11.2	38	10.1
OK	122	4.6	9	3.9	11	4.0	3	3.7	15	5.8	15	4.0
OR	1	0.0	0	0.0	0	0.0	0	0.0	0	0.0	0	0.0
PA	1434	14.3	53	12.3	163	11.6	44	11.8	3	12.7	96	12.2
RI	13	1.6	1	1.5	1	1.5	1	1.6	0	1.6	2	1.5
SC	161	5.3	8	5.0	71	5.4	3	5.0	1	5.6	13	5.0
SD	12	1.7	0	1.7	0	1.6	0	1.6	1	1.8	0	1.7
TN	305	6.3	11	5.7	58	5.4	5	5.3	1	6.2	18	5.7
TX	625	5.4	259	3.3	169	5.5	46	4.3	6	4.8	340	3.4
UT	5	0.2	1	0.3	0	0.2	0	0.2	0	0.4	1	0.3
VA	509	9.7	34	7.8	145	9.2	33	6.9	2	8.7	53	7.7
VT	7	1.1	0	1.1	0	1.1	0	1.1	0	1.1	0	1.2
WA	9	0.2	1	0.2	1	0.2	1	0.2	0	0.2	2	0.2
WI	125	2.6	7	3.0	11	3.0	3	2.5	1	2.5	10	3.0
WV	228	13.5	2	14.2	7	13.0	2	12.6	0	12.3	3	14.1
WY	4	0.8	0	0.9	0	1.3	0	0.9	0	0.7	1	0.9

Natural gas EGUs

State	White Non-Latino deaths	Deaths per 100,000 White Non-Latinos	White Latino deaths	Deaths per 100,000 White Latinos	Black deaths	Deaths per 100,000 Blacks	Asian deaths	Deaths per 100,000 Asians	Native American deaths	Deaths per 100,000 Native Americans	Latino deaths	Deaths per 100,000 Latinos
AL	8	0.2	0	0.2	3	0.3	0	0.2	0	0.3	0	0.2
AR	7	0.3	0	0.3	1	0.3	0	0.3	0	0.3	1	0.3
AZ	1	0.0	1	0.1	0	0.1	0	0.0	0	0.0	1	0.1
CA	19	0.1	13	0.2	3	0.2	7	0.1	0	0.1	22	0.2
CO	2	0.1	0	0.1	0	0.1	0	0.0	0	0.1	1	0.1
CT	6	0.2	1	0.3	1	0.3	0	0.2	0	0.3	2	0.3
DC	0	0.1	0	0.1	0	0.1	0	0.1	0	0.1	0	0.1
DE	2	0.3	0	0.3	1	0.3	0	0.3	0	0.3	0	0.3
FL	57	0.5	15	0.4	15	0.5	3	0.5	0	0.5	19	0.4
GA	14	0.3	1	0.3	11	0.3	1	0.3	0	0.3	2	0.3
IA	2	0.1	0	0.1	0	0.1	0	0.1	0	0.1	0	0.1
ID	0	0.0	0	0.0	0	0.0	0	0.0	0	0.0	0	0.0
IL	7	0.1	1	0.1	2	0.1	0	0.1	0	0.1	2	0.1
IN	7	0.1	0	0.2	1	0.2	0	0.1	0	0.2	1	0.2
KS	5	0.2	0	0.2	0	0.2	0	0.2	0	0.3	1	0.2
KY	4	0.1	0	0.1	0	0.1	0	0.1	0	0.1	0	0.1
LA	22	0.8	1	0.9	13	0.9	1	0.9	0	0.8	2	0.9
MA	7	0.1	0	0.1	1	0.2	1	0.1	0	0.2	1	0.2
MD	4	0.1	0	0.1	2	0.1	0	0.1	0	0.1	0	0.1
ME	1	0.0	0	0.0	0	0.1	0	0.1	0	0.0	0	0.0
MI	9	0.1	0	0.1	2	0.1	0	0.1	0	0.1	1	0.1
MN	2	0.0	0	0.0	0	0.0	0	0.0	0	0.0	0	0.0
MO	8	0.2	0	0.2	1	0.1	0	0.1	0	0.2	0	0.2
MS	5	0.3	0	0.3	4	0.4	0	0.3	0	0.4	0	0.3
MT	0	0.0	0	0.0	0	0.0	0	0.0	0	0.0	0	0.0
NC	10	0.2	1	0.1	3	0.2	0	0.1	0	0.2	1	0.1
ND	0	0.0	0	0.0	0	0.0	0	0.0	0	0.0	0	0.0
NE	1	0.1	0	0.1	0	0.1	0	0.1	0	0.1	0	0.1
NH	1	0.1	0	0.2	0	0.1	0	0.1	0	0.1	0	0.2
NJ	27	0.5	7	0.7	8	0.6	5	0.6	0	0.6	12	0.7
NM	1	0.1	1	0.1	0	0.1	0	0.1	0	0.1	1	0.1
NV	5	0.3	2	0.4	1	0.5	1	0.4	0	0.3	3	0.5
NY	74	0.7	20	1.3	35	1.1	22	1.5	1	0.8	43	1.2
OH	11	0.1	0	0.1	2	0.1	0	0.1	0	0.1	0	0.1
OK	16	0.6	1	0.6	2	0.6	0	0.7	2	0.6	2	0.6
OR	0	0.0	0	0.0	0	0.0	0	0.0	0	0.0	0	0.0
PA	22	0.2	1	0.2	4	0.3	1	0.3	0	0.3	2	0.3
RI	3	0.4	0	0.4	0	0.4	0	0.4	0	0.4	1	0.4
SC	4	0.1	0	0.1	2	0.1	0	0.1	0	0.2	0	0.1
SD	0	0.0	0	0.0	0	0.0	0	0.0	0	0.0	0	0.0
TN	5	0.1	0	0.1	2	0.2	0	0.1	0	0.1	0	0.1
TX	59	0.5	34	0.4	18	0.6	5	0.5	1	0.5	44	0.4
UT	2	0.1	0	0.1	0	0.1	0	0.1	0	0.1	0	0.1
VA	8	0.1	0	0.1	3	0.2	0	0.1	0	0.2	1	0.1
VT	0	0.0	0	0.0	0	0.0	0	0.0	0	0.0	0	0.0
WA	1	0.0	0	0.0	0	0.0	0	0.0	0	0.0	0	0.0
WI	4	0.1	0	0.1	0	0.1	0	0.1	0	0.1	0	0.1
WV	2	0.1	0	0.1	0	0.1	0	0.1	0	0.1	0	0.1
WY	0	0.0	0	0.0	0	0.0	0	0.0	0	0.0	0	0.0

Other fossil fuel EGUs

State	White Non-Latino deaths	Deaths per 100,000 White Non-Latinos	White Latino deaths	Deaths per 100,000 White Latinos	Black deaths	Deaths per 100,000 Blacks	Asian deaths	Deaths per 100,000 Asians	Native American deaths	Deaths per 100,000 Native Americans	Latino deaths	Deaths per 100,000 Latinos
AL	2	0.1	0	0.1	1	0.1	0	0.1	0	0.1	0	0.1
AR	1	0.1	0	0.0	0	0.1	0	0.0	0	0.1	0	0.1
AZ	0	0.0	0	0.0	0	0.0	0	0.0	0	0.0	0	0.0
CA	4	0.0	2	0.0	0	0.0	1	0.0	0	0.0	3	0.0
CO	0	0.0	0	0.0	0	0.0	0	0.0	0	0.0	0	0.0
CT	7	0.3	1	0.3	1	0.3	0	0.3	0	0.3	2	0.3
DC	0	0.2	0	0.2	1	0.2	0	0.2	0	0.2	0	0.2
DE	4	0.6	0	0.6	1	0.6	0	0.6	0	0.6	0	0.6
FL	22	0.2	5	0.1	5	0.2	1	0.2	0	0.2	6	0.1
GA	3	0.0	0	0.0	1	0.0	0	0.0	0	0.0	0	0.0
IA	1	0.0	0	0.0	0	0.0	0	0.0	0	0.0	0	0.0
ID	0	0.0	0	0.0	0	0.0	0	0.0	0	0.0	0	0.0
IL	2	0.0	0	0.0	0	0.0	0	0.0	0	0.0	0	0.0
IN	3	0.1	0	0.1	1	0.1	0	0.1	0	0.1	0	0.1
KS	1	0.0	0	0.0	0	0.0	0	0.0	0	0.1	0	0.0
KY	1	0.0	0	0.0	0	0.0	0	0.0	0	0.0	0	0.0
LA	12	0.4	1	0.5	6	0.4	0	0.5	0	0.5	1	0.5
MA	11	0.2	1	0.2	1	0.2	1	0.2	0	0.2	2	0.2
MD	14	0.4	1	0.3	7	0.4	1	0.3	0	0.4	2	0.3
ME	3	0.2	0	0.2	0	0.3	0	0.3	0	0.2	0	0.2
MI	7	0.1	1	0.2	3	0.2	0	0.1	0	0.1	1	0.2
MN	4	0.1	0	0.1	0	0.2	0	0.1	0	0.1	0	0.1
MO	2	0.0	0	0.0	0	0.0	0	0.0	0	0.0	0	0.0
MS	2	0.1	0	0.1	1	0.1	0	0.1	0	0.2	0	0.1
MT	0	0.0	0	0.0	0	0.0	0	0.0	0	0.0	0	0.0
NC	9	0.1	1	0.1	4	0.2	0	0.1	0	0.2	1	0.1
ND	0	0.0	0	0.0	0	0.0	0	0.0	0	0.0	0	0.0
NE	1	0.0	0	0.1	0	0.0	0	0.0	0	0.0	0	0.1
NH	1	0.1	0	0.1	0	0.1	0	0.1	0	0.1	0	0.1
NJ	29	0.6	5	0.5	7	0.6	4	0.5	0	0.6	9	0.5
NM	0	0.0	0	0.0	0	0.0	0	0.0	0	0.0	0	0.0
NV	0	0.0	0	0.0	0	0.0	0	0.0	0	0.0	0	0.0
NY	37	0.3	7	0.5	13	0.4	8	0.5	0	0.3	16	0.4
OH	6	0.1	0	0.1	1	0.1	0	0.1	0	0.1	0	0.1
OK	1	0.1	0	0.1	0	0.1	0	0.0	0	0.1	0	0.1
OR	2	0.1	0	0.0	0	0.0	0	0.0	0	0.1	0	0.0
PA	42	0.4	2	0.5	8	0.6	2	0.5	0	0.5	4	0.5
RI	2	0.3	0	0.2	0	0.2	0	0.2	0	0.2	0	0.2
SC	4	0.1	0	0.1	2	0.2	0	0.1	0	0.2	0	0.1
SD	0	0.0	0	0.0	0	0.0	0	0.0	0	0.0	0	0.0
TN	1	0.0	0	0.0	0	0.0	0	0.0	0	0.0	0	0.0
TX	14	0.1	6	0.1	5	0.2	1	0.1	0	0.1	7	0.1
UT	0	0.0	0	0.0	0	0.0	0	0.0	0	0.0	0	0.0
VA	17	0.3	1	0.3	9	0.6	1	0.3	0	0.4	2	0.3
VT	0	0.1	0	0.1	0	0.1	0	0.1	0	0.0	0	0.1
WA	2	0.0	0	0.0	0	0.1	0	0.1	0	0.0	0	0.0
WI	3	0.1	0	0.0	0	0.0	0	0.1	0	0.1	0	0.0
WV	1	0.0	0	0.1	0	0.1	0	0.0	0	0.0	0	0.1
WY	0	0.0	0	0.0	0	0.0	0	0.0	0	0.0	0	0.0

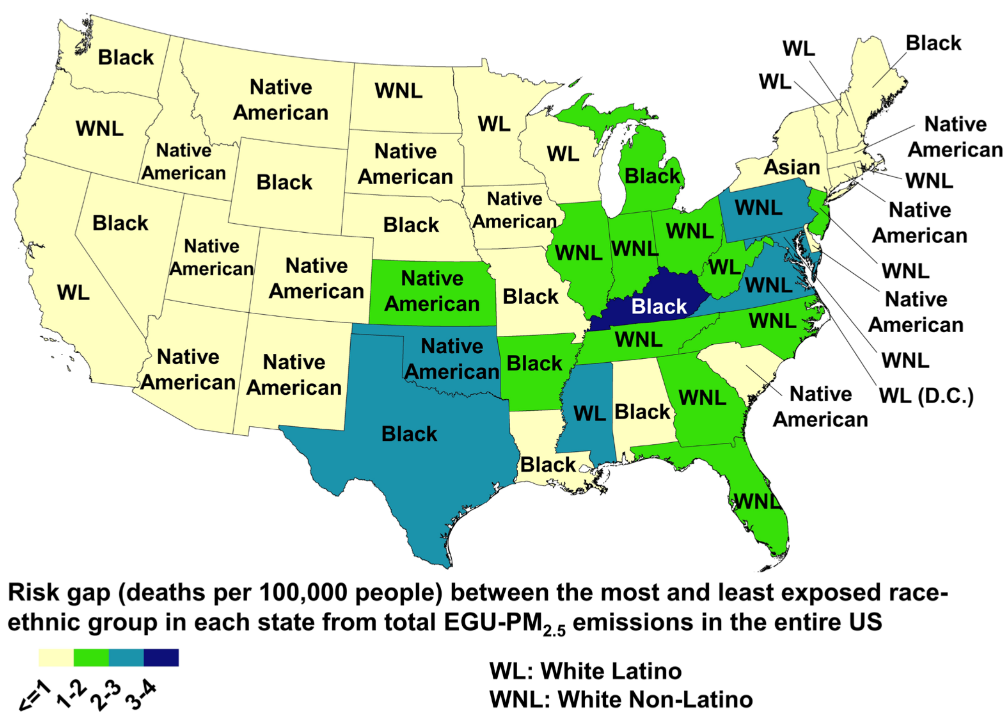

Figure B16. Most exposed racial-ethnic group and risk gap (deaths per 100,000 people) between the most and least exposed racial-ethnic group in each US state from EGU-$PM_{2.5}$ emissions in the entire US. Most exposed group in a state is shown by labels in each state and risk gap is shown by color gradation.

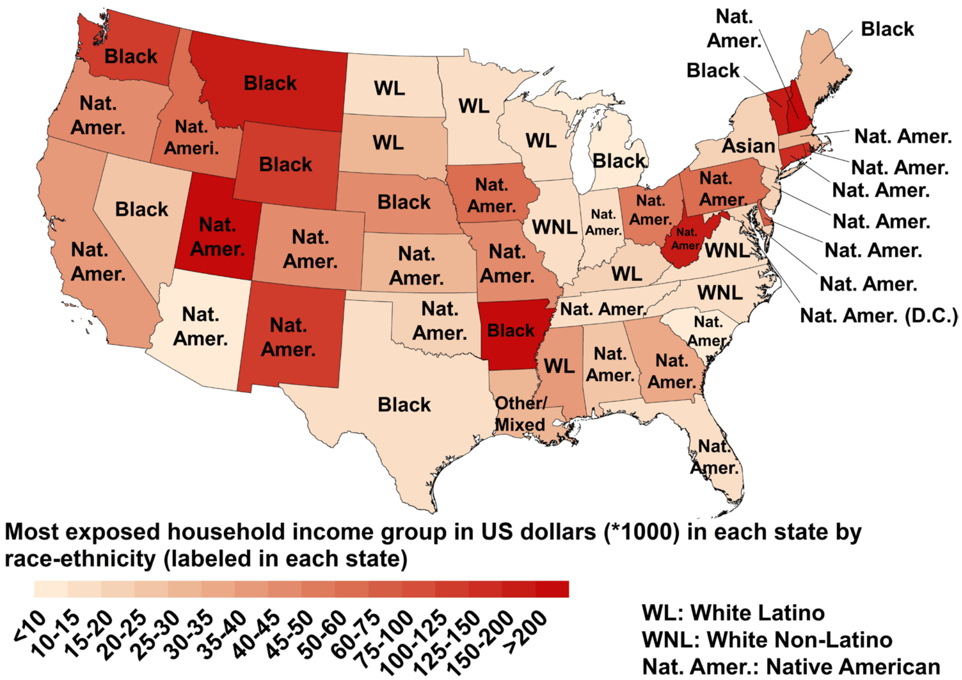

Figure B17. Most exposed household income group in US dollars (*1000) by racial-ethnic group in each US state from EGU-$PM_{2.5}$ emissions in the entire US. Most exposed racial-ethnic group for the most exposed household income group is shown by labels in each state. For example, in Texas, White Non-Latinos with household income group \$10,000 – \$15,000 are the most exposed group.

6. Other relevant plots and tables

6.1 Health impacts at the national scale by race-ethnicity

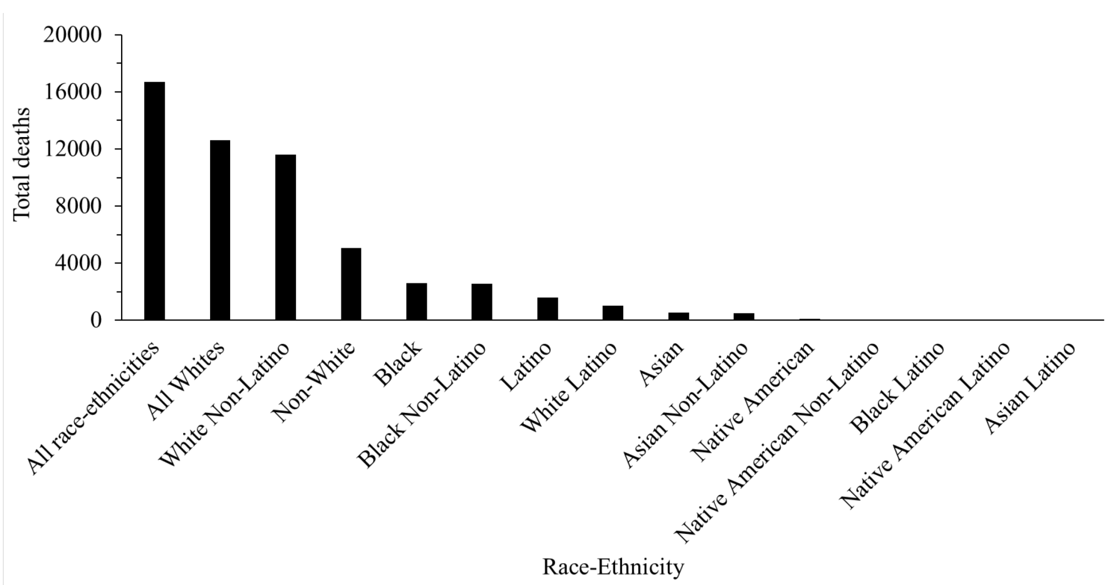

Figure B18. Total premature deaths by race-ethnicity from electricity generation in the entire US for the year 2014. "Non-White" refers to all categories except White Non-Latino; "All Whites" refer to both White Non-Latino and White Latino categories; and "Black", "Asian", "Native", and other categories include both Latino and Non-Latino ethnicities.

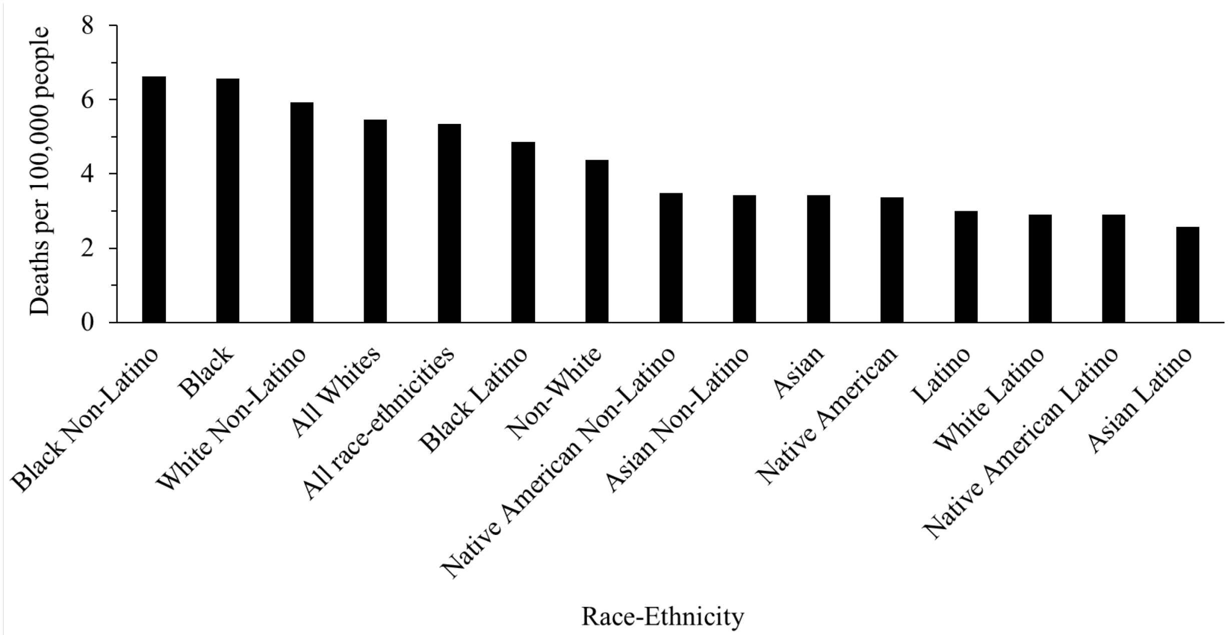

Figure B19. Deaths per 100,000 people by race-ethnicity from electricity generation in the entire US for the year 2014.

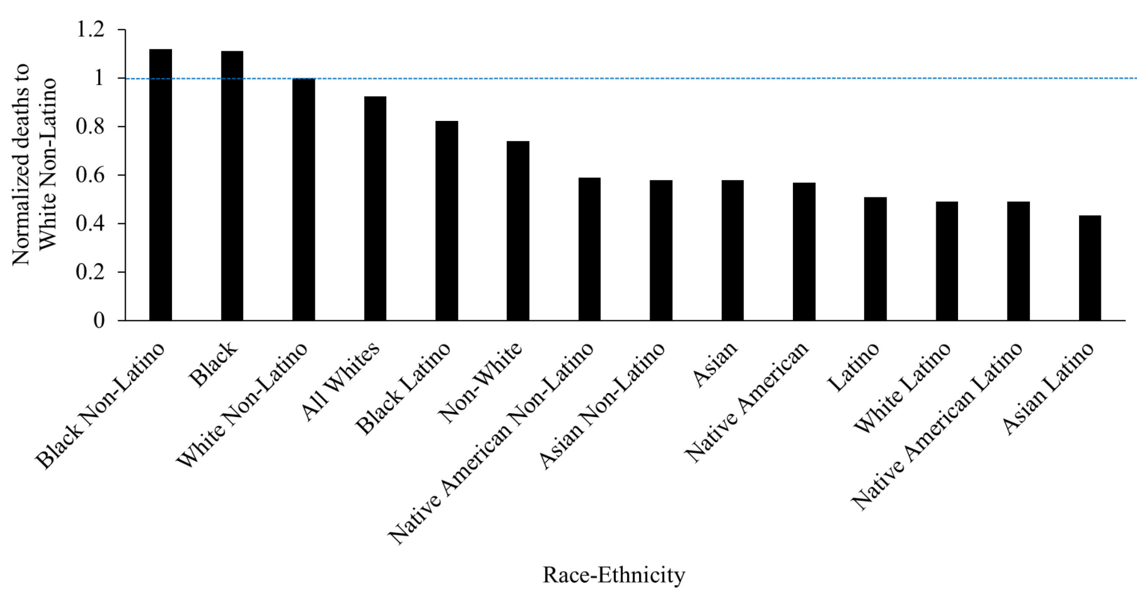

Figure B20. Deaths from electricity generation in the entire US for the year 2014 normalized to deaths among White Non-Latino.

6.2 Health impact analysis for the RTOs

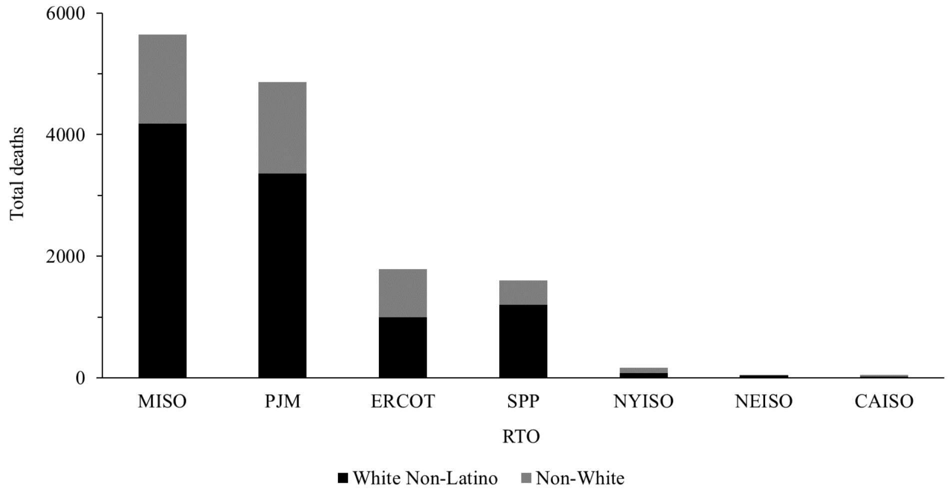

Figure B21. Total deaths among White Non-Latinos and Non-Whites from EGU-$PM_{2.5}$ emissions in each RTO.

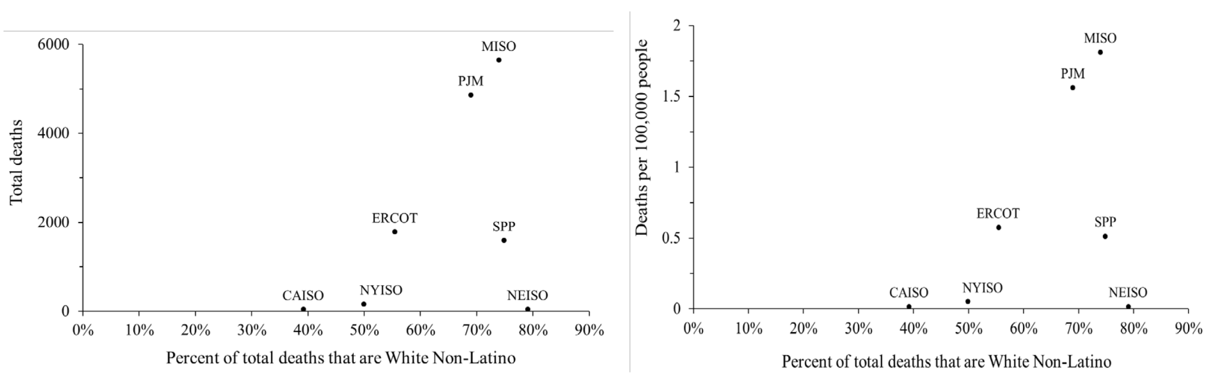

Figure B22. Total deaths (left plot) and deaths per 100,000 people (right plot) vs percent of total deaths for White Non-Latinos in each RTO.

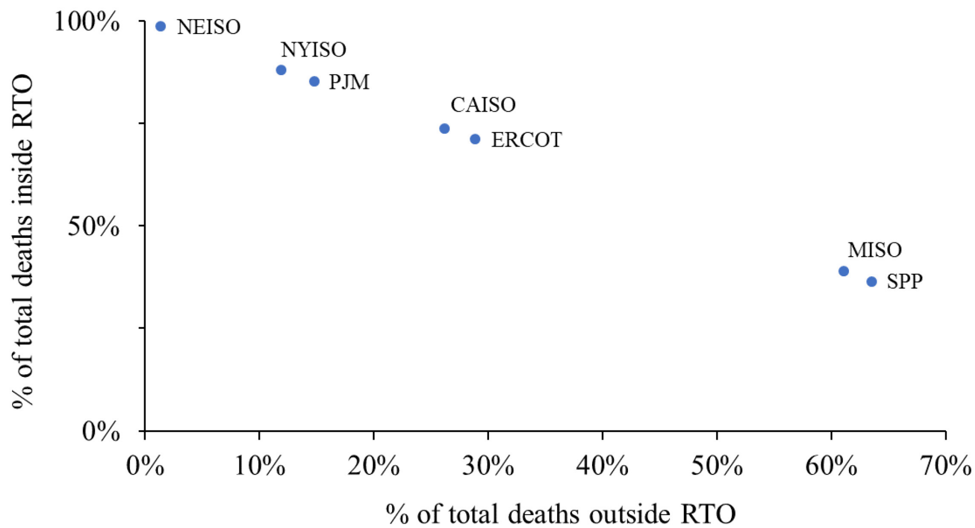

Figure B23. Percentage of total deaths inside and outside of RTOs from EGU-$PM_{2.5}$ emissions in each RTO.

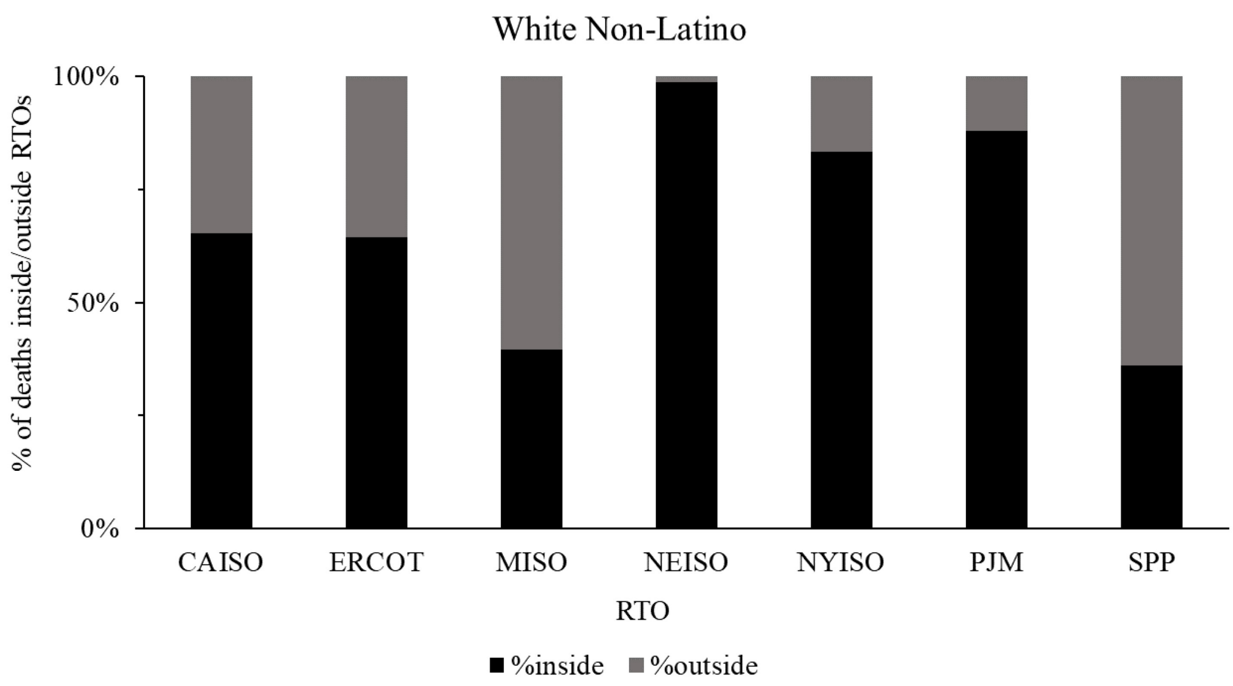

Figure B24. Deaths inside and outside of RTO for White Non-Latinos.

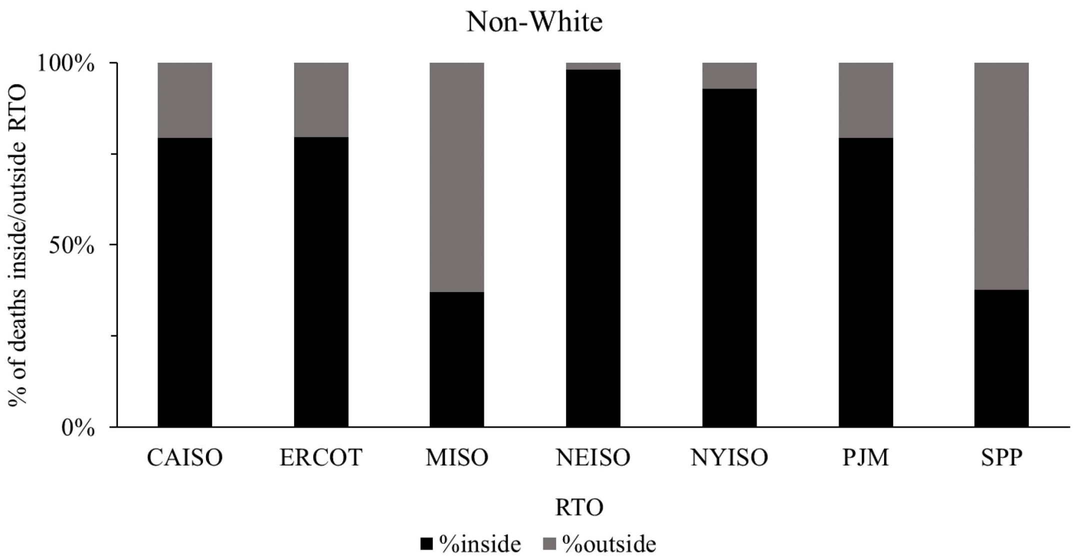

Figure B25. Deaths inside and outside of RTO for Non-Whites.

Table B7. Population weighted average EGU-$PM_{2.5}$ concentration for each US RTO, attributable to emissions in each RTO.

RTO	Population weighted average $PM_{2.5}$ concentration ($\mu g/m^3$)
CAISO	0.003
ERCOT	0.103
MISO	0.264
NEISO	0.002
NYISO	0.009
PJM	0.242
SPP	0.072

6.3 Health impacts from the electricity generation in the US states

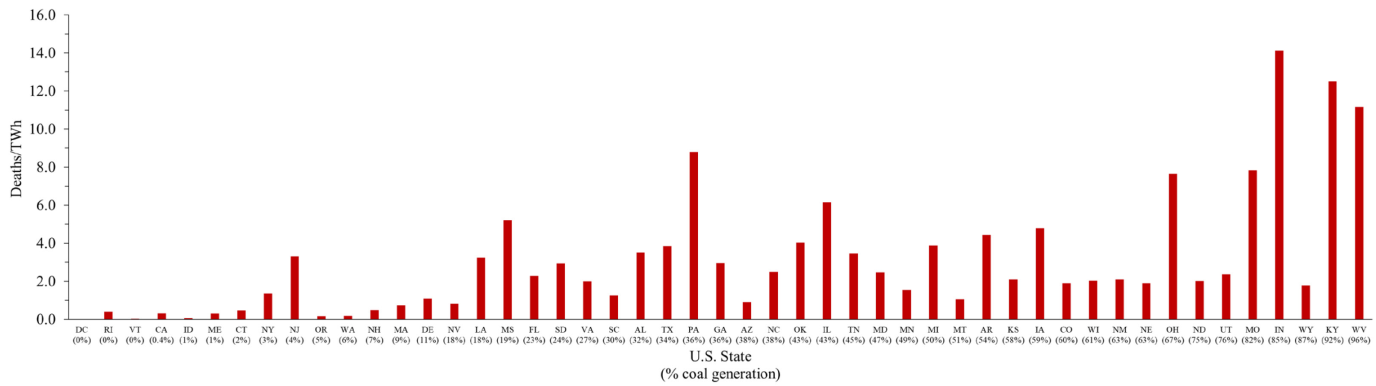

Figure B26. Total deaths in entire US/TWh from EGU-$PM_{2.5}$ emissions in each state (x-axis is sorted by increasing share of coal generation).

Table B8. State population weighted average EGU-$PM_{2.5}$ concentration by state, attributable to electricity generation in the entire US (third column from left) and in that state (fourth column from left).

State abbreviation	State name	Population weighted average $PM_{2.5}$ Concentration (μg/m^3) attributable to electricity generation in the entire US	Population weighted average $PM_{2.5}$ Concentration (μg/m^3) attributable to electricity generation in that state
AL	Alabama	0.948	0.545
AZ	Arizona	0.027	0.022
AR	Arkansas	0.992	0.307
CA	California	0.043	0.032
CO	Colorado	0.319	0.099
CT	Connecticut	0.442	0.042
DC	District of Columbia	1.788	0.000
DE	Delaware	1.963	0.031
FL	Florida	0.402	0.328
GA	Georgia	0.838	0.419
ID	Idaho	0.016	0.0005
IL	Illinois	0.729	0.306
IN	Indiana	1.987	0.920
IA	Iowa	0.586	0.225
KS	Kansas	0.590	0.074
KY	Kentucky	2.167	0.933
LA	Louisiana	1.330	0.505
ME	Maine	0.134	0.033
MD	Maryland	2.067	0.120

MA	Massachusetts	0.248	0.044
MI	Michigan	0.662	0.215
MN	Minnesota	0.296	0.118
MS	Mississippi	1.043	0.416
MO	Missouri	0.832	0.351
MT	Montana	0.021	0.005
NE	Nebraska	0.461	0.095
NV	Nevada	0.094	0.073
NH	New Hampshire	0.208	0.041
NJ	New Jersey	1.218	0.163
NM	New Mexico	0.108	0.030
NY	New York	0.877	0.149
NC	North Carolina	1.129	0.382
ND	North Dakota	0.197	0.150
OH	Ohio	1.565	0.257
OK	Oklahoma	0.695	0.205
OR	Oregon	0.013	0.009
PA	Pennsylvania	1.914	0.945
RI	Rhode Island	0.319	0.023
SC	South Carolina	0.787	0.223
SD	South Dakota	0.268	0.014
TN	Tennessee	0.850	0.208
TX	Texas	0.994	0.857
UT	Utah	0.077	0.064
VT	Vermont	0.178	0.002
VA	Virginia	1.746	0.206
WA	Washington	0.050	0.046
WV	West Virginia	1.556	0.438
WI	Wisconsin	0.432	0.121
WY	Wyoming	0.149	0.056

Appendix C

Supplemental information for Chapter 4

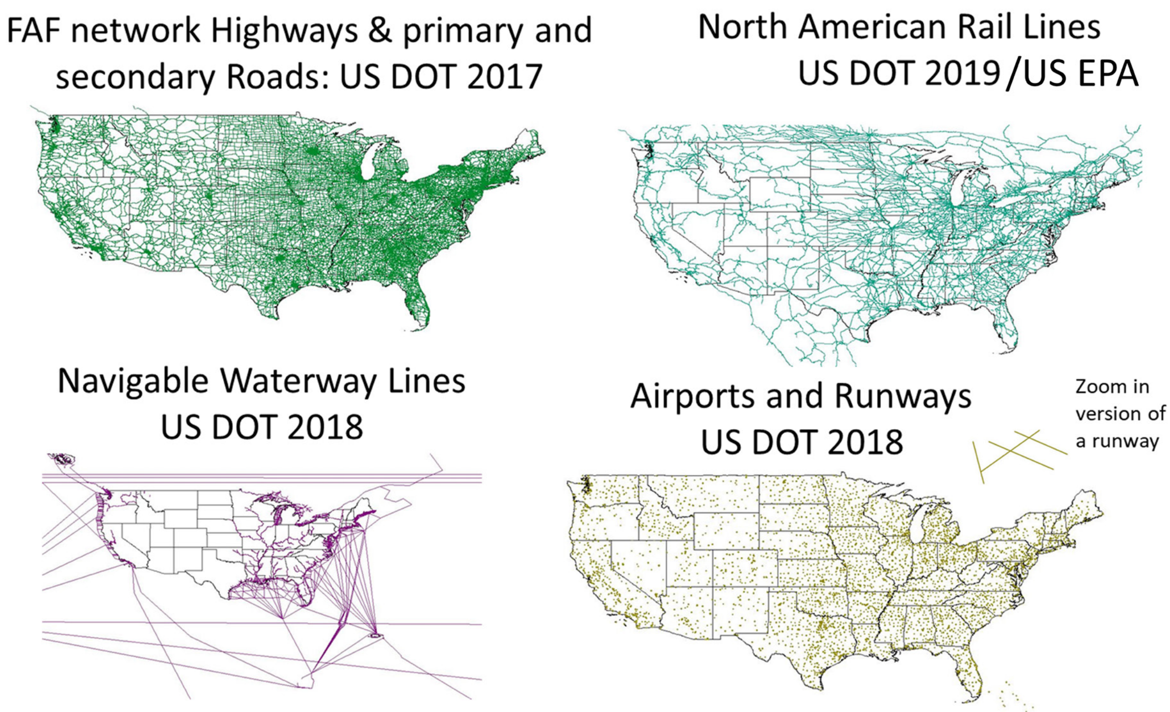

Figure C1. Geospatial network data from U.S. DOT's NTAD and US EPA. (Source: https://data-usdot.opendata.arcgis.com/; https://www.epa.gov/air-emissions-inventories/2014-national-emissions-inventory-nei-data).

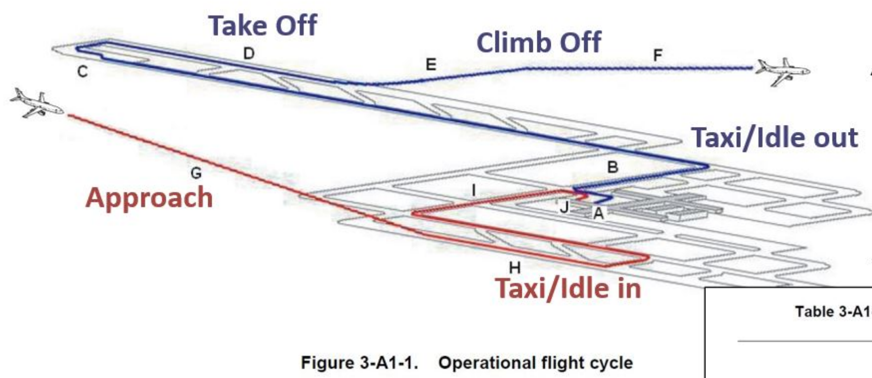

Table 3-A1-1. Reference emissions LTO cycle

Operating phase	Time-in-mode (minutes)		Thrust setting (percentage of rated thrust)
Approach	4.0		30
Taxi and ground idle	26	7.0 (in) 19.0 (out)	7
Take-off	0.7		100
Climb	2.2		85

Figure C2. LTO cycle and time-in-mode table from ICAO's air quality manual (Source: https://www.icao.int/publications/Documents/9889_cons_en.pdf).

Table C1. U.S. DOT ton-miles and estimated ton-miles using shortest route assumptions

Mode	Million Ton-Miles in 2017 (from U.S. DOT's FAF data)	Million Ton-Miles in 2017 (using shortest distance assumption in this research)	Ratio
Truck	1,437,029	1,224,764	1.2
Rail	1,087,651	900,078	1.2
Barge	184,553	196,788	0.9
Air	2,231	2,243	0.99

Table C2. National average estimated deaths and CO_2 emissions metrics

Mode	Billion Ton-Miles in 2017*	Megatons	Total deaths (all age groups)	Total deaths (age≥35 years)	Deaths (all ages) per billion ton-mile	Deaths (≥35 years) per billion ton-mile	Total CO_2 emissions (billion kg)	CO2 emissions kg per ton-mile	Deaths per 100,000 people	Deaths per 100,000 people per billion ton-mile	Risk gap (deaths per 100,000 people)	Risk gap per billion ton-mile
Truck	1,437	3,378	660	611	0.46	0.43	124	0.086	0.206	1.4E-04	0.021	1.5E-05
Rail	1,088	1,117	663	608	0.61	0.56	23	0.021	0.207	1.9E-04	0.035	3.2E-05
Barge	185	291	65	61	0.35	0.33	3.2	0.017	0.020	1.1E-04	0.007	4.1E-05
Air	2	2	2	2	0.81	0.75	1.3	0.588	0.001	2.5E-04	0.0001	6.2E-05

*from U.S. DOT's FAF data

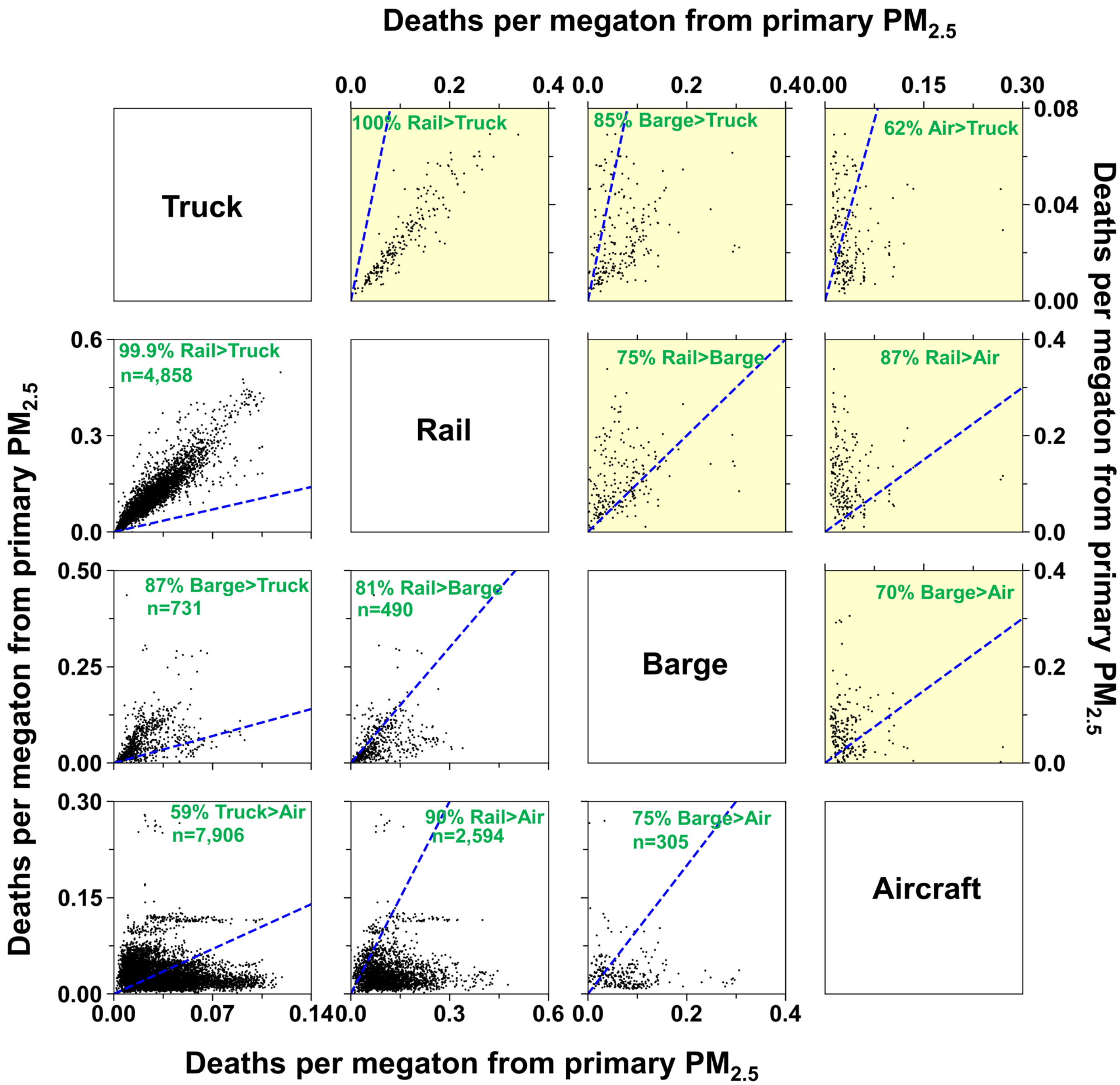

Figure C3. Deaths per megaton from primary $PM_{2.5}$ by mode and O-D pairs.

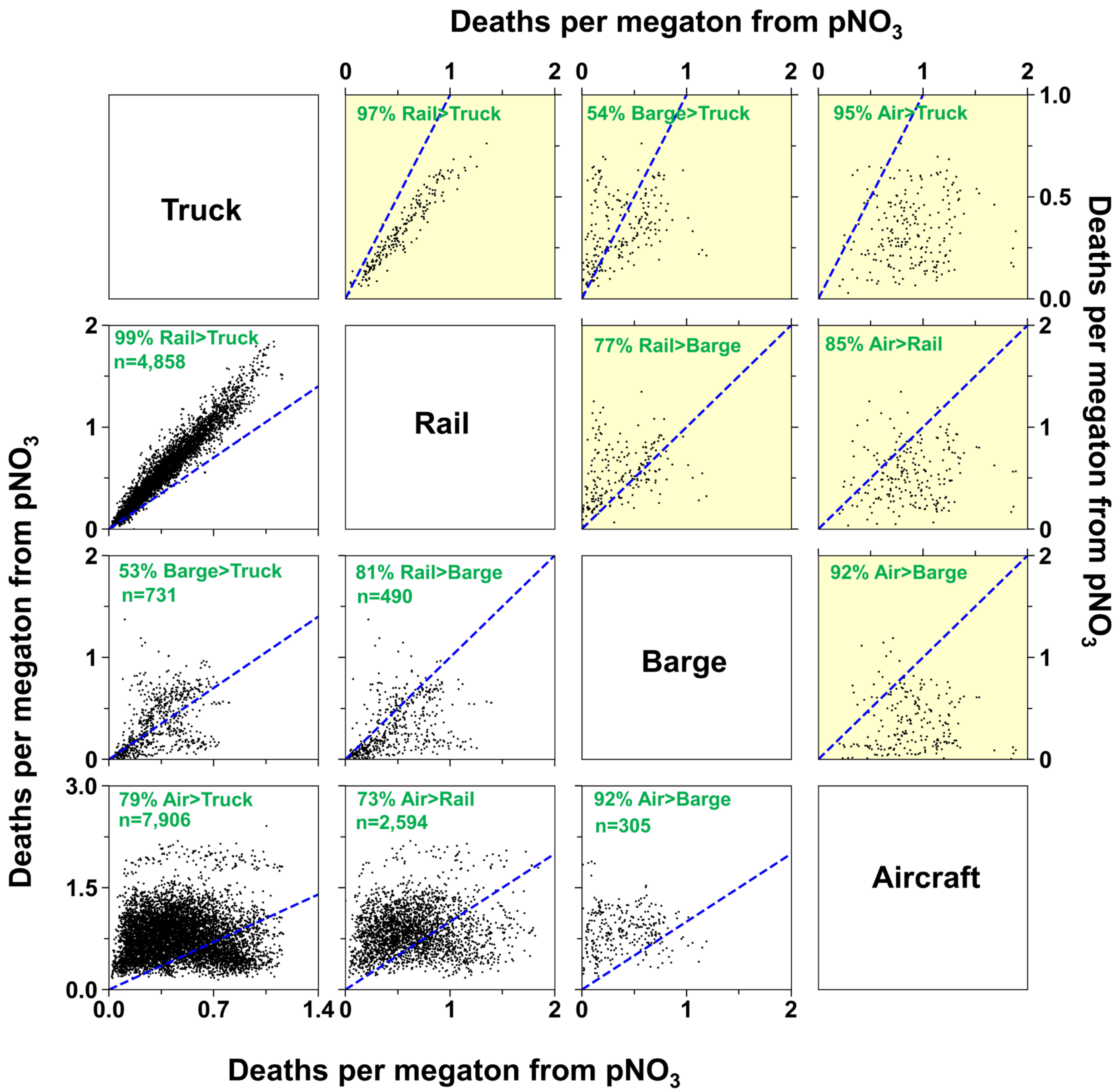

Figure C4. Deaths per megaton from primary particulate nitrate (pNO_3) by mode and O-D pairs.

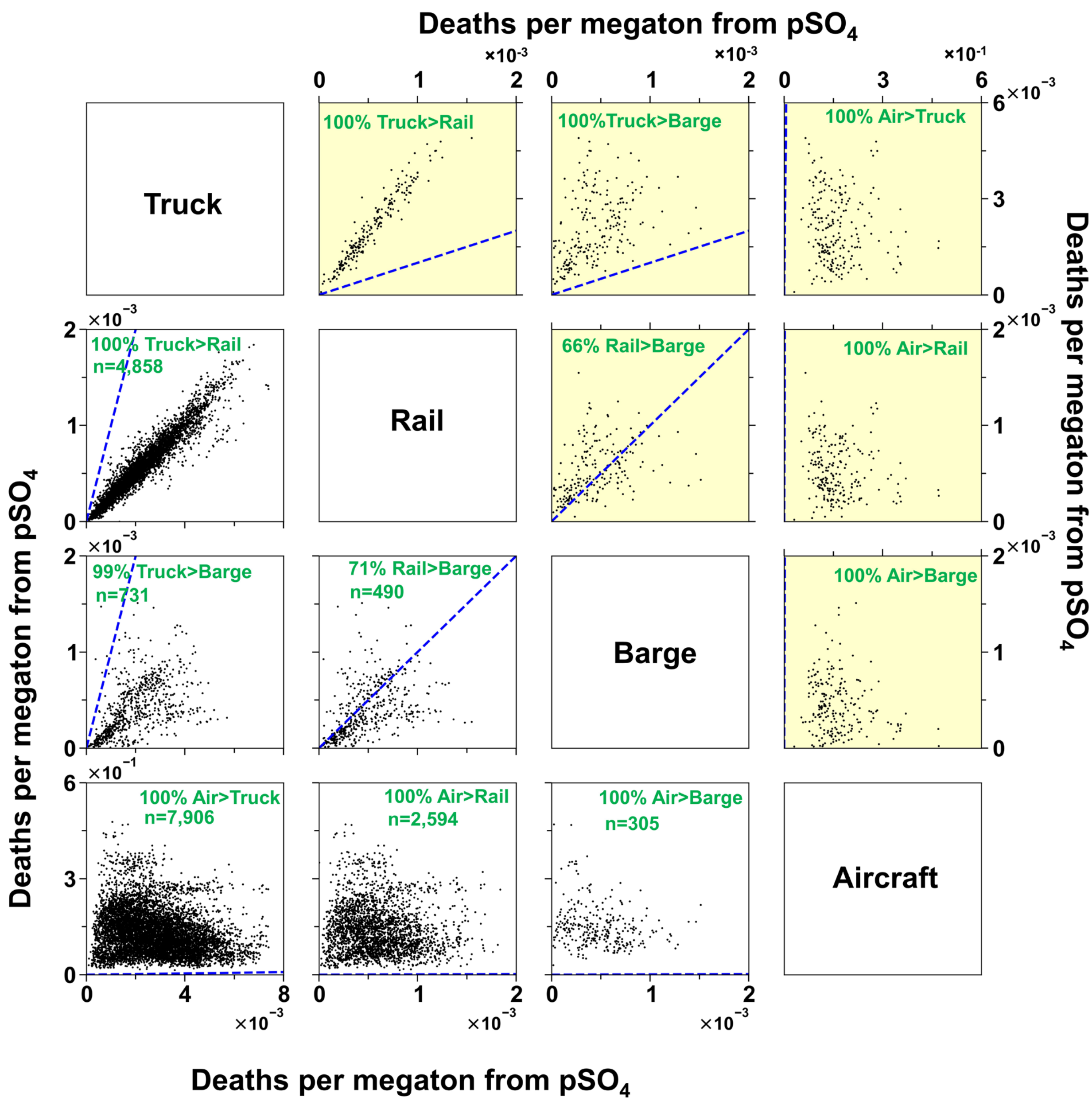

Figure C5. Deaths per megaton from particulate sulfate (pSO_4) by mode and O-D pairs.

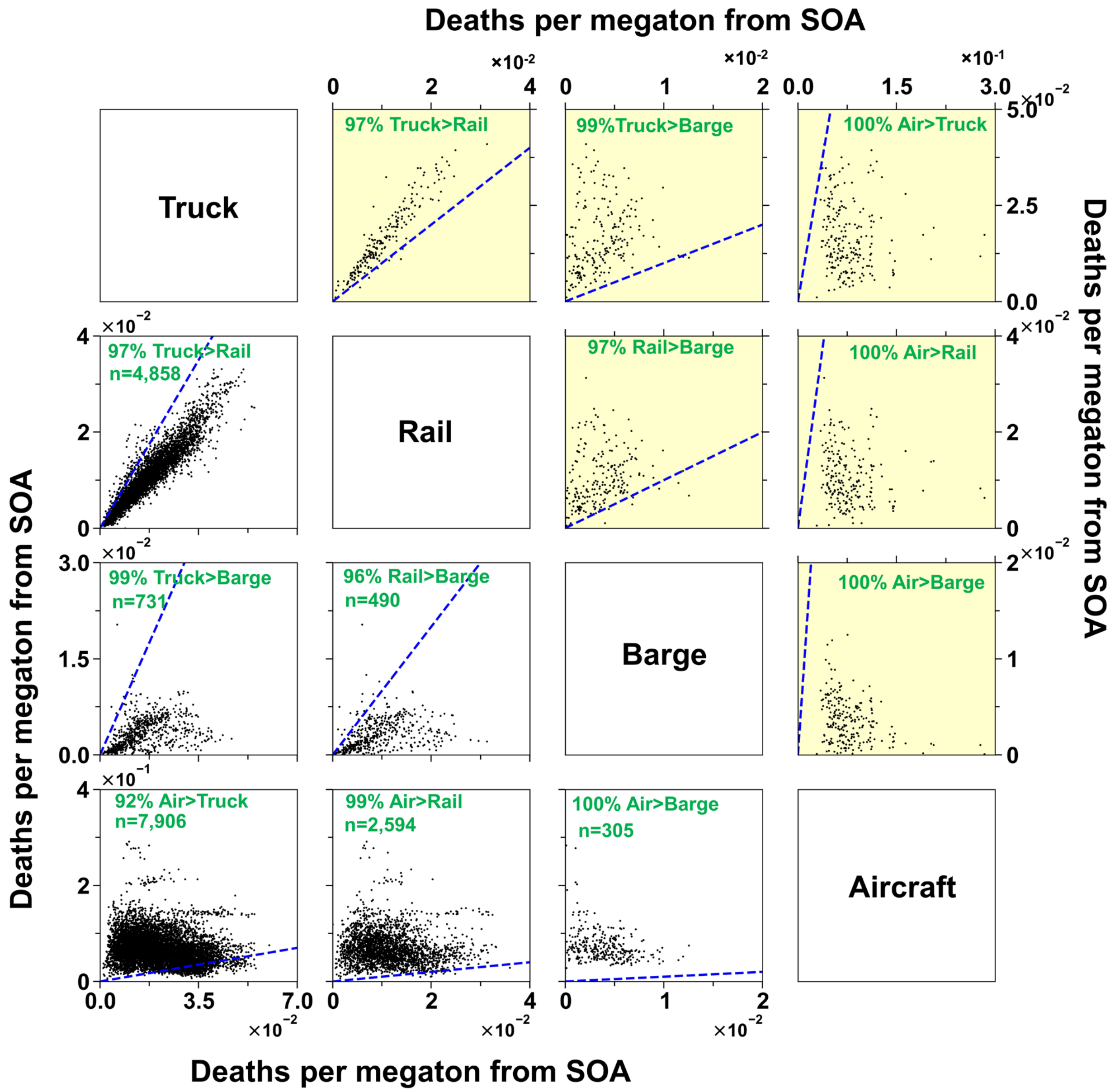

Figure C6. Deaths per megaton from secondary organic aerosols (SOA) by mode and O-D pairs.

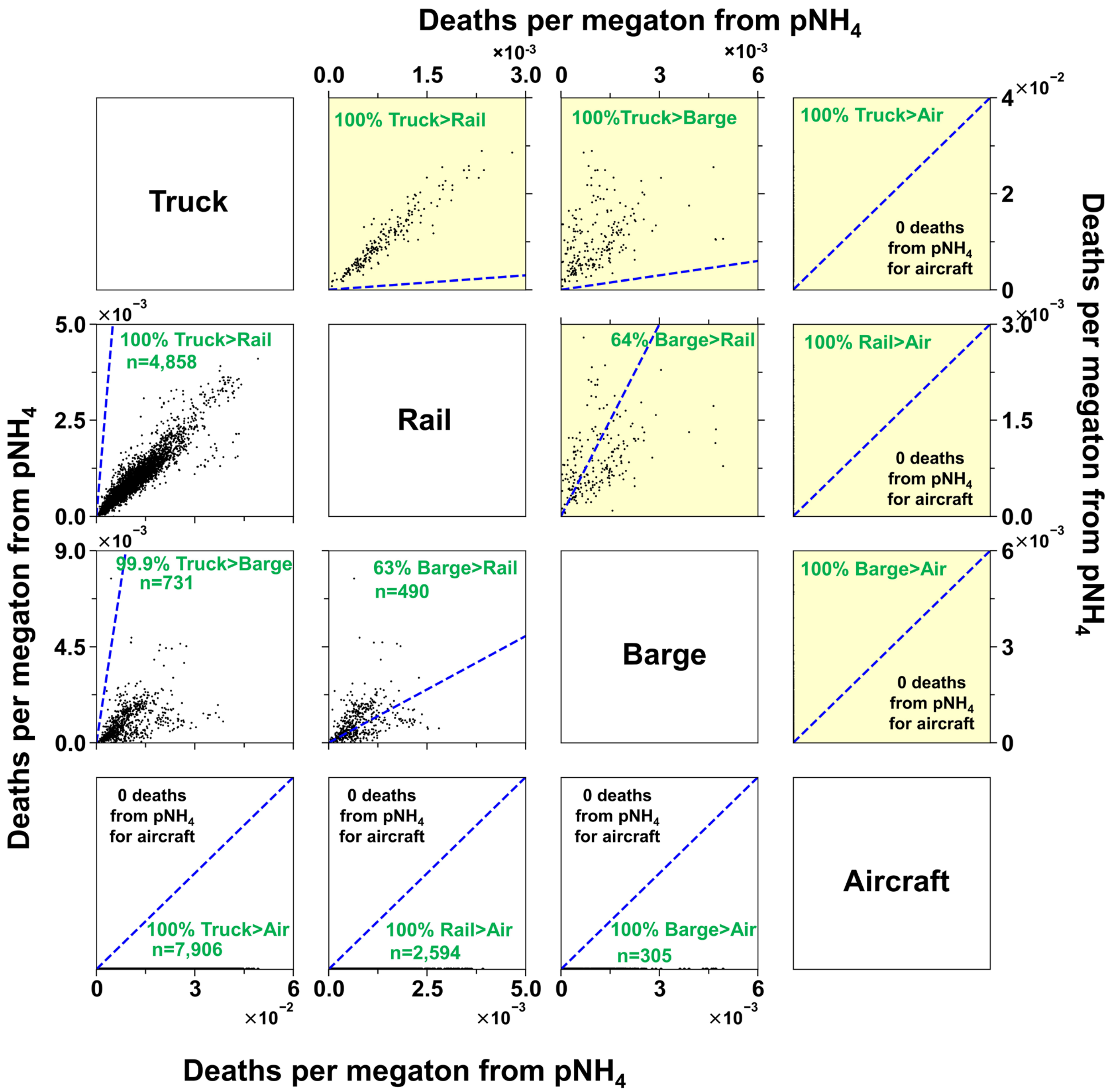

Figure C7. Deaths per megaton from particulate ammonium (pNH_4) by mode and O-D pairs.

Table C3. Z_{SA} for deaths per megaton by mode combinations

	Total $PM_{2.5}$	Primary $PM_{2.5}$	pSO_4	pNO_3	SOA	pNH_4
Rail/Truck	1.62	4.13	0.25	1.55	0.63	0.08
Barge/Truck	1.11	2.61	0.21	1.08	0.22	0.10
Rail/Barge	1.54	1.61	1.23	1.51	2.95	0.80
Air/Truck	1.87	0.87	47.04	1.67	3.16	-
Air/Rail	1.44	0.28	237.05	1.35	6.13	-
Air/Barge	2.36	0.45	317.52	2.19	19.27	-

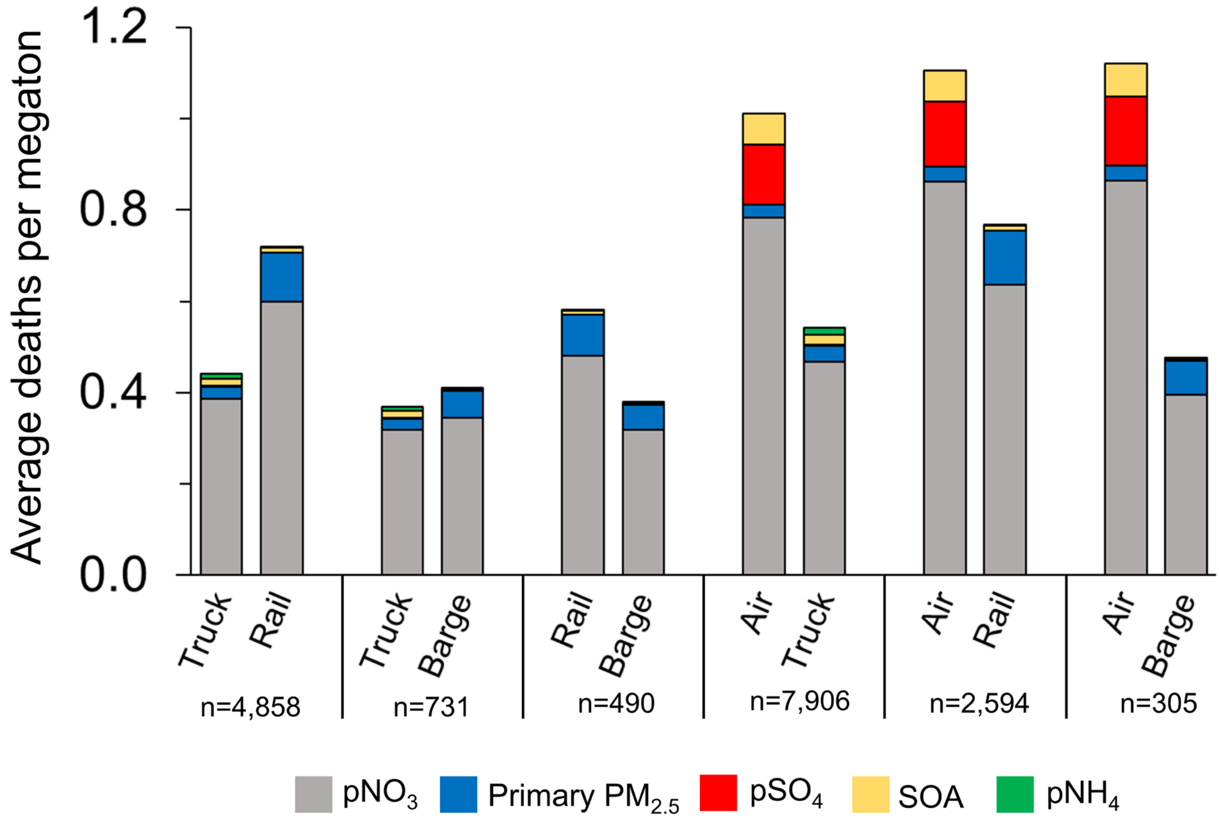

Figure C8. Average deaths per megaton from each $PM_{2.5}$ precursor by mode combinations.

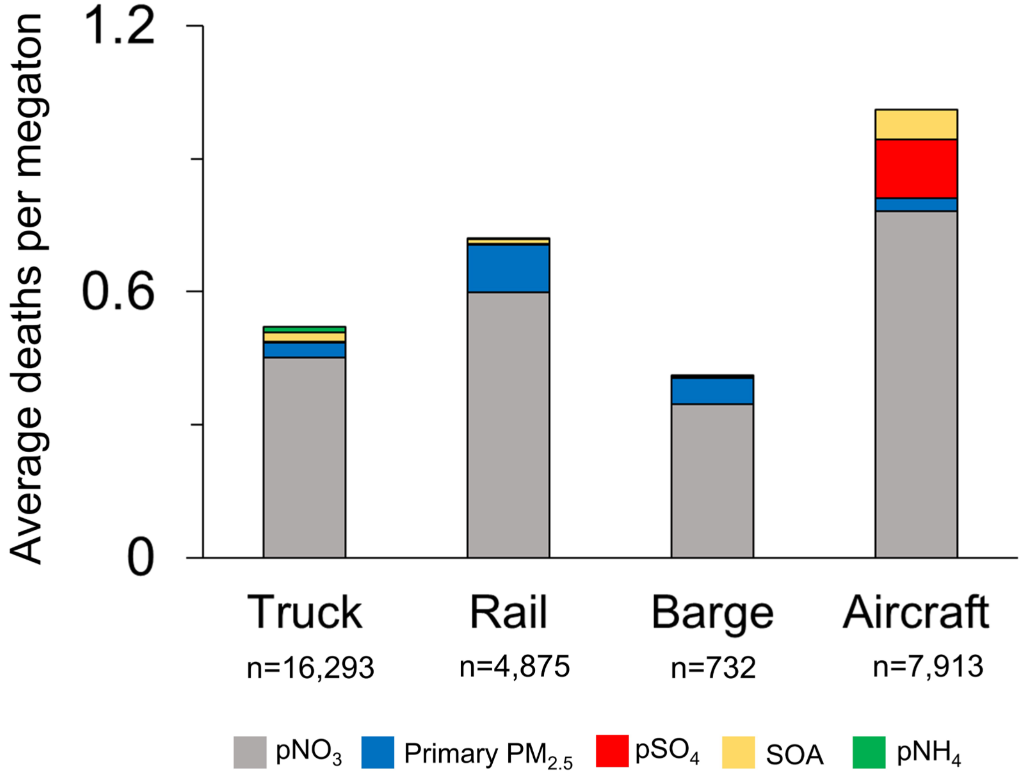

Figure C9. Average deaths per megaton from each $PM_{2.5}$ precursor by mode.

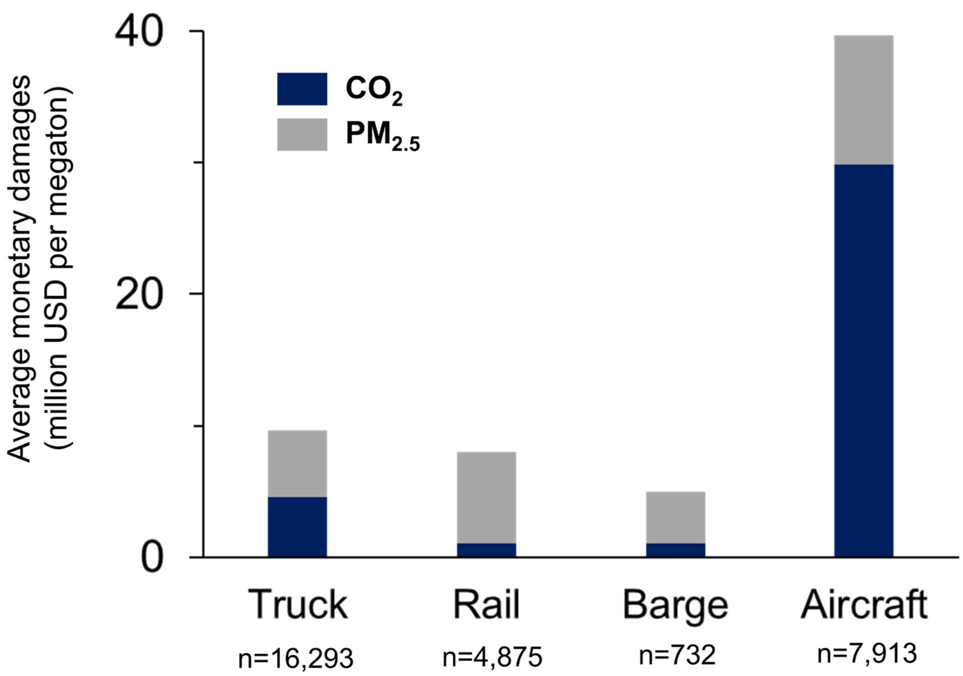

Figure C10. Average health and climate monetary damages (million USD per megaton) from each mode.

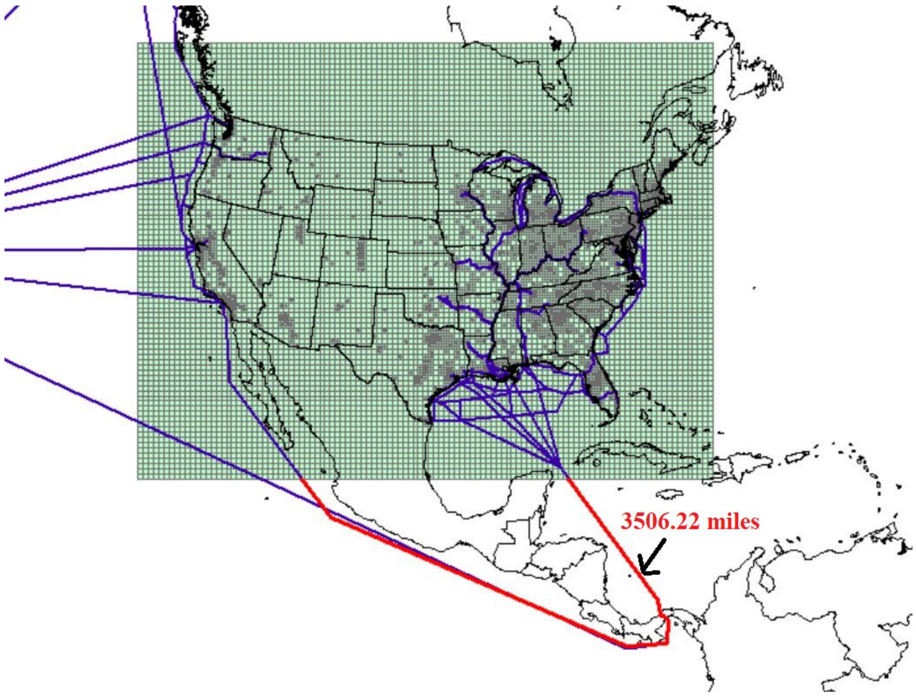

Figure C11. InMAP Source-Receptor Matrix (ISRM) grid, navigable waterway lines, and example of barge route via Panama Canal.